PHOTOINDUCED ELECTRON TRANSFER: DESIGN AND STUDY OF NEW SENSITIZERS TO CONTROL BACK ELECTRON TRANSFER

THESIS SUBMITTED TO
MAHATMA GANDHI UNIVERSITY
IN PARTIAL FULFILMENT OF THE REQUIREMENTS
FOR THE DEGREE OF

DOCTOR OF PHILOSOPHY
IN CHEMISTRY
UNDER THE FACULTY OF SCIENCE

BY

N. MANOJ

PHOTOCHEMISTRY RESEARCH UNIT
REGIONAL RESEARCH LABORATORY (CSIR)
TRIVANDRUM-695 019, KERALA, INDIA

NOVEMBER, 1998

Dedicated to
My Grand Mother

STATEMENT

I hereby declare that the matter embodied in this thesis is the result of investigations carried out by me at the Photochemistry Research Unit of the Regional Research Laboratory (CSIR), Trivandrum, under the guidance of Dr. K. R. Gopidas and the same has not been submitted elsewhere for a degree.

In keeping with the general practice of reporting scientific observations, due acknowledgement has been made wherever the work described is based on the findings of other investigators.

N. Manoj

K. R. GOPIDAS
SCIENTIST

PHOTOCHEMISTRY RESEARCH UNIT
REGIONAL RESEARCH LABORATORY (CSIR)
TRIVANDRUM-695 019, INDIA

Telephone: 91-471-490392 Fax: 91-471-490186
E. Mail: gopidas@csrrltrd.rcn.nic.in

November 05, 1998

CERTIFICATE

Certified that the work embodied in this thesis entitled: **"Photoinduced Electron Transfer: Design and Study of New Sensitizers to Control Back Electron Transfer"** has been carried out by Mr. N. Manoj under my supervision and the same has not been submitted elsewhere for a degree.

K. R. Gopidas
(Thesis Supervisor)

ACKNOWLEDGEMENTS

It is with great pleasure that I place on record my deep sense of gratitude to Dr. K. R. Gopidas, my research supervisor, for suggesting the research problem and for his guidance and encouragement, leading to a successful completion of this work.

I would like to express my sincere thanks to Professor M. V. George for his constant encouragement throughout the tenure of this work.

I wish to thank Dr. G. Vijay Nair, Director, Regional Research Laboratory, Trivandrum and Dr. A. D. Damodaran, former Director, Regional Research Laboratory, Trivandrum for providing me the necessary facilities and for their interest and support in carrying out this work.

I express my gratitude to all my teachers, in particular to, Professor V. N. Rajasekharan Pillai, Vice Chancellor, Mahatma Gandhi University, Professor S. Chandrasekharan, Chairman, Department of Organic Chemistry, Indian Institute of Science, Bangalore, Dr. C. V. Asokan, School of Chemical Sciences and Shri R. Raghunatha Varma, Devaswam Board Pampa College who have motivated me at various stages of my education.

I express my thanks to Dr. Suresh Das, Dr. A. Ajayaghosh, Dr. D Ramaiah, Dr. K. George Thomas and other members of the Photochemistry Research Unit for their suggestions and support extended to me for a successful completion of the work. I acknowledge the help rendered to me by Mrs. Sarada Nair and Mr. Robert Philip during various stages of my work. I also express my thanks to Dr. M. Muneer and all former members of the Photochemistry Research Unit for their

help in initiating the present research work. Thanks are also due to all my friends and well-wishers in various sections of Regional Research Laboratory.

I thank Dr. A. Samantha, School of Chemistry, University of Hyderabad, Dr. P. Ramamurthy, Department of Inorganic Chemistry, University of Madras, Dr. R. Ramaraj, School of Chemistry, Madurai Kamaraj University and Dr. James Joseph, CECRI, Karaikudi for extending their facilities in carrying out some of the experimental work reported in this thesis.

I gratefully acknowledge the Department of Atomic Energy, Government of India for awarding me the Dr. K. S. Krishnan Junior Research Fellowship for carrying out this work.

I wish to express my deepest gratitude to my uncle Dr. M. D. Nair and family for their guidance and help during my studies. Thanks are also due to Dr. K. P. N. Nair and family for their care and support during my stay at Trivandrum.

Finally, I am most grateful to my parents, brother and sisters for their invaluable support and encouragement throughout my life.

Trivandrum

November, 1998

N. Manoj

CONTENTS

PREFACE

Photoinduced electron transfer (PET) is of immense importance to chemistry, primarily because of its potential applications in solar energy conversion and storage. PET involves the use of visible or ultraviolet light to initiate electron transfer from a donor (D) to an acceptor (A) molecule and leads to formation of radical ion products. The energetics and dynamics of PET reactions are shown to depend on the structure of the reactants, the distance separating the reactants, the nature and polarity of the medium and Coulombic effects. A major disadvantage that arises in the use of PET is the energy wasting back electron transfer (BET), which regenerates the starting materials in their ground states. Thus, the challenge confronted in elaborating this area of chemistry lies in controlling the rate of deactivating BET. If the importance of the BET can be diminished, observable, selective chemistry can ensue. The present thesis is an attempt in that direction.

Over the years considerable amount of work has been done in the area of circumventing BET. As a result, several factors that can effectively control BET reactions were identified. Our aim has been to incorporate some of these features into a suitable acceptor chromophore and study their effect on the yields and lifetimes of radical products. We hoped that such an effort would help in the design of sensitizers that can control BET reactions.

We have selected pyrylium cations for our studies. These molecules, being inherently electron deficient in nature, are good electron acceptors in their excited states. We have prepared several pyrylium salts and evaluated their efficiency as sensitizers in terms of the yields and lifetimes of the radical ions generated in PET reactions. Since the kinetics and thermodynamics of PET reactions depend on the redox potentials and excited state properties of the sensitizers, these aspects were also studied in detail.

Chapter 1 of the thesis is a brief review of the fundamental aspects of PET reactions and the various strategies outlined in the literature to circumvent BET reactions. This is followed by a brief discussion of the general properties of the class of sensitizer molecules we have selected for our studies.

In Chapter 2 of the thesis, Photophysical and electron transfer properties of pyrylium salts **1a-f** and thiopyrylium derivatives **2a-d** were investigated. The photophysical studies that we have carried out include absorption spectra, fluorescence spectra, fluorescence quantum yields, fluorescence lifetimes, phosphorescence spectra and triplet-triplet absorption spectra. These studies suggested that the pyrylium cations have two singlet excited states with similar energies and that the substituent and solvent determine which of these has the lowest energy. For cations **1a**, **1f**, and **2a**, the lowest singlet excited state has TICT character. In the case of all other substrates the photophysical properties were better explained by invoking a planar excited state. Laser flash photolysis studies suggested that electron transfer take place from electron rich aromatics to

the singlet and triplet excited states of these compounds. Using biphenyl as donor, we have determined the extinction coefficients and yields of pyranyl and thiopyranyl radicals formed as a result of photoelectron transfer. We have tried to correlate the radical yields to the triplet quantum yields of the sensitizers and also to the stability of the pyranyl radicals. When naphthalene was used as the electron donor, charge separation was very poor due to the formation of a CT complex. Laser flash photolysis in this case led to the formation of the triplet state of the CT complex, which underwent slow deactivation to the ground state.

In Chapter 3, the effect of electronic, steric and Coulombic factors on the rate of BET were examined. A few pyrylium salts, which incorporated these structural features, were synthesized and studied. Pyrylium salts **1-3**, having aromatic substituents at the 4-position, stabilize the pyranyl radicals and this resulted in enhanced lifetimes of the PET products. Substitution of acetyl group as in **4**, led to high quantum yields of triplet formation and this in turn, gave radical products in high yields. The control of BET by steric effect in molecules having bulky substituents has been investigated by using compound **5**. Dicationic pyrylium salts **6** and **7** were prepared in order to impose Coulombic barriers in the BET reactions. In these cases the Coulombic repulsion between the radical cation of the donor molecule and the pyrylium radical cation led to considerable reduction in the rate of BET reactions.

Chapter 4 of the thesis describes the photophysical and electron transfer properties of a few pyrylium salts in aqueous buffer solutions in the absence and

presence of β-cyclodextrin. Our studies have shown that pyrylium salts with suitable hydrophobic moieties can be encapsulated in β-CD cavities. In these cases, the association constants with β-CD were determined using the Benesi-Hildebrand treatment. Electron transfer to the singlet and triplet excited states of the encapsulated pyrylium salts were studied by fluorescence quenching and laser flash photolysis methods. The forward electron transfer rates in the presence of β-CD were slightly lower than those obtained in the absence of β-CD. The back electron transfer rates in the presence of β-CD were approximately 20 times lower. This is attributed to the enhanced binding of the pyranyl radicals to the β-CD cavity.

All these studies were aimed at the identification of the structural elements or environments that can contribute effectively to control BET reactions in these cationic sensitizers. It was hoped that an understanding of these factors might help in the design of electron transfer sensitizers that can be used for practical applications.

Note: The numbers of the various compounds given here correspond to those given under the respective chapters.

CHAPTER 1

PHOTOINDUCED ELECTRON TRANSFER: AN OVERVIEW

1. Introduction

Electron transfer reactions are of fundamental importance to both chemistry and biology. In simple terms, an electron transfer reaction involves the transfer of an electron from a 'donor' to an 'acceptor'. Electron transfer reactions can occur both thermally and photochemically. The latter reactions are referred to as photoinduced electron transfer (PET) reactions. Photoinduced electron transfer is an active area of research at present and a large number of books and reviews dealing with various aspects of PET reactions are currently available.[1-17] In PET reactions, absorption of light activates the donor or acceptor for electron transfer. It has been recognized quite early by Rabinowich[18] that "an electronically excited molecule has an increased tendency to give away an electron, as well as the capacity to replace the one which was removed from its normal level". The quantitative formulation of this conclusion is known as the Rehm-Weller equation[19,20] (vide infra). According to Rehm-Weller equation, absorption of a photon activates molecules to undergo redox reactions, the activation being equal to the excitation energy of the molecule. In fact, nature has used this mode of molecular activation in the photosynthetic reaction centre in order to convert solar energy to chemical energy via charge separation.[1-3] The early events in photosynthesis involve light absorption by antenna chromophores, followed by a series of electron transfers. The transferred electron, in principle, can go back to

the donor through a process known as back electron transfer (BET).[14] Back electron transfer is an energy wasting process as it regenerates the donor and acceptor molecules in their ground states. In the natural photosynthetic system, electron transfer occurs along cascades of donor and acceptor substrates in order to prevent back electron transfer. In an attempt to mimic the natural photosynthesis, chemists have been trying to develop artificial systems containing donor-acceptor moieties and light harvesting antennas to harvest and store solar energy.[1-7] However, the efficiencies of these systems are often limited by facile BET reactions. Efforts have been made by various research groups to circumvent the energy wasting BET process in several donor acceptor systems in homogeneous and heterogeneous media. In the present study, an attempt has been made to examine the effect of structural modifications on the rate of BET reactions.

In this chapter a brief outline of the fundamental aspects of PET reactions is presented. This is followed by a discussion of BET and the various methods devised to circumvent BET. A brief discussion of the general properties of the class of sensitizer molecules we have studied is also presented in this chapter.

1.1. Theories of photoinduced electron transfer

PET involves the use of visible or UV light to initiate electron transfer from a donor (D) to an acceptor (A) molecule. The first step of the reaction is the absorption of light by either the donor or acceptor. A general reaction involving the excitation of A is given in equations (1.1) to (1.3).

$$A \xrightarrow{h\nu} A^* \qquad (1.1)$$

$$A^* + D \xrightarrow{ET} A^{\bullet -} + D^{\bullet +} \qquad (1.2)$$

$$A^{\bullet -} + D^{\bullet +} \xrightarrow{BET} A + D \qquad (1.3)$$

The molecule, which absorbs light and gets excited, is generally referred to as the 'sensitizer' and the other molecule is referred to as the 'quencher'. The excited state involved can be the singlet or the triplet state of the molecule. The energy wasting BET, which regenerates the starting materials in their ground states, is shown in equation (1.3).

The electron transfer reaction described by equation (1.2) proceeds in several discrete steps. For example, consider a general case where the reaction takes place in solution and the reactants are free to move around. The interaction between the excited acceptor and ground state donor creates a series of short-lived intermediates, each possessing a unique geometry and electronic distribution.[1.15] The overall situation is depicted in Figure 1.1. It is shown that the excited acceptor and ground state donor molecules diffuse towards each other by a series of one-dimensional random steps leading to the formation of an encounter complex. Further diffusion towards each other leads to the formation of a collision complex. In excited state electron transfer reactions, a collision complex can be visualized as an ensemble consisting of the sensitizer and the quencher surrounded by several layers of solvent molecules. The sensitizer and the quencher are said to be

contained within a solvent cage, at a centre-to-centre distance (d_{cc}) of ~ 7 Å. The lifetimes of these complexes are usually in the 10^{-9}-10^{-10} s range. Electron transfer within the collision complex or encounter complex leads to the formation of contact ion pair (CIP) or exciplex. The contact ion pair forms a solvent separated ion pair (SSIP), in which the partners may be separated by one or two solvent molecules. The CIP and SSIP are sometimes described as geminate ion pairs.

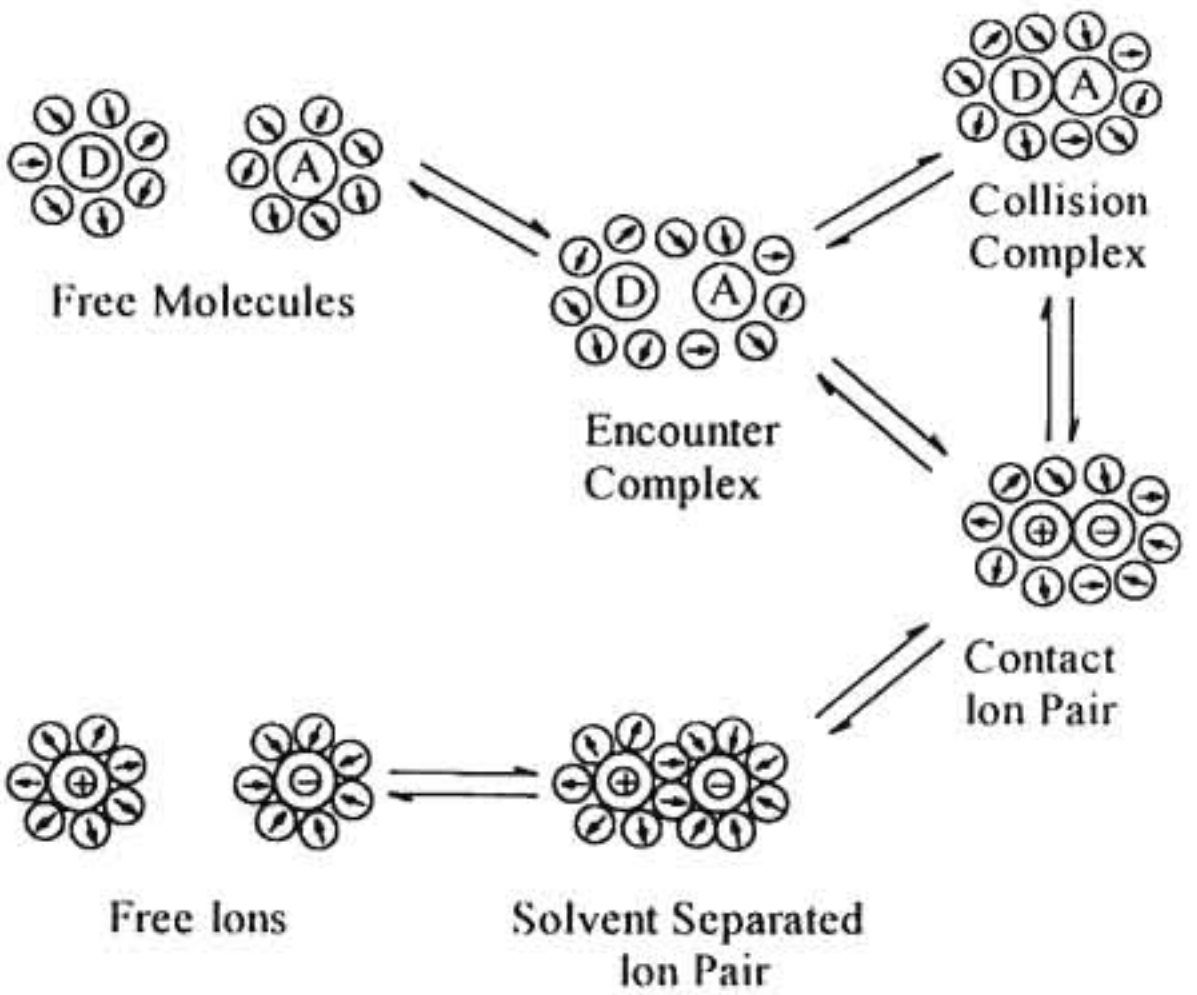

Figure 1.1 A figure summarizing the various events in PET reactions.

Finally, the ions move apart to form free solvated ions. The efficiency of a PET reaction is actually measured in terms of the yield of free ions formed in the reaction. Since the ions are in close contact within the CIP or SSIP, BET is very facile. This severely reduces the yield of free ions. In general, for

bimolecular PET reactions in homogeneous solution, quantum yield is very low.

1.1.1. Energetics

According to definition, electron transfer is energetically feasible when the electron affinity (EA) of the acceptor exceeds the ionization potential (IP) of the donor; i.e.,

$$\Delta E = IP_D - EA_A \tag{1.4}$$

where, ΔE is the change in energy accompanying the electron transfer. When a molecule absorbs a photon, its ionization potential decreases and electron affinity increases according to equations (1.5) and (1.6), respectively.

$$IP_D^* = IP_D - E_{0,0(D)} \tag{1.5}$$

$$EA_A^* = EA_A + E_{0,0(A)} \tag{1.6}$$

$E_{0,0}$ is the energy of the excited state. For the case where the electron donor is in the excited state,

$$\Delta E = IP_D - EA_A - E_{0,0(D)} \tag{1.7}$$

Similarly when the excited state is the electron acceptor,

$$\Delta E = IP_D - EA_A - E_{0,0(A)} \tag{1.8}$$

equations (1.7) and (1.8) are used only to test the feasibility of PET in the gas phase. When PET is carried out in solution, solvation energies (ΔG_{sol}) and Coulombic interaction energies must be added. Under these conditions, the driving force for electron transfer leading to solvent separated ion pair (ΔG_{SSIP}) is given by equation (1.9).

$$\Delta G_{SSIP} = IP_D - EA_A - E_{0,0} + \Delta G_{sol} + w_p - w_r \qquad (1.9)$$

w_p and w_r are the work terms for electrostatic interaction in the product and reactant states, respectively, and is given by equation (1.10).

$$w = Z_A Z_D e^2/d_{cc}\varepsilon_s \qquad (1.10)$$

In equation (1.10), Z_A and Z_D are the charges on the molecules, d_{cc} is the centre-to-centre distance and ε_s is the solvent dielectric constant. ΔG_{sol} is the sum of the solvation energies of the ions, and is given by equation (1.11).

$$\Delta G_{sol} = \Delta G_{(D^+)} + \Delta G_{(A^-)} \qquad (1.11)$$

In solution, the ionization potentials and electron affinities are related to redox potentials as given in equations (1.12) and (1.13), respectively.

$$IP = E^0_{(D^+/D)} - \Delta G_{sol} + \text{Const.} \qquad (1.12)$$

$$EA = E^0_{(A/A^-)} + \Delta G_{sol} + \text{Const.} \qquad (1.13)$$

$E^0_{(D^+/D)}$ is the oxidation potential of the donor and $E^0_{(A/A^-)}$ is the reduction potential of the acceptor measured in the same solvent. Combining equations (1.9) to (1.13) leads to the Rehm-Weller equation (1.14).[19,20]

$$\Delta G_{SSIP} = E^0_{(D^+/D)} - E^0_{(A/A^-)} - E_{0,0} + w_p - w_r \qquad (1.14)$$

The Rehm-Weller equation is useful in calculating the free energy of PET reactions from the redox potentials and excitation energies. It is to be noted that the work term $w_r = 0$ for PET reactions between neutral reactants. Also, the equation $w = e^2/d_{cc}\varepsilon_s$ is valid only if the ions can be treated as point charges (i.e., d_{cc} of the reacting partners is greater than the sum of their molecular radii). The value of this term is small in polar solvents. For example, in acetonitrile ($\varepsilon_s = 37$), $w \sim 0.03$ eV in contrast to a value of 0.3 eV in a

nonpolar solvent ($\varepsilon_s = 4$) for ion pairs at a mean $d_{cc} = 7$ Å. Hence this term is normally neglected in the calculation of ΔG in polar solvents.

Table 1.1 lists the redox potentials and free energies for a few representative examples of PET reactions in polar solvents. The table demonstrates the wide range of ΔG values available for PET reactions.

Table 1.1 Calculated free energies for a few PET reactions.[a]

Donor	Acceptor	$\Delta E_{0,0}$ kcal M^{-1}	$E_{0(D^{+\bullet}/D)}$ V	$E_{0(A/A^{-\bullet})}$ V	ΔG_{el} kcal M^{-1}
TMB	$[Rh_2(dicp)_4]^{2+\bullet}$	38.97	0.32	-1.40	+20.75
Indene	$^3[CN]^{\bullet}$	79.56	1.52	-1.98	-23.06
$[Ru(bpy)_3]^{2+}$	$[Cr(bpy)_3]^{3+\bullet}$	39.43	1.29	-0.26	-3.69
$[Rh_2(dicp)_4]^{2+\bullet}$	MV^{2+}	38.97	0.89	-0.45	-9.45
$[Ru(bpy)_3]^{2+\bullet}$	MV^{2+}	48.89	1.29	-0.45	-10.15
Indene	$^1[CN]^{\bullet}$	89.47	1.52	-1.98	-10.15
Norbornadiene	$^3[Ch]^{\bullet}$	62.26	1.54	+0.02	-28.59

[a] Data collected from Ref. 15 and references therein. Redox potentials are reported vs. SCE. Abbreviations: TMB = *N,N,N',N'*-tetramethylbenzidine, CN = 1-cyano-naphthalene, bpy = 2,2'-bipyridine, dicp = 1,3-diisocyanopropane, MV^{2+} = methylviologen

The success of PET reactions, however, cannot be ensured by favourable energetics alone. Photophysical properties of the sensitizer molecules are also very important. For example, the lifetime of the excited sensitizer must be

sufficiently long to allow quenching by electron transfer to take place. Also, other excited state decay pathways such as luminescence or energy transfer should not compete with electron transfer. Knowledge of the excited state properties of the sensitizers and their redox potentials, as well as the redox potentials of the quenchers are the essential requirements for investigating PET processes.

1.1.2. Rate expressions

An operational format of the various events taking place following excitation of an acceptor molecule is shown in Figure 1.2. The rate constants of the various processes are also shown in this Figure.

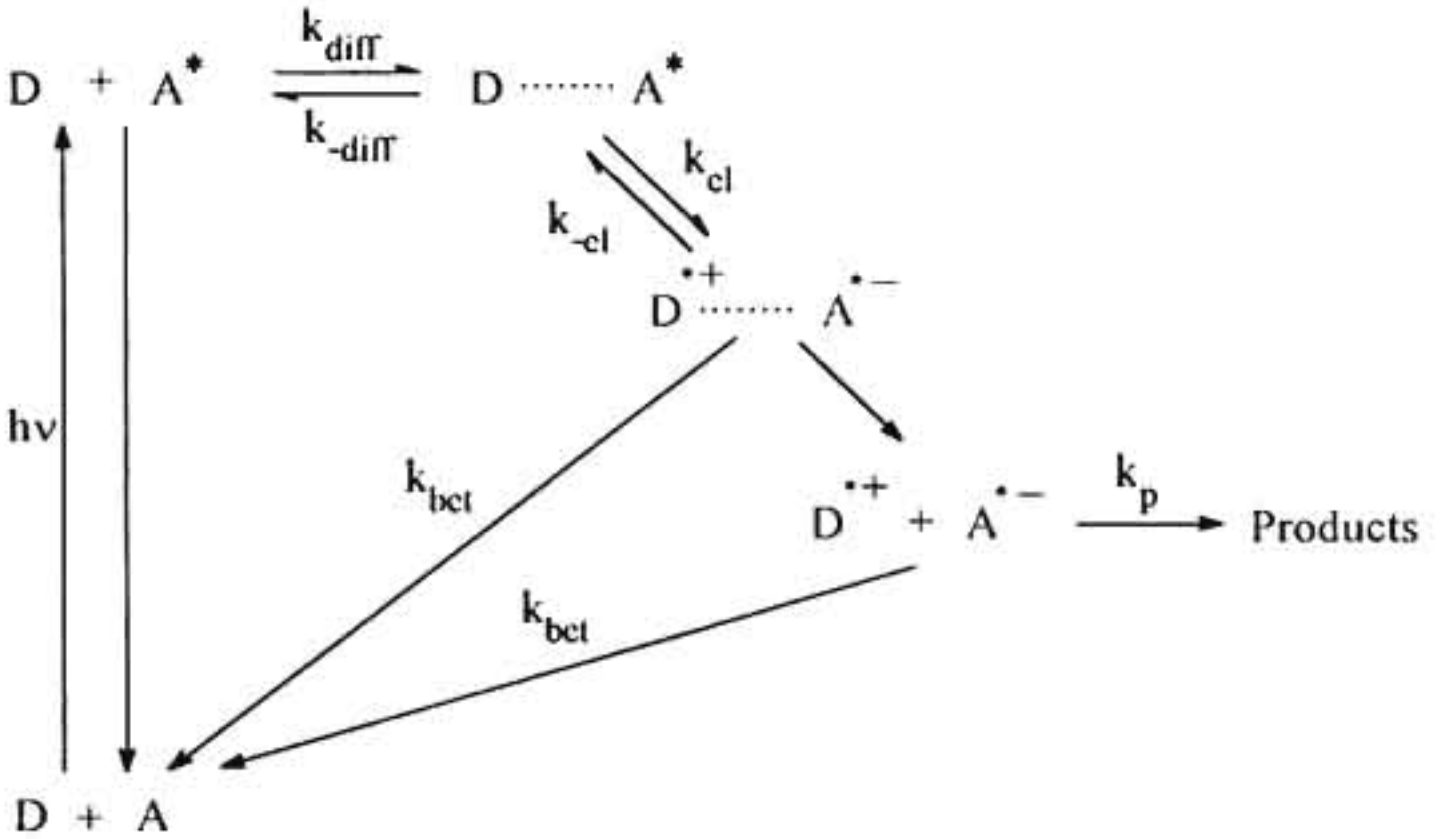

Figure 1.2 Schematic diagram for photoinduced electron transfer showing various processes taking place in solution.

In Figure 1.2, k_{diff} and k_{-diff} are the diffusion controlled rate constants for the formation and dissociation of the encounter complex, respectively, k_{el} is the unimolecular rate of electron transfer within the complex, k_{-el} is the rate

constant for reverse electron transfer and k_{bet} is the rate constant for back electron transfer. A steady-state treatment of the various reactions in Figure 1.2 leads to equation (1.15).

$$k_q = \frac{k_{diff}}{1 + \frac{k_{-diff}}{k_{el}} + \frac{k_{-diff}\ k_{-el}}{k_{el}\,(k_p + k_{bet})}} \qquad (1.15)$$

In equation (1.15), k_q is the bimolecular rate of quenching by electron transfer. The equation can be simplified if we assume that electron transfer is exothermic. Given this assumption, $k_{-el} << k_{el}$, and equation (1.15) becomes,

$$k_q = \frac{k_{el}\ k_{diff}}{k_{el} + k_{diff}} \qquad (1.16)$$

Introducing a further assumption that $k_{diff} = k_{-diff}$, equation (1.16) is simplified to equation (1.17).[21,22]

$$\frac{1}{k_q} = \frac{1}{k_{el}} + \frac{1}{k_{diff}} \qquad (1.17)$$

From equation (1.17) it can be deduced that, under the conditions of rapid electron transfer, i.e., $k_{el} >> k_{diff}$, the observed rate of quenching is simply given by the diffusion rate constants for the reactants in the particular solvent. In this case, the reaction is dominated by diffusion dynamics and is said to be diffusion-controlled. Under conditions of slow electron transfer, i.e., $k_{el} << k_{diff}$, electron transfer is said to be activation controlled. In this case k_{el} can be easily determined from k_q values measured using Stern-Volmer technique and k_{diff}

values calculated using modified Smoluchowski theory[23] or by statistical nonequilibrium thermodynamic theory.[24]

The rate of activation controlled electron transfer k_{el} depends upon the freedom of the excited state and the ground state molecules to explore a given set of electronic and nuclear configurations and ultimately find a suitable arrangement that permits electron transfer. Thus, k_{el} is expressed as a product of nuclear and electronic factors as given in equation (1.18)

$$k_{el} = \nu \kappa_n \kappa_{el} \qquad (1.18)$$

where, ν is the nuclear frequency factor and may range from $\sim 10^{12}$ to $\sim 10^{14}$ s^{-1}. κ_{el} is defined as the electronic factor and κ_n as the nuclear factor. The latter quantities are dimensionless and range between 0 and 1. In the classical theories of electron transfer κ_n is expressed as in equation (1.19)

$$\kappa_n = \exp(-\Delta G^{\ddagger}/RT) \qquad (1.19)$$

where, $\Delta G^{\ddagger}$ is the free energy of activation for the electron transfer. Substituting in equation (1.18), the expression for k_{el} becomes,

$$k_{el} = \nu \kappa_{el} \exp(-\Delta G^{\ddagger}/RT) \qquad (1.20)$$

Two general approaches are used to evaluate the nuclear and electronic factors. In the classical approach by Marcus and others, κ_{el} is assumed to be unity (i.e., electronic barriers are neglected) and $\Delta G^{\ddagger}$ is considered as a function of the nuclear reorganization energy (λ) and free energy change (ΔG) of the reaction. In the nonclassical or quantum mechanical approach, these factors are evaluated from the overlap of the nuclear and electronic wave functions of the initial reactant and final product states.

1.1.3. Marcus theory

Classical theories of Marcus and others assume that the donor and acceptor are within contact distance during electron transfer and, consequently, experience a weak electronic interaction.[25-35] The electronic factor, κ_{el} is assumed to be unity. The nuclear factor (κ_n) is related to the activation energy, $\Delta G^{\ddagger}$, and is given by equation (1.21).

$$\Delta G^{\ddagger} = \frac{(\lambda + \Delta G_{el})^2}{4\lambda} \qquad (1.21)$$

In equation (1.21) ΔG_{el} is the free energy associated with the electron transfer reaction and λ is the total reorganization energy. λ is the sum of λ_v, the inner sphere barrier and λ_s the outer sphere barrier. These nuclear barriers which precede the actual electron transfer, involve bond length changes within the reactants and reorganization of the surrounding solvent dipoles. The reorganization energy due to the bond length changes can be estimated from equation (1.22).

$$\lambda_v = \sum_j \left[\frac{f_i(R)_j \, f_i(P)_j}{f_i(R)_j + f_i(P)_j} \right] [\Delta q_i]^2 \qquad (1.22)$$

where Δq_i are the differences in the equilibrium bond distance between the reactant (R) and product (P) states corresponding to a j^{th} vibration, and f_i is the force constant for this vibration. In practice, all vibrational states are assumed to display harmonic behaviour, and the sum of all force constants and bond distortions of excited and ground state is taken in estimating λ_v.[32]

The outer sphere reorganization energy λ_s refers to the orientational changes in the solvent molecules surrounding the reactants during electron transfer. λ_s can be estimated using equation (1.23).

$$\lambda_s = \Delta e^2 (1/2r_D + 1/2r_A - 1/d_{cc}) (1/\varepsilon_\infty - 1/\varepsilon_s) \qquad (1.23)$$

In equation (1.23), r_D and r_A are the radii of the donor and acceptor, respectively. ε_∞ and ε_s are the refractive index and dielectric constant, respectively, of the solvent. Equation (1.23) is based on a fairly simple physical picture of two spherical reactants surrounded by a cage of solvent molecules. More sophisticated expressions for λ_s are needed if the molecules are not spherical. The equation implies that λ_s is greater in polar solvents compared to nonpolar solvents. Also, λ_s is larger for small molecules. Substituting equation (1.21) in equation (1.20) leads to the Marcus equation (1.24) for the rate constant of electron transfer,

$$k_{el} = \nu \exp\left[\frac{-(\lambda + \Delta G_{el})^2}{4\lambda RT}\right] \qquad (1.24)$$

According to the classical treatment described above, the actual electron transfer occurs at a nuclear geometry midway between the reactant and product states. In PET, the crossing point can be regarded as a transient photoexcited complex having a geometry just between the geometries of the two states. The activation energy consists of solvent and bond contributions and the Marcus treatment can be applied to calculate the energy barriers and rate constants.

1.1.4. The inverted region

According to the Marcus equation (1.24), a plot of k_{el} versus ΔG_{el} will be bell shaped. Initially the rate should increase with an increase in driving force and reaches a maximum at $\Delta G_{el} = -\lambda$. With further increase in the driving force, the rate should progressively decrease. The falling part of the plot beyond the maximum is known as the Marcus inverted region. Experimental evidence for the inverted region has proven to be a formidable and elusive task. Weller, for example, has measured the quenching rate constants for a series of compounds and observed that the rates plateau at large ΔG_{el} values.[19,20] This behaviour is typical of luminescence quenching experiments in solution and is termed as the Rehm-Weller behaviour. Several reasons have been suggested for not observing the inverted region in PET reactions.[36] These include: (1) limiting of the rate constants by diffusion (see equation (1.17)), (2) formation of products in the excited state, (3) presence of extra reaction channels other than electron transfer at high driving forces and (4) lack of a true homogeneous series of donors and acceptors.

The inverted region is now firmly established in electron transfer reactions. Most of these pertain to thermal charge shift reactions in solid matrices[37,38] or charge recombination reaction in covalently linked donor-acceptor systems.[39-46] Presence of the inverted region is also established in back electron transfer reactions of contact and solvent separated ion pairs.[47-57] Although, the evidence for the inverted region is substantial, it is almost nonexistent for bimolecular charge separation reactions except for a few recent reports.[58,59]

1.1.5. Nonclassical theories

The classical theories of electron transfer were formulated on the basic assumption that the donor and acceptor orbitals overlap slightly at a separation distance of ~7 Å within the encounter complex. However, there are many systems where the donor and acceptor are separated by greater distances. For example, in rigid matrices or donor-acceptor systems linked by spacer molecules, the separation distance may be more than ~7 Å. In these systems, electronic as well as nuclear barriers may be rate limiting ($\kappa_{el} \neq 1$) and PET takes place by electron or nuclear tunneling through these energy barriers. A nonclassical treatment is required for these systems where emphasis is placed on the overlap of electronic and nuclear wave functions in the initial and final states rather than on the transition state as in the classical theory.

In the nonclassical theories, the donor, acceptor and the medium are perceived as a supermolecule undergoing high energy bond deformations and low energy solvent dipole orientations.[60-63] PET may then be regarded as a radiationless transition between the initial and final potential energy surfaces. The rate of this process is given by the Fermi 'Golden Rule' equation (1.25).

$$k_{el} = \frac{2\pi}{\hbar} |H_{el}|^2 FC \qquad (1.25)$$

In equation (1.25), H_{el} is the quantum mechanical counter part of the classical electron transfer matrix that couples the reactant and product electronic wave functions and FC is the Franck-Condon factor. H_{el} is identified with κ_{el} in equation (1.20) and is a measure of the probability that the reaction proceeds

from the initial to final state. The Franck-Condon factor is given by equation (1.26).

$$FC = \frac{\exp\left[-(\Delta G_{el} + \lambda)^2/4\lambda k_B T\right]}{(4\pi\lambda k_B T)^{1/2}} \qquad (1.26)$$

Electron transfer can be regarded as taking place in adiabatic, nonadiabatic or in intermediate regions, depending on the magnitude of H_{el}.[55] In the adiabatic region, electronic interaction is strong, and therefore $\kappa_{el} = 1$, and when $\kappa_{el} = 0$, the electron transfer process is classified as nonadiabatic (Figure 1.3). Somewhere between the extremities lies an intermediate region which is called 'weakly adiabatic', i.e., $0 < \kappa_{el} < 1$. This is the region applicable to the classical theories, where the donor and the acceptor are assumed to approach to an approximate encounter distance of ~7 Å to allow for sufficient orbital interactions.

In nonadiabatic PET, emphasis is placed on the effect of H_{el} on k_{el}. The magnitude of H_{el} is affected by factors, which influence the overlap of donor and acceptor orbitals, i.e., separation distance, orientation, shape and nodal character of overlapping orbitals. Orbital interaction may occur via 'through-space' or 'through-bond' pathways.[64] In rigid intramolecular systems, for example, it is generally assumed that electron may tunnel through the bonds of the molecular bridge separating the donor and the acceptor. Two tunneling pathways are possible in such cases (Figure 1.4). In the first, electron travels from the donor to acceptor through the LUMO's of the molecular bridge (path A in Figure 1.4).

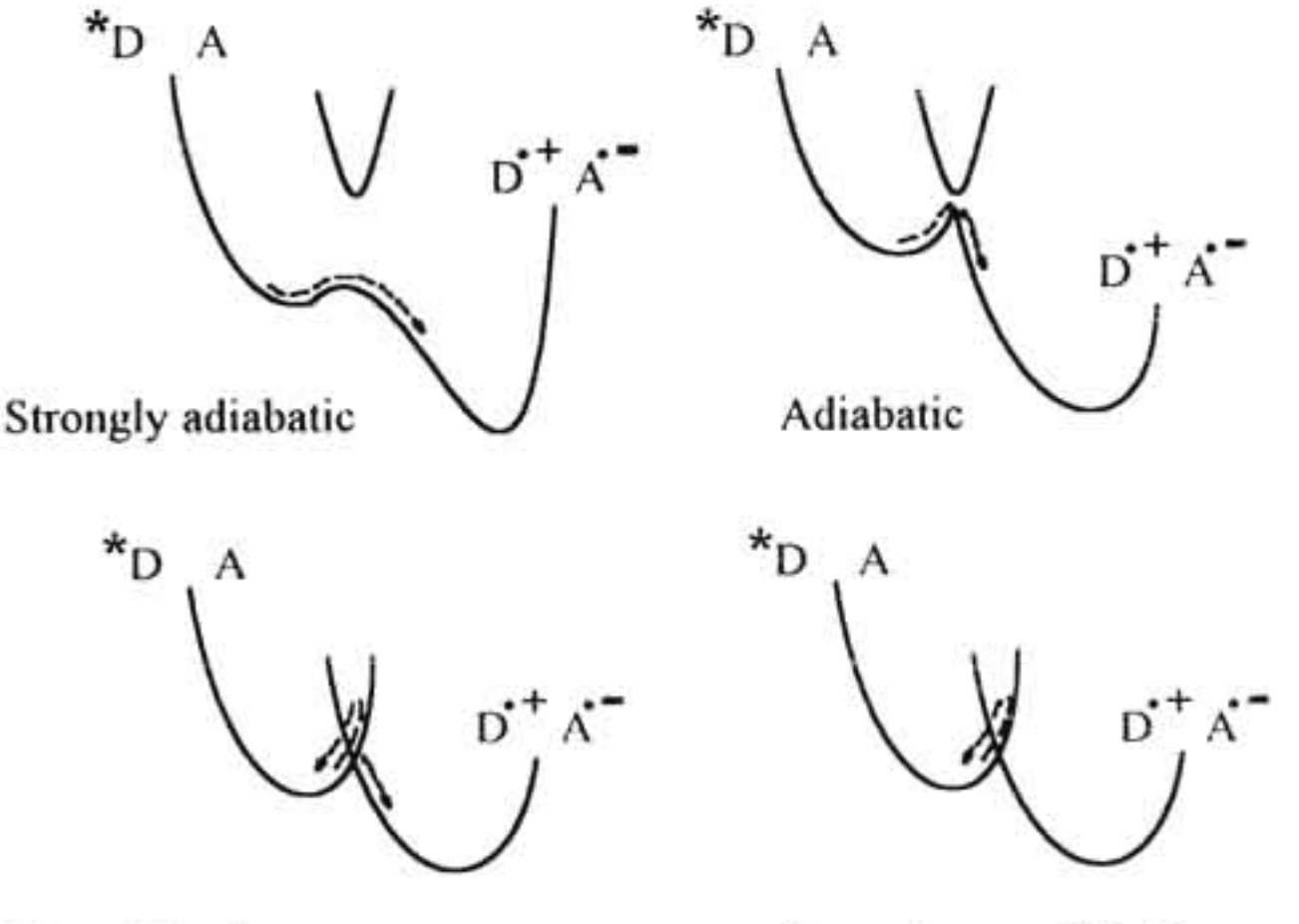

Figure 1.3 Potential Energy descriptions for adiabatic and nonadiabatic electron transfer. Classical theories of electron transfer are applicable to systems which fall somewhere between adiabatic and nonadiabatic, i.e., $0 < \kappa_{el} < 1$.

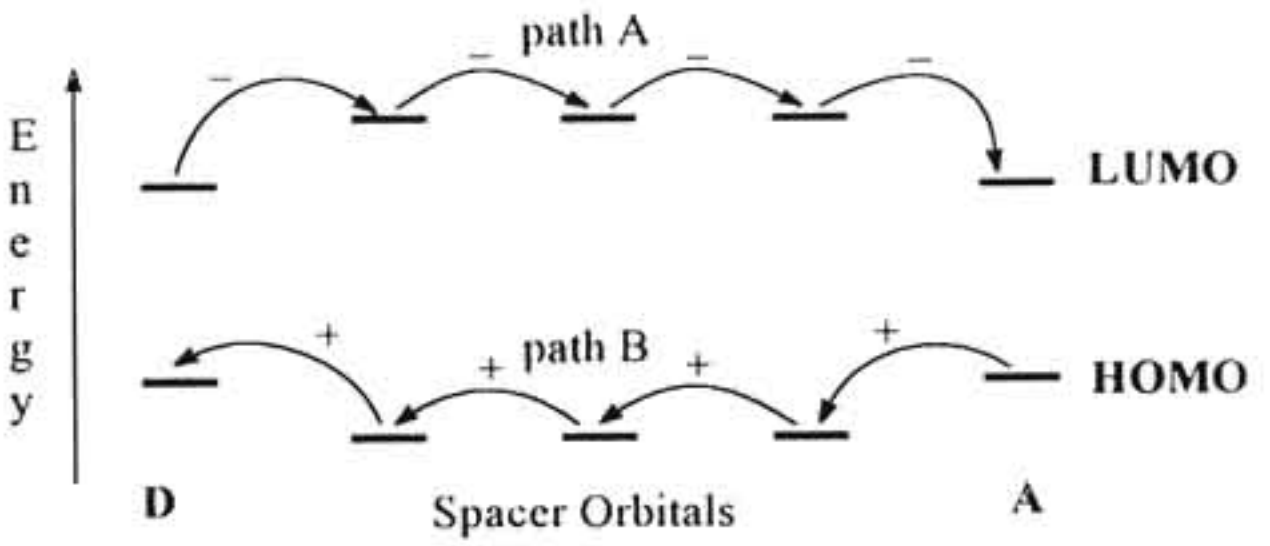

Figure 1.4 Scheme showing electron hopping from the donor orbital along the LUMO of the spacer molecule or by 'hole' hopping from the acceptor orbital along the HOMO of the spacer.

In the second, the electron transfer occurs via a 'hole' mechanism where a positive charge travels from the acceptor to the donor via the HOMO's of the molecular bridge (path B). In these cases, H_{el} decreases exponentially with the number of bonds through which the electron tunnels.[65,66] An example of such a case is provided by the porphyrin-spacer-quinone system **1** (Chart 1.1).[67]

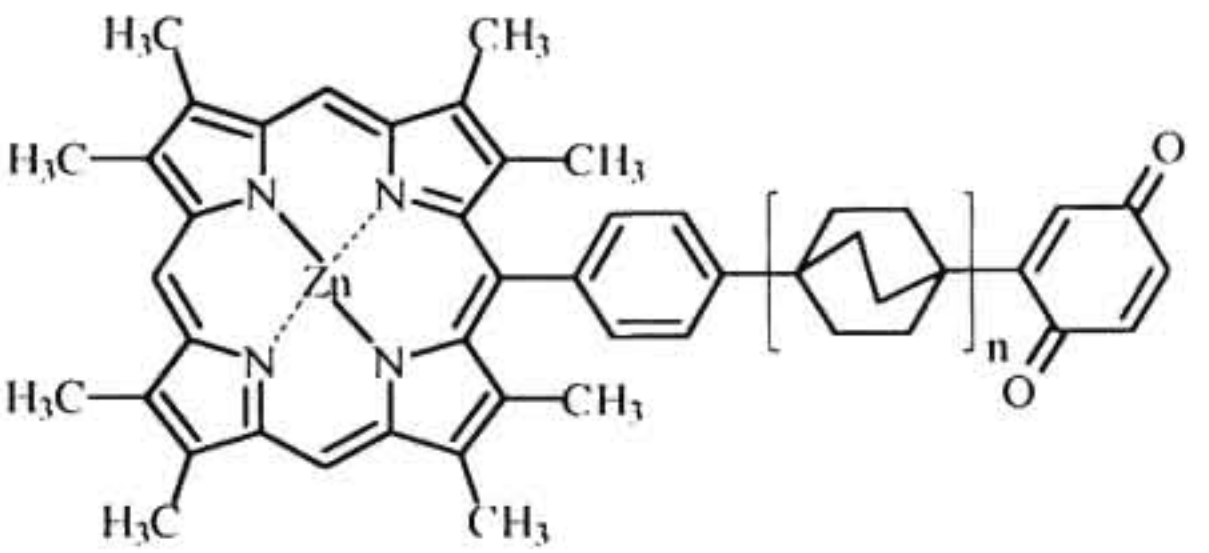

1

Chart 1.1

In **1** (n = 0, 1, 2), the spacer keeps the donor and acceptor well apart and prevents overlap of porphyrin and quinone orbitals. Electron transfer in this case must take place through the bonds of the spacer. An exponential dependence of rate on the separation distance is observed in the above system.

In another study, de Rege et al. varied the type of intervening bonds and studied its effect on the rate of electron transfer process.[68] The porphyrin based donor-acceptor systems **2**, **3** and **4** differ in the type of bridge connecting the donor and acceptor porphyrin moieties (Chart 1.2). The intervening bonds in these cases changed from hydrogen bonded noncovalent in **2** to saturated covalent in **3** to unsaturated covalent in **4**. In all cases, the donor and acceptor are separated by virtually constant distance, thus establishing uniform driving force and

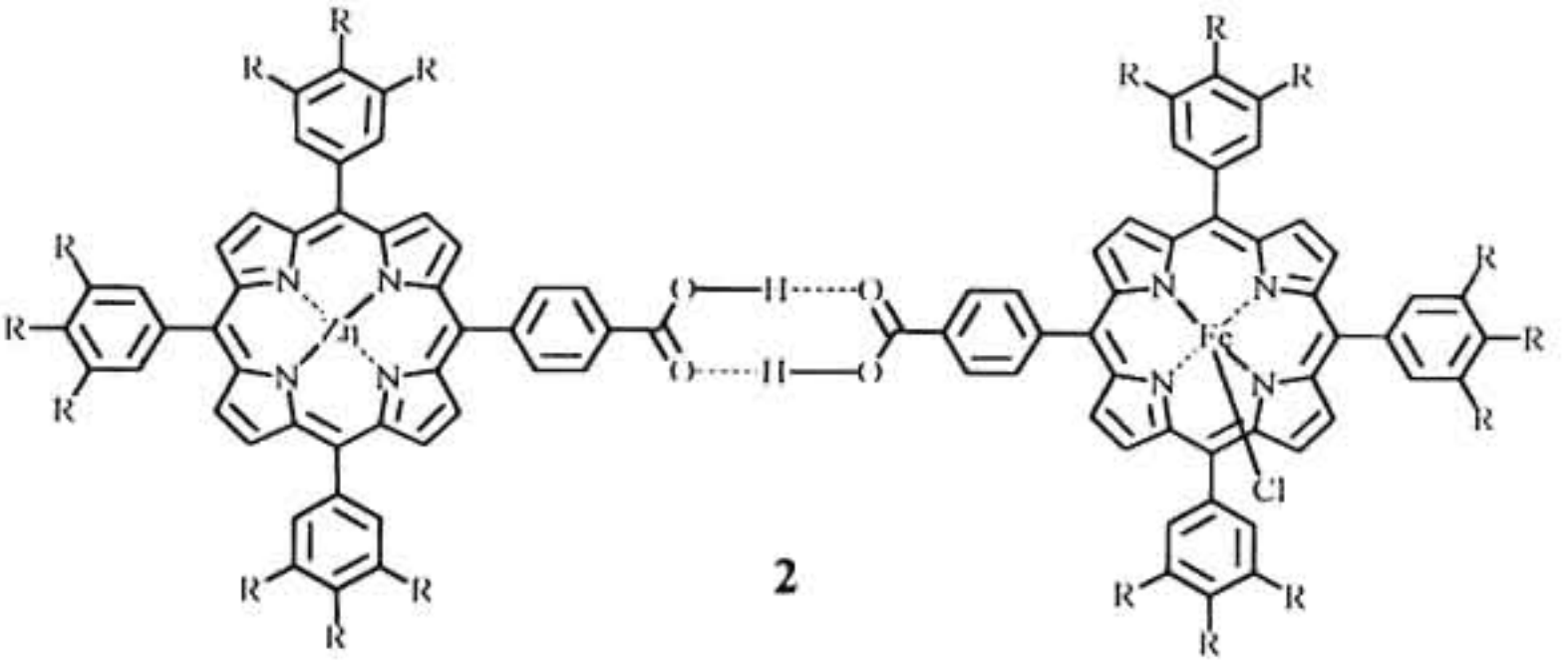

2

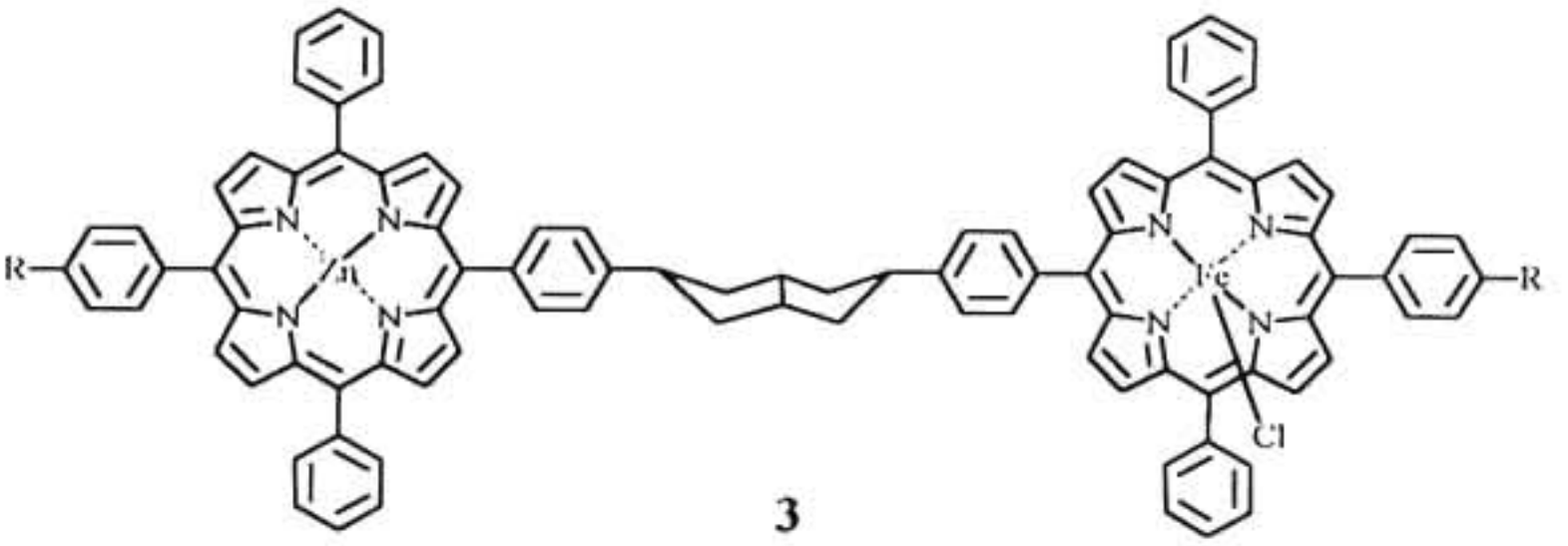

3

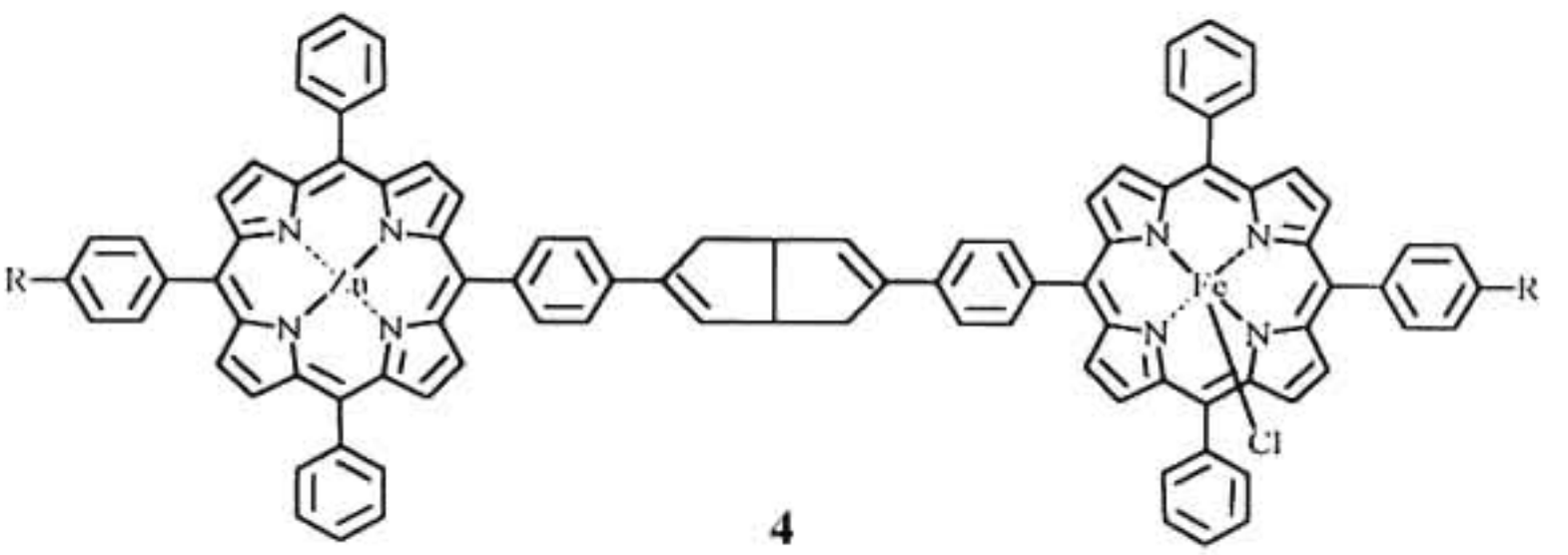

4

R=OMe

Chart 1.2

reorganization energy for electron transfer. The results of their studies showed that the electronic coupling modulated by a hydrogen bond interface is greater than that provided by an analogous interface composed entirely of carbon-carbon σ bonds.

Over the years, substantial amount of work has been carried out to evaluate the effect of various factors on the rate of PET reactions. These factors include free energy, solvent, temperature, donor-acceptor distance and donor-acceptor orientation.[2,3] No attempt will be made in this thesis to summarize the results of all these studies.

1.2. Circumventing back electron transfer

One of the primary objectives in the study of PET reactions is the efficient generation of long-lived radical ion pairs. In the natural photosynthetic reaction centre, the quantum yield of charge separation (Φ_{IP}) is ~95% and the minimum photon energy yield is 30%. The efficiency of charge separation in artificial donor-acceptor systems is considerably lower. Back electron transfer has been identified as the major factor that limits the efficiency of charge separation in artificial systems. Consequently, photochemists have long been preoccupied with the challenge of circumventing back electron transfer in order to generate long-lived ion pair intermediates.[9] Back electron transfer occurs because the products of PET reactions have energies of 1 to 4 eV above the ground states and therefore, BET to generate the starting materials will be highly exothermic. Thus, in order to reduce BET there must be some degree of kinetic forbiddenness to this thermodynamically favoured reverse transition. Several techniques have been

devised in the past few years to increase the yields and lifetimes of radical ion pairs in PET reactions. A brief description of the various factors is given here.

1.2.1. Electron spin

Electron spin is conserved in PET reactions. This means that the radical ions generated from a singlet excited state will have overall singlet multiplicity. Similarly, radical ion pairs generated from a triplet excited state will have triplet multiplicity. Triplet radical ion pairs have to undergo a spin rephasing to singlet radical pairs before undergoing BET. Therefore, BET reaction in triplet radical ion pairs leading to the regeneration of the singlet ground states is said to be spin forbidden. No such forbiddenness exists in the case of charge recombination involving singlet radical ion pairs.

Olmsted and Meyer measured the quantum yields of ion formation in the quenching of a variety of excited donors by methylviologen (MV^{2+}).[70] They found that triplet ion pairs predominantly undergo cage escape to produce free ions, whereas, singlet ion pairs undergo facile BET reaction to generate the starting materials. Working with carbonyl (triplet) and cyanoanthracene (singlet) excited states, Haselbach et al. also made similar observations.[71]

The predominant observation of ion pair products from triplet state as opposed to singlet excited state reactions in solution is due to two reasons: (a) the long lifetime of the triplet state which allows the excited molecule enough time to find the quenchers, and (b) the forbidden nature of BET in triplet radical pairs. It is the latter that results in a finite yield of products. During the few nanoseconds required for spin rephasing in triplet radical ion pairs, the radicals can diffuse apart by 10-30 Å. This leads to enhanced probability of cage escape.

1.2.2. Electron tunneling

The rate of electron tunneling in the forward and backward direction is dependent on the distance between the donor and acceptor moieties as well as the energy gap between the initial and final states.[72,73] If the reactants are too far apart, electron transfer cannot takes place, during the finite lifetime of the excited state. If the reactants are too close together, the reverse electron transfer to the ground state becomes as fast or faster than the forward transfer for the singlet state. Though distance is important, it is the degree of interaction or overlap of wave functions, which is the determining factor. Excitation from a π bonding molecular orbital to a π anti bonding molecular orbital leads to more electron density in the outer region of the molecule. Since the excited state has more electron density on the outside of the molecule, long distance tunneling of the electron is more favourable for the excited state in comparison to the radical ion products.[72,74] In such systems, the back electron transfer is delayed compared to the forward electron transfer. The magnitude of this depends on the ratio of tunneling parameter in both cases.

The energy gap between the ion pair and the ground state can also control the rate of electron return k_{bet} and in effect influence Φ_{IP}. As noted earlier, the rate of electron transfer increases with an increase in the driving force until k_{et} reaches a maximum value, after which the rate begins to decrease (the 'inverted region'). If ΔG_{et} for BET falls within the inverted region, the rate of this process will be low compared to rate of charge separation which ultimately lead to an increase in Φ_{IP}. Using ultra fast laser spectroscopy Mataga et al. obtained values of k_{bet} for several organic donor-acceptor systems.[52,75] His results clearly

demonstrated the above argument. Similar results were obtained by Paddon-Row et al. for PET in linked donor-acceptor systems.[76]

1.2.3. Reactant pair escape and geminate recombination

Electron transfer between neutral molecules in solution leads to the formation of an ion pair. The fractional yield of an ion pair formed at a centre-to-centre distance d_{cc} and recombining at an encounter distance d_e is given by equation (1.27),[77-79]

$$\Phi_{IP} = \frac{\exp(-d_c/d_{cc}) - \exp(-d_c/d_e)}{1 - \exp(-d_c/d_e)} \qquad (1.27)$$

where, d_e is the Coulomb radius and is equal to $e^2/\varepsilon kT$. For singly charged ions, d_e is 7.2 Å in water and 236 Å in toluene.[69] Note that, the diffusion constant and viscosity of the solvent does not appear in the equation. According to equation (1.27), increasing the center to center distance of the reactants, the dielectric constant of the solvent and the temperature of the medium can maximize the ion yield. One can also increase the yield by neutralizing the charge on the ion pairs. Protonation of the radical anion and/or deprotonation of the radical cation can do this and many such cases are known in the literature.[80-82]

1.2.4. Orbital symmetry and orientation

The overlap of π orbitals in intermolecular systems will be largest if the molecules are coplanar or cofacial and aligned along the symmetry axis. If the molecules are aligned along their principal orbital symmetry axis, only symmetric-symmetric or antisymmetric-antisymmetric orbitals will have non-zero overlap. These factors generally impose a method of delaying the reverse

electron transfer. For example, in several cofacial porphyrins, the rate of forward electron transfer is much higher than the rate of BET.[83,84] This is attributed to favourable symmetry factors. Similar behaviour is observed in photoelectron transfer reactions of covalently linked porphyrin-quinone molecules in which the orientation of quinone is varied systematically.[85-86]

Orientation of the donor and acceptor residues in linked donor-acceptor systems has a profound effect on the yield of the charge separated state. For example, the trichromophoric compound **5** can exist in two rigid noninterconverting diastereomeric *syn* and *anti* forms (Chart 1.3).[87-88] It was observed that the rate of BET in the *anti* isomer is two orders of magnitude slower compared to that in the *syn* isomer. This behaviour is probably a consequence of the fact that the *syn* diastereomer possesses a U-shaped geometry, with the terminal chromophores facing each other at a distance of about 15 Å.

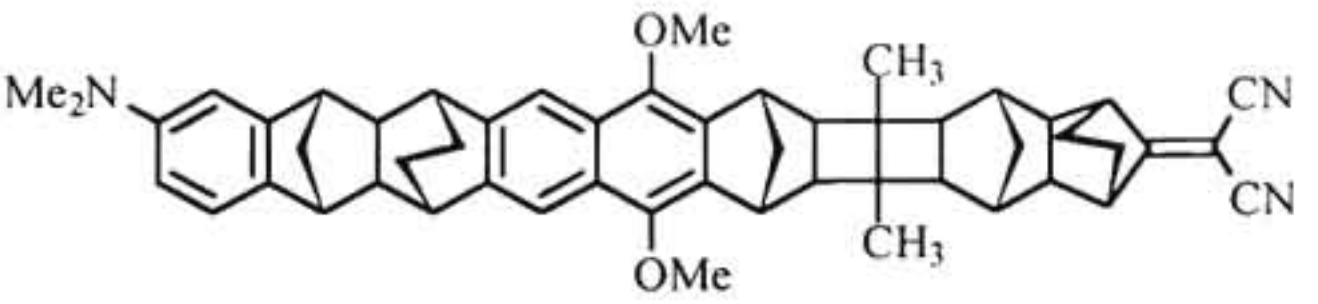

5

Chart 1.3

This orientation of the chromophores is conducive to a facile solvent-mediated BET process that is not available to the *anti* diastereomer. In another example of a giant U-shaped tetrad having porphyrin and methylviologen (MV^{2+}) chromophores,[89] wherein the terminal porphyrin and MV^{2+} units are only about

10 Å apart, photophysical measurements have shown that rapid electron transfer occurs between these units, and the resulting charge separated state is remarkably stable towards BET reaction.

1.2.5. Relays

A simple way to circumvent BET is to use relays in the electron transfer system.[12,13] Here the first photoelectron transfer step is followed by a series of thermal electron transfers which ultimately lead to a spatial separation of charges as shown in Scheme 1.1. If donors and acceptors with suitable redox potentials are selected, unidirectional electron transfer will occur in which the electrons move in one direction and the holes move in the opposite direction. In the final stage, the charges are spatially separated and hence rate of BET will be substantially reduced.[90-100] In porphyrin based systems, it was suggested that the electron and hole may be separated by > 20 Å in two steps.[69]

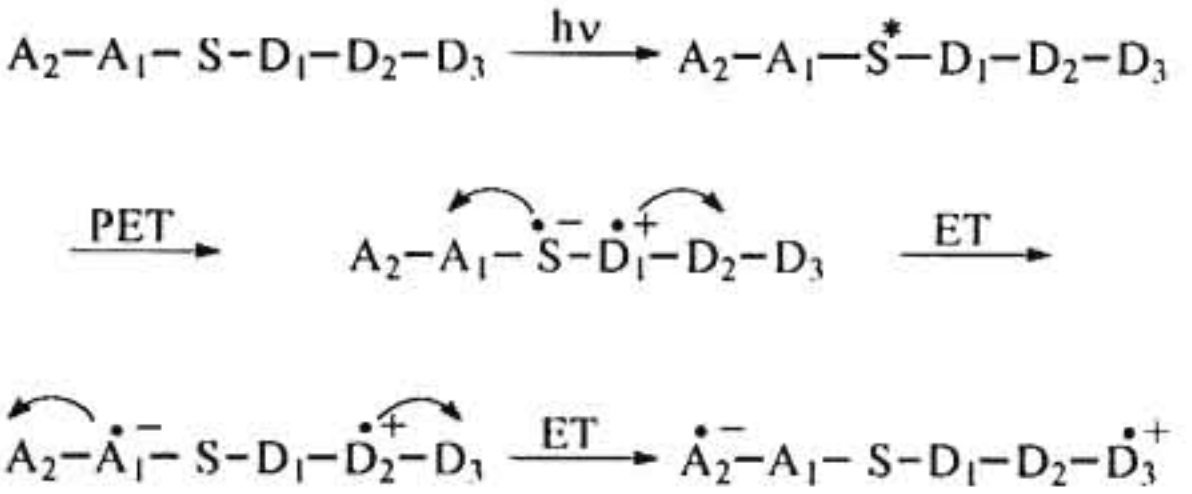

Scheme 1.1

This approach, however, has a major disadvantage. In order for electron transfers to take place as shown in Scheme 1.1, all ET steps should be exothermic. Thus, there is an energy loss associated with each step and this limits the conversion efficiency of light into chemical energy. Nevertheless, this

is the strategy adopted by nature in the photosynthetic reaction centre. Almost all artificial systems that mimic photosynthesis also incorporate this strategy. Two specific examples are discussed below.

Guest and coworkers have made molecular triads, tetrads and pentads which utilize sequential electron transfer steps to control BET.[92-98] The molecular tetrad, **6** consists of a polyene, a porphyrin and two quinones (Chart 1.4). The quinone with more negative redox potential was attached directly to the porphyrin, while, the quinone with less negative redox potential was at the terminus. This arrangement is designed to promote sequential electron transfer from the naphthoquinone to benzoquinone. The initial charge separated species is formed in 15 ps following excitation of the porphyrin. This state lies about 1.6 eV above the ground state. The final charge separated species, with positive charge on the carotenoid moiety and negative charge on the benzoquinone moiety, is formed with a quantum yield of 0.23 and lies about 1.1 eV above the ground state.

Another example is provided by carotene-zinc porphyrin-porphyrin-naphthoquinone-benzoquinone pentad **7** (Chart 1.4).[98] The strategy is once again to maximize the quantum yield of formation and lifetime of the ion pair. With this molecule they have achieved a lifetime of 55 μs and a quantum yield of 0.83. If the Zn atom is removed, the lifetime of the final ion pair increases to 340 μs, while the quantum yield drops to 0.15.

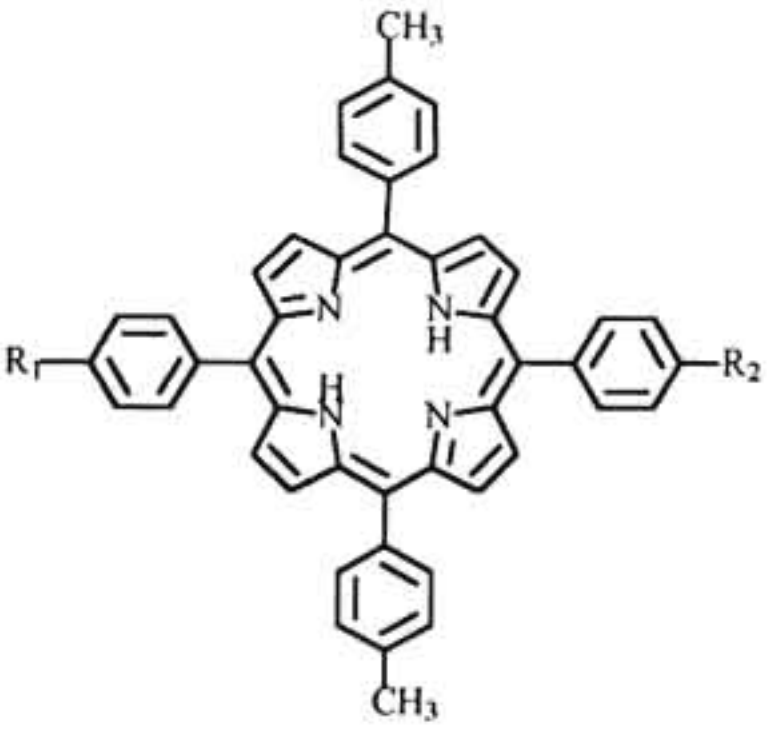
CH3
R1
R2
N
NH
H
N
N
CH3

6

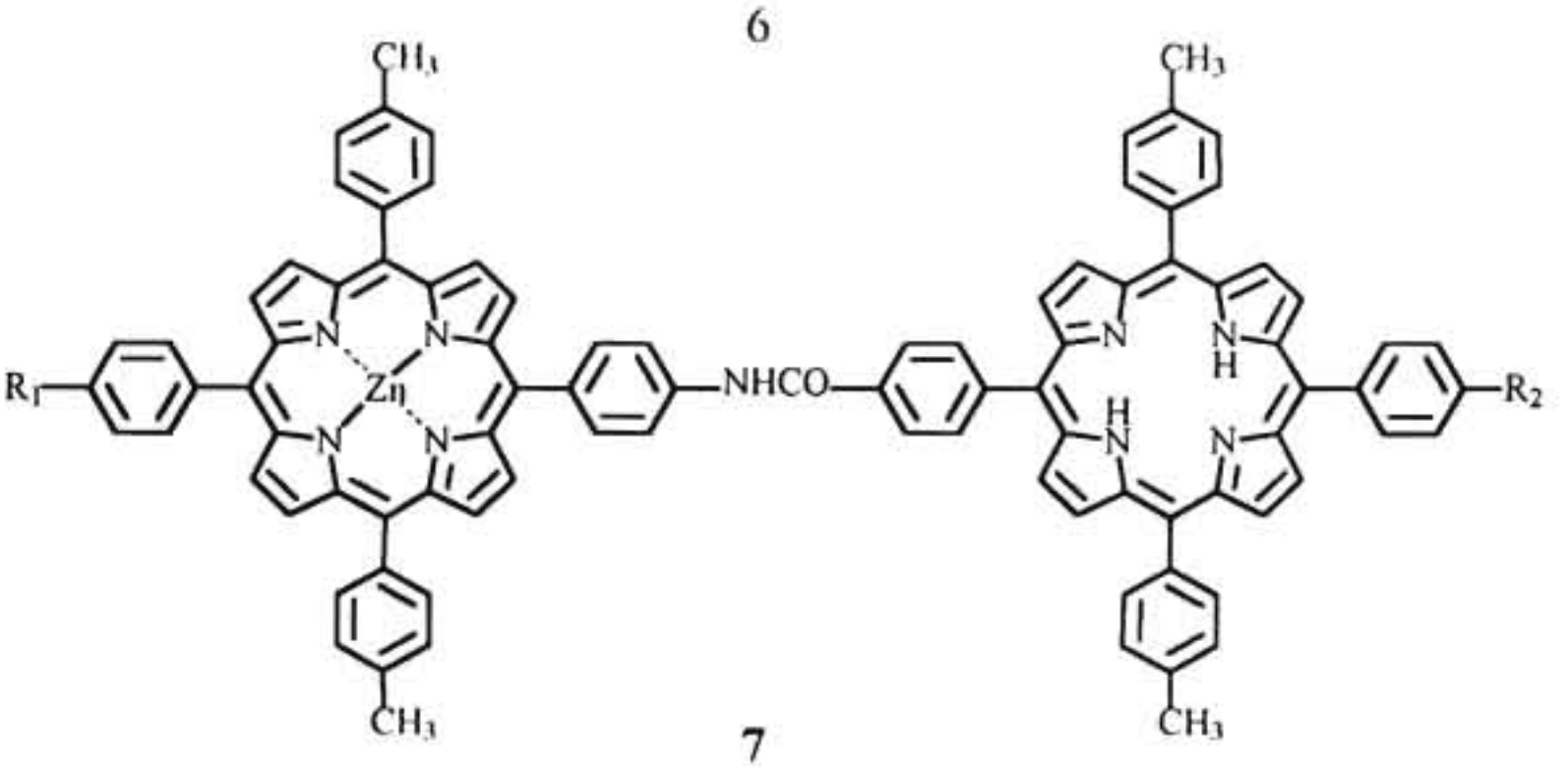
CH3
R1
Zn
N
N
N
N
NHCO
CH3
CH3
N
NH
H
N
N
R2
CH3

7

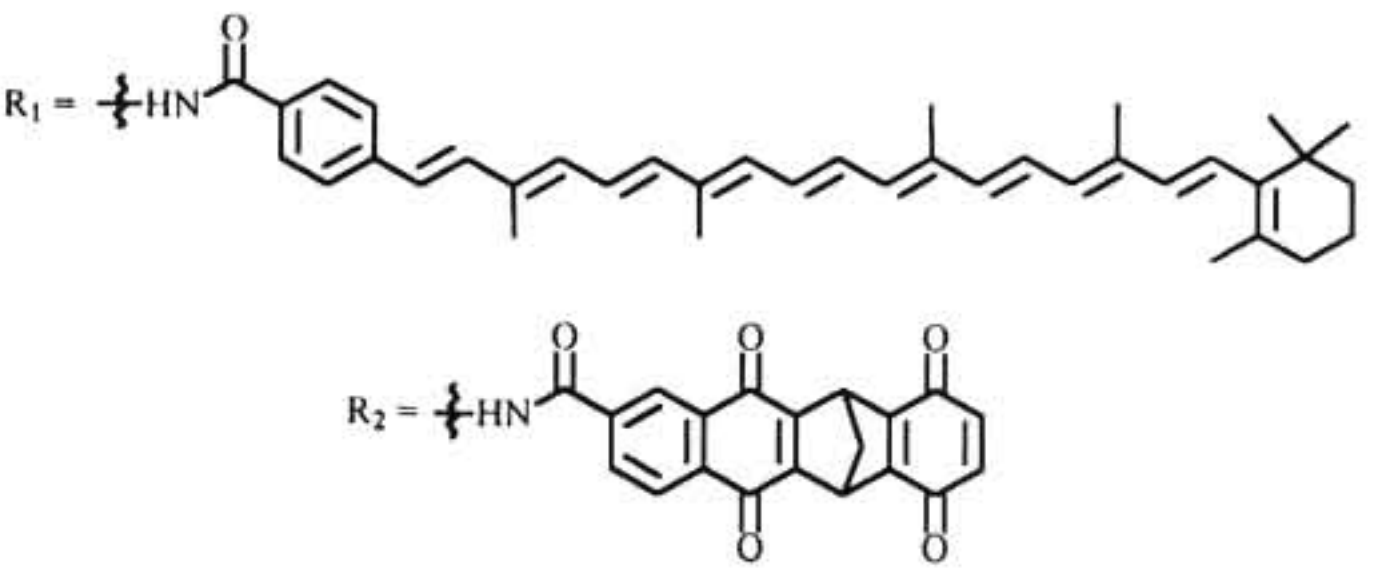
R1 =
HN
O
R2 =
HN
O
O
O
O
O

Chart 1.4

In intermolecular electron transfer reactions in solution, use of a co-sensitizer is found to increase the quantum yield of the reaction. Biphenyl is generally used as co-sensitizer in cyanoaromatics sensitized photoelectron transfer reactions. Gould et al. examined the PET reactions between cyanoaromatics and biphenyl and found that the rate of BET lies in the Marcus inverted region.[99-100] This allows the escape of the biphenyl radical cation into the bulk solution. The biphenyl radical cation can then act as a relay and oxidize other donors present in the system with high overall quantum yield.

1.2.6. Coulomb effects

When electron transfer occurs between neutral molecules, the products formed are oppositely charged radical ions. They are attracted towards each other thereby facilitating BET. But, if one of the reactants is ionic, the products will consist of a neutral radical and an ion, which are not electrostatically attracted. Rate of BET is generally reduced in such cases. [101]

1.2.7. Repulsive collisions

In cases where donor and acceptor carry similar charges, an electrostatic barrier is imposed on both the forward and back electron transfer processes. This can be advantageously utilized to increase the yield of products in PET reactions. Carapellucci and Mauzerall have determined the second order rate constants for the electron transfer between triplet zinc uroporphyrin and a variety of ionically charged acceptors by flash photolysis.[102] They observed that the yield of ions is a function of the charge on the acceptor and ionic strength of the medium. For opposite charges at low ionic strength, a ground state molecular complex is formed, and the yield of the free ions is zero because of very facile BET. Upon

raising the ionic strength to 0.1 M, the complex dissociates and the yield of the PET reaction rises to 80 %. For similarly charged ions the yield reaches to 100 %.

1.2.8. Inhibition of back electron transfer by fragmentation

A different way of inhibiting the reverse electron transfer is through a fragmentation reaction occurring in one of the components after electron transfer.[103-104] This removes the reactive site by one or more atoms and reduces BET. For example, tertiary amines are known to be good donors in PET reactions. The resulting amine radical cation can undergo facile bond cleavage reactions. An example is given in Scheme 1.2.

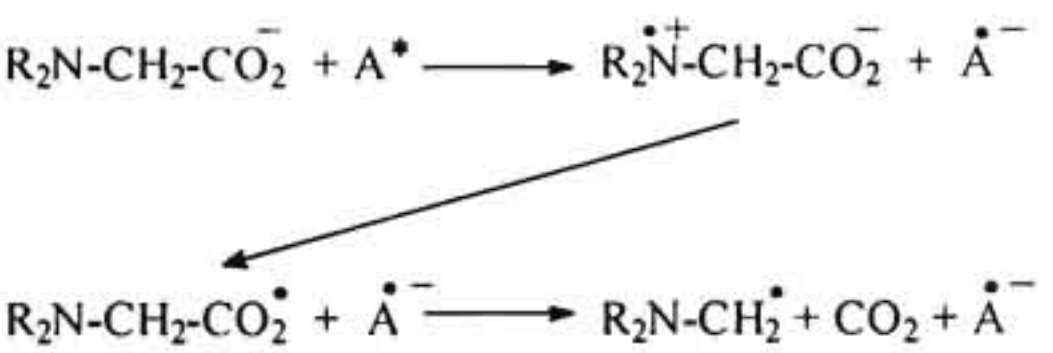

Scheme 1.2

1.2.9. Use of interfaces

A simple way to slow down the reverse electron transfer is to enforce a separation of the donor and the acceptor immediately following PET. Some success has been achieved in this direction by the use of various interfaces, which partition the donors and acceptors. Interfaces employed for this purpose include anionic and cationic micelles, liquid-liquid interfaces, vesicles, micro-emulsions, liposomes, polyelectrolytes, cyclodextrins etc.[104-145]

Electron transfer across liquid-liquid interfaces involves the use of partitioning of components in a mixture of two solvents. Geblewics and

Schiffrin[106] measured the rate of electron transfer across liquid-liquid interfaces, and Marcus developed a theory for the electron transfer rates in such systems.[107-109] Recently, Das and coworkers reported the use of a liquid-liquid interface for PET mediated decarboxylation reactions (Scheme 1.3).[110-111]

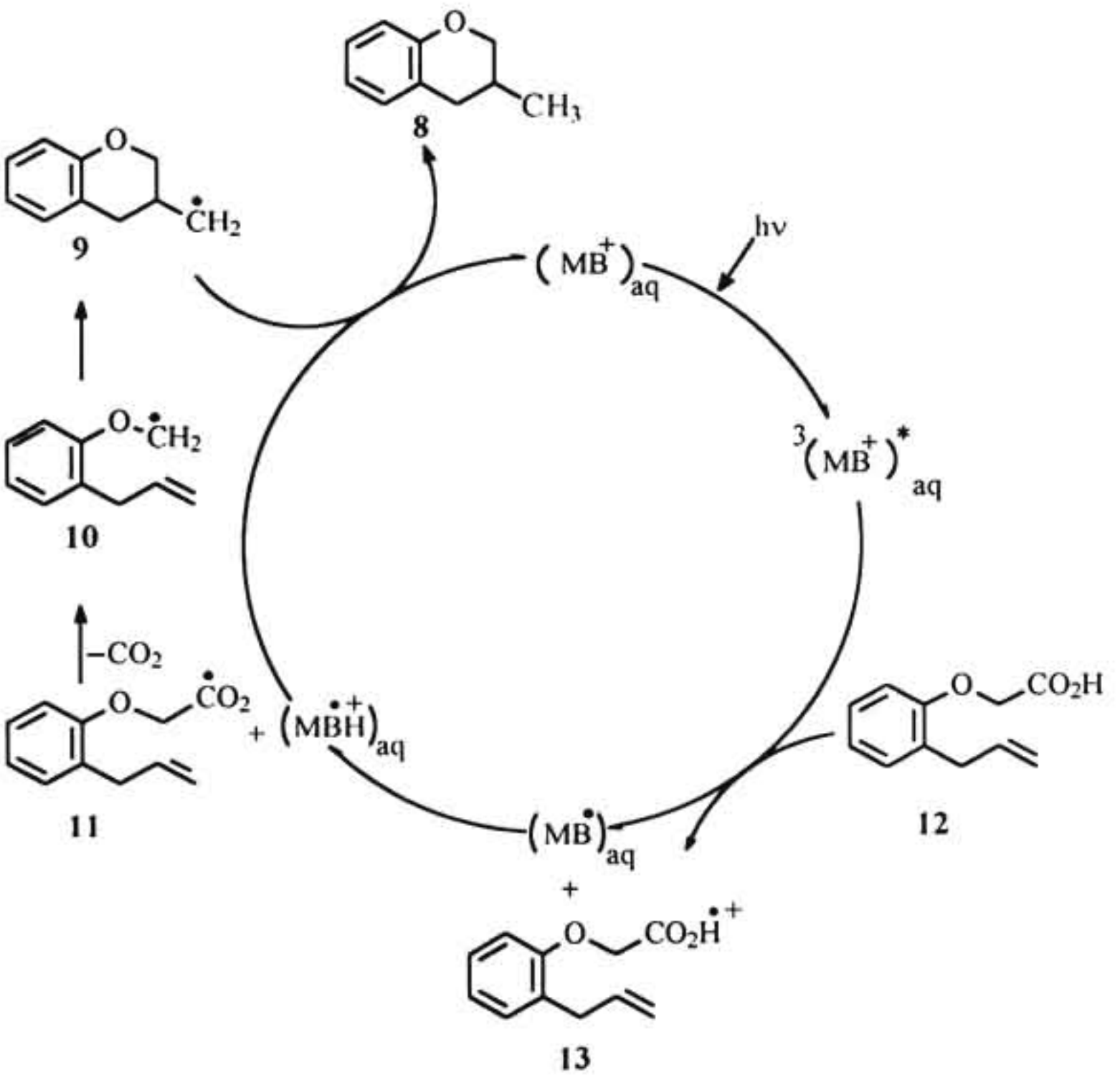

Scheme 1.3

In their study electron transfer takes place across the liquid-liquid interface between triplet excited methylene blue in water and a carboxylic acid in benzene, which will be followed by a proton exchange in order to maintain the charge

balance. The radical cation of the carboxylic acid will undergo rapid decarboxylation to generate the corresponding alkyl radicals (**10**). Further reactions of the radical leads to the observed product (**8**) as shown in Scheme 1.3. The yield of decarboxylation varied inversely with the percentage distribution of the acid in water. These results show that it is the partitioning of the acid and the sensitizer across two liquids that reduces the BET process and leads to enhanced yield of the reaction.

Several micellar systems have been used as media for electron transfer reactions, with a view to circumvent BET.[112-130] Ionic micellar aggregates are characterized by an inner hydrophobic core and a charged outer layer, both of which can play an important role in influencing the reaction course and yields. Consider, for example, the case of donor and acceptor molecules distributed in an anionic micellar system. PET leads to the formation of donor cation radical and acceptor anion radical within the micelle. Electrostatic repulsion will lead to the ejection of the radical anion from the micelle and electrostatic attraction will lead to the stabilization of the radical cation within the micelle. These effects will generally lead to enhanced lifetime and yield of radical ion pairs. In one of the early examples of the use of micelles in PET reactions, Moroi and Grätzel reported the formation of long-lived N-methylphenothiazine radical cation ($NMPT^{+\bullet}$).[130] The $NMPT^{+\bullet}$ generated inside the micelle was found to be stable for several hours. Studies similar to this have been reported in several vesicles and liposomes.[131-139]

Effect of polyelectrolytes in controlling BET has been examined in several systems.[140-141] For example, in the electron transfer quenching of excited

$Ru(bpy)_2(CN)_2$ by $Fe(CN)_6^{3-}$, the cage escape yield (Φ_{IP}) increased from < 0.1 in aqueous solution to 0.93 in the presence of a polyelectrolyte.[142]

Cyclodextrins (CD) have been used to control BET reactions.[143,144] Cyclodextrins are cyclic polysugars composed of glucose units linked by α–glycoside bonds. They are cylindrical in shape with an internal hydrophobic cavity and a hydrophilic exterior. Hydrophobic substrates of proper size and shape can be encapsulated within the cyclodextrin cavity.[145] Molecules encapsulated in cyclodextrin cavities can participate in electron transfer reactions. An example is provided by the electron transfer quenching of the triplet excited state of Zn(II)-meso-tetra(*N*-propylsulfonato)pyrydinium porphyrin, (Zn-TPSPyP, **14**) by anthraquinone-2-sulphonate (**15**) (Chart 1.5).[143]

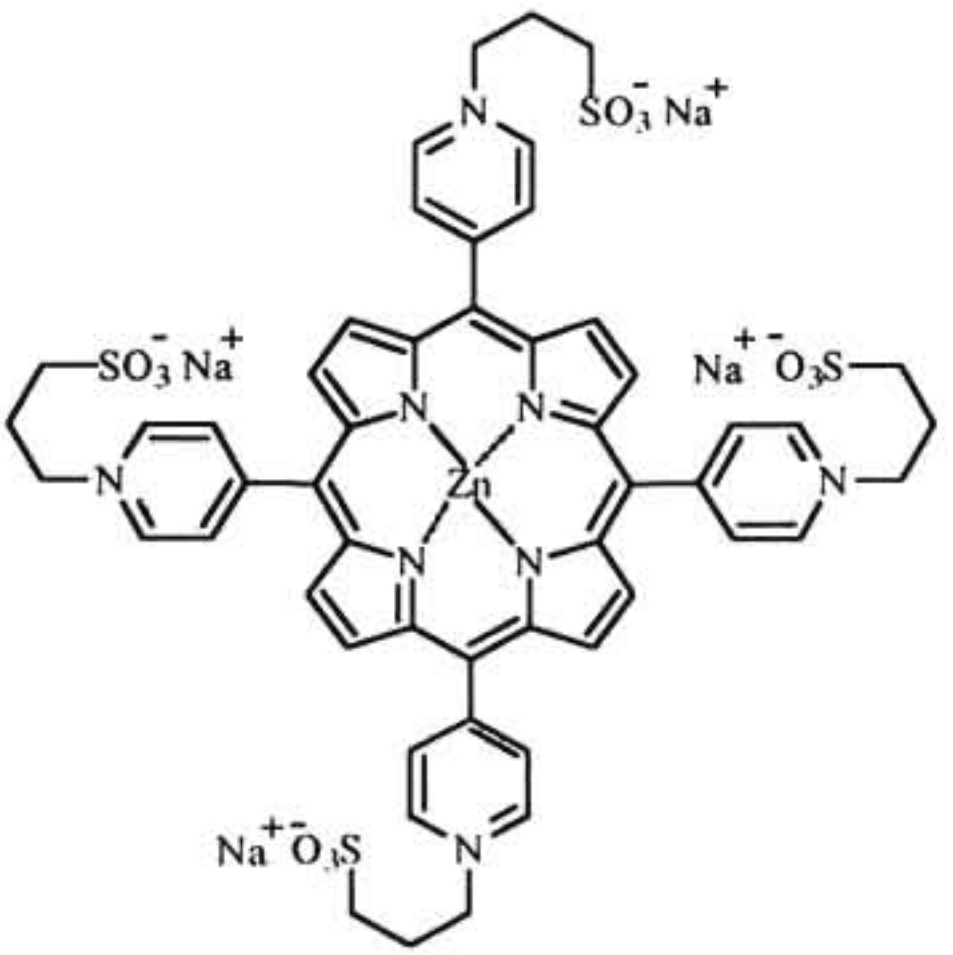

14

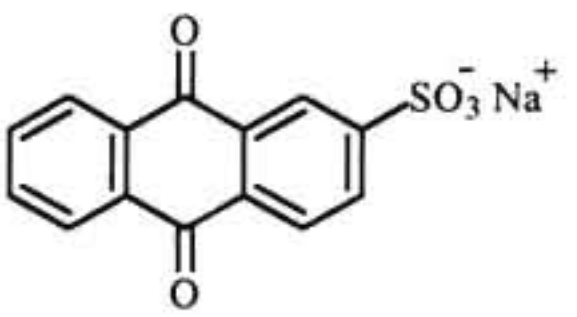

15

Chart 1.5

Porphyrin **14** forms a ground state complex with **15**. Irradiation of **14** in the presence of **15** in aqueous solution did not lead to any observable product. This is attributed to a very facile BET taking place within the complex. Irradiation in the presence of β-CD, however, led to the accumulation of anthraquinone radical anion. β-CD plays a dual role here. It encapsulates the anthraquinone and prevents the formation of the ground state complex. The radical anion formed within the cavity of β-CD is protected from undergoing BET reactions.

1.3. Design and study of new sensitizers to control back electron transfer

In the light of the above discussion on BET, it was interesting to see if structural modification of a given class of potential sensitizers will lead to any noticeable improvement in the control of BET reactions. This aspect forms the subject matter of the present thesis. Our strategy involved (1) selection of a suitable chromophore, (2) modification of its structure in several different ways and (3) evaluation of the effect of these structural changes on the photophysical and electron transfer properties. We have selected pyrylium cation as the prototype molecule because of the following reasons.

Several reviews and reports are available in the literature which discuss various aspects of the chemistry and applications of pyrylium salts.[146-150] These molecules, being cationic, are inherently electron deficient in nature and their electrode potentials are suitably positioned to carry out oxidation reactions of a large number of organic molecules. Generally, pyrylium compounds are stable thermally and photochemically. Their absorption properties can be modified to suit any specific needs. For example, the long wavelength absorption band of pyrylium compounds depends on the type of substituents on the heterocycle and may range from 350-1100 nm (Chart 1.6).[151]

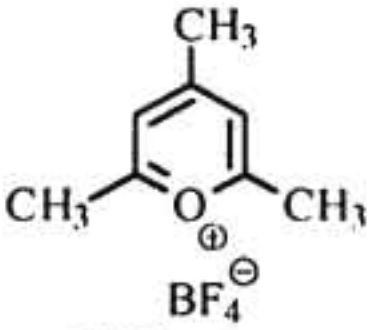

$\lambda_{max}^{CH_2Cl_2}$ = 280 nm

16

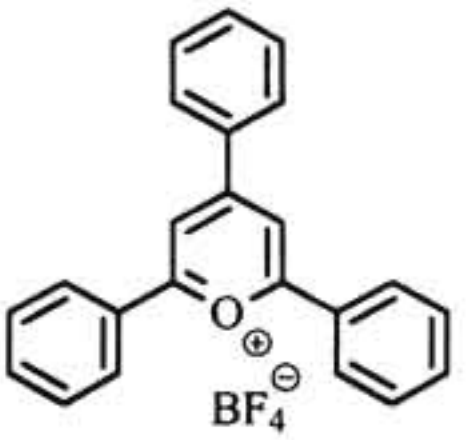

$\lambda_{max}^{CH_2Cl_2}$ = 417 nm

17

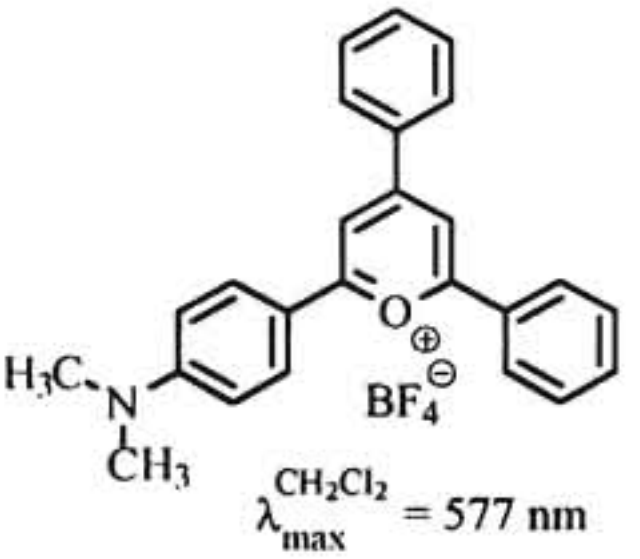

$\lambda_{max}^{CH_2Cl_2}$ = 577 nm

18

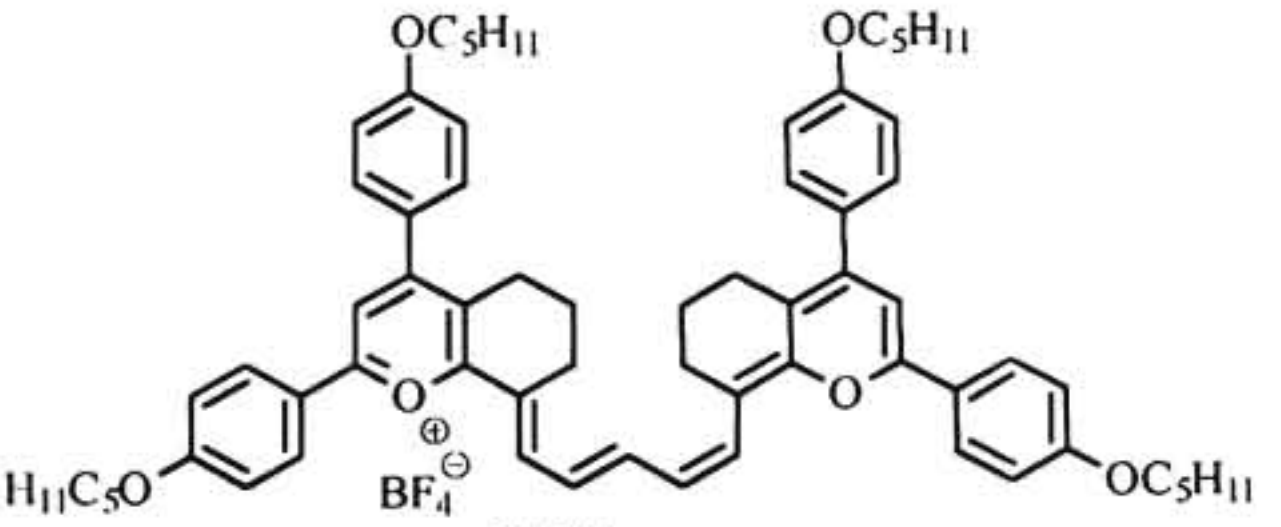

$\lambda_{max}^{CH_3CN}$ = 1062 nm

19

Chart 1.6

These are allowed transitions with very high extinction coefficients. The excited state lifetimes also depend on the substitution and can vary from a few picoseconds to several nanoseconds.[151] In addition, replacement of the ring oxygen atom of the pyrylium moiety by sulfur, selenium or tellurium would lead to other classes of sensitizers with similar or more desirable properties.[150] Potential applications of pyrylium compounds include their use as laser dyes,[152-160] as Q-switches in lasers,[161,162] as initiators in photopolymerization reactions[163,164] and also as sensitizers in electrophotography.[165,166] Their use as liquid crystal forming materials[167-170] and as phototherapeutic[150] agents has also been explored.

A member of this heterocyclic group, namely 2,4,6-triphenylpyrylium (TPP, **17**), as the perchlorate or tetrafluoroborate salt, has been used as sensitizer in several PET reactions. These include, cycloadditions,[171] isomerizations,[172] sigmatropic rearrangements,[173] fragmentation reactions[174] and photo-oxygenation reactions.[175] There are several advantages of using TPP as a sensitizer. It has good absorption in the visible region and this makes selective excitation possible. It is soluble in many organic solvents and also in water and can act as an electron acceptor in both singlet as well as triplet excited states.

A major reason for selecting the pyrylium chromophore is the favourable Coulombic factors that operate when electron transfer occurs in these molecules. PET among neutral molecules lead to the formation of ion pairs which attract each other, thereby leading to enhanced rates of BET. In the case of pyrylium salts, the molecule in the ground state is charged and hence only charge exchange takes place, leading to the formation of the donor radical cation and a pyranyl radical as shown in equation (1.28).

$$^{*}PY^{+} + D \xrightarrow{ET} PY^{\bullet} + D^{\bullet+} \qquad (1.28)$$

Because of the absence of Coulombic factors in the PET reactions of pyrylium derivatives, formation of radical products will be enhanced and deactivation through BET will be reduced in comparison with neutral sensitizers.[149]

Even though a number of reports are available on the electron transfer properties of 2,4,6-triphenylpyrylium tetrafluoroborate, no detailed information is available on the electron transfer properties of other members of this group. Bearing this in mind, we have prepared some new pyrylium salts and studied their photophysical and electron transfer properties. Our aim has been to understand the factors that control the yield as well as the lifetimes of the product radical ions. Chapter 2 of the present thesis deals with the synthesis and study of a series of 4-(*p*-alkylphenyl)-substituted pyrylium and thiopyrylium derivatives. In Chapter 3, the effect of electronic, steric and Coulombic factors on the rate of back electron transfer is examined. Chapter 4 of the thesis deals with the photophysical and electron transfer studies of selected pyrylium salts encapsulated in cyclodextrin cavities. All these studies are aimed at the identification of the structural elements or environments that can contribute effectively to control BET reactions in these cationic sensitizers. An understanding of these factors may help in the design of electron transfer sensitizers that can be used for practical applications.

1. 4. References

1. Kavarnos, G. J. *Fundamentals of Photoinduced Electron Transfer*, VCH, New York, **1993**.
2. Fox, M. A.; Chanon, M. (Eds.), *Photoinduced Electron Transfer. Patrs A – D*, Elsevier, Amsterdam, **1988**.
3. Mattay, J. (Ed.), *Photoinduced Electron Transfer. Parts I – IV*, Springer Verlag, Heidelberg, **1990**.
4. Grätzel, M. (Ed.), *Heterogenous Photoinduced Electron Transfer*, CRC Publishers, Boca Raton, FL, **1988**.
5. Norris, J. R. Jr.; Meisel, D. *Photochemical Energy Conversion*, Elsevier, New York, **1989**.
6. Pelizetti, E.; Serpone, N. (Eds.), *Homogeneous and Heterogeneous Photocatalysis*, D. Reidel Publishing Company, Dordrecht, Holland, **1985**.
7. Pelizzetti, E.; Schiavello, M. (Eds.), *Photochemical Conversion and Storage of Solar Energy*, Kluwer Academic Publishers, Dordrecht, Holland, **1991**.
8. Bolton, J. R.; Mataga, N.; Mc Lendon, G. (Eds.), *Electron Transfer in Inorganic, Organic and Biological Systems*, American Chemical Society, Washington, D. C., **1990**.
9. Mariano, P. A. (Ed.), *Advances in Electron Chemistry. Vol 1-3*, JAI Press, Greenwhich, CT, **1991**.
10. Julliard, M.; Chanon, M. *Chem. Rev.* **1983**, *83*, 425.
11. Mattes, S. L; Farid, S. in *Organic Photochemistry. Vol. 6*, Padwa, A., (Ed.), Dekker, New York, **1983**. p. 233.

12. Balzani, V.; Juris, A.; Scandola, F. in *Homogeneous and Heterogeneous Photocatalysis*, Pelizzetti, E.; Serpone, N. (Eds.), D. Reidel Publishing Company, Dordercht, Holland, **1985**, p. 1.

13. Scandola, F.; Bignozzi, C. A.; Balzani, V. in *Homogeneous and Heterogeneous Photocatalysis*, Pelizzetti, E.; Serpone, N. (Eds.), D. Reidel Publishing Company, Dordercht, Holland, **1985**, p. 29.

14. Fox, M. A. in *Advances in Photochemistry. Vol. 13*, Volman, D. H.; Gollnick, K.; Hammond, G. S. (Eds.), John Wiley and Sons, New York, **1986**, p. 237.

15. Kavarnos, G.; Turro, N. J. *Chem. Rev.* **1986**, *86*, 401.

16. Scandola, F. in *Photocatalysis and Environment: Trends and Applications*, Schiavello, A. (Ed.), Kluwer Academic Publishers, Dordrecht, Holland, **1987**, p. 1.

17. Meyer, T. J. *Acc. Chem. Res.* **1989**, *22*, 163.

18. Rabinowich, E. *Photosynthesis and Related processes*, Interscience, New York, **1945**.

19. Rehm, D.; Weller, A. *Isr. J. Chem.*, **1970**, *8*, 259.

20. Rehm, D.; Weller, A. *Ber. Bunsenges Phys. Chem.* **1969**, *73*, 834.

21. Marcus, R. A. *Int. J. Chem. Kinet.* **1981**, *13*, 865.

22. Sutin, N. *Acc. Chem. Res.* **1982**, *15*, 275.

23. McCammon, J. A.; Northrup, S. H.; Allison, S. A. *J. Phys. Chem.* **1986**, *90*, 390.

24. Keizer, J. *Chem. Rev.* **1987**, *87*, 167.

25. Marcus, R. A. *J. Chem. Phys.* **1956**, *24*, 966.

26. Marcus, R. A. *J. Chem. Phys.* **1956**, *24*, 979.

27. Marcus, R. A. *Faraday Discuss. Chem. Soc.* **1960**, *29*, 21.

28. Marcus, R. A. *Annu. Rev. Phys. Chem.* **1964**. *15*, 155.

29. Marcus, R. A. *J. Chem. Phys.* **1965**. *43*. 679.

30. Marcus, R. A.; Siders, P. *J. Phys. Chem.* **1982**, *86*, 622.

31. Marcus, R. A.; Sutin, N. *Biochim. Biophys. Acta*, **1985**, *811*, 265.

32. Brunschwig, B.; Sutin, N. *J. Am. Chem. Soc.* **1978**, *100*, 7568.

33. Sutin, N. *J. Photochem.* **1979**, *10*, 83.

34. Newton, M. D.; Sutin, N. *Annu. Rev. Phys. Chem.* **1984**, *35*, 437.

35. Hush, N. S. *J. Chem. Phys.* **1958**. *28*. 962.

36. Suppan, P. in *Topics in Current Chemistry. Vol. 163, Photoinduced Electron Transfer. Part IV*, Mattay, J. (Ed.), Springer Verlag, Berlin, **1992**, p. 94.

37. Beitz, J. V.; Miller, J. R. *J. Chem. Phys.* **1979**, *71*, 4579.

38. Miller, J. R.; Beitz, J. V.; Huddleston, R. K. *J. Am. Chem. Soc.* **1984**, *106*, 5057.

39. Miller, J. R.; Calcaterra, L. T.; Closs, G. L. *J. Am. Chem. Soc.* **1984**, *106*, 3047.

40. Closs, G. L.; Miller, J. R. *Science* **1988**, *240*, 440.

41. Wasielewski, M. R.; Niemczyk, M. P.; Svec, W. A.; Pewitt, E. B. *J. Am. Chem. Soc.* **1985**, *107*, 1080.

42. Wasielewski, M. R.; Johnson, D. G.; Svec, W. A. in *Supramolecular Photochemistry*, Balzani, V. (Ed.), D. Riedel Publishing Company, Amsterdam, **1987**, p. 255.

43. Irvine, M. P.; Harrison, R. J.; Beddard, G. S.; Leighton, P.; Sanders, J. K. M. *Chem. Phys.* **1986**, *104*, 315.

44. Harrison, R. J.; Pearce, B.; Beddard, G. S.; Cowan, J. A.; Sanders, J. K. M. *Chem. Phys.* **1987**, *116*, 429.

45. Cowan, J. A.; Sanders, J. K. M.; Beddard, G. S.; Harrison, R. J. *J. Chem. Soc. Chem. Commun.* **1987**, 55.

46. Ohno, T.; Yoshimura, A.; Mataga, N. *J. Phys. Chem.* **1986**, *90*, 3295.

47. Gould, I. R.; Ege, D.; Mattes, S. L.; Farid, S. *J. Am. Chem. Soc.* **1987**, *109*, 3794.

48. Gould, I. R.; Farid, S. *J. Am. Chem. Soc.* **1988**, *110*, 1991.

49. Gould, I. R.; Farid, S. *J. Am. Chem. Soc.* **1988**, *110*, 7242.

50. Gould, I. R.; Farid, S. *J. Am. Chem. Soc.* **1988**, *110*, 7883.

51. Gould, I. R.; Farid, S. *J. Am. Chem. Soc.* **1990**, *112*, 4290.

52. Mataga, N.; Ashai, T.; Kanda, Y.; Okada, T.; Kakitani, T. *Chem. Phys.* **1988**, *127*, 249.

53. Ashai, T.; Mataga, N. *J. Phys. Chem.* **1989**, *93*, 6575.

54. Ashai, T.; Mataga, N.; Takahashi, Y. Miyashi, T. *Chem. Phys. Lett.* **1990**, *171*, 309.

55. Segawa, H.; Takehara, C.; Honda, K.; Schimidzu, T.; Ashai, T.; Mataga, N. *J. Phys. Chem.* **1992**, *96*, 503.

56. Zou, C.; Miers, J. B.; Ballew, R. W.; Dlott, D. D.; Schuster, G. B. *J. Am. Chem. Soc.* **1991**. *113*, 7823.

57. Jayanthy, S. S.; Ramamurthy, P. *J. Phys. Chem.* **1997**, *101*, 2016.

58. Turro, C.; Zaleski, J. M.; Karabatsos, Y. M.; Nocera, D. G. *J. Am. Chem. Soc.* **1996**, *118*, 6060.

59. Thanasekaran, P.; Rajendran, T.; Rajagopal, S.; Srinivasan, C.; Ramaraj, R.; Ramamurthy, P.; Venkatachalapathy, B. *J. Phys. Chem.* **1997**, *101*, 8195.

60. Engleman, R.; Jortner, J. *J. Mol. Phys.* **1970**, *18*, 145.

61. Freed, K. F. *Acc. Chem. Res.* **1975**, *11*, 74.

62. Freed, K. F.; Jortner, J. *J. Chem. Phys.* **1970**, *52*, 6272.

63. Liang, N.; Closs, G.; Miller, J. *J. Am. Chem. Soc.* **1990**, *112*, 5353.

64. Siders, P.; Cave, R. J.; Marcus, R. A. *J. Chem. Phys.* **1984**, *81*, 5613.

65. Wasielewski, M. R.; Niemczyk, M. P. in *Porphyrins –Excited States and Dynamics*, Gouterman, M.; Rentzepis, P. M.; Straub, K. D. (Eds.), American Chemical Society, Washington, D. C., **1986**, p. 154.

66. Wasielewski, M. R. in *Photoinduced electron transfer. Part A*, Fox, M. A.; Chanon, M. (Eds.), Elsevier, Amsterdam, **1988**, p. 161 and references cited therein.

67. Joran, A. D.; Leland, B. A.; Geller, G. G.; Hopfield, J. J.; Dervan, P. B. *J. Am. Chem. Soc.* **1984**, *106*, 6090.

68. De Rege, P. J. F.; Williams, S. A.; Therien, M. J. *Science* **1995**, *269*, 1409.

69. Mauzerall, D. in *Photoinduced Electron Transfer. Part A*, Fox, M. A.; Channon, M. (Eds.), Elsevier, Amsterdam, **1988** p. 228.

70. Olmsted III, J.; Meyer, T. J. *J. Phys. Chem.* **1987**, *97*, 1649.

71. Haselbach, E.; Vauthey, E.; Suppan, P. *Tetrahedron*, **1988**, *44*, 7335.

72. Mauzerall, D. *Brookhaven Symp. in Biol.* **1976**, *28*, 64.

73. Mauzerall, D. in *The Porphyrin. Vol. 5*, Dolphin, D. (Ed.), Academic Press, New York, **1978**, p. 29.

74. Dexter, D. L. *Phys. Rev.* **1954**, *93*, 985.

75. Mataga, N.; Kanka, Y; Asahi, T; Miyasaka, H.; Okada, T.; Kakitani, T. *Chem. Phys.* **1988**, *127*, 239.

76. Paddon – Row, M. N.; Oliver, A. M.; Warman, J. M.; Smit, K. J.; de Hass, M.; Overing, H.; Veroheven, J. W. *J. Phys. Chem.* **1988**, *92*, 9658.

77. Mauzerall, D.; Ballard, S. G. *Ann. Rev. Phys. Chem.* **1982**, *33*, 377.

78. Schulten, Z.; Schulten, K. *J. Chem. Phys.* **1977**, *66*, 4616.

79. Hong, K. M.; Noolandi, J. *J. Chem. Phys.* **1978**, *69*, 5026.

80. Shizuka, H., *Acc. Chem. Res.* **1985**, *18*, 141.

81. Lewis, F. D., *Acc. Chem. Res.* **1986**, *19*, 401.

82. Lee, L. Y. C.; Schanze, K. S.; Giannotti, C.; Whitten, D. G. in *Homogeneous and Heterogeneous Photocatalysis*, Pelizzetti, E.; Serpone, N. (Eds.), D. Riedel Publishing Company, Dordrecht, Holland, **1985**, p. 147.

83. Fujita, I.; Fajer, J.; Chang, C.-K.; Wang, C. B.; Bergkamp, M. A.; Netzel, T. L. *J. Phys. Chem.* **1982**, *86*, 3754.

84. Netzel, T. L.; Bergkamp, M. A.; Chang, C. -K. *J. Am. Chem. Soc.* **1982**, *104*, 1952.

85. Lindsey, J.; Mauzerall, D.; Linschitz, H. *J. Am. Chem. Soc.* **1983**, *105*, 6528.

86. Wasielewski, M. R.; Niemczyk, M. P.; Svec, W. A.; Pewitt, E. B. *J. Am. Chem. Soc.* **1985**, *107*, 5562.

87. Lawson, J. M.; Craig, D. C.; Oliver, A. M.; Paddon-Row, M. N. *J. Am. Chem. Soc.* **1997**, *119*, 5355.

88. Roest, M. R.; Verhoven, J. W.; Schuddeboom, W.; Warman, J. M.; Lawson, J. M.; Paddon-Row, M. N. *J. Am. Chem. Soc.* **1996**, *118*, 1762.

89. Jolliffe, K. A.; Bell, T. D. M.; Ghiggino, K. P.; Langford, S. J.; Paddon-Row, M. N. *Angew. Chem. Int. Ed. Engl.* **1998**, *37*, 916.

90. Ross, R. T. *Biochim. Biophys. Acta*, **1977**, *459*, 321.

91. Warshel, A. *Isr. J. Chem.* **1981**, *21*, 341.

92. Guest, D.; Moore, T. A.; Liddel, P. A..; Nemeth, G. A.; Makings, L. R.; Moore, A. L.; Barret, D.; Pessiki, P. J.; Bensasson, R. V.; Rougee, M.; Chachaty, C.; De Schryver, F. C.; Van der Auwerner, M.; Holzworth, A. R.; Conolly, J. S. *J. Am. Chem. Soc.* **1987**, *109*, 846.

93. Moore, T. A.; Guest, D.; Mathis, P.; Mialocq, J.; Chachaty, C.; Bensasson, R. V.; Land, E. J.; Doizi, D.; Liddel, P. A.; Lehman, W. R.; Nemeth, G. A.; Moore, A. L. *Nature* **1984**, *307*, 630.

94. Guest, D.; Moore, T. A.; Moore, A. L.; Barret, D.; Harding, L. O.; Makings, L. R.; Liddel, P. A.; De Schryver, F. C.; Van der Auwerner, M.; Bensasson, R.; Rougee, M. *J. Am. Chem. Soc.* **1988**, *110*, 321.

95. Guest, D.; Moore, T. A.; Moore, A. L.; Makings, L. R.; Seely, G. R.; Liddel, P. A.; Ma, X. C.; Trier, T. T.; Gao, F. *J. Am. Chem. Soc.* **1988**, *110*, 7567.

96. Guest, D.; Moore, T. A.; Moore, A. L.; Seely, G. R.; Liddel, P. A.; Barrett, D.; Harding, L. O.; Ma, X. C.; Lee, S. J.; Gao, F. *Tetrahedron* **1989**, *45*, 4867.

97. Guest, D.; Moore, T. A.; Moore, A. L.; Gao, F.; Luttrull, D. K.; De Graziano, J. M.; Ma, X. C.; Makings, L. R.; Lee, S. J.; Trier, T. T.; Bittersmann, E.;

Seely, G. R.; Woodward, S.; Bensasson, R. V.; Rougee, M.; De Schryver, F. C.; Van der Auweraer, M. *J. Am. Chem. Soc.* **1991**, *113*, 3638.

98. Guest, D.; Moore, T. A.; Moore, A. L.; Lee, S. J.; Bittersmann, E.; Luttrull, D. K.; Rehm, A. A.; DeGraziano, J. M.; Ma, X. C.; Gao, F.; Belford, R. E.; Trier, T. T. *Science* **1990**, *248*, 199.
99. Gould, I. R.; Farid, S. *Acc. Chem. Res.* **1996**, *29*, 522.
100. Gould, I. R.; Ege, D.; Moser, J. E.; Farid, S. *J. Am. Chem. Soc.* **1990**, *112*, 4290.
101. Rackocsky, S.; Sherr, H. *Biochim. Biophys. Acta* **1982**, *681*, 152.
102. Carapellucci, P.; Mauzerall, D. *Ann. N. Y. Acad. Sci.*, **1975**, *244*, 214.
103. Cristol, S. J.; Seapy, D. G.; Aeling, E. O. *J. Am. Chem. Soc.* **1979**, *101*, 5707.
104. Mauzerall, D. *J. Am. Chem. Soc.* **1960**, *82*, 1832.
105. Kalyanasundaram, K. *Photochemistry in Microheterogeneous Systems*, Academic Press, New York, **1987**.
106. Geblewicz, G.; Schiffrin, D. J. *J. Electroanal. Chem.* **1988**, *244*, 27.
107. Marcus, R. A. *J. Phys. Chem.* **1990**, *94*, 4152.
108. Marcus, R. A. *J. Phys. Chem.* **1990**, *94*, 7742.
109. Marcus, R. A. *J. Phys. Chem.* **1991**, *95*, 2010.
110. Das, S.; Thanulingam, T. L.; Rajesh, C. S.; George, M. V. *Tetrahedron Lett.* **1995**, *36*, 1337.
111. Rajesh, C. S.; Thanulingam, T. L.; Das, S. *Tetrahedron* **1997**, *53*, 16817.
112. Kalyanasundaram, K. *J.Chem.Soc., Chem. Commun.* **1978**, 627.
113. Pileni, M. P.; Braun, A. M.; Grätzel, M. *Photochem. Photobiol.* **1980**, *31*, 423.
114. Brugger, P. A.; Grätzel, M. *J. Am. Chem. Soc.* **1980**, *102*, 2461.

115. Rodgers, M. J.; Becker, J. C. *J. Phys. Chem.* **1980**, *84*, 2762.

116. Schmehl, R. H.; Whitten, D. G. *J. Am. Chem. Soc.* **1980,** *102*, 1938.

117. Schmehl, R. H.; Whitten, D. G. *J. Phys. Chem.* **1981**,*85*, 3473.

118. Matsuo, T.; Sakamoto, T.; Takuma, K.; Sakura, K.; Ohsaka, T. *J. Phys. Chem.* **1981**, *85*, 1277.

119. Foreman, T. K.; Sobol, W. M.; Whitten, D. G. *J. Am. Chem. Soc.* **1981**, *103*, 5333.

120. Schmehl, R. H.; Whitesell, L. G.; Whitten, D. G. *J. Am. Chem. Soc.* **1981**, *103*, 3761.

121. Infelta, P. P.; Brugger, P. -A. *Chem. Phys. Lett.* **1981**, *82*, 462.

122. Brugger, P. A.; Infelta, P. P.; Braun, A. M.; Grätzel, M. *J. Am. Chem. Soc.* **1981**, *103*, 320.

123. Nakamura, T.; Kurihara. T.; Matsuo, T. *J. Phys. Chem.* **1982**, *86*, 4368.

124. Brugger, P. A.; Grätzel, M. Gaurr, T.; McLendon, G. *J. Phys. Chem.* **1982**, *86*, 944.

125. Miyashita, T.; Murakata, T.; Matsuda, M. *J. Phys. Chem.* **1983**, *87*, 4529.

126. Kurihara, K.; Tundo, P.; Fendler, J. H. *J. Phys. Chem.* **1983**, *87*, 3777.

127. Kiwi, J.; Kalyanasundaram, K.; Grätzel, M. *Struct. Bonding (Berlin)* **1982** *49*, 37.

128. Harriman, A.; West, M. A. (Eds.), *Photogeneration of Hydrogen*, Academic Press, New York, **1982**.

129. Grätzel, M., (Ed.), *Energy Resources through Photochemistry and Catalysis*. Academic Press, New York, **1983**.

130. Moroi, Y.; Grätzel, M. *J. Am. Chem. Soc.* **1979**, *101*, 567.

131. Radda, G. K.; Vanderkooi, J.; *Biochim. Biophys. Acta* **1972**, *265*, 509.

132. Nichols, P.; West, J.; Bangham, A. D. *Biochim. Biophys. Acta* **1974**, *363*, 190.

133. Mangel, M. *Biochim. Biophys. Acta* **1976**, *430*, 459.

134. Ford, W. E.; Otvos, J. W.; Calvin, M. *Nature (London)* **1978**, *274*, 507.

135. Ford, W. E.; Otvos J. W.; Calvin, M. *Proc. Natl. Acad. Sci. U.S.A.* **1979**, *76*, 3590.

136. Laane, C.; Ford. W. E.; Otvos, J. W.; Calvin, M. *Proc. Natl. Acad. Sci. U.S.A.* **1981**, *78*, 2017.

137. Kurihara, K.; Sukigara, M.; Toyoshima, Y, *Res. Commu.* **1979**, *88*, 320.

138. Matsuo, T.; Itoh, K.; Takuma, K.; Hashimoto, K.; Nagamura, T. *Chem. Lett.* **1980**, 1009.

139. Matsuo, T.; Takuma, K.; Tsutsui, Y.; Nishijima, T. *J. Coord. Chem.* **1980**, *10*, 187.

140. Morishima, Y. Itoh, Y. Nozakura, S. Ohno, T.; Kato, S. *Macromolecules*, **1984**, *17*, 2264.

141. Kurimura, Y.; Schinozaki, N.; Ito, Y.; Urtani, K.; Schigehara, K.; Tschuida, E.; Kaneko, M. Yamada, A. *Bull. Chem. Soc. Jpn.* **1982**, *55*, 380.

142. Sasson, R. E.; Rabani, J. *J. Phys. Chem.* **1980**, *84*, 1319.

143. Adar, E.; Degani, Y.; Goren, Z.; Willner, I. *J. Am. Chem. Soc.* **1986**, *108*, 4696.

144. Wilner, I.; Adar, E.; Goren, Z.; Steinberger, B. *New J. Chem.* **1987**, *11*, 769.

145. Bender, M. L.; Kamiyama, M. *Cyclodextrin Chemistry.* Springer Verlag, Berlin, **1978**.

146. Balaban, A. T.; Sahini, V.E.; Keplinger,E. *Tetrahedron* **1960**, *9*, 163.

147. Balban, A. T.; Dinculescu, A.; Dorofeyenko, G. N. ; Fischer, G. W.; Koblik, A. V.; Mezheritzkii, V. V.; Schroth, W. *Pyrylium salts: Synthesis, Reactions and Physical Properties*. Katrizky, A. R. , (Ed.), *Advances in Heterocyclic Chemistry*; Academic Press: New York, **1982**; Suppliment 2.

148. Haucke, G.; Czerney, P.; Cebulla, F. *Ber. Bunsenges Phys. Chem.* **1992**, *96*, 880.

149. Miranda, M. A.; Garcia, H. *Chem. Rev.* **1994**, *94*, 1063 and references there in.

150. Detty, M. R.; Merkel, P. B. *J. Am. Chem. Soc.* **1990**, *112*, 3845.

151. Tripathi, S. L. *Handbook of Photochemistry*; Marcel Dekker: New York, **1973**.

152. Valat, P; Triphati, S; Wintgens, V.; Kossanyi, J. *New J. Chem.* **1990**, *14*, 825.

153. Basting, D.; Schäefer, F. P.; Steyer, B. *Appl. Phys.* **1974**, *3*, 81.

154. Seilmeier, A.; Kopainsky, B.; Kaiser, W. *Appl. Phys.* **1980**, *22*, 355.

155. Czerney, P.; Haucke, G. *Appl. Fluoresc. Technol.* **1989**, *1*, 13.

156. Deligeorgiev, T.; Gadzhev, N. *Dyes Pigm.* **1990**, *12*, 157.

157. Kopainsky, B.; Qiu, P.; Kaiser, W.; Sens, B.; Drexhage, K. H. *Appl. Phys. (Part B)* **1982**, *29*, 15.

158. Tripathi, S.; Wintgens, V.; Valat, P.; Toscano, V.; Kossanyi, J.; Bos, F. *J. Luminescence* **1987**, *37*, 149.

159. Kotowski, T.; Skubiszak, W.; Soroka, J. A.; Soroka, K. B.; Stacewiez, T. *J. Luminescence* **1991**, *50*, 39.

160. Rulliere, C.; Declemy, A.; Balaban, A. T. *Can. J. Phys.* **1985**, *63*, 191.

161. Williams, J. L. R.; Reynolds, G. A. *J. Appl. Phys.* **1968**, *39*, 5327.

162. Kopainsky, B.; Kaiser, W.; Drexhage, K. H. *Opt. Commun.* **1980**, *32*, 451.

163. Kawamura, K.; Okamoto, Y. *Ger. Offen.* DE 3,834,960; *Chem. Abstr.* **1989**, *111*, 222173.

164. Matsumoto, T.; Minoshima, Y.; Nakachi, O. *Jpn. Kokai Tokkyo Koho* **1988** JP 63 278,903; *Chem. Abstr.* **1989**, *110*, 213634.

165. Van Allan, J. A.; Natalc, C. C.; Rauner, F. J. *Belg. Pat.* **1963**, 623,972; *Chem. Abstr.* **1965**, *63*, 10102.

166. Leubner, G. H.; Unruh, C. C. *Brit. Pat.* **1964**, 949,919; *Chem. Abstr.* **1964**, *61*, 8435.

167. Veber, M.; Sotta, P.; Davidson, P.; Levelut, A. M.; Jallabert, C.; Strzelecka, H. *J. Phys.(Paris)* **1990**, *51*, 1283.

168. Markovitsi, D.; Lecuyer, I.; Clergeot, B.; Jallabert, C.; Strzelecka, H.; Veber, M. *Liq. Cryst.* **1989**, *6*, 83.

169. Davidson, P.; Jallabert, C.; Levelut, A. M.; Strzelecka, H.; Veber, M. *Mol. Cryst. Liq. Cryst.* **1987**, *161 B*, 395.

170. Strzelecka, H.; Jallabert, C.; Veber, M.; Davidson, P.; Levelut, A. M.; Malthete, J.; Sigaud, G.; Skoulios, A.; Weber, P. *Mol. Cryst. Liq. Cryst.* **1987**, *161 B*, 403.

171. Muller, F.; Mattay, J. *Chem. Rev.* **1993**, *93*, 99.

172. Corma, A.; Fornes, V.; Garcia, H, Miranda, M. A.; Primo, J.; Sabater, K. *J. Am. Chem. Soc.* **1994**, *16*, 2276.

173. Wiest, O.; Steckhan, E.; *Angew. Chem. Int. Ed. Engl.* **1993**, *32*, 901.

174. Adam, W.; Sendelbach, J. *J. Org. Chem.* **1993**, *58*, 5316.

175. Manoj, N.; Gopidas, K. R. *J. Photochem. Photobiol. A: Chem.* **1995**, *85*, 53.

CHAPTER 2

PHOTOPHYSICAL AND ELECTRON TRANSFER STUDIES OF A FEW 2,6-DIMETHYL-4-(ALKYLPHENYL)PYRYLIUM AND THIOPYRYLIUM DERIVATIVES

2.1. Abstract

Photophysical and electron transfer properties of pyrylium salts **1a-f** and the thiopyrylium derivatives **2a-d** were investigated. Photophysical studies include: absorption spectra, fluorescence spectra, fluorescence quantum yields, fluorescence lifetimes, phosphorescence spectra and triplet-triplet absorption spectra. Our results indicated that these cations have two singlet excited states with similar energies and that the substituent and solvent determine which of these has the lowest energy. For cations **1a**, **1f**, and **2a**, the lowest singlet excited state has TICT character. In the case of all other substrates, the photophysical properties are better explained by invoking a planar excited state. Laser flash photolysis studies suggest that electron transfer takes place from electron rich aromatics to the singlet and triplet excited states of these compounds. Using biphenyl as donor, we have estimated the extinction coefficients, as well as the yields of the pyranyl/thiopyranyl radicals formed as a result of photoelectron transfer. Ion yields were higher than those observed with other cationic sensitizers. We have tried to correlate the radical yields to the triplet quantum yields and also to the stability of the pyranyl radicals. When naphthalene was used as the electron donor, charge separation was very poor due to the formation of a CT complex. Laser

flash photolysis in this case leads to the formation of the triplet state of the CT complex which undergoes slow deactivation to the ground state.

2.2. Introduction

Several spectroscopic studies, both experimental and theoretical, have been carried out on pyrylium salts and their structural analogs.[1-19] Balaban and coworkers, for example, correlated the absorption bands in simple pyrylium systems to those in benzene, pyridine and pyridinium salts.[1-3] Absorption bands in the pyrylium systems were designated as *x*-bands and *y*-bands, depending on the direction of polarization of the bands. Effect of substitution in the ring on the absorption bands was also studied. It was observed that substituents in the 2- and 6- positions affect the *x*-band and substituents in the 4- position affect the *y*-band, predominantly. These observations were in agreement with the projection of the substituents in the *x* and *y* axes, respectively (see Chart 2.1 for axis convention). Thus, in 2,6-dimethyl-4-phenylpyrylium salt (**1a**), the 300 nm band observed in acetonitrile, was assigned as the *x*-band and the 326 nm band as the *y*-band. Simalty and coworkers made similar assignments for several styryl-substituted pyrylium salts.[4-8] Recent calculations, however, do not agree with the above assignments. Rullière et al., for example, suggested that the 326 nm band in **1a** is a superposition of two closely lying bands: $S_0 \rightarrow S_1$ band at 334 nm polarized along the *x*-axis and $S_0 \rightarrow S_2$ band at 325 nm polarized along the *y*-axis.[16] They could not, however, observe the $S_0 \rightarrow S_1$ band and suggested that this weak band is hidden by the strong $S_0 \rightarrow S_2$ band. Studies on the 2,4,6-triaryl-substituted pyrylium salts also suggested that the long-wavelength absorption is a superposition of two closely lying bands.[18,19]

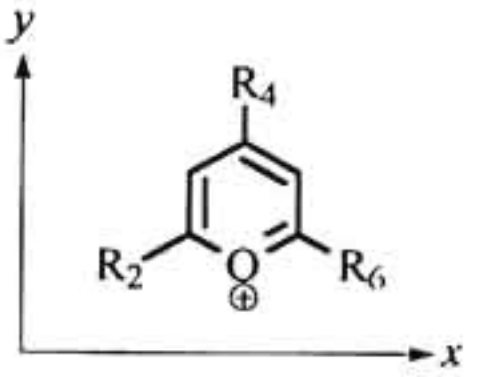

Chart 2.1

Although, there are several reports on the absorption spectra of simple pyrylium salts, studies of their fluorescence properties are very few.[20-24] In a recent report, Lin and Schuster reported that fluorescence quantum yields of 2,6-di-*tert*-butyl-4-arylpyrylium salts depend on the substitution in the aryl ring.[22] This was attributed to the presence of two closely lying excited states in these molecules. A few laser flash photolysis studies, which characterize the triplet states and radicals of pyrylium salts are also available in the literature.[25-37] Most of these studies deal with the well known electron transfer sensitizer, 2,4,6-triphenylpyrylium perchlorate. Other derivatives of this group have not been studied in detail. In view of this, a detailed study of the photophysical and electron transfer properties of a few 2,6-dimethyl-4-arylpyrylium derivatives have been undertaken and the results are presented in this thesis.

In the first part of this chapter, photophysical properties of 2,6-dimethyl-4-(alkylphenyl)pyrylium salts **1a-f** are presented. These studies include: absorption spectra, fluorescence spectra, fluorescence quantum yields, fluorescence lifetimes, phosphorescence spectra and triplet-triplet absorption spectra. This is followed by laser flash photolysis studies of these salts in the presence of electron donors. In

the second part, similar experiments for thiopyrylium salts **2a-d** are presented. Finally, a comparison of the quantum yields of ion formation in these two classes of compounds is attempted. The structures of the compounds studied in this chapter are presented in Chart 2.2

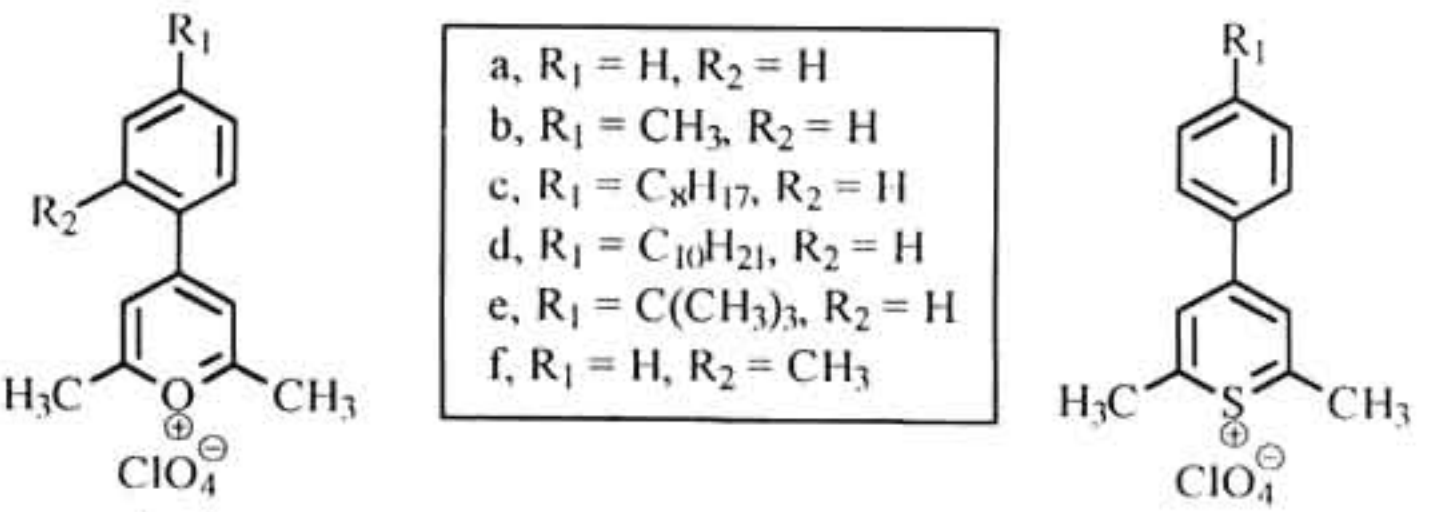

1a-f **2a-d**

Chart 2.2

2.3. Results and Discussion

2.3.1. 2,6-Dimethyl-4-(alkylphenyl)pyrylium salts 1a-f

2.3.1.1. Absorption spectra

The pyrylium salt **1a** exhibits two absorption bands of relatively high intensity in the UV-Visible region. The higher energy band at 300 nm remains largely unaffected by solvent, whereas, the lower energy band at 326 nm in acetonitrile, undergoes a red shift in nonpolar solvents. A red shift of the long-wavelength absorption in nonpolar solvents is observed for several pyrylium derivatives.[20] Substitution of an alkyl group in the 4-phenyl ring, as in **1b-f**, leads to major changes in the absorption spectrum. We have undertaken a detailed study of this aspect in order to understand and explain these changes and the results are summarized below.

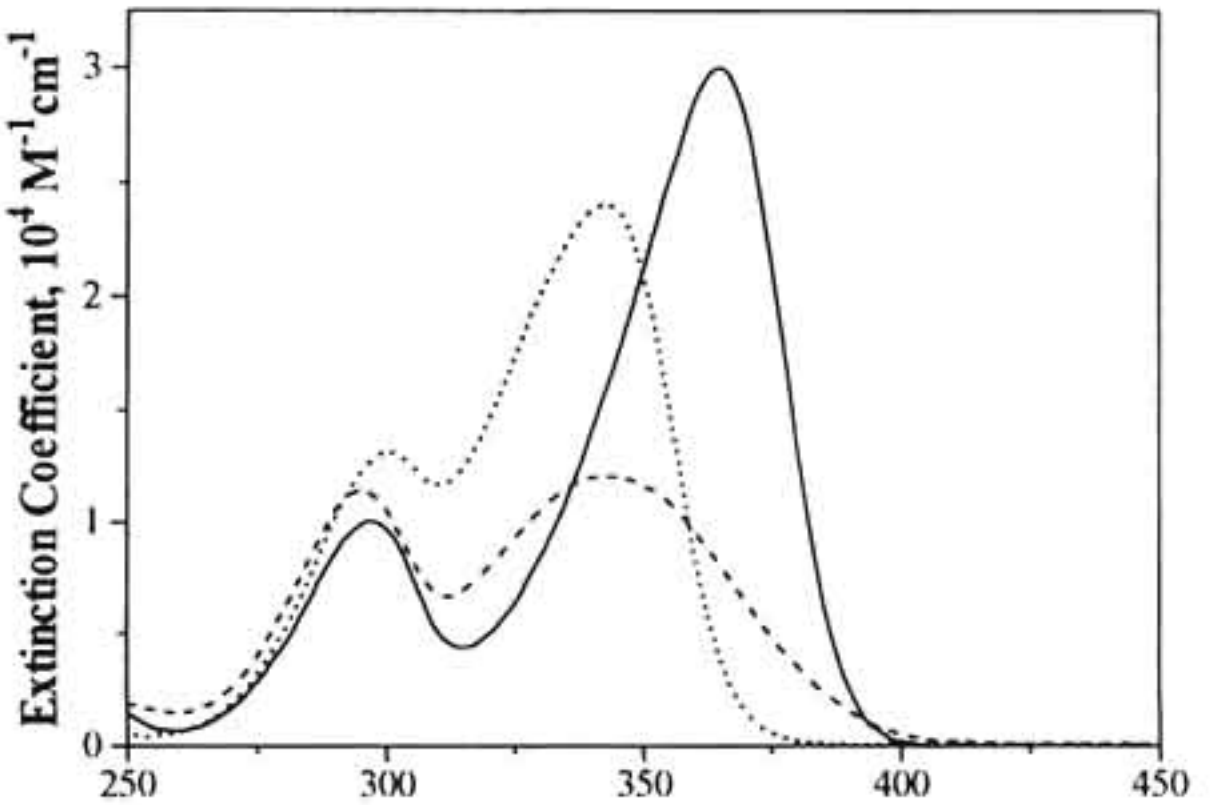

Figure 2.1 Absorption spectra of pyrylium perchlorates **1a** (••••); **1b** (—) and **1f** (- - -) in dichloromethane.

Figure 2.1 shows the absorption spectra of **1a**, **1b** and **1f** in dichloromethane and Figure 2.2 shows the same in acetonitrile. These compounds differ only by the presence of a methyl group in the *ortho* or *para* position of the 4-phenyl ring. This minor change, however, is sufficient to create substantial changes in the long-wavelength absorption in these compounds. As is clear from Figure 2.1, substitution of methyl group in the *para* position (as in **1b**), leads to a red shift of the band by 22 nm in dichloromethane solution. This is associated with an increase in the extinction coefficient and a reduction in bandwidth. Substitution of methyl group in the *ortho* position (as in **1f**), on the other hand, leads to a decrease in the extinction coefficient and an increase in the bandwidth. The

absorption maximum remained unchanged in this case. Spectra in acetonitrile also showed similar trends.

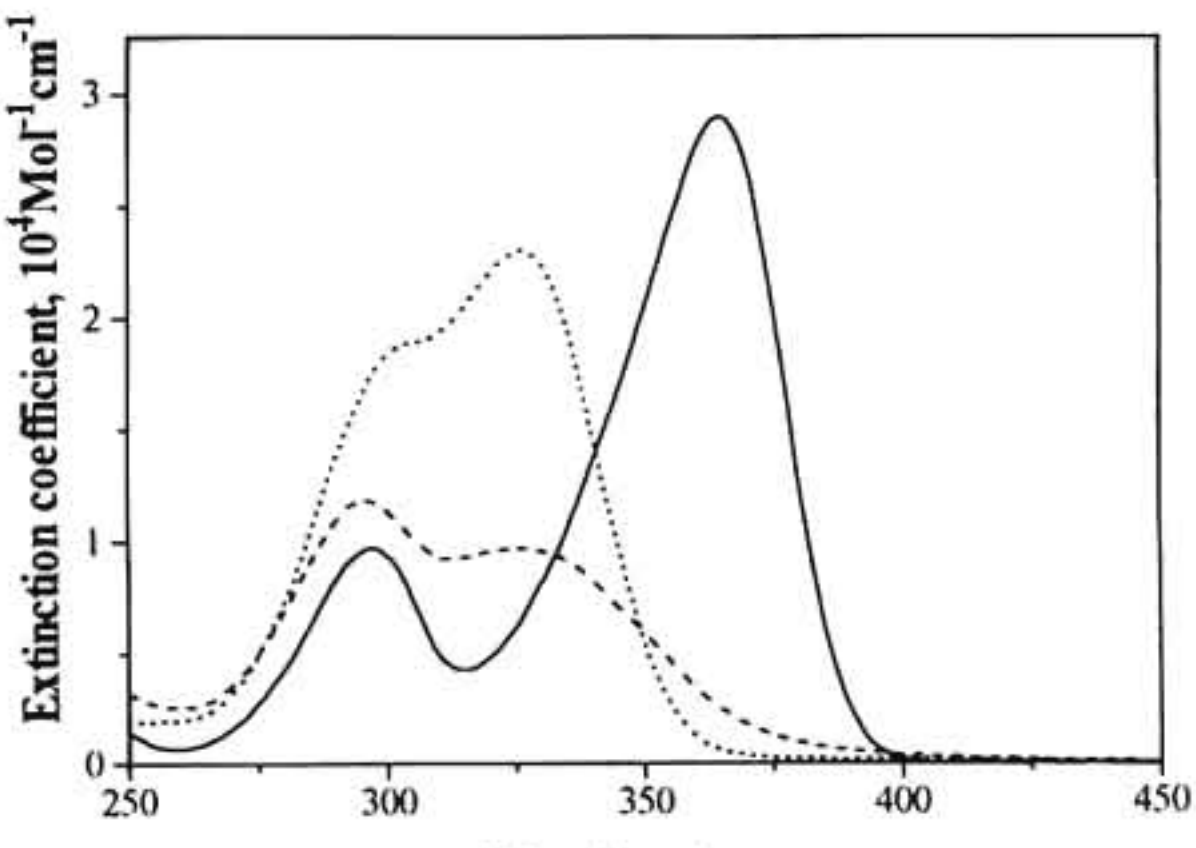

Figure 2.2 Absorption spectra of pyrylium perchlorates **1a** (••••); **1b** (—) and **1f** (- - -) in acetonitrile.

Table 2.1 summarizes the absorption maxima, extinction coefficients and full width at reciprocal '*e*' (FWRE) values for the lowest energy absorption bands of **1a-f**. For **1a** and **1f**, the two absorption bands overlap in acetonitrile and hence FWRE values could not be determined in this solvent. As is clear from Table 2.1, the nature of the alkyl groups (methyl, *n*-dodecyl or *tert*-butyl), does not play any role because their effect is the same as that of the methyl group. In the following section, an attempt is made to explain the above observations.

Table 2.1 Absorption maxima (λ_{max}), extinction coefficients (ε_{max}), and full width at reciprocal *e* (FWRE) values for pyrylium salts 1a-f in dichloromethane. Values in parenthesis are those obtained in acetonitrile.

Compound	λ_{max}, nm	ε_{max}, $M^{-1}cm^{-1}$	FWRE, cm^{-1}
1a	343 (326)	2.4×10^4 (2.3×10^4)	4585
1b	365 (347)	3.0×10^4 (2.9×10^4)	3650
1c	370 (350)	3.4×10^4 (2.9×10^4)	3575
1d	370 (350)	3.4×10^4 (2.9×10^4)	3575
1e	365 (345)	3.4×10^4 (2.9×10^4)	3617
1f	343 (327)	1.2×10^4 (0.97×10^4)	6332

According to Rullière et al., the absorption band at 326 nm for **1a** in acetonitrile is a superposition of two closely lying bands, namely, the weak $S_0 \rightarrow S_1$ band (calculated λ_{max} = 334 nm, polarized along the *x*-axis) and the strong $S_0 \rightarrow S_2$ band (calculated λ_{max} = 325 nm, polarized along the *y*-axis).[16] The band separation is very small (9 nm, corresponds to $\Delta E = 825\ cm^{-1}$) and hence these bands could not be resolved. The FWRE value for **1a** ($4585\ cm^{-1}$) indeed suggests that this band is a superposition of two absorption bands. It should be mentioned

here that, the existence of two closely lying bands has been confirmed in a few pyrylium salts by fluorescence polarization measurements.[18,19]

Substituents affect the absorption spectra of pyrylium cations depending on whether they are in the *x*-direction or *y*-direction.[1-8] *Ortho* substitution as in **1f**, has its major component projected along the *x*-axis and affect the *x*-band predominantly. Thus in **1f**, the $S_0 \rightarrow S_1$ band (*x*-band) is expected to shift bathochromically relative to the $S_0 \rightarrow S_2$ band leading to increased separation of the bands. This is confirmed by the observation of larger FWRE values (6332 cm^{-1}) and a red shift in the onset of absorption for **1f**, as seen in Figures 2.1 and 2.2. On the other hand, substitution of a methyl group at the *para* position as in **1b**, will affect the *y*-band predominantly. Thus, in **1b** we expect the $S_0 \rightarrow S_2$ band to shift bathochromically relative to the *x*-band. If this relative red shift is more than 9 nm, it would lead to a reversal of the energy levels. A methyl group generally induces a bathochromic shift of 20 nm. Hence we believe that the S_1 and S_2 levels of **1a** (or **1f**) are actually reversed in **1b**. There is very little effect on further increasing the size of the alkyl group. The absorption maxima of **1c-e** are similar to those observed for **1b**. Note that in **1b-e**, the FWRE values are very small. These values are typical of single absorption bands.[38] This suggests that the $S_0 \rightarrow S_1$ band of **1a** (and **1f**) is extremely weak or even absent in **1b-e**.

4-Phenylpyrylium cations like **1a** are structurally similar to biphenyl and 4-phenylpyridine derivatives, where it is well known that the two aromatic rings are not coplanar.[39] Calculations have recently shown that in 2,4,6-triphenylpyrylium cation, the 4-phenyl ring makes an angle (θ_4) of 40^0 with the

plane of the pyrylium ring.[19] The twist angle $\theta_4 = 40^0$ for the minimum energy conformation, is a result of competition between conjugation (leading to stabilization of planar conformation) and steric hindrance (leading to twisted conformation). The twist angle was found to be reduced to 30^0 when the *para* position of the 4-phenyl ring was substituted by an electron donating dimethylamino group (more stabilization of the planar conformation).[18] The twist angle is expected to increase if the *ortho* position of the phenyl group is substituted. Thus, we expect **1f** to be more twisted and **1b-e** more planar compared to **1a**. This argument is supported by the low extinction coefficients of absorption for **1a** and **1f**, compared to other derivatives (Figures 2.1 and 2.2). Thus, an analysis of the absorption spectra of **1a-f** has given us some insight into the structure and orbital ordering in these molecules.

2.3.1.2. Fluorescence properties

Pyrylium salts **1a-f** exhibit fluorescence emission in the 350-650 nm region. The fluorescence maxima of all these compounds are red shifted in acetonitrile by ~20 nm. Figure 2.3 shows the emission spectra of **1a**, **1b** and **1f** in dichloromethane and Figure 2.4 shows the same in acetonitrile. Fluorescence spectra of **1c-e** are similar to that of **1b** in both solvents. Note that the fluorescence maxima of **1a** and **1f** are very much red shifted in both solvents relative to that of **1b-e**. For all these compounds, the Stokes shifts (ν_{st}) were calculated from the values of the absorption and fluorescence maxima. A blue shift in the absorption maxima and red shift in the fluorescence maxima led to very high values of ν_{st} for **1a** and **1f**.

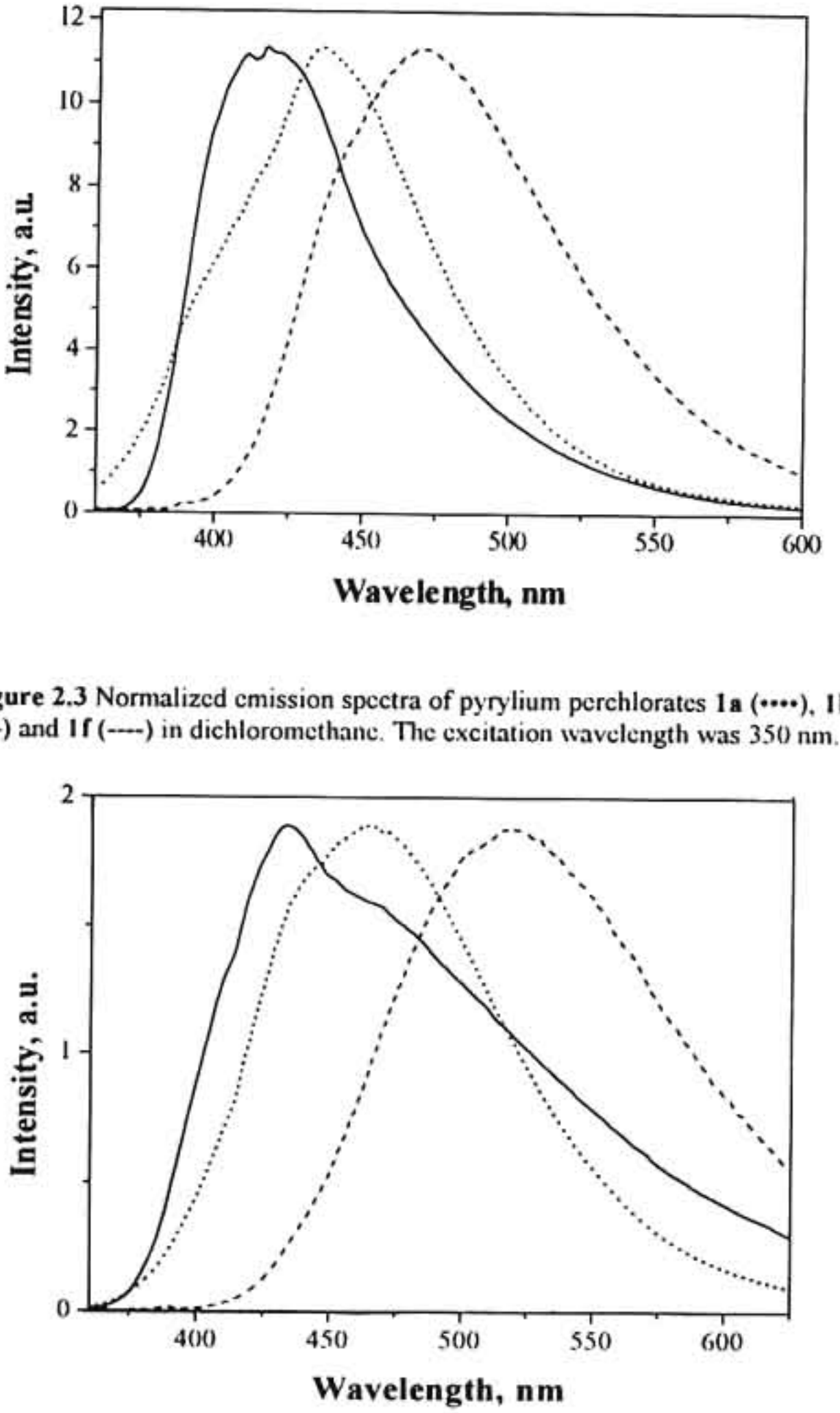

Figure 2.3 Normalized emission spectra of pyrylium perchlorates **1a** (••••), **1b** (—) and **1f** (----) in dichloromethane. The excitation wavelength was 350 nm.

Figure 2.4 Normalized emission spectra of pyrylium perchlorates **1a** (••••), **1b** (—) and **1f** (----) in acetonitrile. The excitation wavelength was 350 nm.

The fluorescence quantum yields (Φ_f) of **1a-f** were measured in dichloromethane and acetonitrile using optically matched solutions. A solution of quinine sulphate in 1 N sulphuric acid (Φ_f = 0.54) was used as the reference in these measurements. For **1a** and **1f**, fluorescence quantum yields were very low in dichloromethane. These values slightly improved in acetonitrile. For other derivatives relatively high Φ_f values were noted in both solvents.

Fluorescence lifetimes (Φ_f) of **1a-1f** were determined in dichloromethane and acetonitrile using single photon counting technique. For **1a**, the fluorescence lifetime is ~15 times longer in acetonitrile compared to its value in dichloromethane (Figure 2.5). For other derivatives the difference was smaller. From the Φ_f and τ_f values, the radiative (k_R) and nonradiative (k_{NR}) rate constants were calculated according to equations (2.1) and (2.2), respectively.

$$k_R = \frac{\Phi_f}{\tau_f} \qquad (2.1)$$

$$k_{NR} = k_R \left(\frac{1}{\Phi_f} - 1 \right) \qquad (2.2)$$

Table 2.2 summarizes the fluorescence maxima, quantum yields, fluorescence lifetimes, Stokes shift values, radiative rate constants and the nonradiative rate constants for **1a-f** in two solvents. Based on the data in Table 2.2, the compounds can be grouped in to two: **1b-e** form one group and **1a** and **1f** form another.

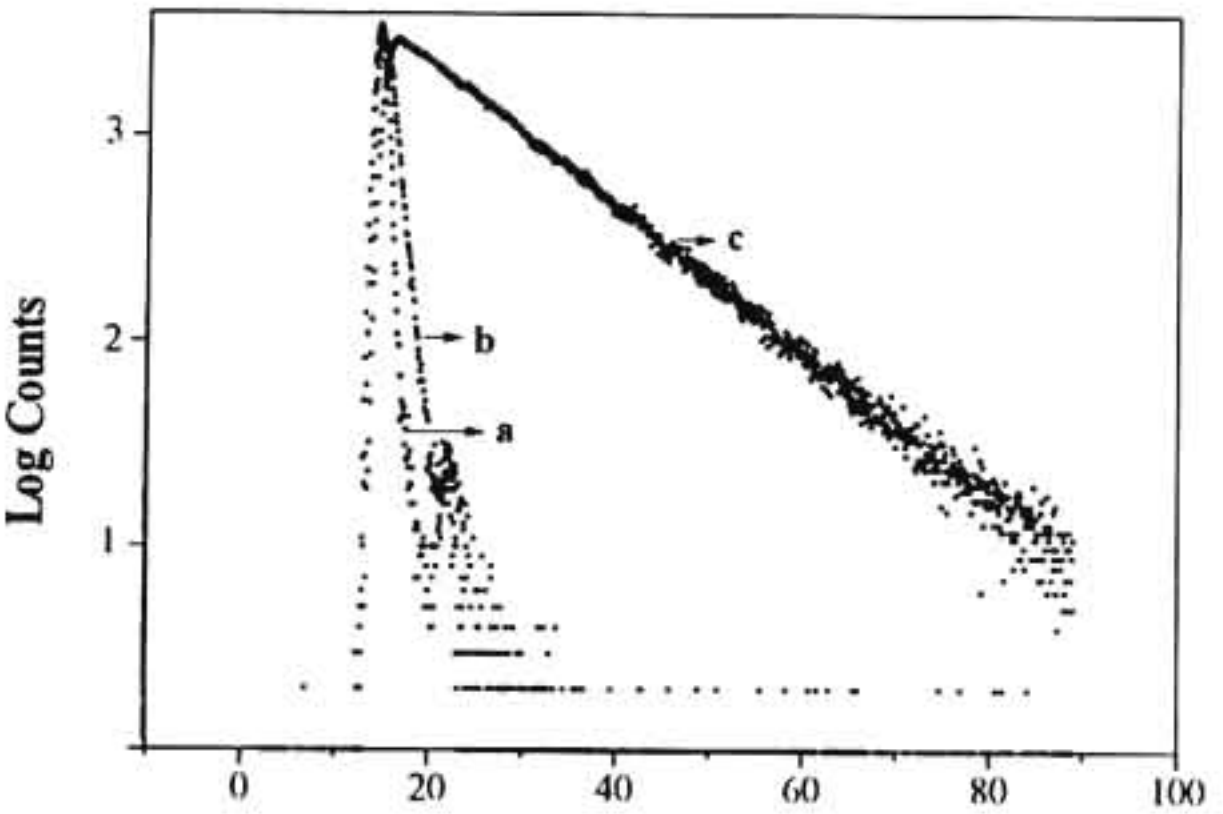

Figure 2.5 Fluorescence decay profile of **1a**. (a) lamp profile, (b) decay profile in dichloromethane and (c) decay profile in acetonitrile. Excitation wavelength was 350 nm.

1a and **1f** exhibit very large Stokes shift values in both solvents. To a first approximation, the Stokes shift is a property of the refractive index (n) and dielectric constant (ε) of the solvent and is described by equation (2.3),[40]

$$\nu_{st} = \frac{2(\mu_g - \mu_e)^2 \Delta f}{hca^3} + \text{Constant} \qquad (2.3)$$

where μ_e and μ_g are the excited and ground state dipole moments, respectively, 'h' is the Planck's constant, 'c' is the speed of light and 'a' is the radius of the cavity in which the fluorophore resides. Δf is known as the solvent polarity parameter and is given by equation (2.4).

$$\Delta f = \left[\frac{\varepsilon - 1}{2\varepsilon + 1} \right] - \left[\frac{n^2 - 1}{2n^2 + 1} \right] \qquad (2.4)$$

Table 2.2 Emission maxima (λ_{max}), Stokes shift (ν_{st}) values, fluorescence quantum yields (Φ_f), fluorescence lifetimes (τ_f), radiative decay rates (k_R) and nonradiative decay rates (k_{NR}) for pyrylium salts 1a-f in dichloromethane. Values in parenthesis are those obtained in acetonitrile.

Compound	λ_{max}, nm	ν_{st}, cm^{-1}	Φ_f	τ_f, ns	k_R, $10^6\ s^{-1}$	k_{NR}, $10^8\ s^{-1}$
1a	434 (462)	6114 (9030)	0.011 (0.10)	0.78 (12.1)	14.1 (8.3)	12.7 (0.74)
1b	417 (435)	3416 (5830)	0.27 (0.28)	3.3 (8.7)	81.8 (32.2)	2.2 (0.83)
1c	418 (435)	3104 (5583)	0.35 (0.32)	3.1 (8.0)	112.9 (40.0)	1.7 (0.59)
1d	418 (435)	3104 (5583)	0.37 (0.36)	3.1 (8.1)	119.4 (44.4)	2.0 (0.79)
1e	417 (430)	3416 (5730)	0.25 (0.36)	2.1 (8.0)	119.1 (45.0)	3.6 (0.80)
1f	469 (518)	7833 (11276)	0.05 (0.10)	4.6 (12.2)	10.9 (8.2)	2.1 (0.78)

Equation (2.3) is known as the Lippert equation[40]. According to this equation, a plot of ν_{st} *vs.* Δf gives $2\Delta\mu^2/hca^3$ as slope (*m*), from which $\Delta\mu$ can be

calculated. In order to determine *m*, Stokes shift values were determined for representative cases in four solvents. ν_{st} values were then plotted against Δf (Figure 2.6). Straight lines were obtained in all cases. From the slopes of these plots and assuming a = 4 Å, $\Delta\mu$ values were calculated. The Stokes shift and $\Delta\mu$ values for substrates **1a**, **1b** and **1f** are given in Table 2.3. These experiments suggested that the dipole moments of the pyrylium salts change by 13.8 -16.9 Debye units upon excitation.

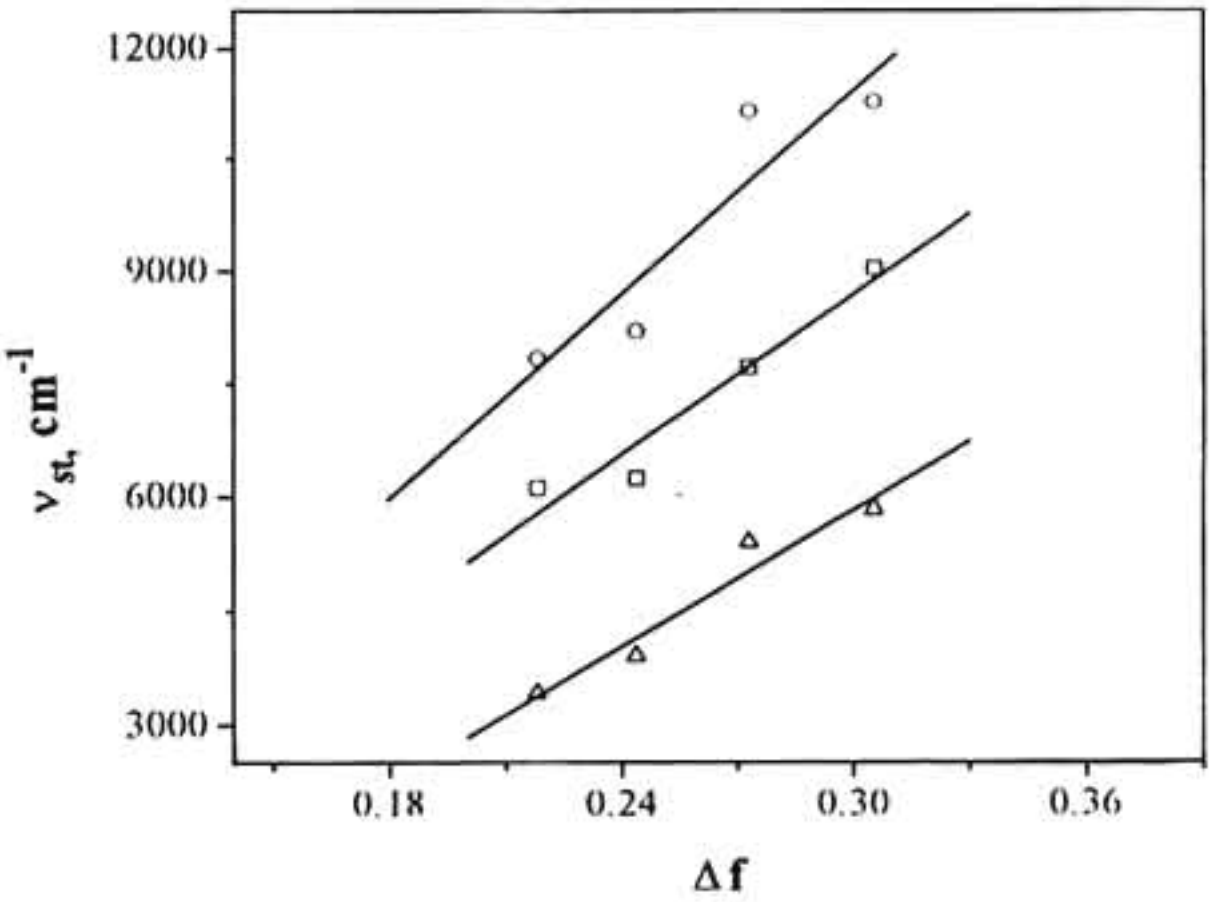

Figure 2.6 Plot of Stokes shift values (ν_{st}) vs solvent polarity parameter (Δf) for **1a** (Δ), **1b** (O) and **1f** ($\square$).

Table 2.3 Stokes shift values (ν_{st}) in different solvents, solvatochromic slopes (m), and $\Delta\mu$ values for pyrylium salts 1a, 1b and 1f.

Compound	Stokes Shift, ν_{st} cm^{-1}				m, cm^{-1}	$\Delta\mu^{a}$, D
	CH_2Cl_2	$C_2H_4Cl_2$	$(CH_3)_2CHOH$	CH_3CN		
1a	6114	6241	7719	9030	35644	15.1
1b	3416	3908	5397	5830	29927	13.8
1f	7833	8198	11146	11276	44972	16.9

[a] Calculated assuming a = 4Å

It is clear from Table 2.2 and Figures 2.3 and 2.4 that the fluorescence properties of **1b-e** are different from those of **1a** and **1f**. In the following section, an attempt is made to explain the observed differences in the fluorescence properties of **1a-f** in terms of molecular structure and geometry. **1b-e** exhibit slight structure in the fluorescence spectra in dichloromethane. This factor, along with the small Stokes shift (3400 cm^{-1}), higher Φ_f and relatively short τ_f values, suggests that these compounds have planar excited states. Their behaviour can be compared with that of biphenyl, where 0_4 = 23° in the ground state and 0° in the excited state and a Stokes shift of 3300 cm^{-1} is observed in nonpolar solvents.[38] The fluorescence quantum yields of **1b-e** remain relatively unchanged in acetonitrile indicating that the excited state remains the same in this solvent. It was suggested that the first two singlet transitions of 4-phenylpyrylium cations are charge transfer in nature.[13] As a consequence of this charge transfer, the phenyl

ring bears approximately the entire positive charge. The effective change in the positive charge centers (pyrylium→phenyl) is reflected in the large change in dipole moment subsequent to excitation. Assuming planar geometries for ground and excited states, .Bigelow calculated μ_g = -3.67 D and μ_e = 10.29 D (polarizations along the y-axis) for 2,6-dimethyl-4-phenylpyrylium cation.[13] The $\Delta\mu$ value we obtained for **1b** (13.8 D) is very close to the 13.96 D predicted by Bigelow. This again supports our suggestion that **1b-e** exhibit planar singlet excited states.

For **1a** and **1f**, the large Stokes shifts in acetonitrile suggest the presence of a relaxed excited state. Such large values are normally observed for compounds which exhibit twisted intramolecular charge transfer (TICT) or other adiabatic photoreaction channels.[41,42] The concept of TICT was initially advanced by Grabowski and coworkers to account for the dual fluorescence of dimethylaminobenzonitrile (DMABN).[43-45] It was postulated that the lowest energy conformation in DMABN is one in which the dimethylamino group has twisted 90° relative to the rest of the molecule. The red shifted fluorescence band of DMABN is attributed to the twisted form. In principle, any electron donor-acceptor system connected to a conjugated system by a single bond can exhibit the TICT phenomenon.[41,42] Although, suitably substituted pyrylium cations are good candidates to study TICT phenomenon, only one of its derivatives, namely, 2,6-diphenyl-4-(*p*-dimethylaminophenyl)pyrylium tetrafluoroborate, is reported to possess the TICT excited state.[18] In this case, calculations showed the formation of a non-fluorescent TICT state involving the rotation of the dialkylaminophenyl group without energy barrier. Our results suggest that the lowest excited states in

1a and **1f** have TICT character, whereas, for compounds **1b-e** the photophysical properties are best explained by invoking a planar excited state.

Absorption spectral studies have suggested that the 4-phenyl ring in **1a** and **1f** is twisted relative to the pyrylium ring by > 40° (vide supra). The Franck-Condon (FC) excited states in these cases can relax either to a planar excited state ($\theta_4 = 0°$) or a TICT state ($\theta_4 = 90°$). The twist involved in both the cases is similar and which state is preferentially populated depends on the stabilization of these states in the particular solvent. Since polar solvents stabilize the TICT state, we expect this state to be populated in polar solvents. The higher Φ_f and τ_f values in acetonitrile for **1a** are in accordance with the above observations. For **1a**, nonradiative processes predominate in dichloromethane indicating that the TICT state is not stabilized in this solvent. This leads to smaller τ_f values and short decay times for **1a** in dichloromethane. For **1f**, twisting of the FC state to a planar state is not possible because of steric factors. Hence the TICT state is the only state to which the FC state can relax. This is reflected in the larger Φ_f and τ_f values of **1f** relative to **1a.**

Eventhough both **1a** and **1f** exhibit similar TICT states, the Stokes shift observed for **1f** is much larger. This can be attributed to the different donor groups (phenyl *vs.* *o*-toluyl) present in these compounds. The toluyl group stabilizes a positive charge better, leading to a larger red shift in the emission maximum. In this context it should be mentioned that, to the best of our knowledge, TICT states in which an unsubstituted phenyl group is acting as the donor moiety have not been reported so far. In the case of **1a**, the acceptor strength of the pyrylium moiety coupled with the pre-twisting that existed in the

molecule prior to excitation may be responsible for the formation of the TICT state.

Thus, pyrylium salts **1a-f** belong to a group of compounds where small structural changes bring about large variations in the photophysical properties. Introduction of a methyl group at the *ortho* or *para* position of the 4-phenyl ring is all that is required to bring about this change. Increasing the length or steric size of the alkyl chain further has very little influence on the observed effect. In the case of **1a** and **1f**, the lowest energy S_1 state has a minimum at a twist angle of 90° in polar solvents. In the case of **1b-e**, the lowest excited state (this corresponds to the S_2 state of **1a** and **1f**) has a minimum at the planar geometry. Hence emission occurs from the planar state and the TICT state is not observed even in polar solvents. Thus, the differences in the observed photophysical properties were attributed to a reversal in the ordering of the excited state energy levels induced by alkyl substitution.

2.3.1.3. Phosphorescence spectra

Phosphorescence emission spectra of pyrylium salts **1a** and **1b** were measured in order to estimate the triplet energies of these compounds. Figure 2.7 shows the phosphorescence spectra of **1a** and **1b** in glycerol glass at 77 K. The spectra showed moderate structure. The short-wavelength band was assigned to the 0,0 transition. The triplet energies were calculated based on this assignment. Values of 63.1 and 61.1 kcal M^{-1} were thus obtained for the triplet energies of **1a** and **1b**, respectively.

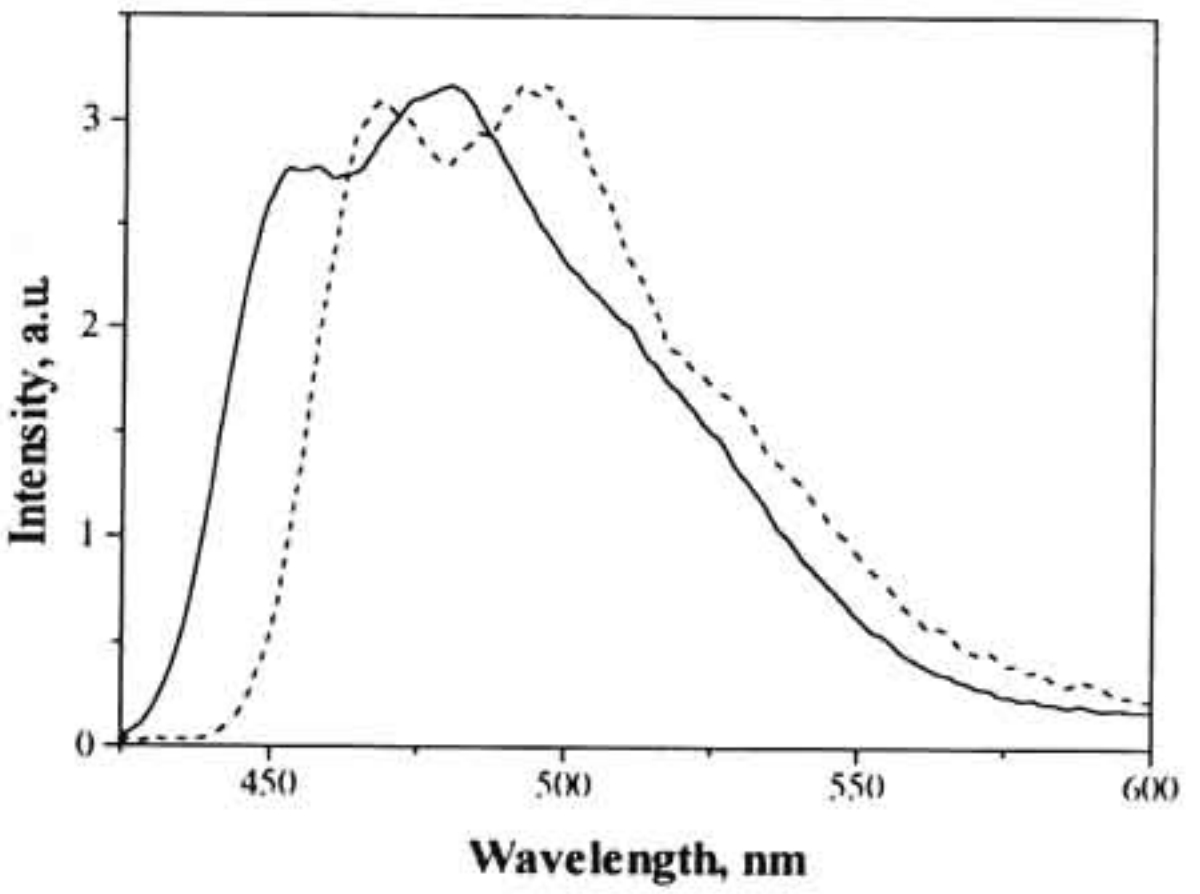

Figure 2.7 Normalized phosphorescence emission spectra of **1a** (—) and **1b** (- - -) in glycerol at 77 K.

2.3.1.4. Laser flash photolysis studies

Laser flash photolysis of **1a-f** in dichloromethane saturated with argon led to the formation of transients, characterized by strong bleaching below 400 nm and broad absorption above 400 nm. Representative examples of the transient absorption spectra are given in Figure 2.8. The transients in all cases decay with first order kinetics and the decays were independent of the concentration of these materials (i.e., no self-quenching was evident). The transient absorption spectra were recorded in acetonitrile also. In this case, a small blue shift of the absorption maxima was noted for all these compounds. In acetonitrile, transients of all these compounds have a lifetime of ~3 μs. The transients from all these compounds were quenched by oxygen. Hence we assign the transients as triplets of the substrates. We have determined the oxygen quenching rate constants ($k_q(O_2)$) in

all the cases. $k_q(O_2)$ values we obtained are similar to the values reported in earlier studies by others.[28]

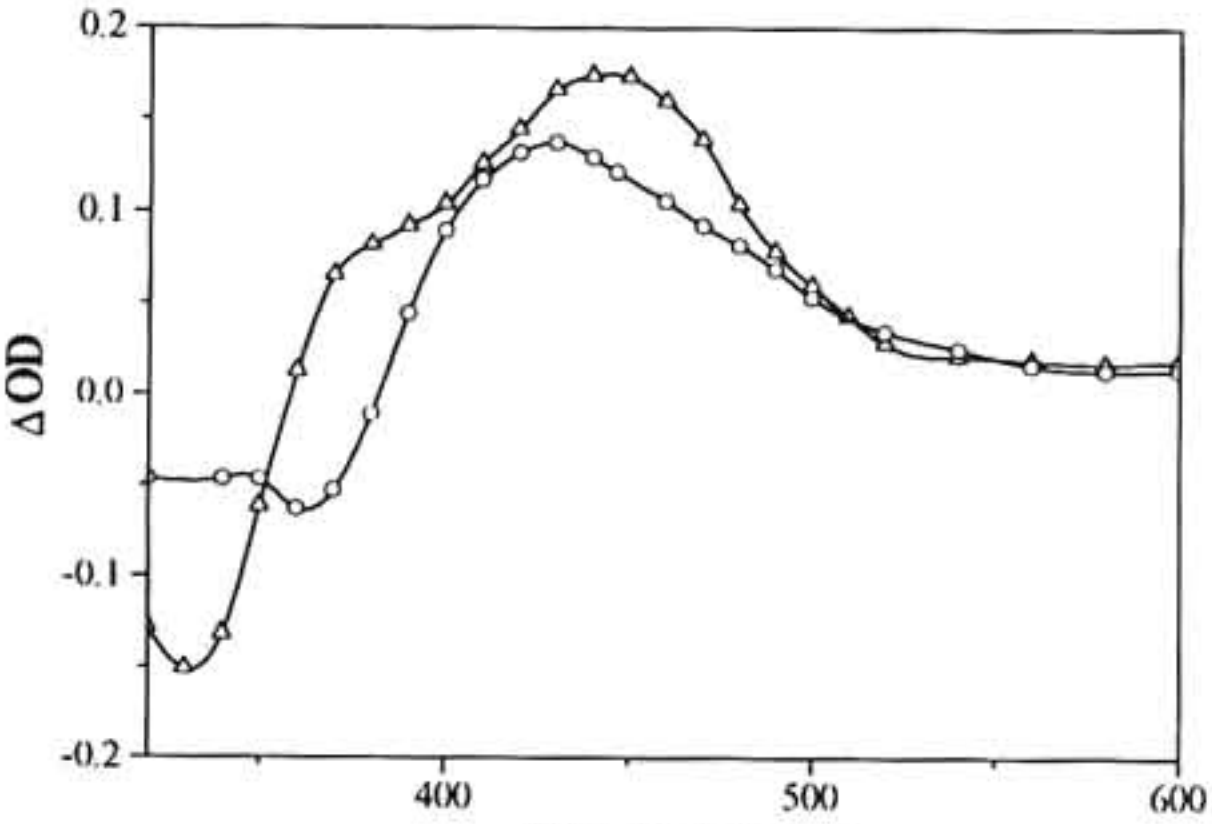

Figure 2.8 Transient absorption spectra of **1a** (Δ) and of **1c** (O) in dichloromethane, recorded at 60 ns and 200 ns respectively.

As mentioned above, transient absorption spectra from all the compounds showed strong bleaching in the region of their ground state absorptions. This enabled us to determine the extinction coefficients of the triplet absorptions by the singlet depletion method.[46] This method assumes that the triplets do not absorb in the spectral region where the singlet depletion is monitored. This assumption is not found to be valid in acetonitrile solution, where the maxima of the singlet depletion did not match with the absorption maxima of the compounds. In dichloromethane solution better matching of the two maxima was observed. Hence these studies were carried out in dichloromethane solution. Using the extinction coefficients thus obtained, we have determined the triplet quantum yields (Φ_T) for all the substrates by the relative

actinometry method.[47] An optically matched solution of benzophenone in benzene was used as a reference and Φ_T values were calculated using equation (2.5).

$$\Phi_T = \Phi_R \frac{\Delta OD_U \varepsilon_R}{\Delta OD_R \varepsilon_U} \qquad (2.5)$$

In equation (2.5), 'U' and 'R' refer to unknown and reference, respectively. Φ's are the quantum yields, ε's are the extinction coefficients and ΔOD's represent the end-of-pulse optical densities of the transients. For the reference compound benzophenone, we used values of $\Phi_R = 1$ and $\varepsilon_R = 7600\ M^{-1}\ cm^{-1}$ (at 530 nm), for the calculations.[48] Table 2.4 summarizes the triplet-triplet absorption maxima, extinction coefficients, triplet quantum yields, triplet lifetimes and oxygen quenching rate constants for pyrylium derivatives **1a-f**.

Note that **1a** and **1f** have higher triplet quantum yields. These values were comparable to that of 2,4,6-triphenylpyrylium perchlorate reported in the literature.[25] For **1b-e**, triplet quantum yields were much lower. We have suggested earlier that the lowest singlet excited states in **1a** and **1f** have TICT character. TICT formation reduces the energy of the singlet excited state. This in turn reduces the energy gap between the lowest singlet and triplet excited states. According to the energy gap law of nonradiative transitions, this leads to enhanced intersystem crossing efficiencies. Hence it is generally observed that TICT formation leads to enhanced triplet yields.[49] Higher Φ_T values in **1a** and **1f** are thus attributed to the formation of a TICT state in these molecules. Another important factor to note here is that $\Phi_f + \Phi_T < 1$ in these compounds. This suggests the involvement of other nonradiative decay channels in these molecules.

Table 2.4 Triplet-triplet absorption maxima (λ^{T}_{max}), extinction coefficients (ε^{T}_{max}), triplet quantum yields (Φ_T), triplet lifetimes (τ_T) and oxygen quenching rate constants (k_q (O_2)) for pyrylium derivatives 1a-f.

Compound	λ^{T}_{max}(Abs), nm	ε^{T}_{max}(Abs), M^{-1} cm^{-1}	Φ_T	τ_T μs	k_q (O_2) M^{-1} s^{-1}
1a	440	2.7×10^4	0.47	0.2	1.5×10^8
1b	430	5.2×10^4	0.19	2.4	5.9×10^7
1c	430	5.4×10^4	0.19	2.7	4.8×10^7
1d	430	6.0×10^4	0.18	2.7	5.1×10^7
1f	460	1.7×10^4	0.43	0.8	--

2.3.1.5. Electron transfer studies

2.3.1.5.1. Fluorescence quenching studies

We have observed that electron rich aromatic hydrocarbons such as biphenyl (BP) and naphthalene (NP) quench the fluorescence of **1a-f** very efficiently. It is known in the literature that pyrylium salts form charge transfer (CT) complexes with polycyclic condensed arenes and substituted benzenoid compounds.[50,51] If CT complexes are formed, then fluorescence quenching would involve both static as well as dynamic mechanisms. In order to see whether any CT complex is formed, the

absorption spectra of the pyrylium salts **1a-e** were recorded in the presence of various concentrations of NP and BP.

Figure 2.9 shows the absorption spectra of **1a** in acetonitrile, in the absence and presence of 0.1 M of naphthalene. The red end of the absorption shifts to longer wavelengths in the presence of naphthalene, indicating the formation of a CT complex. The difference absorption spectrum (λ_{max} 372 nm), shown in Figure 2.9, corresponds to the CT complex. It can be noted from Figure 2.9 that CT formation is very weak at 0.1 M naphthalene concentration. Similar behaviour was noted for **1b-e**. Complex formation was also noticed in dichloromethane solution for **1a-e**.

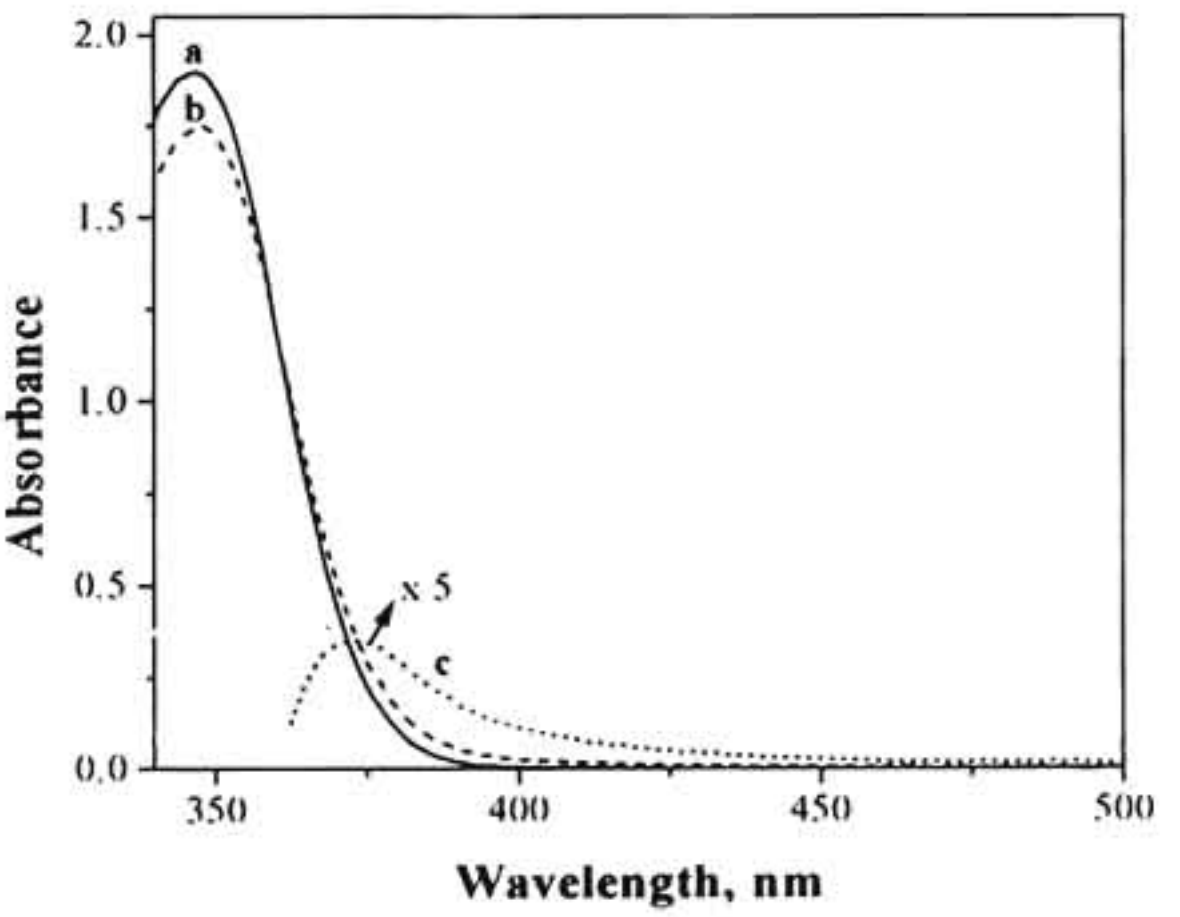

Figure 2.9 (a) Absorption spectrum of **1a** (—), (b) absorption spectrum of **1a** in the presence of naphthalene (0.1 M) (- - -) and (c) the difference absorption spectrum (••••) obtained by subtracting (a) from (b). All the spectra were recorded in acetonitrile solution.

However, we did not observe any complex formation when biphenyl was added to the pyrylium salt solutions. We also did not observe any emission from the CT complexes in acetonitrile solutions.

When biphenyl is used as the quencher, plots of the fluorescence intensity *vs.* biphenyl concentration [Q], fitted the Stern-Volmer equation (2.6),

$$\frac{I_o}{I} = 1 + K_{SV}[Q] \qquad (2.6)$$

where, K_{SV} ($= k_q^S \tau_f$) is the Stern-Volmer constant. The K_{SV} values obtained were in the range 98-188 M^{-1}. The bimolecular fluorescence quenching rate constants (k_q^S) were calculated from the K_{SV} values.

Quenching of the fluorescence of **1a-e** by NP were also analyzed according to equation (2.6). We have observed CT formation between the substrates and NP. CT formation sometimes leads to an upward curvature in the Stern-Volmer plots, indicating a combined dynamic and static quenching process.[52] In the present case, no curvature was observed and fits to equation (2.6) were very good (correlation coefficient 99%). This indicated that only dynamic quenching is taking place in the concentration range studied.

2.3.1.5.2. Electrochemical studies

As will be discussed below, the fluorescence quenching of **1a-e** with electron rich aromatics occurs by electron transfer quenching of the singlet excited state of these salts as indicated in equation (2.7),

$$^*P^+ + Q \longrightarrow P^\bullet + Q^{\bullet+} \qquad (2.7)$$

where, 'P' stands for the pyrylium salt and 'Q' for the quencher hydrocarbon. In order to estimate the free energy change (ΔG_{el}) associated with this electron transfer reaction, we have measured the reduction potentials of **1a-e** in acetonitrile using cyclic voltammetry. In acetonitrile solution, the first reduction peak for these substrates appeared in the range -0.48 to -0.65 V *vs.* SCE. The cyclic voltammograms of these substrates did not show the reverse anodic peak. Absence of the reverse anodic peak in the cyclic voltammogram is reported in the literature for several pyrylium salts.[53-55] In general, pyrylium salts substituted with H and CH_3 in position 2- or 4- of the ring show no reverse anodic peak in the reduction peak. This behavior is attributed to a rapid and irreversible dimerization reaction of the pyranyl radicals formed in the reduction.[53]

The oxidation potential of the donor molecules were known in the literature.[56] Using the redox potentials the free energy for electron transfer, from the donors to the singlet excited states of the salts **1a-e,** can be calculated by the Weller equation[57] (2.8),

$$\Delta G_{el} = 23.06\left[\left(E_{A/A^-} + E_{D^+/D}\right) - \frac{e^2}{\varepsilon d}\right] - E_{0,0} \qquad (2.8)$$

where, $E_{D^+/D}$ and E_{A/A^-} are the electrochemical oxidation potential of the donor and the reduction potential of the acceptor, respectively. $E_{0,0}$ is the excitation energy of the acceptor salts. $E_{0,0}$ values were determined from the point of intersection of the absorption and fluorescence spectra of **1a-e**. The term $e^2/\varepsilon d$ in equation (2.8) represents the energy gained in bringing the radical or radical ion species into an encounter distance 'd' in a solvent of relative permitivity 'ε'. In the

present case this term can be ignored because the pyrylium salts are positively charged and hence there is no net change of charge during electron transfer.

The singlet energies, reduction potentials, free energies of electron transfer to the singlet state, Stern-Volmer quenching constants, and bimolecular quenching rate constants (k_q^S) for the quenching of the singlets of pyrylium salts **1a-d** by BP and NP, are presented in Table 2.5.

Table 2.5 Excitation energies ($E_{0,0}$), reduction potentials (E_{red}), free energies of electron transfer to the singlet state (ΔG_{et}^S), Stern-Volmer quenching constants (K_{SV}) and singlet quenching rate constants (k_q^S) for the pyrylium salts 1a-d in acetonitrile solution.

Compound	$E_{0,0}$ kcal mol^{-1}	E_{red}, V *vs.* SCE	Biphenyl			Naphthalene		
			ΔG_{et}^S, kcal M^{-1}	K_{SV}, M^{-1}	k_q^S, M^{-1} s^{-1}	ΔG_{et}^S, kcal M^{-1}	K_{SV}, M^{-1}	k_q^S, M^{-1} s^{-1}
1a	77.5	-0.48	-21.2	188	1.6×10^{10}	-24.9	213	1.8×10^{10}
1b	75.5	-0.62	-16.0	104	1.2×10^{10}	-19.7	130	1.5×10^{10}
1c	74.9	-0.63	-15.1	103	1.3×10^{10}	-18.8	118	1.5×10^{10}
1d	74.9	-0.63	-15.1	98	1.2×10^{10}	-18.8	123	1.5×10^{10}

The free energy for the electron transfer reaction ranged from -15.1 to -24.9 kcal M^{-1} and should lie in the normal region according to the Marcus equation.[58] The quenching rate constants calculated are in the range $1.2\text{-}1.6 \times 10^{10}$ M^{-1} s^{-1}. The diffusion rates calculated using the Smoluchowski equation, assuming a radius of

4 Å for the molecules, is 1.75 x 10^{10} M^{-1} s^{-1}. We can see that the quenching rates obtained are close to the diffusion-controlled limit.

2.3.1.5.3. Laser flash photolysis studies

Triplet quenching experiments. The quenching of the triplets of **1a-e** by electron donors such as BP, NP and 4,4'-dimethoxystilbene (DMS) were attempted by laser flash photolysis. The bimolecular triplet quenching rate constants (k_q^T) were obtained by measuring the pseudo-first-order rate constants (k_{obs}), at different quencher concentrations [Q] and plotting the data according to equation (2.9),

$$k_{obs} = k_0 + k_q^T[Q] \qquad (2.9)$$

where, k_0 is the rate in the absence of the quencher. In these experiments, the quencher concentration [Q], was varied over a narrow range of 1-4 x 10^{-4} M^{-1}. When BP was used as the quencher, good single exponential fits were obtained for the decay and we obtained k_q^T in the range 3.5-20 x 10^8 M^{-1} s^{-1}. When NP was the quencher, fits to equation (2.9) were not very good, especially at higher NP concentrations. Nevertheless, k_q^T values were determined using these data. For the DMS quencher, k_q^T values were measured for only **1a** and **1b** and the values obtained were in the range 1-2 x 10^9 M^{-1} s^{-1}. As mentioned earlier, triplet energies of **1a-b** were calculated from the 0,0 band in the phosphorescence spectra. For **1c-e**, the triplet energy is assumed to be the same as that of **1b**. Using these values, free energy for electron transfer (ΔG_{et}^T) from the hydrocarbons to the triplet excited states of **1a-d** were calculated using the Weller equation. The triplet energies, free energies of electron transfer to the triplet states and the bimolecular quenching rate constants for the pyrylium salts **1a-d** are presented in Table 2.6. Note from

Table 2.6 that ΔG_{et}^{T} values obtained are in the range -1.4 to -10.6 kcal M^{-1}. ΔG_{et}^{T} values are only weakly exothermic and lie in the normal region according to Marcus theory. Consequently, the quenching rate constants are all low (3.5-20 x 10^8 M^{-1} s^{-1}) and there is a good correlation between ΔG_{et}^{T} and k_q^{T} values in these cases.

Table 2.6 Triplet energies ($E_{0,0}^{T}$), free energies of electron transfer to the triplet state (ΔG_{et}^{T}), and triplet quenching rate constants (k_q^{T}) for the pyrylium salts 1a-d in acetonitrile solution.

Compound	$E_{0,0}^{T}$, kcal M^{-1}	Biphenyl		Naphthalene	
		ΔG_{et}^{T}, kcal M^{-1}	k_q^{T}, $M^{-1}s^{-1}$	ΔG_{et}^{T}, kcal M^{-1}	k_q^{T}, $M^{-1}s^{-1}$
1a	63.13	-6.9	1.8×10^{9}	-10.6	1.1×10^{10}
1b	61.11	-1.6	9.4×10^{8}	-5.3	8.5×10^{9}
1c	61.11	-1.4	9.9×10^{8}	-5.1	8.4×10^{9}
1d	61.11	-1.4	8.2×10^{8}	-5.1	8.3×10^{9}

At the very low concentration used for these studies (4×10^{-4} M), quenching of the singlets of **1a-e** by the quenchers are negligible (2-7% for **1a** and somewhat lower for other substrates, based on K_{SV} values). Hence transient absorption spectra recorded under these conditions is expected to give us information about the intermediates involved in the triplet quenching reaction. The transient absorption spectra of **1a** in the presence of DMS (2×10^{-4} M) obtained at

different time intervals, following the laser pulse are shown in Figure 2.10. The spectrum, immediately following the pulse, showed mainly the absorption due to the triplet at 440 nm. The absorption at 520 nm is identical to the $DMS^{\cdot-}$ absorption reported in the literature.[56] The growth of this absorption was concomitant with the decay of the triplet absorption. The insets in Figure 2.10 clearly show the decay of the triplet and concomitant growth of the radical cation. It is clear from Figure 2.10 that the decay of the triplet directly leads to the formation of radical ions by an electron transfer mechanism. The absorption due to the pyranyl radical was not observed in this case, most probably due to the low extinction coefficients of these absorptions (vide infra).

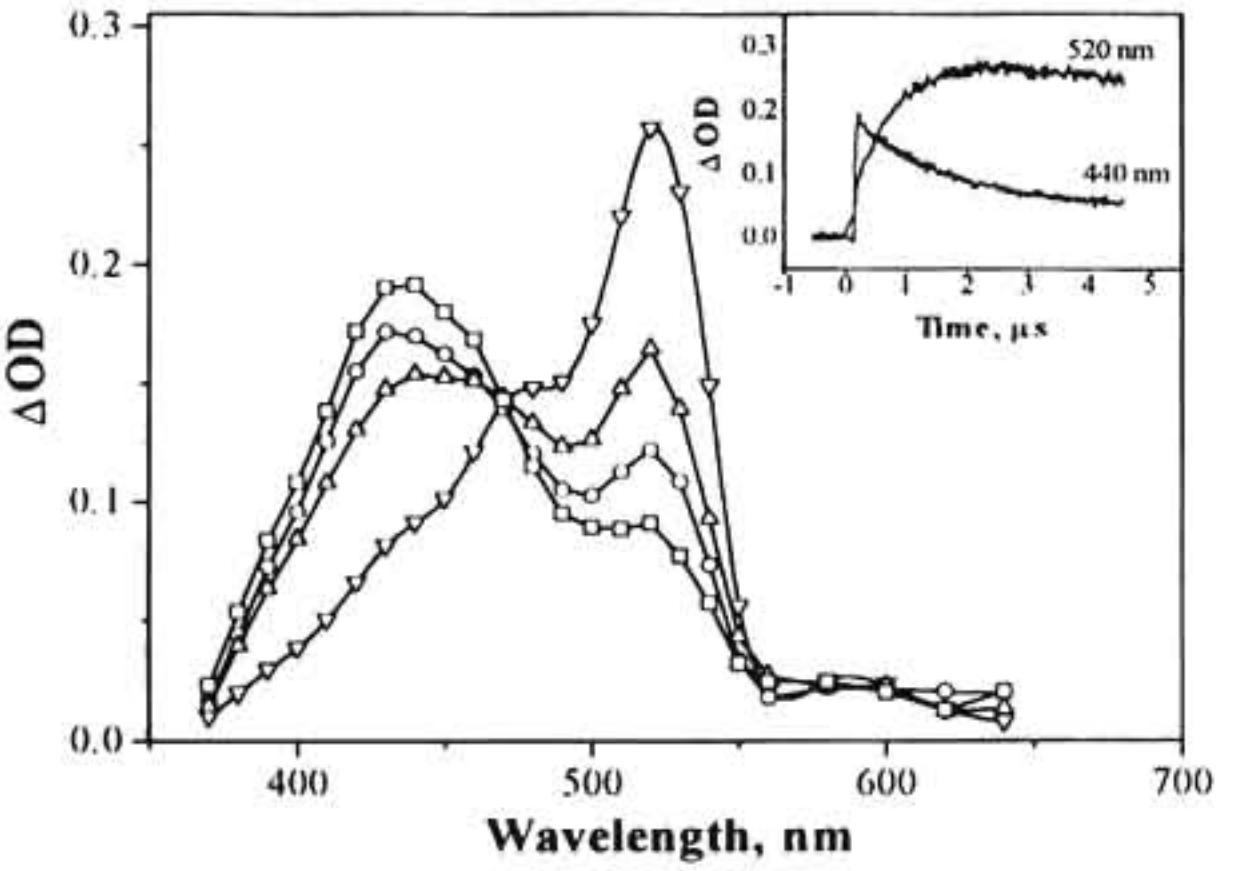

Figure 2.10 Transient absorption spectra at (■) 0.2, (O) 0.35, (Δ) 0.55 and (▽) 2 μs, following the 355 nm laser pulse excitation of **1a** (2×10^{-4} M) in the presence of 4,4'-dimethoxystilbene (2×10^{-4} M) in acetonitrile. Inset shows the decay of the transient at 440 nm and growth at 520 nm.

Transient absorption spectra of **1a** recorded in the presence of NP and BP (10^{-4} M) also showed peaks at 440 nm due to the triplets and very weak absorptions above 650 nm corresponding to the radical cations of the donors. A growth of the radical cation, however, is not observed in these cases. This is again attributed to the lower extinction coefficients of the radicals, compared to those of the triplets. In the case of DMS, the growth becomes very noticeable because of the very high extinction coefficient of $DMS^{\bullet+}$ ($\varepsilon = 65{,}000\ M^{-1}\ cm^{-1}$)[56]

Singlet quenching experiments. Transient absorption spectra of **1a-f** were recorded in the presence of 0.1 M biphenyl and naphthalene. Transient absorption spectrum in the presence of DMS at high concentrations was not recorded because this compound has substantial absorption at 355 nm under these conditions. At 0.1 M concentration of BP, more than 90% of the singlets of **1a-f** were quenched by BP. The transient absorption spectra obtained in the case of **1a** and **1c** are shown in Figures 2.11 and 2.12, respectively.

In the case of **1a-f**, the transient spectra in the presence of BP (0.1 M) were characterized by absorptions at 385 nm and at 680 nm. The 680 nm peak is due to the well known BP radical cation ($BP^{\bullet+}$)[56] and hence we assign the 385 nm peak to the pyranyl radicals formed as a result of electron transfer as per equation (2.7). According to equation (2.7), the concentration of $BP^{\bullet+}$ should be the same as the concentration of pyranyl radical formed. This enabled us to determine the extinction coefficients of the radical absorptions using equation (2.10).

$$\varepsilon_{PY^{\bullet}} = \frac{\Delta OD_{PY^{\bullet}} \cdot \varepsilon_{BP^{\bullet+}}}{\Delta OD_{BP^{\bullet+}}} \qquad (2.10)$$

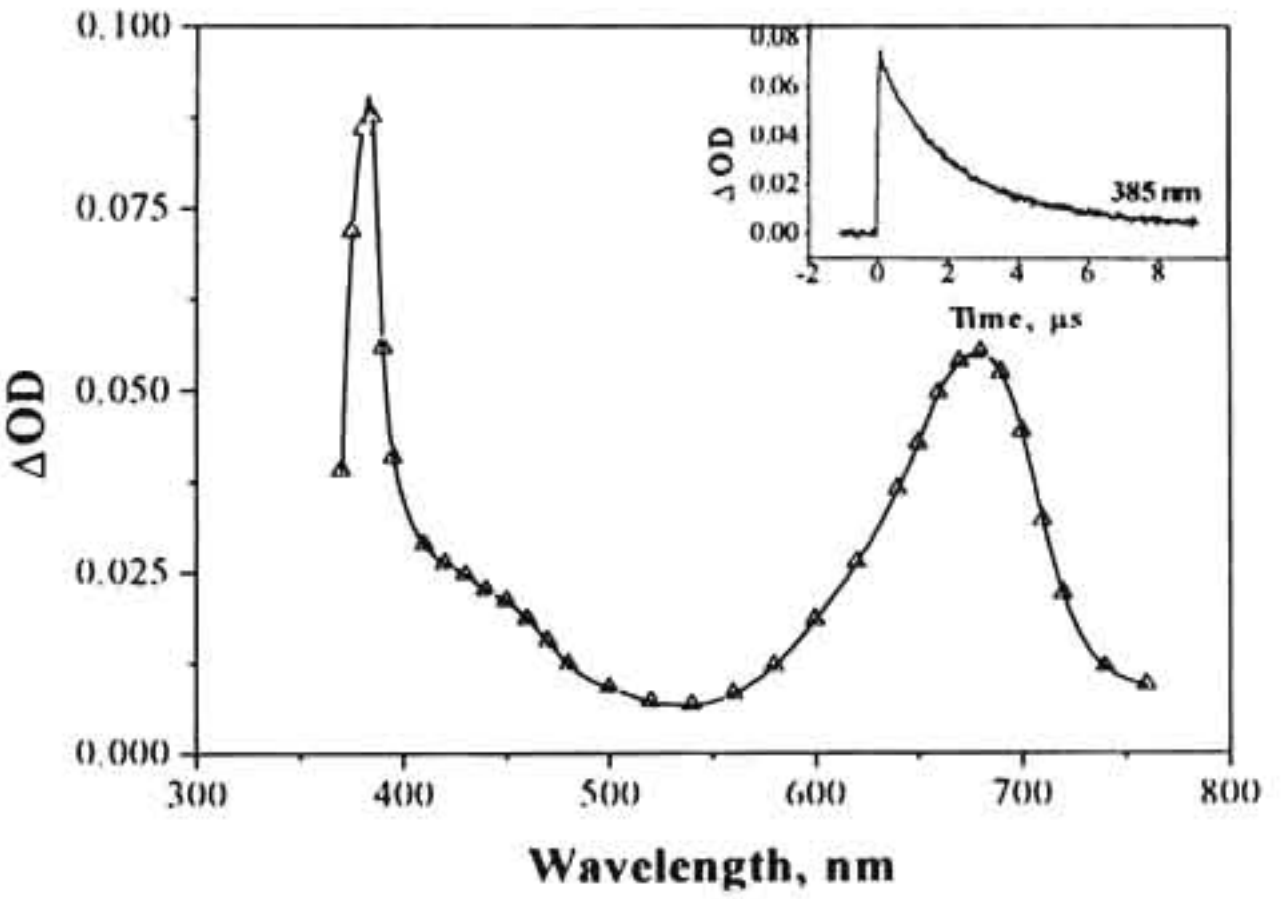

Figure 2.11 Transient absorption spectrum of **1a** (2×10^{-4} M) in the presence of biphenyl (0.1 M) at 200 ns following the laser pulse. Inset shows the decay of the transient at 385 nm.

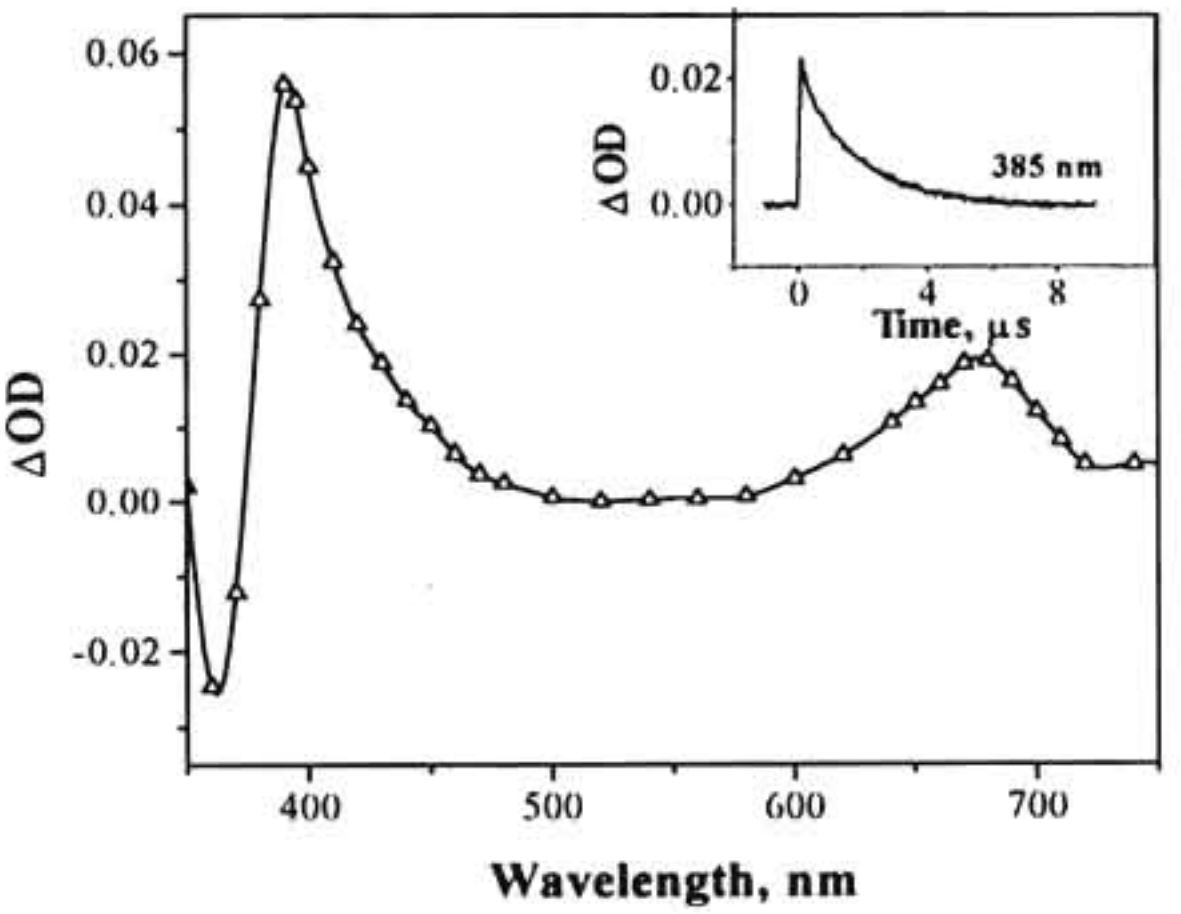

Figure 2.12 Transient absorption spectrum of **1c** (2×10^{-4} M) in the presence of biphenyl (0.1 M) at 200 ns after the laser pulse. The inset shows the decay of the transient at 385 nm.

In equation (2.10), ε's are the extinction coefficients and ΔOD's are the end-of-pulse optical densities at the corresponding absorption maxima. A value of 14.5 x 10^3 M^{-1} cm^{-1} for the extinction coefficient of $BP^{\bullet+}$ was used in the calculation.[56]

The decay of the radical ions followed second order kinetics. Since no long-lived absorptions due to product formation were observed, it was assumed that decay occurs by BET. Monitoring the decay of $BP^{\bullet+}$ at 680 nm, the decay rates were calculated by second order equal concentration kinetics. The value of the rate constant obtained (= k_2/ε) were in the range 1-1.2 x 10^7 cm s^{-1}. Substituting for ε, we get k_2 in the range 1.5 x 10^{11} M^{-1} s^{-1}. This value is an order of magnitude slower compared to the BET rates in DCN/BP system studied under identical conditions.

With BP as the donor, the yields of the radicals (Φ_{ion}) in the case of **1a-f** were determined as follows. Optically matched solutions of benzophenone in benzene (actinometer) and of pyrylium salts containing BP (0.1 M) in acetonitrile were deaerated and flash photolysed at 355 nm. Φ_{ion} were then calculated according to the equation (2.11).

$$\Phi_{ion} = \Phi_T^R \frac{\Delta OD_{BP^{\bullet+}}\ \varepsilon_T^R}{\Delta OD_T^R\ \varepsilon_{BP^{\bullet+}}} \qquad (2.11)$$

In equation (2.11), ΔOD's are the end-of-pulse absorbance changes, ε's are the extinction coefficients. 'R' refers to the reference compound benzophenone. From the known values of Φ_T^R, ε_T^R and $\varepsilon_{BP^{\bullet+}}$ (vide supra), Φ_{ion} values were calculated. Table 2.7 summarizes the absorption maxima, extinction coefficients and quantum yield of pyranyl radicals formed from **1a-f**.

The Φ_{ion} values obtained are much larger than those observed for similar cationic sensitizers.[59,60] The pyrylium derivatives **1a** and **1f** exhibits much higher Φ_{ion} values than **1b-e**. We believe that the primary factor responsible for the high values of Φ_{ion} in these cases is the higher triplet yields. It is well established that electron transfer involving triplet excited states leads to efficient separation of ion pairs.[61,62] This is a consequence of the fact that recombination in the geminate triplet radical pair to regenerate the starting materials is spin forbidden. An inspection of Tables 2.4 and 2.7 shows that there is good correlation between the triplet yields and Φ_{ion} values.

Table 2.7 Absorption maxima (λ_{max}^{R}), extinction coefficients (ε_{max}^{R}) and quantum yields of formation (Φ_{ion}) for the pyranyl radicals obtained from 1a-c.

Compound	λ_{max}^{R} nm	ε_{max}^{R} $M^{-1}cm^{-1}$	Φ_{ion}
1a	385	1.9×10^4	0.42
1b	385	2.6×10^4	0.20
1c	385	2.6×10^4	0.17
1d	385	2.5×10^4	0.19
1f	385	2.0×10^4	0.52

In contrast to the behavior of BP, the transient absorption spectra of **1a-e**, in the presence of NP (0.1 M) in acetonitrile did not show absorptions due to $NP^{\cdot}$ at 660 nm or the pyranyl radicals at 385 nm. Instead, the transient absorption spectrum showed maxima at 460 and 560 nm (Figure 2.13). These absorptions were observed within the laser pulse. The absorptions have slightly different decay rates, with the 460 nm species decaying faster than the 560 nm species. Addition of $LiClO_4$ (0.1 M) or saturating the solution with oxygen did not lead to any noticeable change in the spectra. Decay rates were marginally affected by the presence of oxygen. The spectrum in dichloromethane, however, was slightly different (Figure 2.13). In this case, the 560 nm peak was much more intense compared to the 460 nm peak.

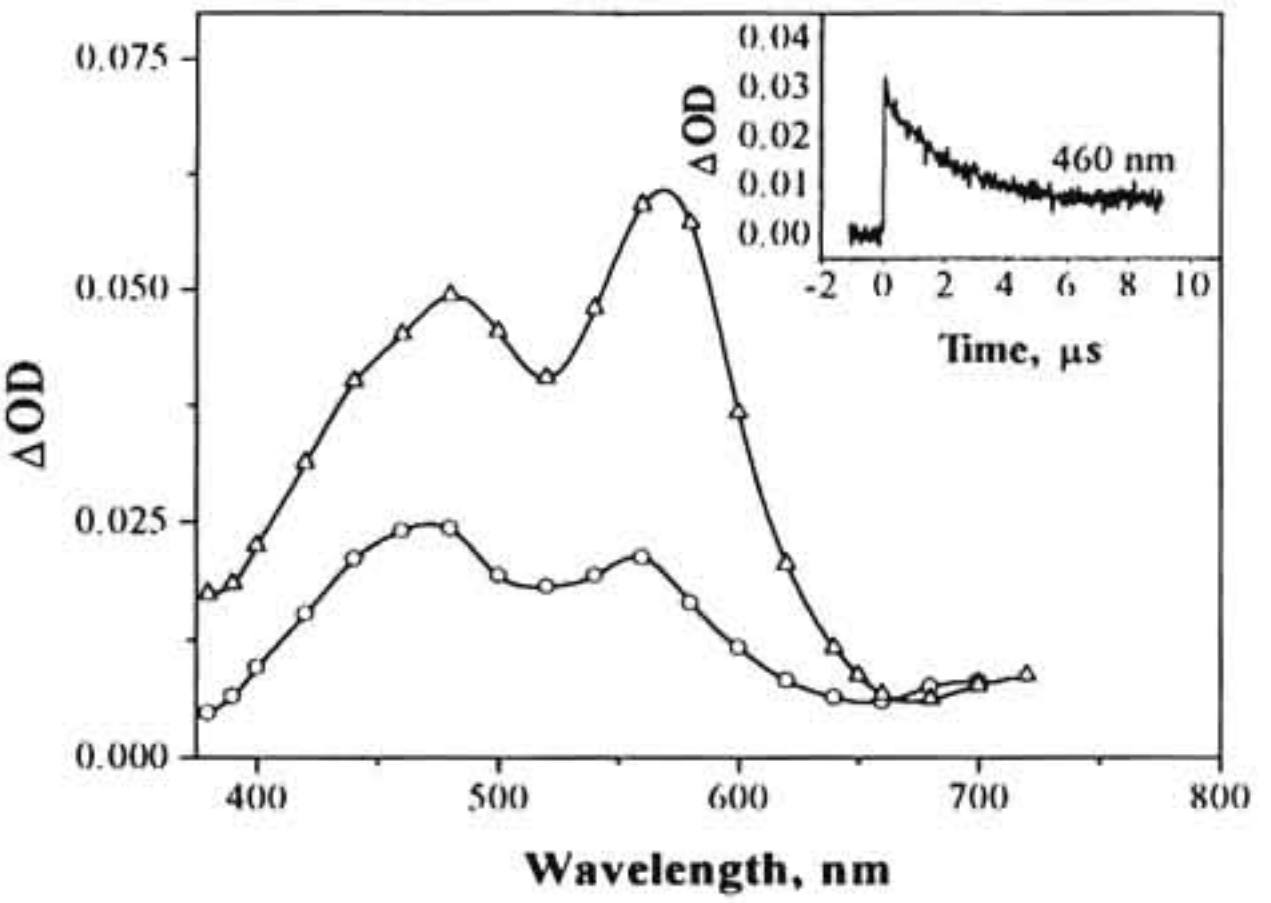

Figure 2.13 Transient absorption spectra of **1a** (2×10^{-4} M) at 300 ns after the laser pulse in the presence of naphthalene (0.1 M) in (O) acetonitrile and (Δ) in dichloromethane. Inset shows the decay of the transient at 460 nm in acetonitrile.

In the case of **1a**/NP system, irradiation leads to the excitation of the CT complex. The photochemistry of CT complexes has been reviewed by several authors.[63-65] According to Mulliken's theory,[66] excitation of CT complex leads to the ion pair state. In general, three mechanistic pathways are available for the excited states of these complexes. Path I leads to the formation of the triplet state of the donor arising from a fast ISC process occurring in the non equilibrated FC state, as observed by Orbach and Ottolenghi.[63] The second pathway leads to the formation of separated ion pairs, which undergo BET in microsecond time scales.[67] The third route involves fast formation of the ion pairs which undergo extremely rapid BET (30-300 ps).[68,69] In the last case, the transient absorption will not be observed on the nanosecond time scales. In the present case of **1a**/NP system, the first two pathways can be ruled out due to the lack of spectroscopic evidence (absorptions due to radicals or triplets are not detected in these experiments).

In a similar study, Lin and Schuster have shown that 2,6-di-*tert*-butyl-6-arylpyrylium cation forms CT complex, when 2-naphthalenesulfonate anion was used as the counter ion.[22] Excitation of this CT complex in dimethyl carbonate solution led to the formation of ion radicals as evidenced by the absorptions at 485 nm (pyranyl radical) and 650 nm (naphthalene radical cation). These radicals were short-lived and decayed to the ground state by BET within 330 ps. In the present case we did not see the absorptions due to the radicals, most probably due to the short lifetime of this ion pair singlet state. A fraction of these ions decays to the observed transient species (Figure 2.13) and we assign this species as the triplet excited state of the CT complex.

It is widely recognized (based on the enhancement of phosphorescence in CT complexes) that intermolecular CT interactions may provide a general mechanism for the induction of spin-orbit coupling, leading to triplet formation.[70,71] Lim et al.[72] suggested a 'selection rule' for ISC in CT complexes which states that, effective ISC to the $^3(CT)^\bullet$ state requires a locally excited triplet state, $^3LE^\bullet$, in proximity to the CT singlet state. In the light of these studies, we assign the 460 nm species to a LE triplet state and the 560 nm species to the $^3(CT)^\bullet$. The $^3LE^\bullet$ has the excitation localized more on the pyrylium moiety. This assignment is supported by the fact in dichloromethane solution, where the CT complex is more rigid, the absorption due to the $^3(CT)^\bullet$ at 560 nm is much more intense than that at 460 nm due to $^3LE^\bullet$. In these experiments, we have noted that decay of these species leads to small residual absorptions indicating the formation of products at longer time scales. However, the transient absorption spectra recorded at long delay times were very weak and definite assignment could not be made. We believe that a major fraction of the triplet excited states of the CT complex decays to the ground state to regenerate the starting materials.

2.3.2. Thiopyrylium derivatives 2a-d

2.3.2.1. Absorption spectra

Thiopyrylium derivatives **2a-d** also exhibit two absorption bands in the UV-Visible region. Figure 2.14 shows the absorption spectra of **2a** and **2b** in acetonitrile solution. Spectroscopic properties of **2c** and **2d** were similar to those of **2b**. The spectra are red shifted by ~20 nm in dichloromethane solution. Table 2.8 summarizes the absorption properties of **2a-d**. From a comparison of Tables 2.1. and 2.8. we can make the following conclusions.

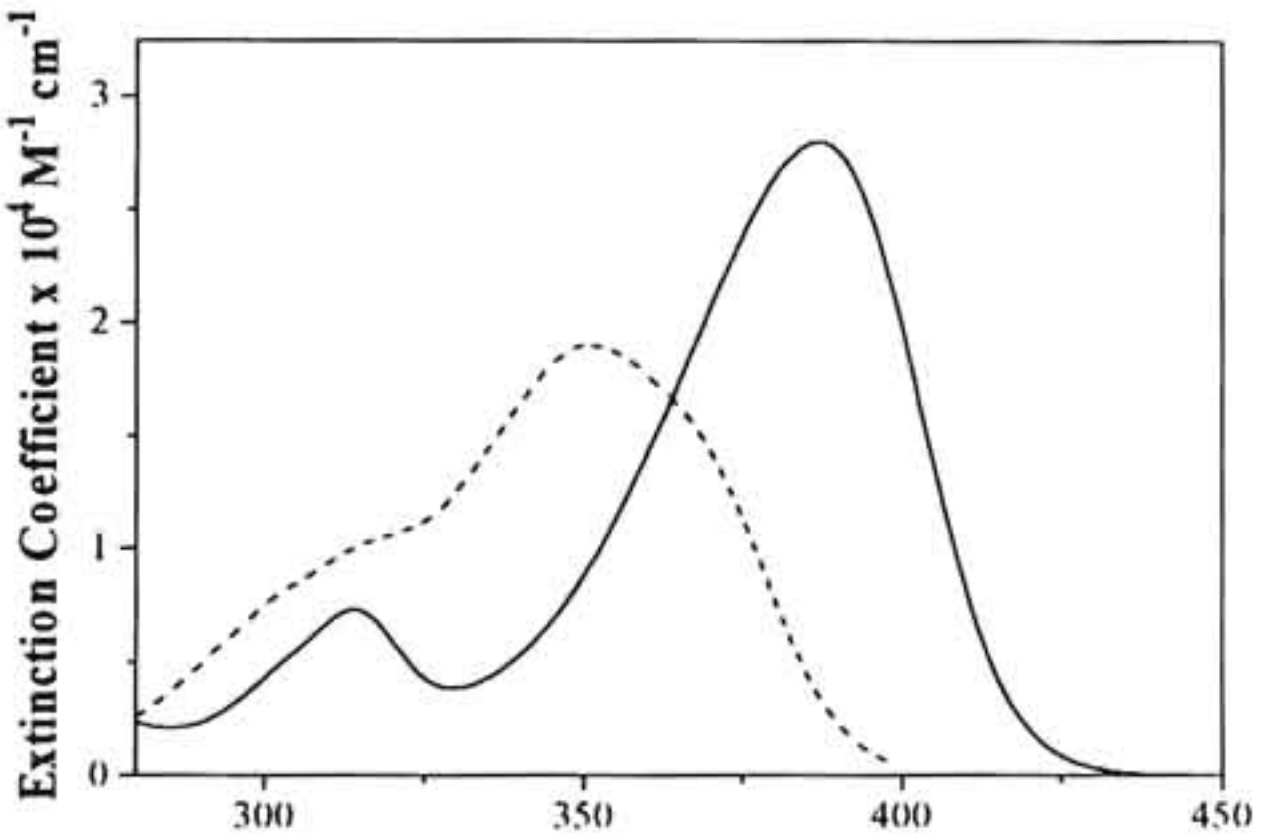

Figure 2.14 Absorption spectra of **2a** (----) and **2b** (—) in dichloromethane.

Table 2.8 Absorption maxima (λ_{max}), extinction coefficients (ε_{max}), and full width at half maximum (FWHM) values for thiopyrylium salts 2a-d in dichloromethane. Values in parenthesis are those obtained in acetonitrile.

Compound	λ_{max}, nm	ε_{max}, $M^{-1} cm^{-1}$	FWRE, cm^{-1}
2a	350 (335)	1.9×10^4 (1.88×10^4)	7289
2b	387 (365)	2.8×10^4 (2.5×10^4)	4211
2c	387 (365)	2.7×10^4 (2.5×10^4)	4211
2d	387 (365)	2.7×10^4 (2.5×10^4)	4443

(1) The long wavelength absorption of **2a** is a superposition of the $S_0 \rightarrow S_1$ band and $S_0 \rightarrow S_2$ band as in the case of **1a**, (2) these band positions are reversed in **2b-d** and (3) the 4-phenyl ring in **2a** is more twisted in the ground state compared to those in **2b-d**.

2.3.2.2. Emission properties

Thiopyrylium derivatives **2a-d** exhibit emission in the 350-650 nm range. The fluorescence spectra of **2a** and **2b** in acetonitrile are shown in Figure 2.15. The emission maxima are blue shifted in dichloromethane by ~30 nm.

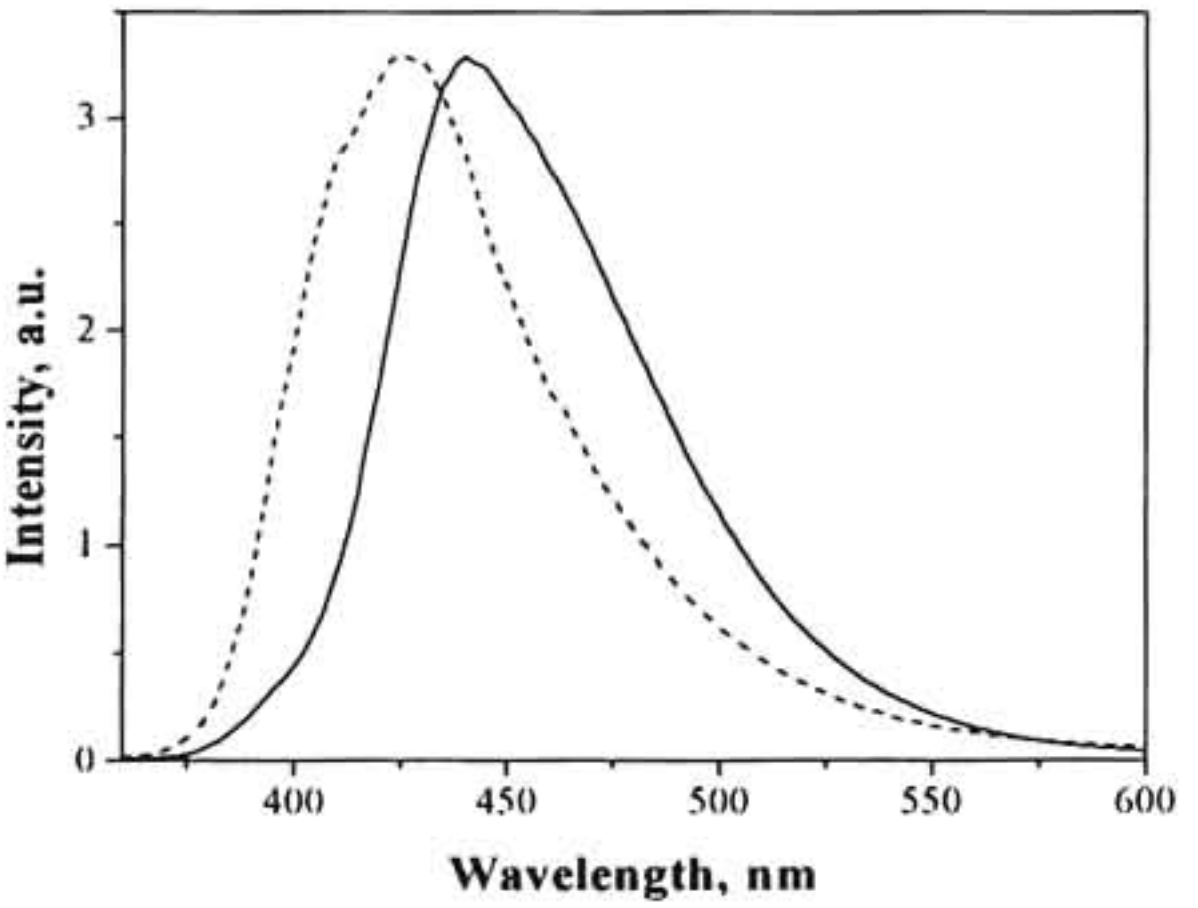

Figure 2.15 Normalized emission spectra of **2a** (----) and **2b** (—) in dichloromethane.

As in the case of **1a-f**, all the fluorescence parameters were determined for **2a-d** in two solvents and the data are presented in Table 2.9. A comparison of data

in Tables 2.2 and 2.9 shows that **2b-d** have similar fluorescence properties as **1b-d**, and we suggest a planar S1 state in these cases. **2a** exhibits some similarities with **1a**, but there are differences as well. For example, the Stokes shift observed for **2a** is small compared to **1a**. But Φ_f and τ_f values are very similar to that of **1a** in both solvents. These similarities prompted us to believe that, as in the case of **1a**, the lowest excited state of **2a** has some TICT character.

Table 2.9 Emission maxima (λ_{max}), Stokes shift (ν_{st}) values, fluorescence quantum yields (Φ_f), fluorescence lifetimes (τ_f) and radiative decay rates (k_R) for thiopyrylium salts 2a-d in dichloromethane. Values in parenthesis are those obtained in acetonitrile.

Compound	λ_{max}, nm	ν_{st}, cm^{-1}	Φ_f	τ_f, ns	k_R, $10^6\ s^{-1}$
2a	428 (471)	5207 (8619)	0.029 (0.07)	0.62 (12.3)	46.8 (5.7)
2b	440 (471)	3112 (6166)	0. 35 (0.34)	3.8 (5.1)	92.1 (66.7)
2c	445 (471)	3367 (6166)	0.45 (0.46)	3.6 (5.8)	125.0 (79.3)
2d	445 (471)	3367 (6166)	0.44 (0.45)	3.5 (5.7)	125.7 (78.9)

The phosphorescence emission spectra of **2a** and **2b** are given in Figure 2.16. The spectra differ from those of **1a,b** in the position and intensity of the

0,0 band. The 0,0 band occurs at shorter wavelengths and hence **2a** and **2b** have higher triplet energies compared to **1a** and **1b.** Since **2b-d** has similar spectroscopic properties, the triplet energies of **2c** and **2d** were assumed to be the same as that of **2b**.

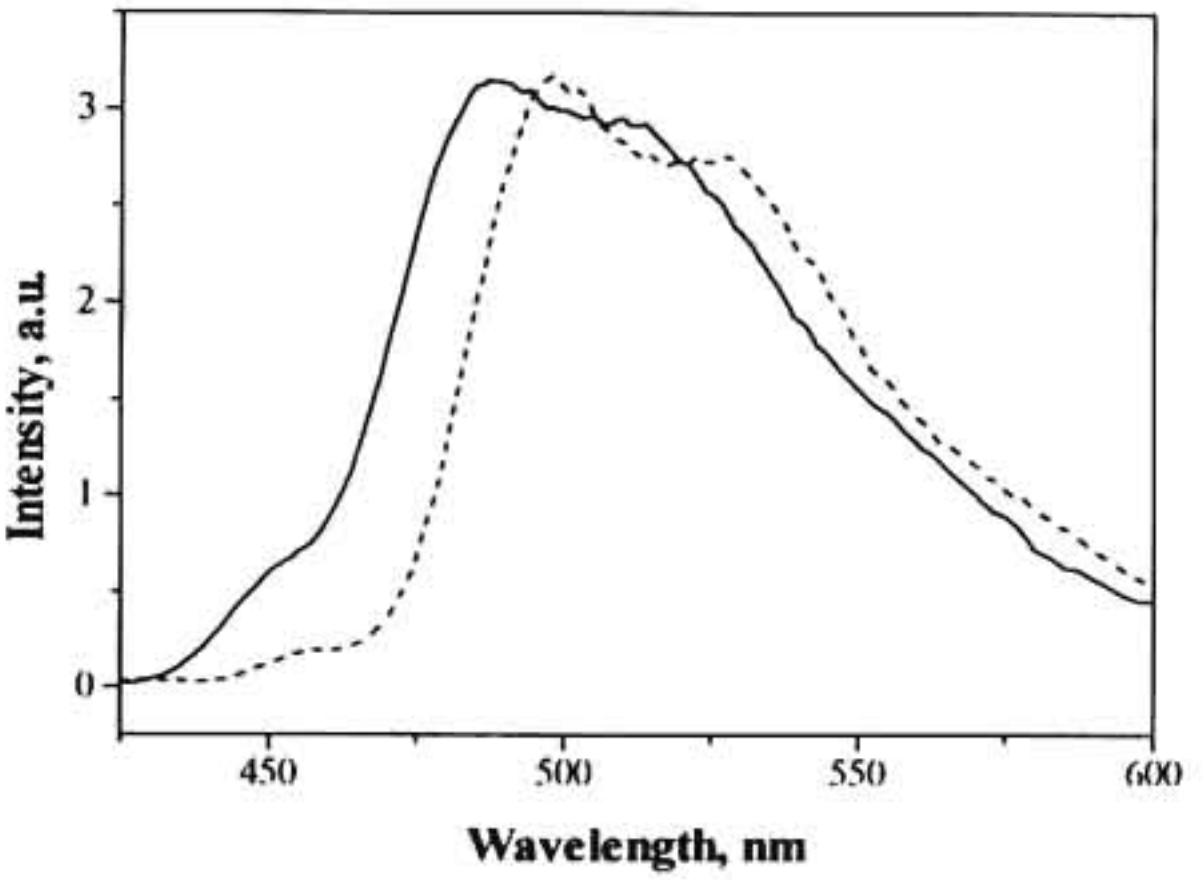

Figure 2.16 Normalized phosphorescence spectra of **2a** (—) and **2b** (----) in glycerol glass at 77 K.

2.3.2.3. Laser flash photolysis studies

Laser flash photolysis of **2a-d** in degassed dichloromethane or acetonitrile led to the formation of transients, which are assigned to the triplets of these molecules. Representative triplet-triplet absorption spectra are shown in Figure 2.17 The T-T absorption maxima are red shifted for these compounds compared to their oxygen analogs by ~30 nm. As in the case of the pyrylium derivatives **1a-d**, all triplet state parameters were determined for **2a-d** and the

data are collected in Table 2.10. One can note the close analogy between **1a** and **2a** here also. In accordance with the assignment made in the case of **1a**, the higher triplet quantum yield of **2a** was assigned to the presence of a TICT state. Except for **2a**, all other thiopyrylium derivatives have higher triplet quantum yields compared to their oxygen analogs. This most probably is due to the presence of the sulphur atom, which is considered as a 'heavy atom'. Thus, increased triplet yields for the thiopyrylium derivatives are attributed to an internal heavy atom effect. Others have made similar observations in the past.[36,73]

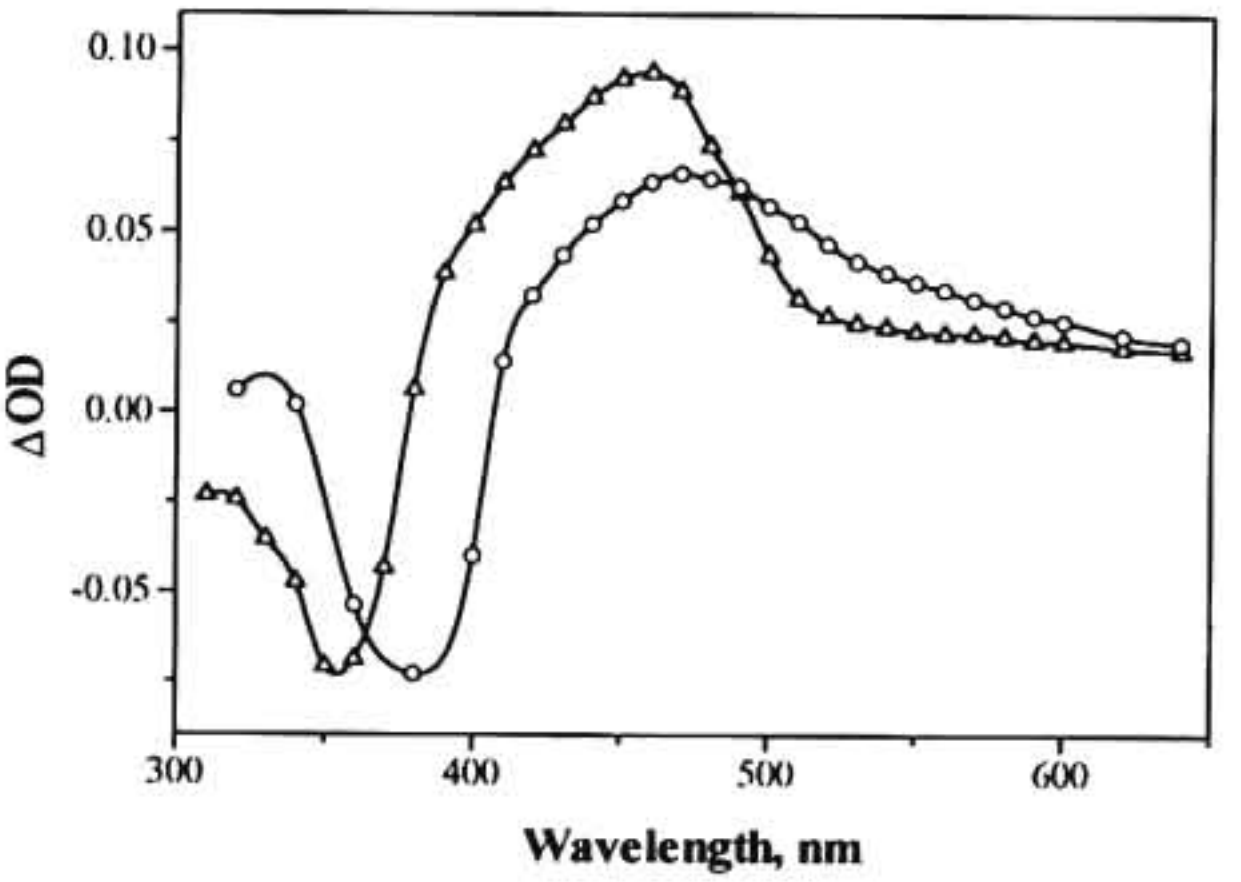

Figure 2.17 Transient absorption spectra of **2a** (Δ) and of **2c** (O) in dichloromethane recorded at 100 ns after the laser pulse, respectively.

Table 2.10 Triplet-triplet absorption maxima (λ^{T}_{max}), extinction Coefficients (ε^{T}_{max}), triplet quantum yields (Φ_T), triplet lifetimes (τ_T) and oxygen quenching rate constants ($k_q(O_2)$) for thiopyrylium derivatives 2a-d in dichloromethane solution.

Compound	λ^{T}_{max}(Abs), nm	ε^{T}_{max}(Abs), M^{-1} cm^{-1}	Φ_T	τ_T µs	$k_q(O_2)$ M^{-1} s^{-1}
2a	460	2.2×10^4	0.44	2.9	9.9×10^7
2b	470	1.4×10^4	0.30	3.0	3.8×10^7
2c	470	1.4×10^4	0.30	3.0	3.7×10^7
2d	470	1.6×10^4	0.32	3.0	3.9×10^7

2.3.2.4. Electron transfer studies

Fluorescence quenching studies: Fluorescence of **2a-d** were quenched efficiently by electron rich hydrocarbons such as BP and NP. We have noticed the formation of CT complex between NP and **2a-d**. The quenching rate constants were determined using the Stern–Volmer treatment. From the known values of the oxidation potentials of the donors and the measured values of the reduction potentials of **2a-d**, the free energies of singlet quenching were calculated. These data are presented in Table 2.11. ΔG_{et} values ranged between -12.4 to -20 kcal M^{-1}. Hence we expected diffusion controlled quenching rates in all cases. However, k_q^s obtained for **2a** was much smaller. For others the values were in the diffusion controlled range.

Table 2.11 Excitation energies ($E_{0,0}$), reduction potentials (E_{red}), free energies of electron transfer to the singlet state (ΔG_{et}^{S}), Stern-Volmer quenching constants (K_{SV}) and singlet quenching rate constants (k_q^{S}) for the thiopyrylium dalts 2a-d in acetonitrile solution.

Compound	$E_{0,0}$ kcal mol^{-1}	E_{red}, V *vs.* SCE	Biphenyl			Naphthalene		
			ΔG_{et}^{S}, kcal M^{-1}	K_{SV}, M^{-1}	k_q^{S}, M^{-1} s^{-1}	ΔG_{et}^{S}, kcal M^{-1}	K_{SV}, M^{-1}	k_q^{S}, M^{-1} s^{-1}
2a	74.8	-0.57	-16.1	48	3.9×10^{9}	-20.0	57	4.6×10^{9}
2b	70.3	-0.55	-12.4	67	1.3×10^{10}	-16.1	97	1.9×10^{10}
2c	71.0	-0.58	-12.4	80	1.4×10^{10}	-16.1	91	1.6×10^{10}
2d	70.9	-0.57	-12.4	73	1.3×10^{10}	-16.1	83	1.5×10^{10}

Laser flash photolysis studies: Rate constants for the quenching of the triplets of **2a-d** by BP and NP were measured as in the case of the pyrylium salts. The rate constants obtained, along with the calculated ΔG_{et} values for triplet quenching rates, are presented in Table 2.12. Because of ground state CT formation, the data for NP could not be fitted properly. The higher quenching rates obtained for NP may be due to the CT formation. ΔG_{et} values are only moderately exothermic and consequently, k_q^{T} values are lower than the diffusion controlled rates.

Table 2.12 Triplet energies ($E_{0,0}^{T}$), free energies of electron transfer to the triplet state (ΔG_{el}^{T}), and triplet quenching rate constants (k_q^{T}) for the thiopyrylium salts 2a-d in acetonitrile solution.

Compound	$E_{0,0}^{T}$, kcal mol^{-1}	Biphenyl		Naphthalene	
		ΔG_{el}^{T}, kcal M^{-1}	k_q^{T}, M^{-1}s^{-1}	ΔG_{el}^{T}, kcal M^{-1}	k_q^{T}, M^{-1}s^{-1}
2a	64.27	-5.9	9.4×10^{9}	-9.6	1.1×10^{10}
2b	64.45	-6.6	4.9×10^{8}	-10.3	1.0×10^{9}
2c	-	-5.9	2.6×10^{8}	-9.8	1.1×10^{9}
2d	-	-6.1	3.4×10^{8}	-9.6	1.0×10^{9}

Laser flash photolysis of **2a-d** were carried out in the presence of higher concentrations of BP and NP. Transient absorption spectra in the presence of BP showed the biphenyl radical cation at 680 nm and the thiopyranyl radical in the 385-430 nm region. A representative example is given in Figure 2.18. As in the case of the pyranyl radicals, the extinction coefficients and quantum yields of formation of the thiopyranyl radicals were determined by relative actinometry. These values, along with the thiopyranyl radical absorption maxima, are presented in Table 2.13. When NP was the quencher, laser flash photolysis did not lead to the formation of radicals. As in the case of **1a** (see Figure 2.13) we obtained transient absorption with maxima at 480 and 560 nm. In accordance with the

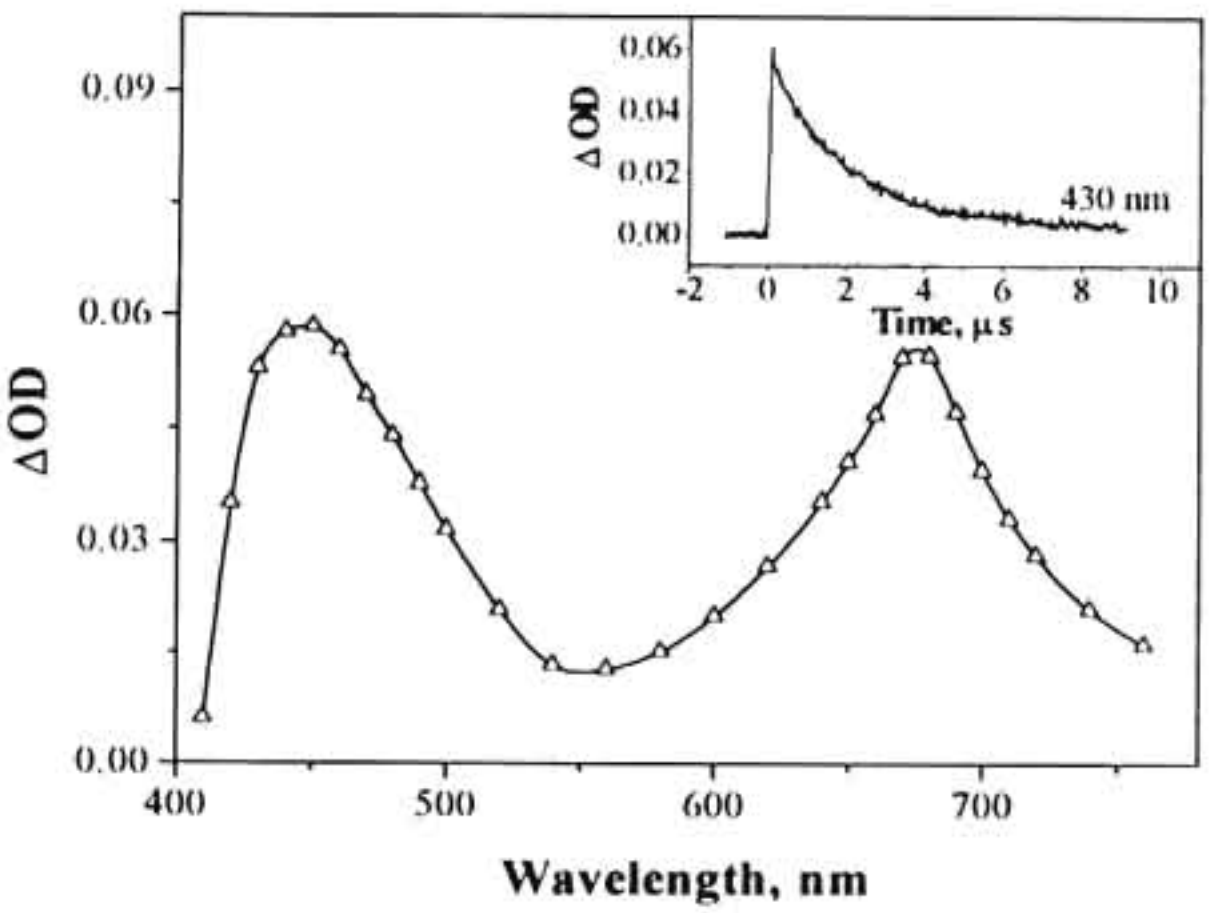

Figure 2.18 Transient absorption spectrum of **2c** (2×10^{-4} M) in the presence of biphenyl (0.1 M) at 200 ns after the laser pulse. The inset shows the decay of the transient at 430 nm.

Table 2.13 Absorption Maxima (λ_{max}^{R}), Extinction Coefficients (ε_{max}^{R}) and Quantum Yields of Formation (Φ_{ion}) for the Thiopyranyl Radicals obtained from 2a-d.

Compound	λ_{max}^{R} nm	ε_{max}^{R} M^{-1} cm^{-1}	Φ_{ion}
2a	385	2.2×10^{4}	0.51
2b	430	1.4×10^{4}	0.38
2c	430	1.4×10^{4}	0.35
2d	430	1.6×10^{4}	0.35

assignments made in the case of **1a**/NP system, these absorption bands were assigned to the ^{3}(LE)* and ^{3}(CT)* state, respectively.

An inspection of Table 2.13 reveals that Φ_{ion} value obtained for **2a** is higher compared to those obtained for **2b-d**, and this is attributed to the higher triplet yield of **2a.** Compared to the oxygen analogs **1a-d** (Table 2.7), **2a-d** showed higher Φ_{ion} values. A major factor responsible for the variation in the Φ_{ion} values is the relative stability of the pyranyl and thiopyranyl radicals. For example, Niizuma and coworkers have studied the formation of pyranyl and thiopyranyl radicals by photoillumination of several pyrylium and thiopyrylium salts in THF solution.[74,75] They have observed high Φ_{ion} values for the thio- derivatives compared to the oxygen analogs. They also observed that electron- donating substituents decrease the Φ_{ion} values. These authors have suggested that electron-donating substituents destabilize the lowest unoccupied molecular orbital (LUMO) of the cation and as a consequence, destabilize the highest occupied molecular orbital (HOMO) of the radical. This argument is supported by the observation that pyrylium salts substituted with electron donating groups have a higher absolute value of reduction potentials.[50,54] Comparing the pyranyl and thiopyranyl radicals, the oxygen atom destabilizes the radical more than what sulfur does, and hence the radical yields will be lower in the case of pyrylium salts. The Φ_{ion} values that we have observed are also in tune with these observations.

In this Chapter, we have described the photophysical and electron transfer properties of a group of pyrylium salts and their sulphur analogs. Our aim has been to determine the efficiency of radical ion formation and relate this to structural factors. The studies showed that these compounds are good electron

acceptors in their singlet and triplet excited states. Efficiencies of ion pair formation were much better compared to xanthenium and thioxanthenium cations studied earlier.[59,60] The BET rates were low compared to DCN sensitized PET reactions carried out under similar conditions. Our studies also suggest a direct correlation between the triplet yields and ion yields in these compounds. Increasing the twist or nonplanarity in the pyrylium molecule increases the triplet quantum yield. This aspect is further examined in Chapter 3, where, we have cited examples of increased steric bulk of the 4-substituent hoping that this would lead to enhanced intersystem crossing yields. Another aspect we have noted is that, formation of a CT complex leads to quenching of excited state without formation of ion pairs. For pyrylium and thiopyrylium salts, CT formation was observed with planar donor molecules such as naphthalene. Disruption of the planarity of the pyrylium moiety also, in principle, should reduce the chances of CT formation. Pyrylium salts with bulky substituents in the 4-position or *tert*-butyl groups in the 2- and 6 positions, therefore, are expected to reduce CT formation and enhance the yield of radical ion formation. Some of these aspects are addressed in Chapter 3.

2.4. Experimental

Measurements: All melting points are uncorrected and were determined on a Büchi Model 530 melting point apparatus. IR spectra were recorded on a Perkin Elmer Model 882 IR spectrometer. ^{1}H NMR spectra were recorded on a JEOL EX-90 spectrometer. Mass spectra (FAB) were recorded on a JEOL JMS AX503 mass spectrometer. The absorption spectra were recorded on a Shimadzu UV-2100 or a GBC double beam UV-VIS spectrophotometer. Fluorescence spectra were recorded on a SPEX Fluorolog F 112X spectrofluorimeter with a right angle

geometry using 1 x 10^{-5} M solutions. Phosphorescence spectra of the compounds in glycerol glass at 77 K were recorded on a SPEX 1934D phosphorimeter. Fluorescence lifetimes were determined using a IBH 5000 U or a Edinburgh Instruments FL900CD single photon counting system. Electrochemical experiments were performed with a Wenking Model POS 73 potentioscan and pulse generator. Solutions of the pyrylium or thiopyrylium salts (1 x 10^{-3} M) in acetonitrile, containing 0.1 M tetra-*n*-butylammonium perchlorate as supporting electrolyte were thoroughly degassed before use. A glassy carbon electrode was used as the working electrode and a platinum gauze was used as the counter electrode. Laser flash photolysis experiments were carried out by employing an Applied Photophysics Model LKS-20 Laser Kinetic Spectrometer using GCR-12 Series Quanta Ray Nd:YAG laser. The analyzing and laser beams were fixed at right angles to each other. The laser energy was 60 mJ at 355 nm.

Materials: The pyrylium derivatives **1a-f** and thiopyrylium derivatives **2a-d** were synthesized by the general route[76] outlined in Scheme 2.1.

The appropriate Grignard reagent was prepared through the reaction of 1-(bromophenyl)alkane (20 mM) and magnesium (20 mM) in dry THF (20 mL). This reagent was added to a suspension of 2,6-dimethyl-4-pyrone (20 mM) in dry THF (50 mL) at 0 °C. The solution was allowed to warm up to room temperature and stirred for 30 minutes. Ice cold solution of 10% perchloric acid (100 mL) was added and the precipitated pyrylium salt was collected by filtration. The salt thus obtained was dissolved in dichloromethane and reprecipitated by adding ether. This process was repeated until a constant melting point was obtained.

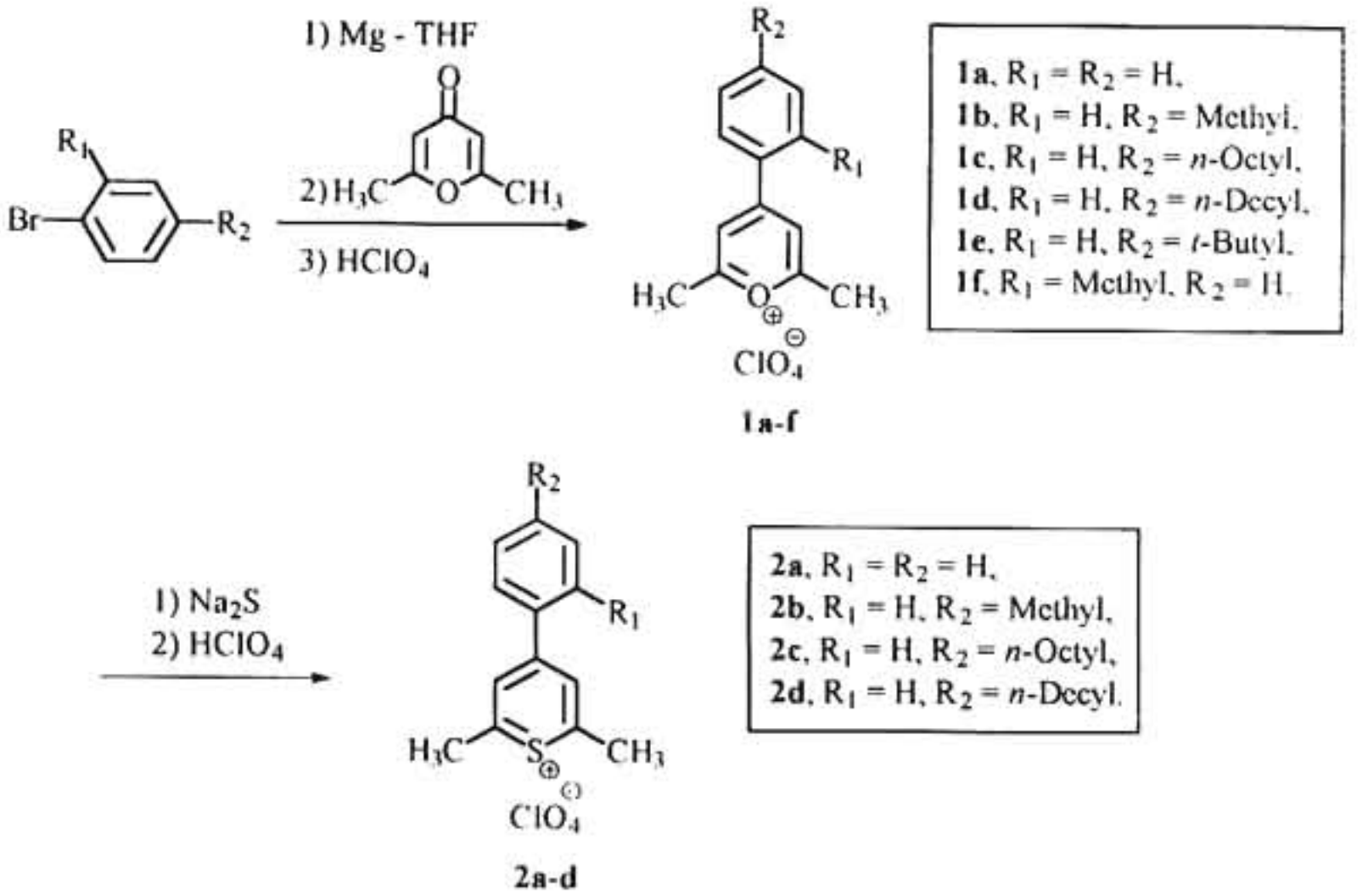

1a, $R_1 = R_2 = H$,
1b, $R_1 = H$, R_2 = Methyl,
1c, $R_1 = H$, $R_2 = n$-Octyl,
1d, $R_1 = H$, $R_2 = n$-Decyl,
1e, $R_1 = H$, $R_2 = t$-Butyl,
1f, R_1 = Methyl, $R_2 = H$.

1a-f

2a, $R_1 = R_2 = H$,
2b, $R_1 = H$, R_2 = Methyl,
2c, $R_1 = H$, $R_2 = n$-Octyl,
2d, $R_1 = H$, $R_2 = n$-Decyl.

2a-d

Scheme 2.1

2,6-Dimethyl-4-phenylpyrylium perchlorate (1a): Yield 34%; mp 224-225 °C (reported melting point 217-220 °C).[76]

2,6-Dimethyl-4-(*p*-methylphenyl)pyrylium perchlorate (1b): Yield 34%; mp 211-212 °C; IR (ν_{max}): 3094, 2931, 2860, 1643, 1092 cm^{-1}; ^1H NMR (90 MHz, $CDCl_3$), δ 2.35 (s, 3 H), 2.9 (s, 6 H), 7.3 - 8.2 (m, 6 H); Anal. Calcd for $C_{14}H_{15}O_5Cl$: C, 56.36; H, 5.07. Found: C, 56.21; H, 5.34.

2,6-Dimethyl-4-(*p*-*n*-octylphenyl)pyrylium perchlorate (1c): Yield 34%; mp 129 -130 °C; IR (ν_{max}): 3095, 2933, 2860, 1649, 1094 cm^{-1}; ^1H NMR (90 MHz, $CDCl_3$), δ 0.9 - 1.5 (m, 15 H), 2.75 (t, 2 H), 2.9 (s, 6 H), 7.3 - 8.2 (m, 6 H); HRMS

(FAB) calcd for $C_{21}H_{29}O^+$ (cation), 297.2218, found 297.2232; Anal. Calcd for $C_{21}H_{29}O_5Cl$: C, 63.61; H, 7.38. Found: C, 63.26; H, 7.77.

2,6-Dimethyl-4-(*p*-*n*-decylphenyl)pyrylium perchlorate (1d): Yield 33%; mp 131 - 132 °C; IR (ν_{max}): 3098, 2931, 2859, 1642, 1097 cm^{-1}; ^1H NMR (90 MHz, $CDCl_3$), δ 0.9 - 1.5 (m, 19 H), 2.75 (t, 2 H), 2.9 (s, 6 H), 7.3 - 8.2 (m, 6 H); HRMS (FAB) calcd for $C_{23}H_{33}O^+$ (cation), 325.2531, found 325.2530; Anal. Calcd for $C_{23}H_{33}O5Cl$: C, 65.06; H, 7.84. Found: C, 65.05; H, 8.11.

2,6-Dimethyl-4-(*p*-*t*-butylphenyl)pyrylium perchlorate (1e): Yield 16%; mp 169-170 °C; IR (ν_{max}): 3096, 2928, 1090 cm^{-1}; ^1H NMR (90 MHz, $CDCl_3$): δ 1.3 (s, 9H), 2.9 (s, 6H), 7.5 - 8.2 (m, 6H). HRMS (FAB) calcd for $C_{17}H_{21}O^+$ (cation), 241.1592, found 241.1598; Anal. Calcd for $C_{17}H_{21}O_5Cl$: C, 59.98; H, 6.22. Found: C, 59.91; H, 6.25.

2,6-Dimethyl-4-(*o*-methylphenyl)pyrylium perchlorate (1f): Yield 10%; mp 164-165 °C; IR (ν_{max}): 3082, 2931, 2868, 1088 cm^{-1}; ^1H NMR (90 MHz, $CDCl_3$): δ 2.5 (s, 3H), 3.0 (s, 6H), 7.2 - 7.8 (m, 6H). HRMS (FAB) calcd for $C_{14}H_{15}O^+$ (cation), 199.1123, found 199.1122; Anal. Calcd for $C_{14}H_{15}O_5Cl$: C, 56.36; H, 5.07. Found: C, 54.80; H, 5.00.

The thiopyrylium derivatives **2a-d** were prepared from **1a-d**. In a typical run, a solution of Na_2S (2 mM) in water (5 mL) was added to a cold solution of **1a** (1 mM) in acetone, maintained at 5 °C. The solution was allowed to stand for 30 minutes and acidified with 5 mL of 10% perchloric acid. The mixture was cooled and filtered to yield the thiopyrylium perchlorate (**2a**). Similar procedures were adopted for the preparation of **2b-d.** These were purified by repeated dissolution in dichloromethane, and followed by reprecipitation by adding ether.

2,6-Dimethyl-4-phenylthiopyrylium perchlorate (2a): Yield 66%; mp 224-225 °C; IR (ν_{max}): 3098, 2930, 1642, 1086 cm^{-1}; ^1H NMR (90 MHz, DMSO), δ 3.1 (s, 6 H), 7.3 - 8.0 (m, 5 H), 8.55 (s, 2 H).

2,6-Dimethyl-4-(*p*-methylphenyl)thiopyrylium perchlorate (2b): Yield 66%; mp 204-205 °C; IR (ν_{max}): 3098, 2930, 2860, 1644, 1090 cm^{-1}; ^1H NMR (90 MHz, $CDCl_3$), δ 2.4 (s, 3 H), 3.1 (s, 6 H), 7.3 - 7.8 (m, 4 H), 8.55 (s, 2 H); Anal. Calcd for $C_{14}H_{15}O_4SCl$: C, 53.50; H, 4.81. Found: C, 53.48; H, 5.01.

2,6-Dimethyl-4-(*p*-*n*-octylphenyl)thiopyrylium perchlorate (2c): Yield 85%; mp 78-79 °C; IR (ν_{max}): 3098, 2933, 2861, 1644, 1090 cm^{-1}; ^1H NMR (90 MHz, $CDCl_3$), δ 0.9 - 1.5 (m, 15 H), 2.7 (t, 2 H), 3.1 (s, 6 H), 7.3 - 8.0 (m, 4 H), 8.55 (s, 2 H); HRMS (FAB) calcd for $C_{21}H_{29}S^+$ (cation), 313.1990, found 313.1969; Anal. Calcd for $C_{21}H_{29}O_4SCl$: C, 61.14; H, 7.09. Found: C, 60.99; H, 7.53.

2,6-Dimethyl-4-(*p*-*n*-decylphenyl)thiopyrylium perchlorate (2d): Yield 83%; mp 82-83 °C; IR (ν_{max}): 3099, 2927, 2859, 1645, 1091 cm^{-1}; ^1H NMR (90 MHz, $CDCl_3$), δ 0.9 - 1.5 (m, 19 H), 2.7 (t, 2 H), 3.1 (s, 6 H), 7.3 - 8.0 (m, 4 H), 8.55 (s, 2 H); HRMS (FAB) calcd for $C_{23}H_{33}S^+$ (cation), 341.2303, found 341.2289; Anal. Calcd for $C_{23}H_{33}O_4SCl$: C, 62.70; H, 7.56. Found: C, 62.53; H, 8.04.

All the quenchers used were commercial samples and were recrystallized before use from suitable solvents. Spectroscopic grade solvents were used throughout and solutions for flash photolysis experiments were deaerated with argon for 15 minutes, prior to the experiments.

2. 5. References

1. Balaban, A. T.; Sahini, V. E.; Keplinger, E. *Tetrahedron* **1960**, *16*, 163.
2. Balaban, A. T.; Simon, Z. *Tetrahedron* **1962**, *18*, 315.
3. Balaban, A. T.; Simon, Z. *Rev. Roum. Chim.* **1965**, *10*, 1059.
4. Maroni-Barnaud, Y.; Maroni, P.; Simalty, M.; Madaule, Y. *Bull. Soc. Chim. Fr.* **1970**, 1398.
5. Simalty, M.; Carretto, J.; Sib, S. *Bull. Soc. Chim. Fr.* **1970**, 3920.
6. Simalty, M.; Carretto, J.; Sib, S. *Bull. Soc. Chim. Fr.* **1970**, 3926.
7. Simalty, M.; Strzelecka, H.; Khedija, H. *Tetrahedron* **1971**, *27*, 3503.
8. Khedija, H.; Strzelecka, H.; Simalty, M. *Bull. Soc. Chim. Fr.* **1972**, 3173.
9. Boyd, G. V.; Singer, N. *Tetrahedron* **1965**, *21*, 1263.
10. Singer, N.; Whittington, P. R.; Boyd, G. R. *Tetrahedron* **1970**, *26*, 3731.
11. Mistr, A.; Vávra, M.; Skoupý, J.; Zahradnik, R. *Collect. Czech. Chem. Commun.* **1972**, *37*, 1520.
12. Wilt, J. R.; Reynolds, G. A. *Tetrahedron* **1973**, *23*, 795.
13. Bigelow, R. W. *J. Chem. Phys.* **1977**, *67*, 4498.
14. Bigelow, R. W. *J. Chem. Phys.* **1980**, *73*, 3864.
15. Saeva, F. D.; Olin, G. R. *J. Am. Chem. Soc.* **1980**, *102*, 299.
16. Rullière, C.; Declemy, A.; Balaban, A. T. *Can. J. Chem.* **1985**, *63*, 191.
17. Wintgens, V.; Pouliquen, J.; Valat, P.; Kossanyi, J.; Canonica, S.; Wild, U. *Chem. Phys. Lett.* **1986**, *123*, 282.
18. Markovitsi, D.; Sigal, H,; Ecoffet, C.; Millié, P.; Charra, F.; Fiorini, C.; Nunzi, J. M.; Strzelecka, H.; Veber, M.; Jallabert, C. *Chem. Phys.* **1994**, *182*, 69.

19. Ecoffet, C.; Markovitsi, D.; Millié, P.; Jallabert, C.; Strzelecka, H.; Veber, M. *J. Chem. Soc. Faraday Trans.* **1993**, *89*, 457.

20. Karmazin, V. P.; Kayazhanskii, M. I.; Olenkhnovich, E. P.; Dorofeenko, G. N. *Zh. Prikl. Spektrosk.* **1975**, *22*, 234.

21. Haucke, G.; Czerney, P.; Cebulla, F. *Ber. Bunsenges Phys. Chem.* **1992**, *96*, 880.

22. Lin, Z.; Schuster, G. B. *J. Org. Chem.* **1994**, *59*, 1119.

23. Chen, Y.; Wang, P.-F.; Wu, S.-K. *J. Luminescence* **1995**, *65*, 257.

24. Chen, Y.; Wu, S. –K. *J. Photochem. Photobiol. A: Chem.* **1997**, *102*, 203.

25. Miranda, M. A.; Garcia, H. *Chem. Rev.* **1994**, *94*, 1063.

26. Akaba, R.; Aihara, H.; Sakuragi, H.; Tokumaru, K. *J. Chem. Soc. Chem. Commun.* **1987**, 1262.

27. Akaba, R.; Ohshima, K.; Kawai, Y.; Negishi, A.; Sakuragi, H.; Tokumaru, K. *Tetrahedron* **1991**, *32*, 109.

28. Akaba, R.; Aihara, S.; Sakuragi, H.; Tokumaru, K. *J. Chem. Soc. Perkin Trans.2*. **1991**, 291.

29. Akaba, R.; Niimura, Y.; Fukushima, T.; Kawai, Y.; Tajima, T.; Karugemi, T.; Negishi, A.; Kamata, M.; Sakuragi, H.; Tokumaru, K. *J. Am. Chem. Soc.* **1992**, *114*, 4460.

30. Valat, P.; Tripathi, S.; Wintgens, V.; Kossanyi, J. *New. J. Chem.* **1990**, *14*, 825.

31. Manoj, N.; Gopidas, K. R. *J. Photochem. Photobiol. A: Chem.* **1995**, *85*, 53.

32. Ramamurthy, P.; Morlet-Savary, F.; Fouassier, J. P. *J. Chem. Soc. Faraday Trans.* **1993**, *89*, 465.

33. Ramamurthy, P.; Parret, S.; Morlet-Savary, F.; Fouassier, J. P. *J. Photochem. Photobiol. A: Chem.* **1994**, *83*, 205.

34. Sivakumar, A.; Parimala, S.; Ramamurthy, P. *J. Photochem. Photobiol. A: Chem.* **1996**, *94*, 129.

35. Jayanthi, S. S.; Ramamurthy, P. *J. Phys. Chem.* **1997**, *101*, 2016.

36. Jayanthi, S. S.; Ramamurthy, P. *J. Phys. Chem. A* **1998**, *102*, 511.

37. Lampre, I.; Marguet, S.; Markovitsi, D.; Delysse, S.; Nunzi, J. M. *Chem. Phys. Lett.* **1997**, *272*, 496.

38. Berlman, I. B. *Handbook of Fluorescence of Aromatic Molecules*, Academic Press, New York, **1971**.

39. Fromherz, P.; Heilemann, A. *J. Phys. Chem.* **1992**, *96*, 6864.

40. Lippert, E. Z. *Naturforsch.* **1955**, *10 A*, 541.

41. Rettig, W. *Angew. Chem. Int. Ed. Engl.* **1986**, *25*, 971.

42. Rettig, W. in *Topics in Fluorescence Spectroscopy. Vol. 4*, Lakowicz, J. R. (Ed.), Plenum Press, New York, **1994**, p. 109.

43. Rotkiewicz, K.; Grellmann, K. H.; Grabowski, Z. R. *Chem. Phys. Lett.* **1973**, *19*, 315.

44. Rotkiewicz, K.; Grabowski, Z. R.; Krowczynski, A.; Kuhnle, W. *J. Luminescence.* **1976**, *12*, 877.

45. Grabowski, Z. R.; Rotkiewicz, K.; Siemiarczuk, A.; Cowley, D. J.; Baumann, W. *Nouv. J. Chim.* **1979**, *3*, 443.

46. Carmichael, I.; Hug, G. L. *J. Phys. Chem. Ref. Data* **1986**, *15*, 1.

47. Lutz, H.; Breheret, E.; Lindquist, L. *J. Phys. Chem.* **1973**, *77*, 1758.

48. Bensasson, R.; Land, E. J. *J. Photochem. Photobiol. Rev.* **1978**, *3*, 163.

49. Bhattacharyya, K.; Chowdhury, M. *Chem. Rev.* **1993**, *93*, 507.

50. Wintgens, V.; Pouliquen, J.; Simalty, M.; Kossanyi, J.; Justesen, F. K.; Eriksen, J. *J. Photochem.* **1984**, *26*, 131.

51. Wintgens, V.; Pouliquen, J.; Kossanyi, J. *Nouv. J. Chim.* **1985**, *9*, 229.

52. Lakowicz, J. R. *Principles of Fluorescence Spectroscopy*, Plenum Press, New York, **1983**.

53. Pragst, F.; Ziebig, R.; Seydewitz, U.; Driesel, D. *Electrochim. Acta* **1980**, *25*, 341.

54. Wintgens, V.; Pouliquen, J.; Kossanyi, J.; Heintz, M. *Nouv. J. Chim.* **1986**, *10*, 345.

55. Klima, J.; Volke, J.; Urban, J. *Electrochim. Acta* **1991**, *36*, 73.

56. Gould, I. R.; Ege, D.; Moser J. E.; Farid, S. *J. Am. Chem. Soc.* **1990**, *112*, 4290.

57. Rehm, D.; Weller, A. *Isr. J. Chem.* **1970**, *8*, 259.

58. Marcus, R. A. *Annu. Rev. Phys. Chem.* **1964**, *15*, 155.

59. Samanta, A.; Gopidas, K. R.; Das, P. K. *Chem. Phys. Lett.* **1990**, *167*, 165.

60. Samanta, A.; Gopidas, K. R.; Das, P. K. *J. Phys. Chem.* **1993**, *97*, 1583.

61. Olmsted III, J.; Meyer, T. J. *J. Phys. Chem.* **1987**, *91*, 1649.

62. Haselbach, E.; Vauthey E.; Suppan, P. *Tetrahedron* **1988**, *44*, 7335.

63. Orbach, N.; Ottolenghi, M. in *The Exciplex*, Gordon M.; Ware, W. R. (Eds.), Academic Press, New York, **1975**.

64. Jones II, G. in *Photoinduced Electron Transfer. Part A*, Fox, M. A.; Chanon, M. (Eds.), Elsevier, Amsterdam, **1988**.

65. Mattay, J.; Vondenhof, M. in *Photoinduced Electron Transfer. Part III*, Mattay, J. (Ed.), Springer-Verlag, Heidelberg, **1990**.

66. Mulliken, R. S.; Person, W. B. *Molecular Complexes*, Wiley Interscience, New York, **1969**.

67. Masuhara, H.; Mataga, N. *Acc. Chem. Res.* **1981**, *14*, 312.

68. Hilinski, E. F.; Masnovi, J. M.; Amatore, C.; Kochi, J. K.; Rentzepis, P. M. *J. Am. Chem. Soc.* **1983**, *105*, 6167.

69. Kochi, J. K. *Angew. Chem. Int. Ed. Engl.* **1988**, *27*, 1227.

70. McGlynn, S. P.; Azumi, T.; Kinoshita, M. *Molecular Spectroscopy of the Triplet State*, Prentice-Hall, New Jersy, **1969**.

71. Christodouleas N.; McGlynn, S. P. *J. Chem. Phys.* **1964**, *40*, 166.

72. Lim, B. T.; Okajima, S.; Chandra A. K.; Lim, E. C. *Chem. Phys. Lett.* **1981**, *79*, 22.

73. Tripathi, S.; Wintgens, V.; Valat, P.; Toscano, V.; Kossanyi, J.; Bos, F. *J. Lumin.* **1987**, *37*, 149.

74. Niizuma, S.; Sato, N.; Kawata, H.; Suzuki, Y.; Toda T.; Kokubun, H. *Bull. Chem. Soc. Jpn.* **1985**, *58*, 2600.

75. Kawata, H.; Niizuma, S. *Bull. Chem. Soc. Jpn.* **1989**, *62*, 2279.

76. Balaban, A. T.; Dinculescu, A.; Dorofeyenko, G. N.; Fischer, G. W.; Koblik, A. V.; Mezheritzkii, V. V.; Schroth, W. *Pyrylium salts: Synthesis, Reactions and Physical Properties*. Katrizky, A. R., (Ed.), *Advances in Heterocyclic Chemistry*; Academic Press: New York, **1982**; Suppliment 2.

77. Ohta, M.; Kato, H. *Bull. Chem. Soc. Jpn.* **1959**, *32*, 707.

CHAPTER 3

PHOTOPHYSICAL AND ELECTRON TRANSFER PROPERTIES OF A FEW 2,6-DIALKYL-4-ARYLPYRYLIUM SALTS AND DICATIONIC PYRYLIUM SALTS

3.1. Abstract

Photophysical and electron transfer properties of pyrylium salts 1-7 are reported. Design of these substrates was based on the strategies that are in use for the control of BET reactions outlined in Chapter 1. By employing biphenyl as the donor, quantum yields of ion formation and rates of back electron transfer were determined for all these substrates. Yields of radicals were higher for these pyrylium salts (Φ_{ion} = 0.3-0.7) compared to those of 2,6-dimethyl-4-(*p*-alkylphenyl)-pyrylium salts reported in Chapter 2 of this thesis. Pyrylium salts **4** and **5** gave very high yields of ion radicals and have great potential as PET sensitizers. Although pyrylium salts **1-3** gave only moderate yields of ion radicals, their absorption at $\lambda > 400$ nm makes them suitable for use in the visible region. Dicationic pyrylium salts (**6** and **7**) also absorb in the visible region, but they tend to form CT complexes with electron rich molecules, thereby reducing the yield of radical ions. These salts can be employed as sensitizers at very low substrate concentrations.

3.2. Introduction

In this Chapter, photophysical and electron transfer properties of pyrylium salts listed in Chart 3.1 are presented. As mentioned earlier, our aim has been to

elucidate the structural features that contribute towards the enhancement of yield and lifetime of radicals generated in PET reactions in this class of compounds. Selection of these derivatives for our study was guided by the various strategies, that are in use for the control of BET reactions[1] (see Chapter 1 for details).

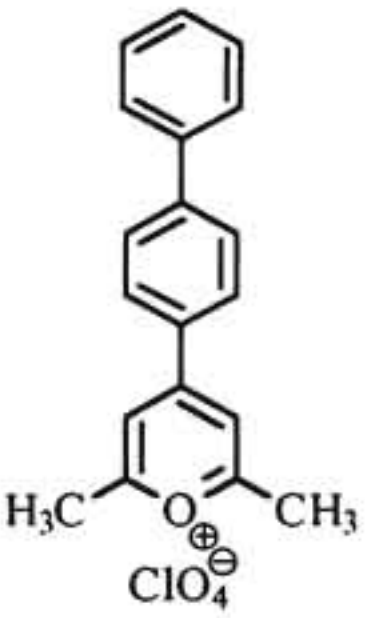

1

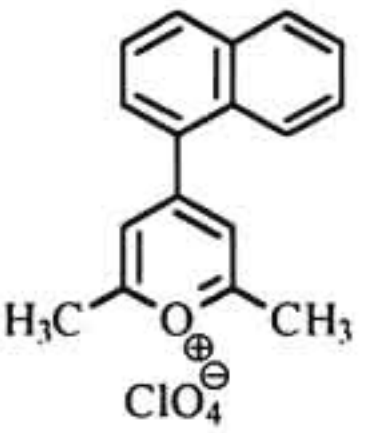

2

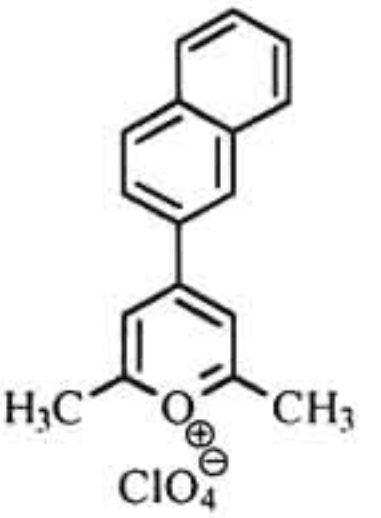

3

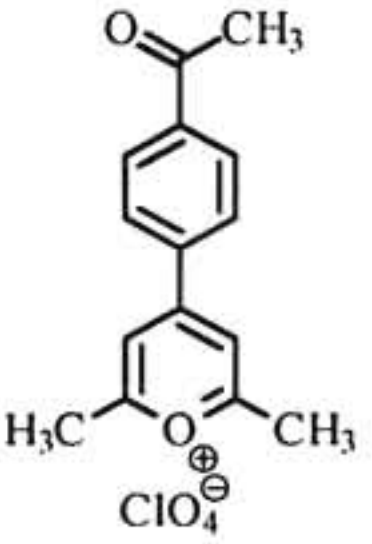

4

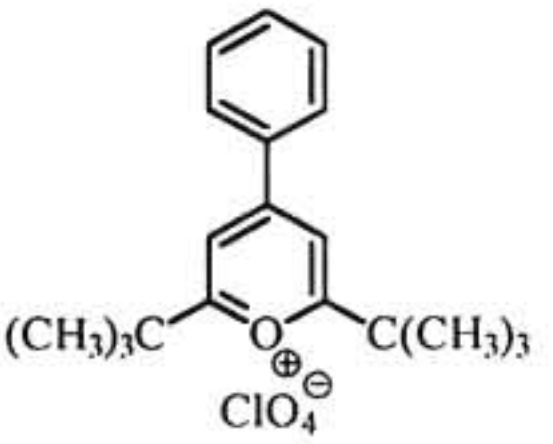

5

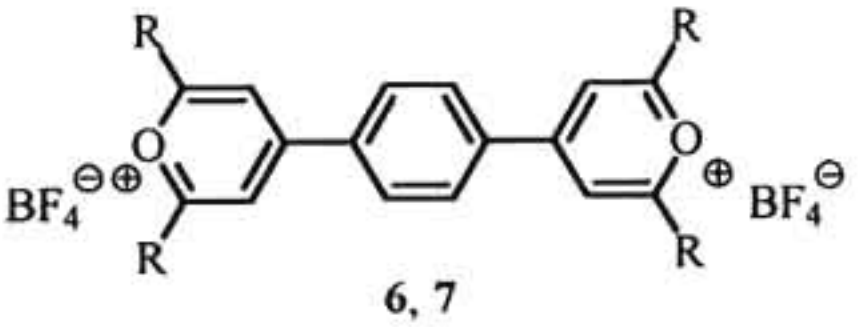

6, 7

6, R = -C_6H_5
7, R = -C_6H_4-Br(*p*)

Chart 3.1

Electrochemical reductions of a large number of pyrylium salts were studied by cyclic voltammetry and polarography.[2-15] The pyranyl radicals generated by these techniques were investigated by EPR[7-10] and UV-Near IR spectroscopy[4,13] and also by electrogenerated chemiluminescence.[3,4] According to EPR spectra and quantum chemical calculations,[10] the pyranyl radicals exhibit a higher spin density at position 4- of the heterocyclic ring. Thus, it was suggested that, if the 4- position is substituted with groups that can delocalize the odd electron, the pyranyl radical would be more stable.[13] Such a strategy has prompted us to design substrates **1-4**. Pyranyl radicals of these substrates are expected to be long-lived, which in turn would lead to a reduction in the rates of BET reactions.

An additional factor that may operate in the case of **4** is the possible enhancement of triplet quantum yield due to the presence of a carbonyl group in the molecule. Compounds containing carbonyl groups generally undergo enhanced intersystem crossing leading to generation of triplet states in high yields.[16] It was observed that PET reactions involving triplet excited states of sensitizers lead to higher yields of radical ions and lower rates for BET reactions.

Compound **5** has been designed to study the effect of steric factors on BET reactions. The bulky *tert*-butyl groups present in this molecule reduce the chances of CT complex formation. These groups may also induce additional nonplanarity in the molecule due to steric crowding and lead to enhanced rates of triplet formation. Both these factors are expected to enhance the yield of radical ions in PET reactions.

The dicationic pyrylium salts **6** and **7** were designed to evaluate the effect of Coulombic repulsion in PET reactions of pyrylium salts. When these sensitizers

are excited in the presence of a donor (D), PET would lead to the generation of two radical cations as shown in equation (3.1).

$$^{*}P^{2+} + D \longrightarrow P^{\bullet+} + D^{\bullet+} \quad (3.1)$$

The two radical cations repel each other and create a kinetic barrier to BET reactions. Several such examples are known in the literature.[17] In addition to this, **7** contains four bromine atoms which can enhance the yield of triplet formation by heavy atom effect.

In all these cases, yields of radicals were determined by laser flash photolysis experiments using biphenyl (BP) as the donor. Electron transfer from BP to all these pyrylium salts were exothermic and flash photolysis led to the formation of the well-characterized biphenyl radical cation ($BP^{\bullet+}$). Quantum yields of the PET reactions were measured from the optical densities of $BP^{\bullet+}$ absorption at 680 nm (ε = 1.45 x 10^4 M^{-1} cm^{-1}).[18] Rate constants for BET reactions were determined by fitting the decay of the $BP^{\bullet+}$ absorptions to second-order equal-concentration kinetics.

3.3. Results and Discussion

3.3.1. Photophysical and electron transfer properties of 2,6-dimethyl-4-arylpyrylium salts 1-3

3.3.1.1. Absorption spectra

Pyrylium salts **1-3** show strong absorption in the 300-450 nm region. Figure 3.1 shows the absorption spectra of **1** in acetonitrile and dichloromethane. The absorption maximum for this compound is blue shifted in acetonitrile by 27 nm.

The blue shift in acetonitrile is associated with a considerable decrease in the extinction coefficient of the long wavelength absorption as shown in Figure 3.1.

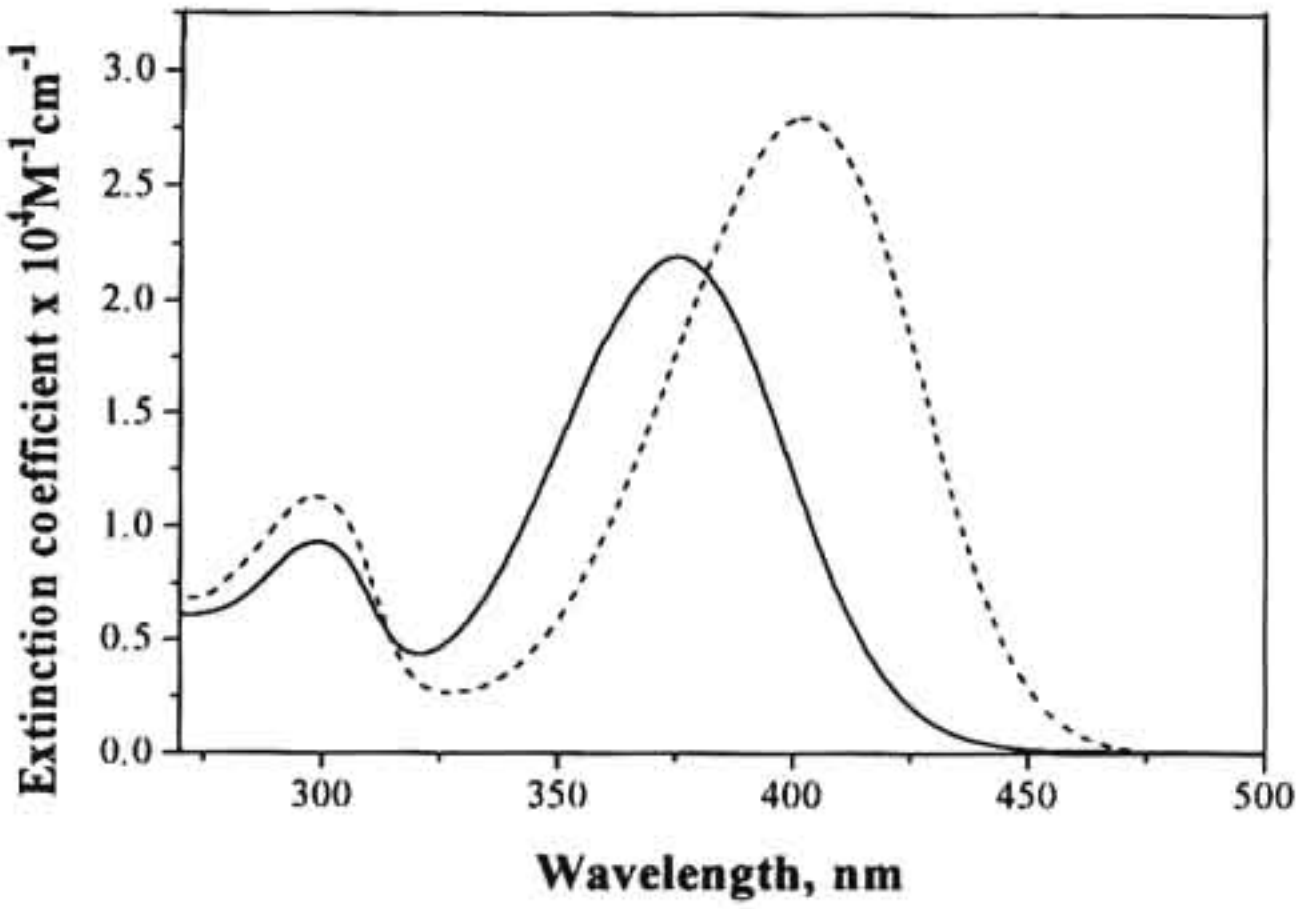

Figure 3.1 Absorption spectra of **1** in dichloromethane (- - -) and acetonitrile (—).

Pyrylium salts **2** and **3** differ only by the position of attachment of the naphthyl ring to the 2,6-dimethylpyrylium moiety. Yet they exhibit markedly different absorption spectra. Figure 3.2 shows the absorption spectra of **2** and **3** in dichloromethane and Figure 3.3 shows the same in acetonitrile. The β-naphthyl substituted derivative exhibits absorption maxima at 367 and 430 nm. In the α-naphthyl substituted derivative **2**, the 367 nm band is not noticeable and is present only as a small shoulder. Although, the long wavelength absorption bands of **2** and **3** differ slightly in dichloromethane, they show complete overlap in the 400-475 nm region in acetonitrile solution.

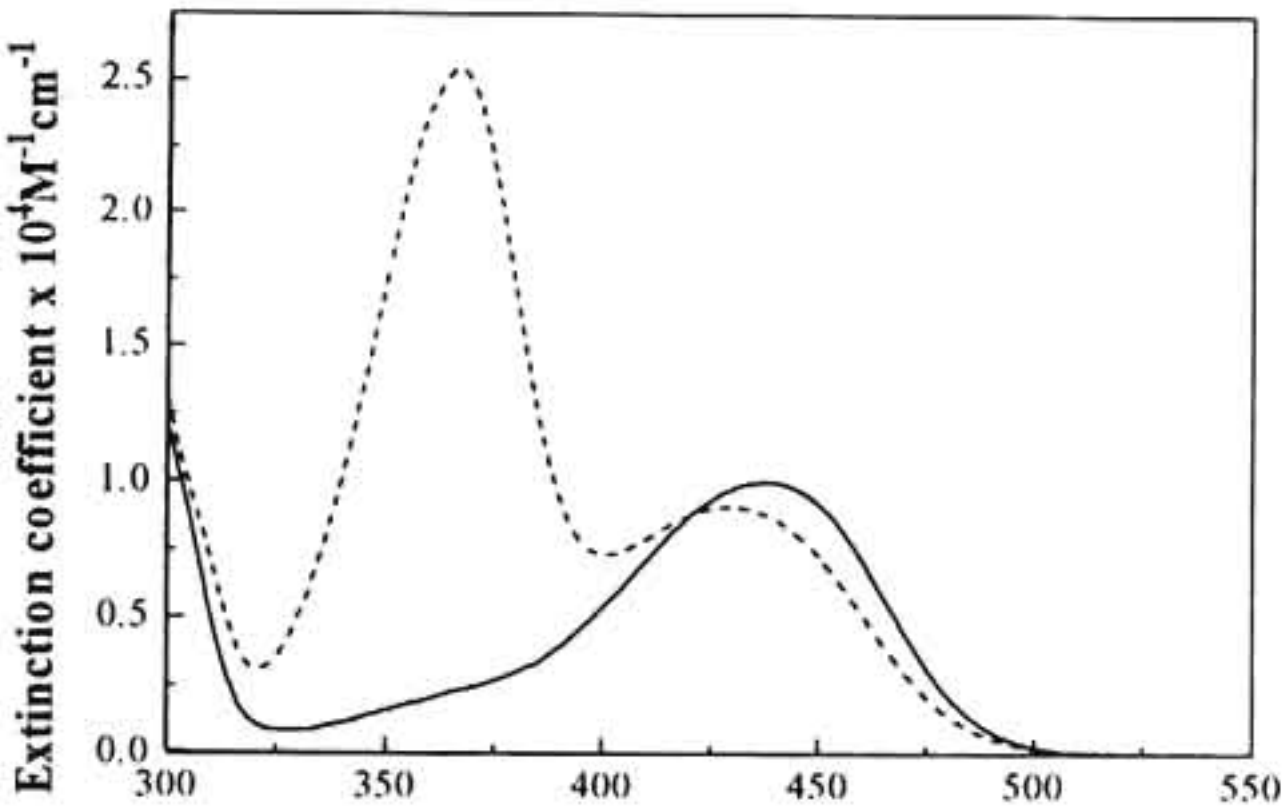

Figure 3.2 Absorption spectra of **2** (—) and **3** (- - - -) in dichloromethane.

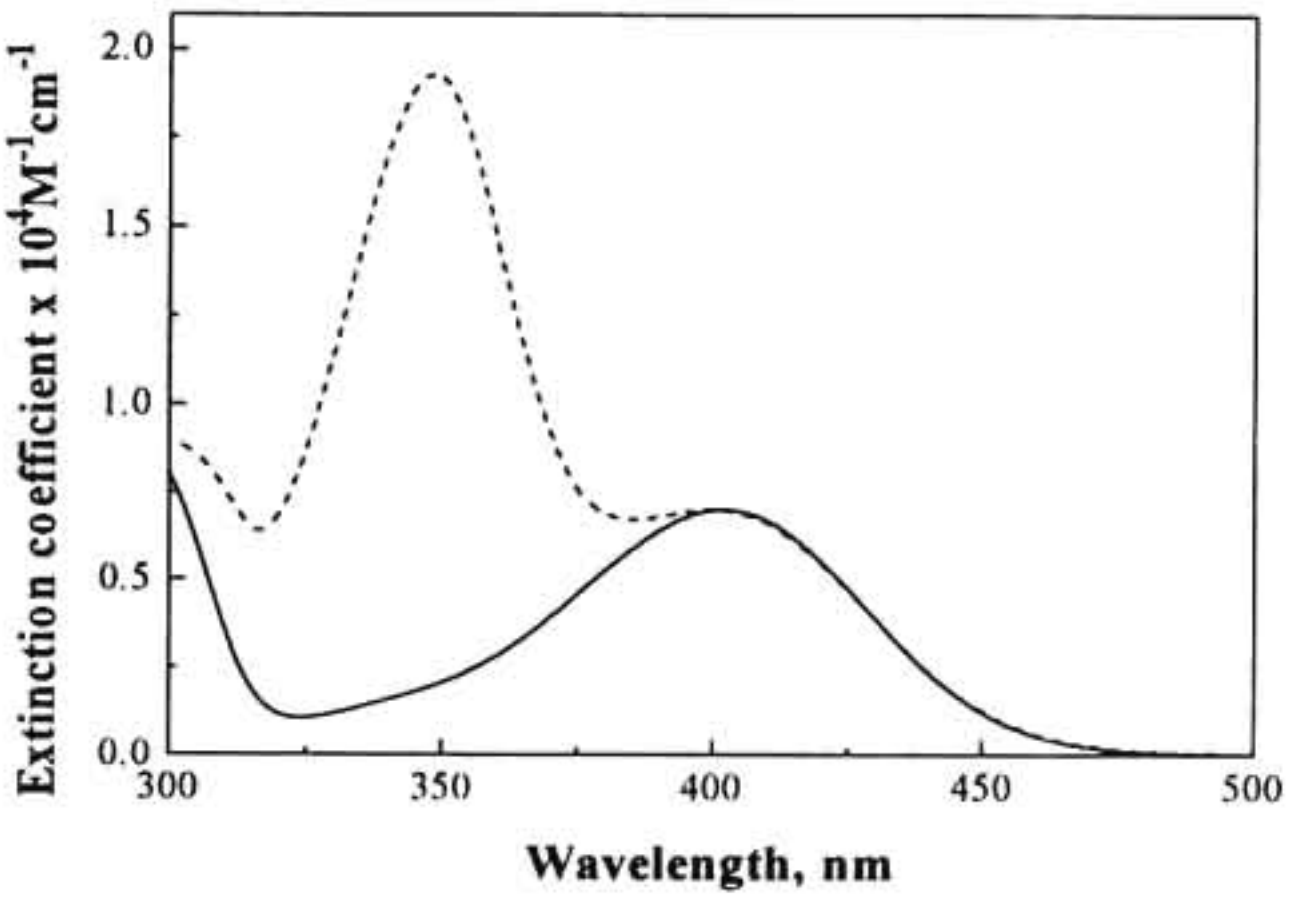

Figure 3.3 Absorption spectra of **2** (—) and **3** (- - -) in acetonitrile.

Table 3.1 summarizes the absorption maxima, extinction coefficients and full width at half maximum (FWHM) values for pyrylium salts **1-3** in two solvents. For all the absorption bands, the FWHM values were small. These values are typical for single absorption bands[19] and hence we rule out the presence of any submerged absorption bands in these cases.

Table 3.1 Absorption maxima (λ_{max}), extinction coefficients (ε_{max}), and full width at half maximum (FWHM) values for pyrylium salts 1-3 in dichloromethane. Values in parenthesis are those obtained in acetonitrile.

Compound	λ_{max}, nm	ε_{max}, $M^{-1}cm^{-1}$	FWHM, cm^{-1}
1	402 (375)	2.8×10^4 (2.2×10^4)	3895 (4139)
2	438 (402)	1.0×10^4 (7.0×10^3)	3783 (4166)
3	367, 430 (348, 402)	2.5×10^4, 9.0×10^3 $(1.9 \times 10^4, 7.0 \times 10^3)$	3099, 4032 (3481, 4166)

It was shown in Chapter 2 of the thesis, that the long wavelength absorption band of 2,6-dimethyl-4-phenylpyrylium salt (**8**, Scheme 3.1) is a superposition of the intense *y*-band at 326 nm and the very weak *x*-band at 334 nm. When the phenyl group is substituted by alkyl groups, the absorption spectra exhibited changes, which depended on the position of the substituent. Substitution in the *para* position of the 4-phenyl ring will have its entire contribution projected along the *y*-direction (see Scheme 3.1 for axis convention). These substituents can be called '*y*-substituents' and they affect only the *y*-band. On the other hand,

substitution in the *ortho* or *meta* positions of the 4-phenyl ring will have its major contribution projected along the *x*-direction. Substituents in these positions can be called '*x*-substituents' and they affect the *x*-band predominantly. The *y*-band may also be present in these cases. Based on these ideas, we have tried to explain the absorption spectra of **1-3** using Scheme 3.1.

According to Scheme 3.1, **1** can be considered as a *p*-phenyl substituted derivative of **8**. This is an example of a *y*-substitution in which the electrons can delocalize over three additional π-bonds of the phenyl substituent. Hence we expect the *y*-band to shift bathochromically by 60-70 nm. Because of the additional delocalization, the extinction coefficient is also expected to be high. The absorption spectrum of **1** is in very good agreement with this suggestion.

The α-naphthyl substituted derivative **2** can be considered as *ortho*, *meta*-disubstituted derivative of **8** (Scheme 3.1). The two *x*-substituents are expected to produce a large red shift in the *x*-band with an associated increase in the extinction coefficient. The *y*-band will be relatively unaffected. In accordance with this suggestion, **2** shows only one absorption band at 437 nm. The *y*-band appears as a very small shoulder at < 350 nm.

The β-naphthyl substituted pyrylium salt **3** can be considered as a *meta*, *para*- disubstituted derivative of **8**. According to the arguments presented earlier, the *x* and *y* bands should show bathochromic shifts and increase in extinction coefficients. The absorption spectrum of **3** is in very good agreement with this guideline. In this case, the red shift in the *x*-band is more pronounced than the shift in the *y*-band and lead to a separation of the two bands.

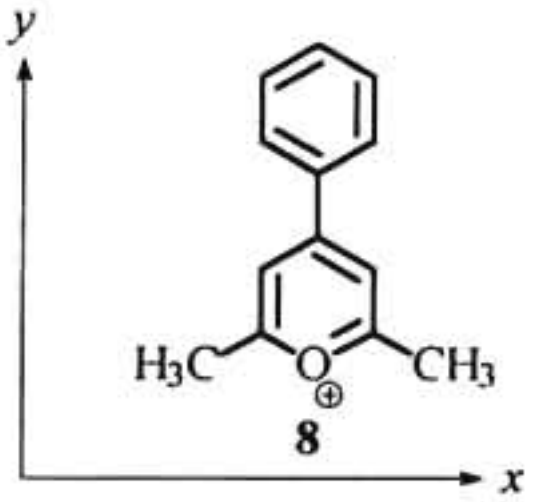

8

y-band 326 nm (ε~20,000)

x-band 334 nm (ε very low)

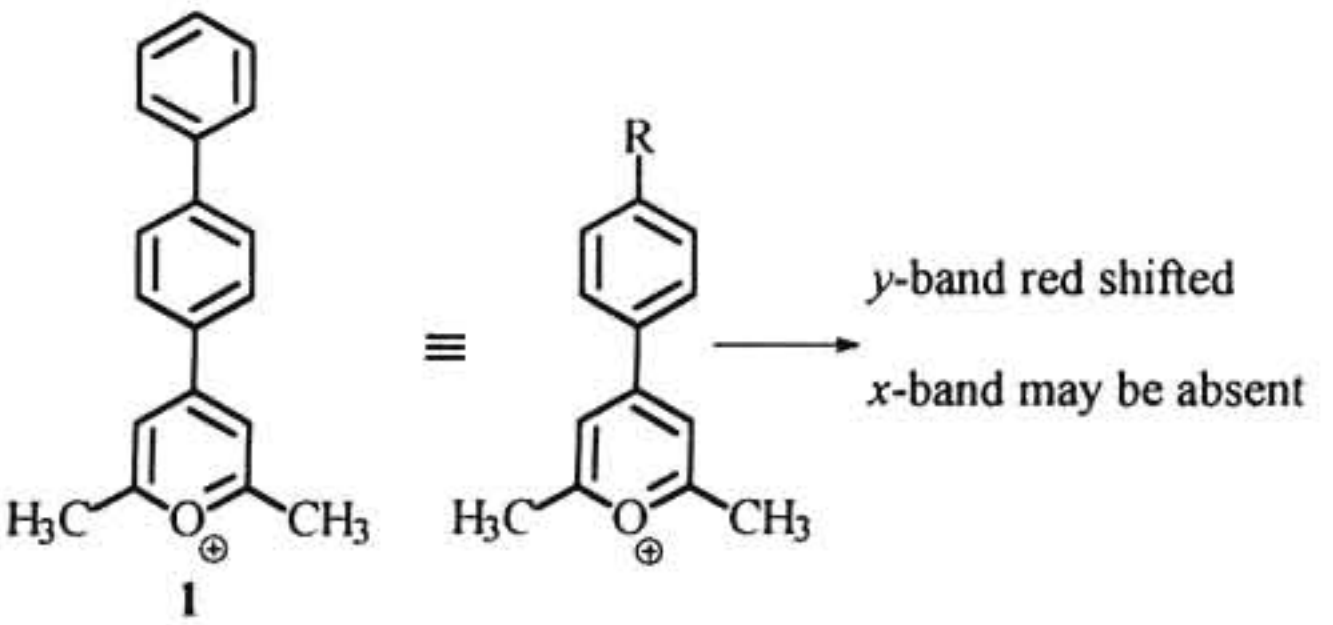

1

y-band red shifted

x-band may be absent

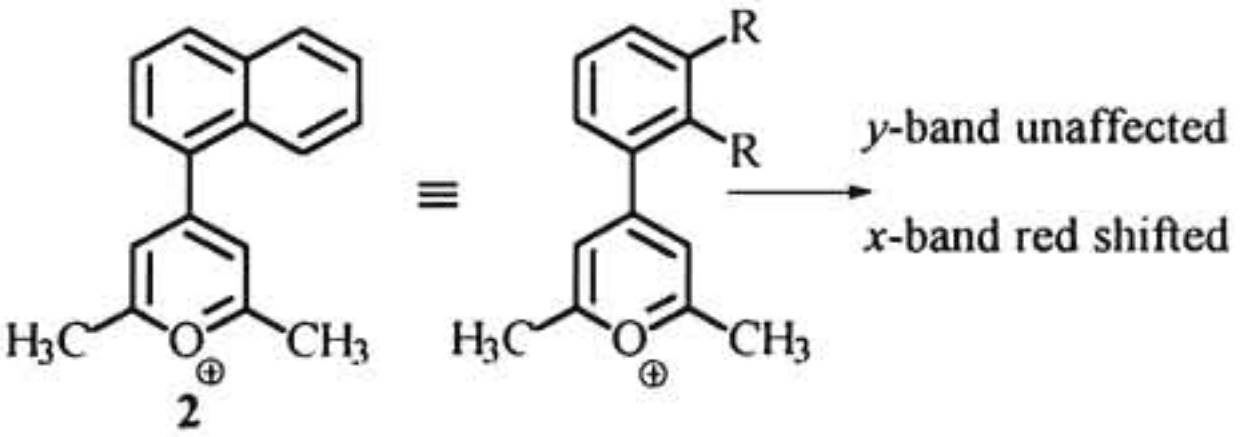

2

y-band unaffected

x-band red shifted

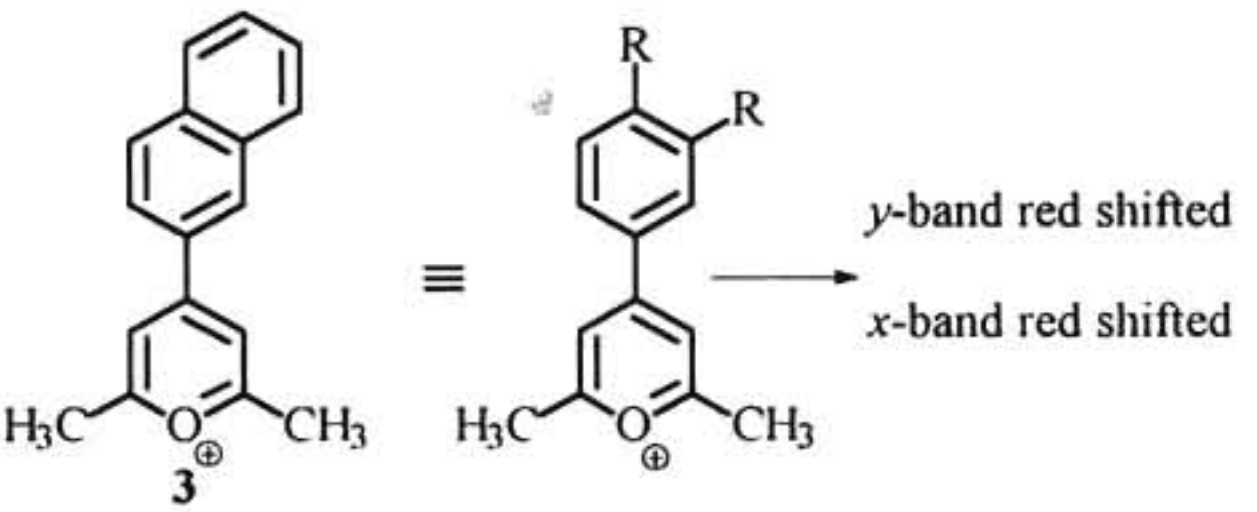

3

y-band red shifted

x-band red shifted

Scheme 3.1

The absorption maximum of the *y*-band in **1** is more red shifted compared to that of **3**. This is due to more delocalization available in **1** (three π-bonds compared to two in **3**). However, the *x*-band in **2** (two *x*-substituents) appeared at similar wavelengths compared to **3** (one *x*-substituent). In fact, the *x*-bands of **2** and **3** overlap in acetonitrile solution. Hence, position of the substituents may not be the only factor that determines the red shifts of the *x* and *y* bands in these cases.

In order to resolve this question, we have resorted to geometry optimization calculations using Austin Method 1 (AM1) of the PC SPARTAN package.[20,21] Calculations showed that **1** and **3** have near-planar conformations (θ_4 = 23° and 26°, respectively), whereas, **2** is twisted (θ_4 = 43°) in the ground state. This indicates that delocalization of electrons into the naphthyl ring is poor in **2** compared to that in **3**. Hence the bathochromic effect due to the substituents will not be the same in **2** and **3**.

It has been stated in Chapter 2 that, in the case of pyrylium salts, excitation involves transfer of charge from the 4-substituent into the pyrylium ring. In order to look into this aspect we have calculated the HOMO and LUMO surfaces of these derivatives using AM1. Figure 3.4 gives a graphical representation of the HOMO and LUMO surfaces of **2** and **3**. The HOMO surfaces of **2** and **3** have more electron density localized on the naphthyl substituent. In the LUMO surfaces the electron density is more localized on the pyrylium ring. Thus it is clear from these calculations and Figure 3.4, that excitation in these cases is associated with almost complete transfer of an electron from the naphthyl group to the pyrylium ring. The extent of charge separation actually depends on the solvent. In polar solvents like acetonitrile, complete charge separation may occur and the excited state may be represented as ($PY^{\bullet}$—$NP^{\bullet+}$).

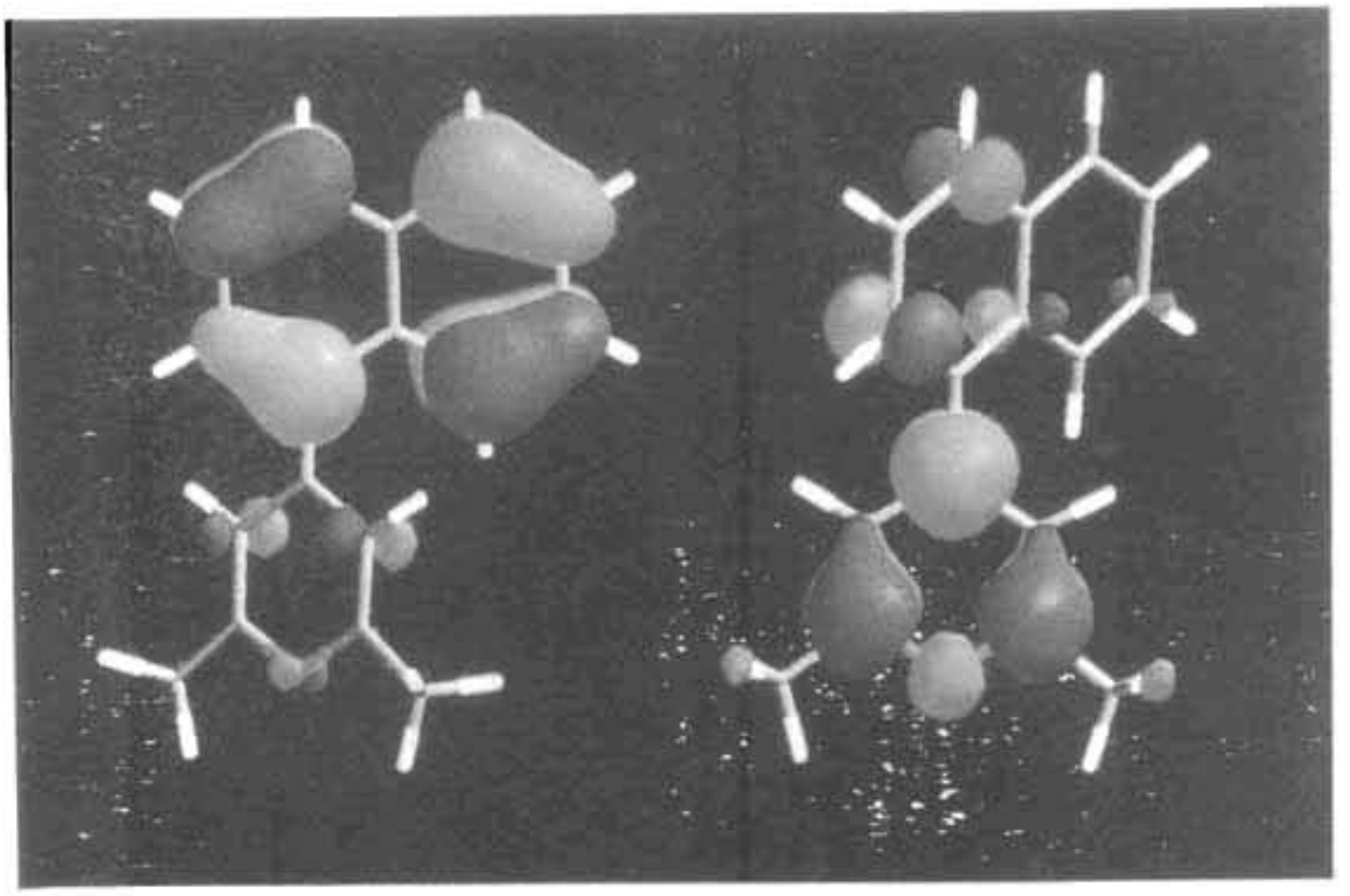

2 - HOMO

2 - LUMO

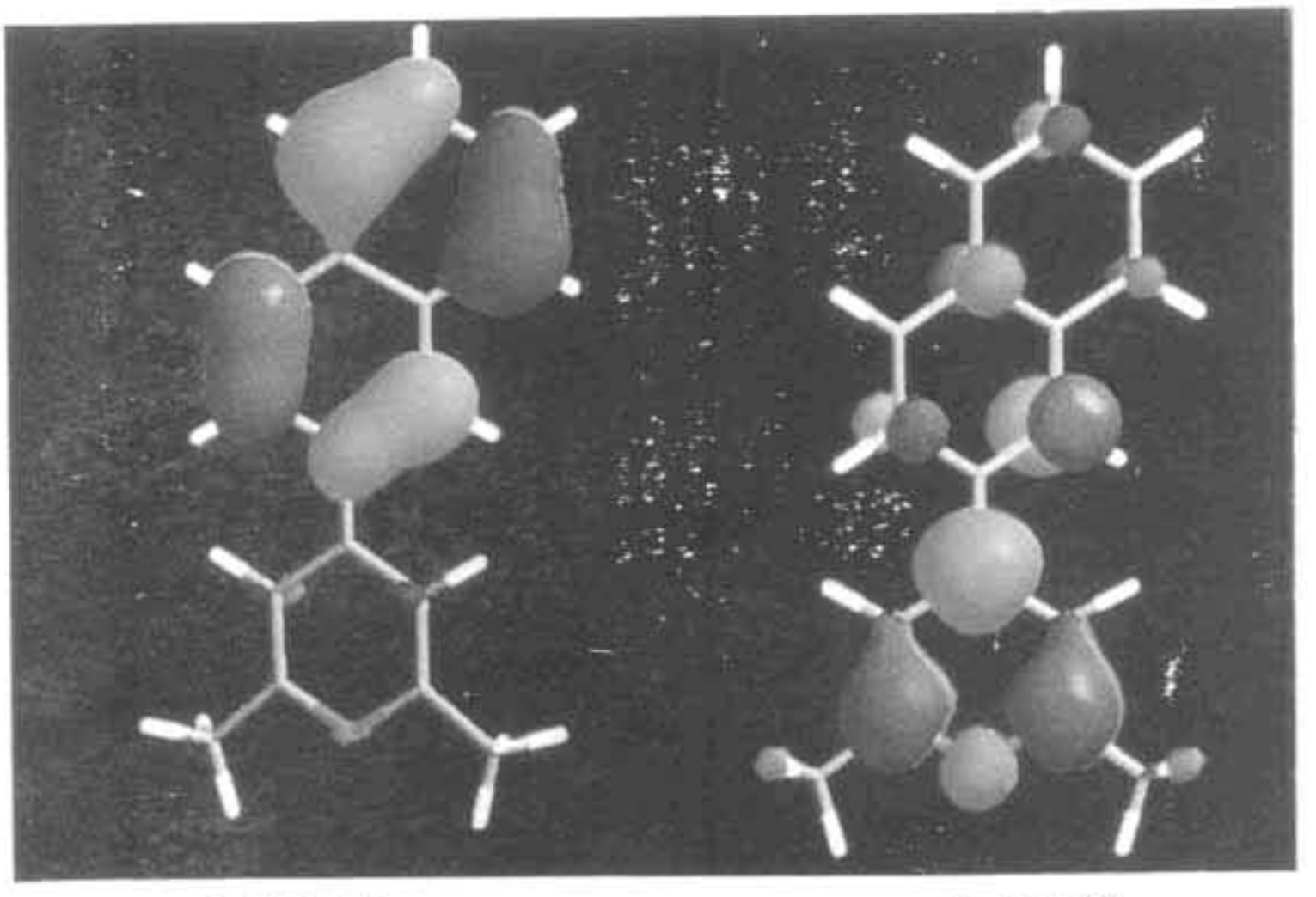

3 -HOMO

3 - LUMO

Figure 3.4. HOMO and LUMO surfaces of **2** and **3** obtained by AM1.

3.3.1.2. Fluorescence properties

Pyrylium salts **1-3** exhibit moderate to strong fluorescence emission in the 400-700 nm region. Figure 3.5 shows the fluorescence spectra of **1** in dichloromethane and acetonitrile and Figure 3.6 shows the fluorescence spectra of **2** and **3** in dichloromethane. The fluorescence maxima of all these compounds are red shifted in acetonitrile compared to those in dichloromethane. This behaviour is typical of all pyrylium salts and is attributed to the charge transfer nature of the excitation.[22] The fluorescence maxima, quantum yields, lifetimes and radiative rates for **1-3** are listed in Table 3.2.

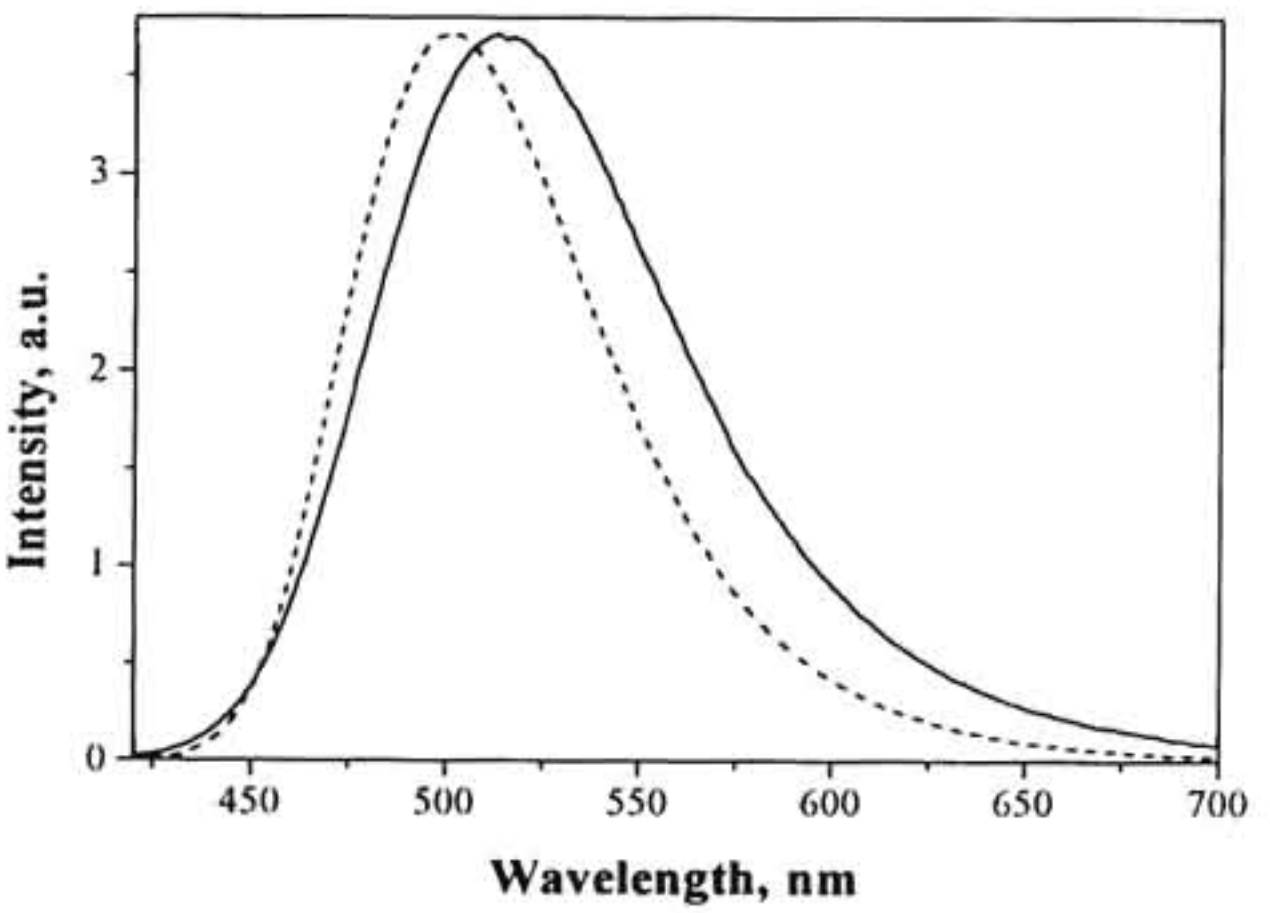

Figure 3.5 Normalized emission spectra of **1** (- - -) in dichloromethane and (—) in acetonitrile.

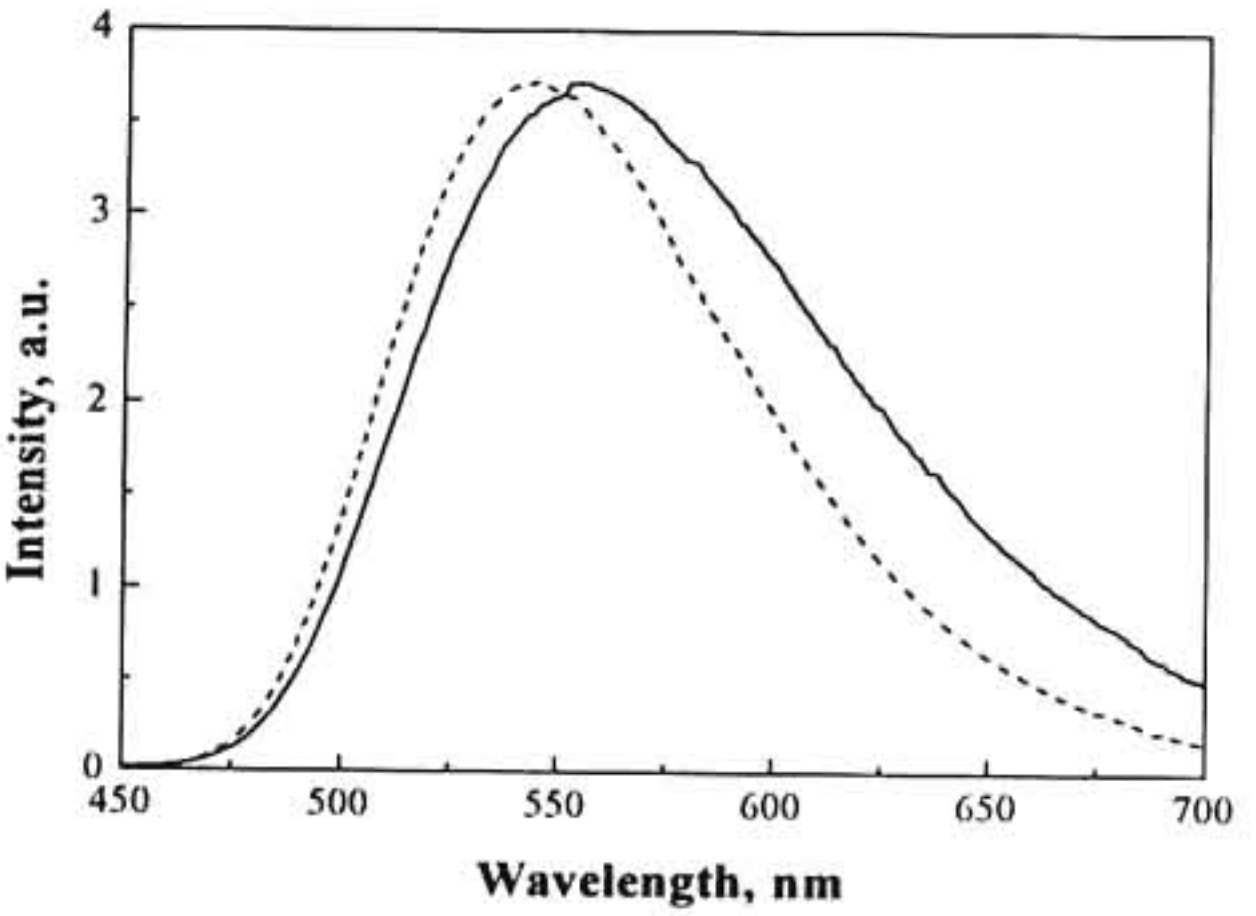

Figure 3.6 Normalized emission spectra of **2** (—) and **3** (- - -) in dichloromethane.

Table 3.2 Emission maxima (λ_{max}), Stokes shift (ν_{st}) values, fluorescence quantum yields (Φ_f), fluorescence lifetimes (τ_f) and radiative decay rates (k_R) for pyrylium salts 1-3 in dichloromethane. Values in parenthesis are those obtained in acetonitrile.

Compound	λ_{max}, nm	ν_{st}, cm^{-1}	Φ_f	τ_f, ns	k_R, $10^6\ s^{-1}$
1	501 (511)	4916 (7097)	0.78 (0.21)	3.4 (2.1)	229 (100)
2	554 (582)	4780 (7694)	0.22 (0.02)	13.4 (14.1)	16.4 (1.41)
3	544 (580)	4873 (7634)	0.64 (0.02)	16.7 (14.6)	39.0 (1.37)

Note that the fluorescence quantum yields of **1-3** are considerably reduced in acetonitrile. In acetonitrile solution, fluorescence properties of **2** and **3** are very similar. They gave overlapping fluorescence spectra. Fluorescence quantum yields and lifetimes were also the same. This can be explained only by invoking a charge separated state in this solvent. Our studies have shown that the charge separated states have considerably lower fluorescence quantum yields. Charge separation was very low for **1** in acetonitrile.

Since **1-3** exhibited intramolecular charge transfer behaviour, excitation in these cases will be associated with large changes in dipole moment. The change in dipole moments ($\Delta\mu$) were calculated by employing the Lippert equation[23] (see Chapter 2 for details). The Stokes shift values obtained in four solvents were plotted against the solvent polarity parameter. Linear plots were obtained in all cases (Figure 3.7). $\Delta\mu$ values were calculated from the slopes of these plots. In these calculations, the molecules were assumed to be spherical with a radius of 4.5 Å. $\Delta\mu$ values along with Stokes shifts obtained in four solvents are presented in Table 3.3. Note that the change in dipole moment observed for **2** is large compared to other derivatives. This can be attributed to the formation of a TICT state in this case.[24,25] Notice that **2** is twisted by 43° in the ground state and hence formation of a TICT state may be very facile in this case.

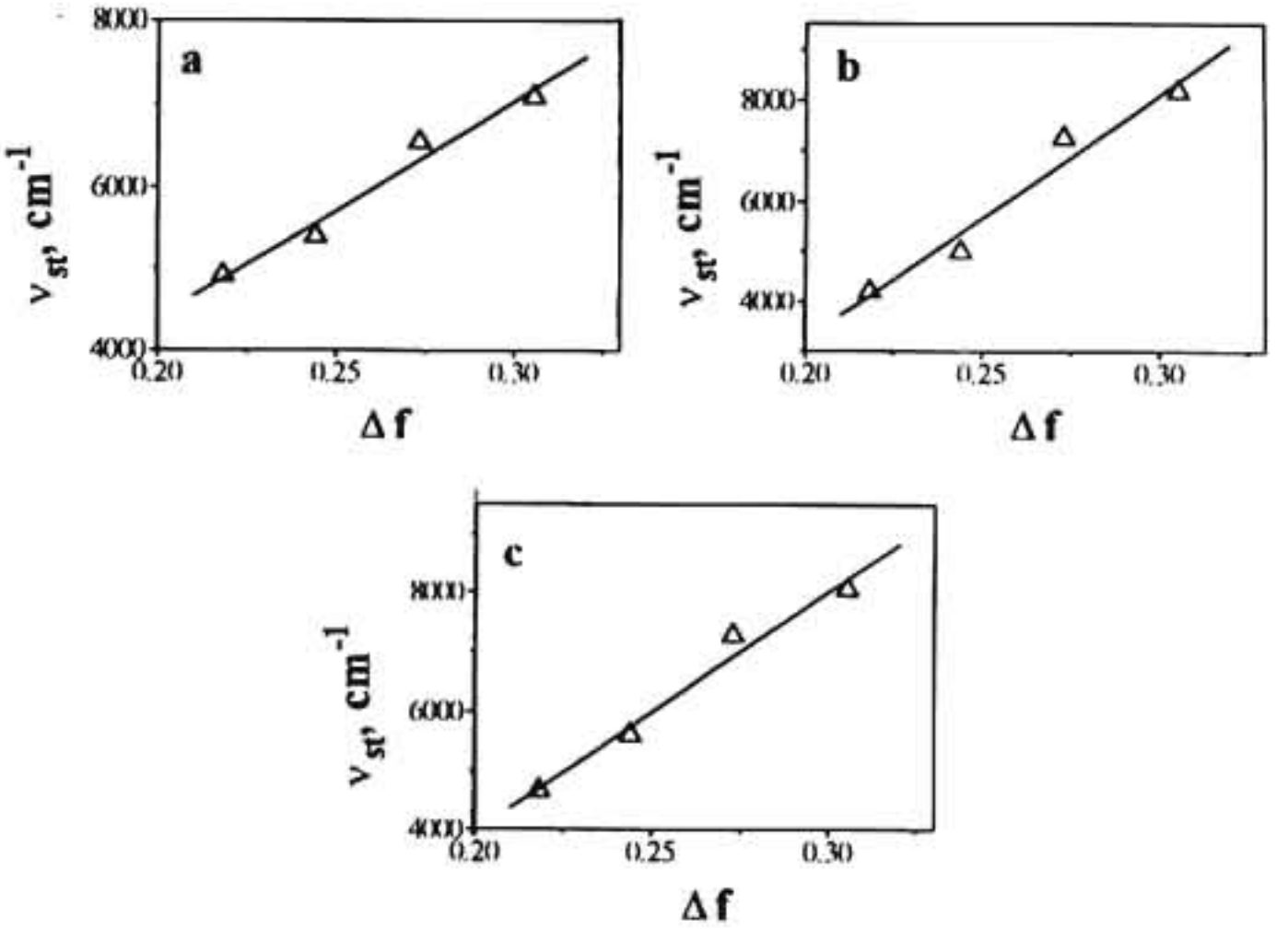

Figure 3.7 Plot of Stokes shift values (ν_{st}) *vs.* solvent polarity parameter (Δf) for **1** (a), **2** (b) and **3** (c).

Table 3.3 Stokes shift values (ν_{st}) in different solvents, solvatochromic slopes (m), and $\Delta\mu$ values for pyrylium salts 1-3.

Compound	Stokes Shift, ν_{st} cm^{-1}				m, cm^{-1}	$\Delta\mu$, D
	CH_2Cl_2	$C_2H_4Cl_2$	$(CH_3)_2CHOH$	CH_3CN		
1	4916	5392	6553	7097	26424	15.5
2	4780	5367	6784	7693	34923	21.0
3	4873	5599	7023	7634	33215	17.3

Pyrylium salts **1-3** did not exhibit phosphorescence emission in glycerol glass at 77 K. Thus, our attempts to record these spectra were not successful and the triplet energies of these molecules could not be measured.

3.3.1.3. Laser flash photolysis studies

Pyrylium salts **1-3** did not give good transients in acetonitrile solution. They, however, exhibited moderate absorption in dichloromethane solution. In addition to the ground state depletion, bands at 500-520 nm and at 680 nm were observed in these transient spectra (Figures 3.8-3.10). The transients were quenched by oxygen and hence we assign them to the triplet excited states of these molecules.

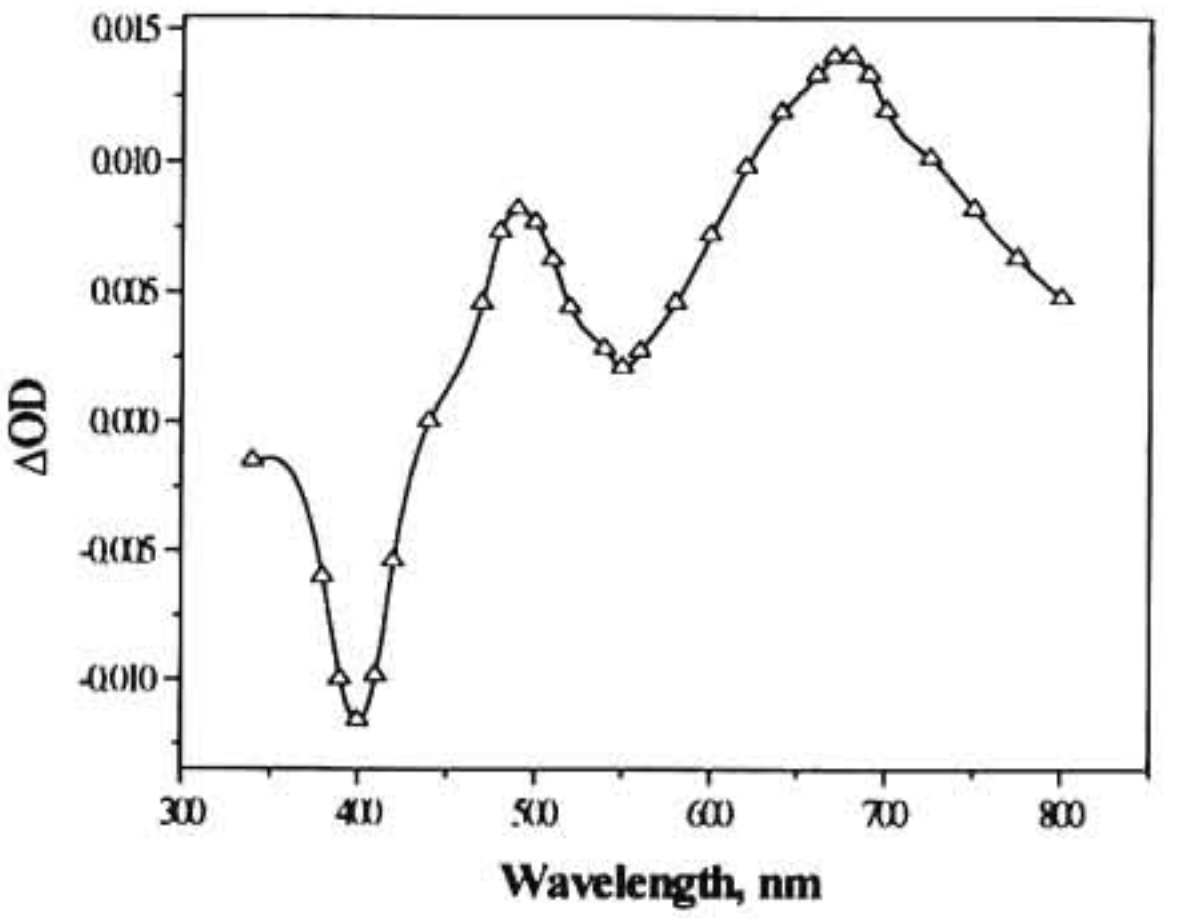

Figure 3.8 Transient absorption spectrum of **1** in dichloromethane recorded at 100 ns after the laser pulse.

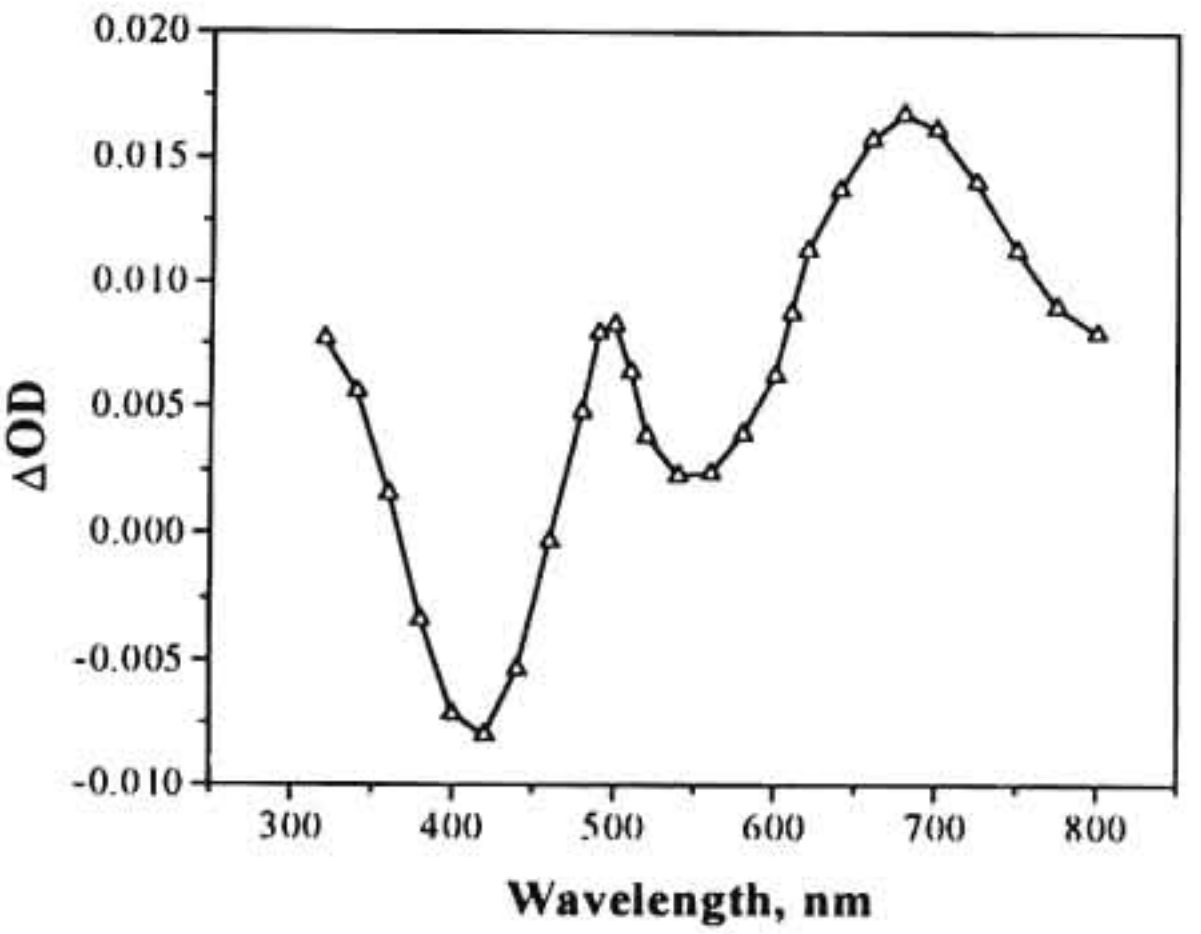

Figure 3.9 Transient absorption spectrum of **2** in dichloromethane recorded at 100 ns after the laser pulse.

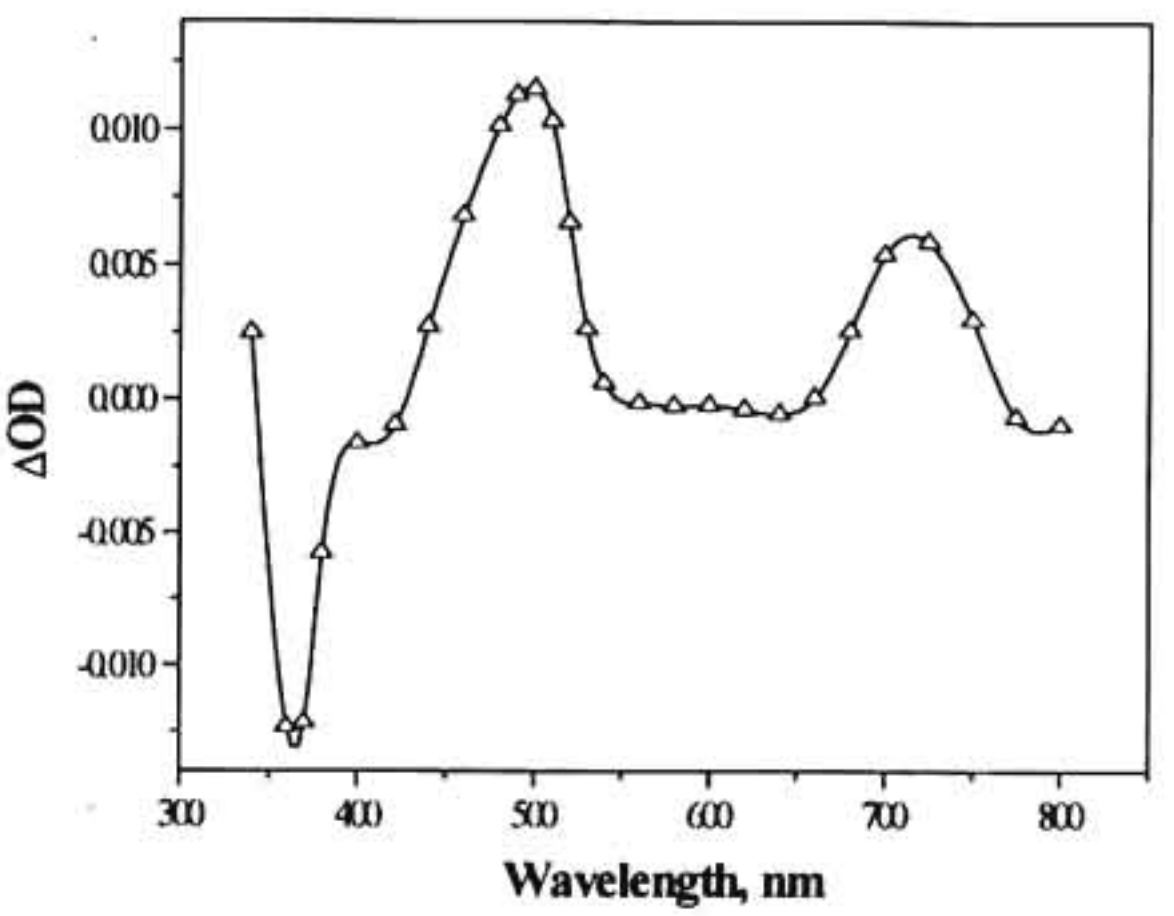

Figure 3.10 Transient absorption spectrum of **3** in dichloromethane recorded at 100 ns after the laser pulse.

In all these cases, the bleaching maxima coincided with the absorption maxima in dichloromethane solution. This enabled us to calculate the extinction coefficients of these absorptions by the singlet depletion method.[26] The quantum yields of triplet formation were then determined by relative actinometry.[27] Table 3.4 presents the absorption maxima, extinction coefficients, quantum yields, triplet lifetimes and oxygen quenching rate constants for **1-3**.

Table 3.4 Triplet-triplet absorption maxima (λ^{T}_{max}), extinction coefficients (ε^{T}_{max}), triplet quantum yields (Φ_T), triplet lifetimes (τ_T) and oxygen quenching rate constants ($k_q(O_2)$) for pyrylium derivatives 1-3.

Compound	λ^{T}_{max}(Abs), nm	ε^{T}_{max}(Abs), M^{-1} cm^{-1}	Φ_T	τ_T μs	$k_q(O_2)$ M^{-1} s^{-1}
1	500 (680)	4.0×10^4	0.03	2.2	4.9×10^7
2	520 (680)	5.5×10^4	0.13	6.1	3.3×10^9
3	520 (680)	1.5×10^4	0.09	3.5	4.2×10^9

Notice that the oxygen quenching rate constants for **2** and **3** are very large compared to **1** and other pyrylium salts reported in the literature.[28] This is attributed to the charge transfer character of the excited state in these cases. Notice that the excited states have pronounced diradical character and this leads to enhanced quenching by oxygen.

3.3.1.4. Electron transfer studies

3.3.1.4.1. Fluorescence quenching studies

Fluorescence of **1-3** were quenched very efficiently by BP. Plots of fluorescence intensity *vs.* BP concentration were linear in all cases and were analyzed by the Stern-Volmer treatment. Stern-Volmer constants (K_{SV}) obtained from these plots were used in the calculation of the bimolecular fluorescence quenching rate constants (k_q^S). These values are given in Table 3.5.

Quenching of the fluorescence of pyrylium salts by BP occurs by electron transfer mechanism. In order to calculate the free energy changes (ΔG) associated with these PET reactions, the reduction potentials of these salts were required. The reduction potentials of **1-3** were measured in acetonitrile solution using cyclic voltammetry. The first reduction peak of these substrates appeared in the -0.44 to -0.49 V range (*vs.* SCE). The cyclic voltammograms of **1-3** did not show the reverse anodic peak and this is attributed to fast dimerization of the pyranyl radicals.

The oxidation potential of BP is 1.91 V *vs.* SCE in acetonitrile solution.[18] ΔG_{et}^S values of the PET reactions were calculated using the Weller equation.[29] ΔG_{et}^S values along with reduction potentials and k_q^S values are presented in Table 3.5. An inspection of Table 3.5 shows that ΔG values are only moderately exothermic in these cases. These values lie in the normal region of the Marcus plot and we expect the rate constants to be lower than the diffusion controlled value.[30,31] k_q^S values we have obtained are in agreement with this observation.

Table 3.5 Excitation energies ($E_{0,0}$), reduction potentials (E_{red}), free energies of electron transfer to the singlet state (ΔG_{el}^{S}), Stern-Volmer quenching constants (K_{SV}) and singlet quenching rate constants (k_q^{S}) for the pyrylium salts 1-3 in dichloromethane solution.

Compound	$E_{0,0}$ kcal mol^{-1}	E_{red}, V vs. SCE	Biphenyl		
			ΔG_{el}^{S} kcal M^{-1}	K_{SV}, M^{-1}	k_q^{S}, M^{-1} s^{-1}
1	63.6	-0.44	-8.3	16.3	4.8×10^9
2	58.9	-0.49	-2.4	16.1	1.2×10^9
3	59.6	-0.47	-3.6	77.2	4.7×10^9

3.3.1.4.2. Laser flash photolysis studies

Quenching of the triplets of **1-3** by BP were not very efficient. These reactions are expected to be endothermic. Note from Table 3.5 that the singlet energies of these derivatives are low. Since these compounds did not exhibit phosphorescence emission, we could not determine their triplet energies. If we assume that the triplets of **1-3** lie ~10 kcal M^{-1} below their singlet excited states, PET involving the triplet states will be endothermic. Because of this, transient absorption spectra under triplet quenching conditions were not recorded for these substrates.

Transient absorption spectra of **1-3** were recorded in the presence of BP under singlet quenching conditions ([BP] ~ 0.1 M). Under these conditions more than 90% of the singlets will be quenched by electron transfer, leading to

the formation of $BP^{\bullet+}$ and the corresponding pyranyl radicals. Transient absorption spectra recorded in all cases showed the $BP^{\bullet+}$ absorption at 680 nm. The pyranyl radical absorptions appeared in the 370-450 nm region (see Figures 3.11 - 3.13).

It can be seen in Figures 3.11-3.13 that, the absorption spectra of the radicals in the 370-450 nm region were distorted by the ground state bleaching due to the pyrylium salts. Transient absorption spectra in such cases can be corrected using equation (3.2).[27]

$$\varepsilon_{PY^{\bullet}} = \frac{\Delta OD_{obsd}}{l[PY^{\bullet}]} + \varepsilon_{PY^{+}} \qquad (3.2)$$

In equation (3.2), ε's are the extinction coefficients (of the pyranyl radicals and pyrylium cations), ΔOD_{obsd} is the observed difference absorption and l is the optical path length (1 cm). The term $[PY^{\bullet}]$ represents the concentration of the pyranyl radicals. This term could not be measured directly. Since $PY^{\bullet}$ and $BP^{\bullet+}$ are formed in equal amounts in electron transfer reactions, this term can be replaced in equation (3.2) by $[BP^{\bullet+}]$. Values of $[BP^{\bullet+}]$ were calculated from the transient absorption at 680 nm and used in equation (3.2) to obtain the corrected spectra of the radicals. The corrected absorption spectra of the radicals are presented along with the transient absorption spectra in Figures 3.11-3.13. Note that the absorption spectrum of $\mathbf{2}^{\bullet}$ shows two bands. Absorption spectra of $\mathbf{1}^{\bullet}$ and $\mathbf{2}^{\bullet}$ were similar to the spectra of pyranyl radicals reported in Chapter 2 of this thesis.

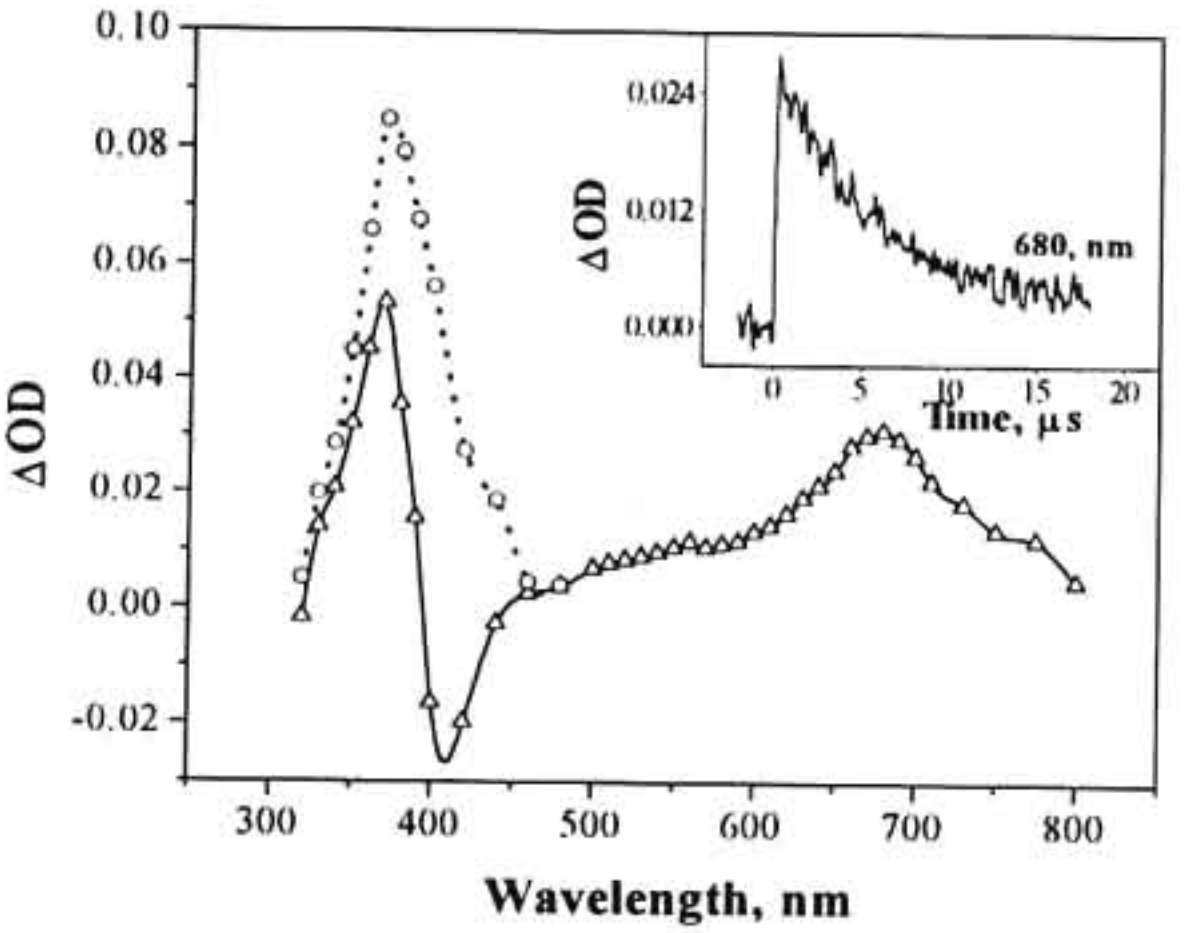

Figure 3.11 Transient absorption spectrum (Δ) of **1** (2 x 10^{-5} M) in the presence of biphenyl (0.1 M) at 100 ns following the laser pulse. Inset shows the decay of the transient at 680 nm. The corrected spectrum of the radical is also shown (- - O - -).

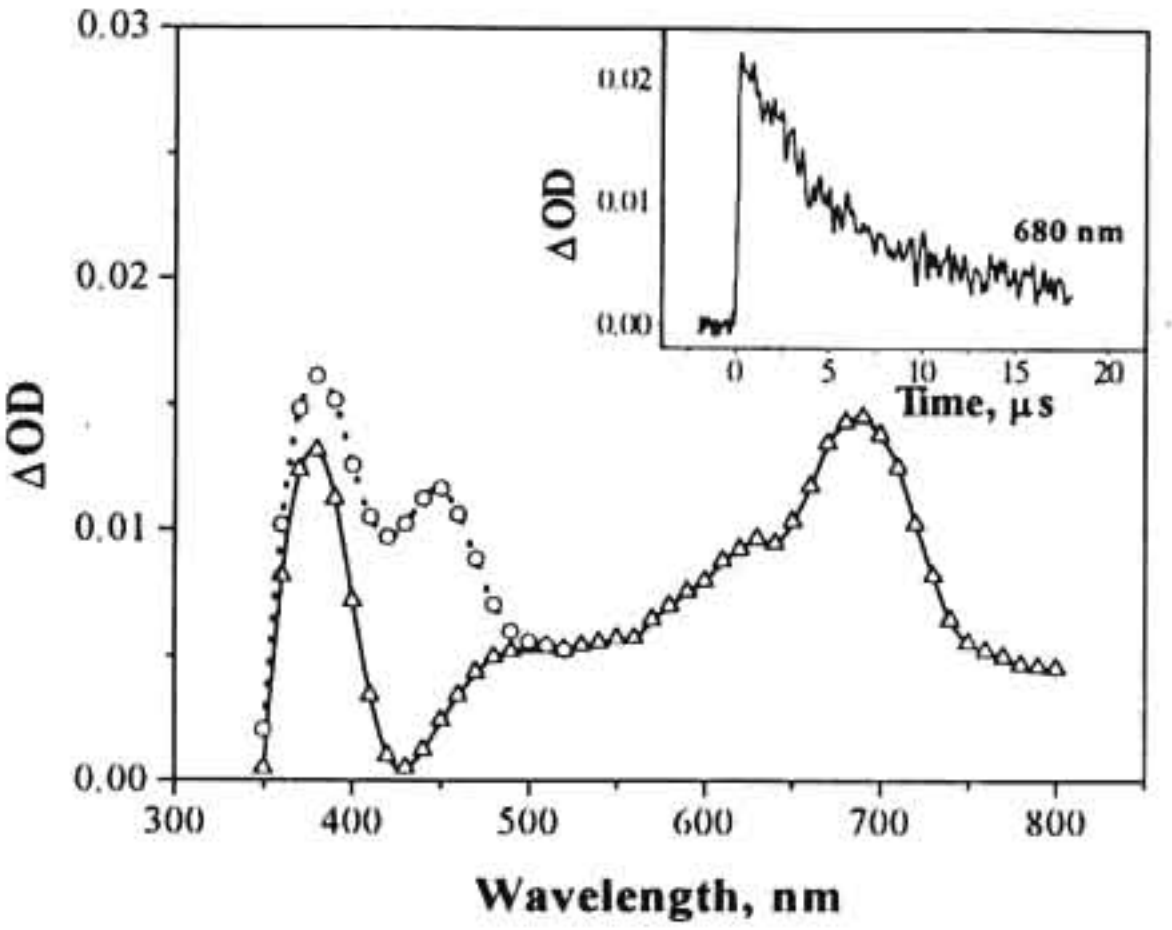

Figure 3.12 Transient absorption spectrum (Δ) of **2** (2 x 10^{-5} M) in the presence of biphenyl (0.1 M) at 100 ns following the laser pulse. Inset shows the decay of the transient at 680 nm. The corrected spectrum of the radical is also shown (- - O - -).

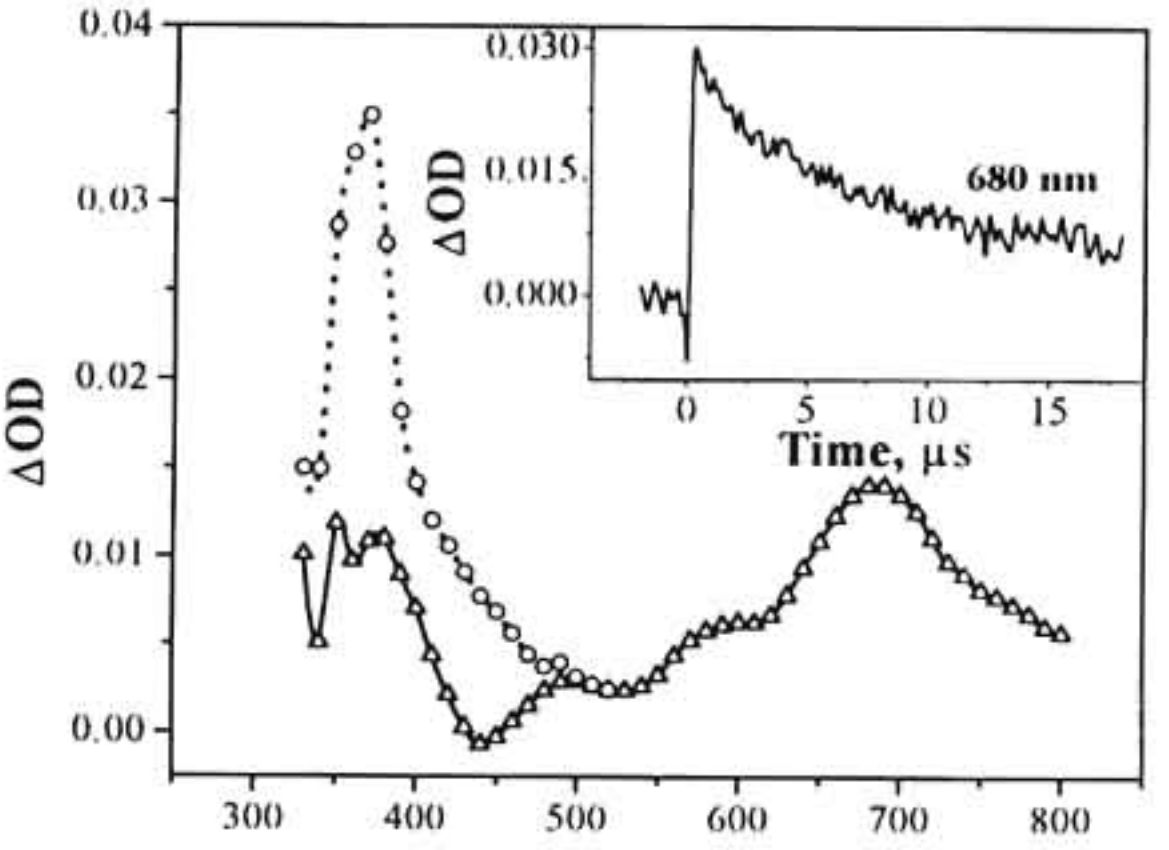

Figure 3.13 Transient absorption spectrum (Δ) of 3 (2×10^{-5} M) in the presence of biphenyl (0.1 M) at 100 ns following the laser pulse. Inset shows the decay of the transient at 680 nm. The corrected spectrum of the radical is also shown (- - O - -).

The decay of the radical ions followed second order kinetics. Since no long- lived absorptions due to product formation were observed, it was assumed that decay occurs by BET reactions. Monitoring the decay of the $BP^{\bullet+}$ absorption at 680 nm, the decay rates were calculated by second order, equal concentration kinetics. Values of the rate constants obtained ($= k_2/\varepsilon$) were in the range (6-9) x 10^6 cm s^{-1}. Substituting for ε, we obtained k_2 in the range (5.9-13.0) x 10^{10} M^{-1} s^{-1}. These values are an order of magnitude smaller compared to those observed for pyrylium salts studied in Chapter 2. We believe that extended delocalization of the odd electron (in $PY^{\bullet}$) into the naphthyl or biphenyl substituents, is responsible for the observed reduction in the BET rates in these cases.

The yields of radical formation in these cases were determined by relative actinometry (see Chapter 2 for details). These values along with the pyranyl radical absorption maxima, extinction coefficients and back electron transfer rates are presented in Table 3.6.

Table 3.6 Absorption maxima (λ_{max}^{R}), extinction coefficients (ε_{max}^{R}), rate of back electron transfer (k_{bet}) and quantum yields of formation (Φ_{ion}) for the pyranyl radicals obtained from 1-3.

Compound	λ_{max}^{R} nm	ε_{max}^{R} $M^{-1}cm^{-1}$	k_{bet} $M^{-1}s^{-1}$	Φ_{ion}
1	370	4.0×10^{4}	9.5×10^{10}	0.36
2	380 450	1.6×10^{4} 1.2×10^{4}	1.3×10^{11}	0.30
3	370	3.6×10^{4}	9.5×10^{10}	0.26

Φ_{ion} values obtained are relatively high. It was suggested earlier that the triplets of **1-3** might not be involved in electron transfer reactions with BP because of energetic reasons ($\Delta G_{et}^{T} > 0$). Thus PET reactions in these cases can involve only the singlet excited states. Generally, yields of ions from PET reactions involving singlet states are very low. The high yields of ions obtained in case of **1-3** are explained by invoking a relay effect as illustrated in Scheme 3.2.

In pyrylium salts **1-3**, the electron deficient pyrylium rings are connected to electron rich donor moieties such as biphenyl or naphthalene by a single bond. These systems are examples of donor-acceptor dyads. In the case of **1-3**, AM1

calculations have shown that excitation involve charge transfer from the donor to the acceptor moiety as shown in Scheme 3.2 (D = NP or BP). When an external quencher BP is present, a collision complex is formed which has configuration similar to a A-D-D triad. Electron transfer in these systems occurs by a relay effect[32,33] (see Chapter 1). This leads to a slight separation of the charge centers and enhances the yield of radical ions.

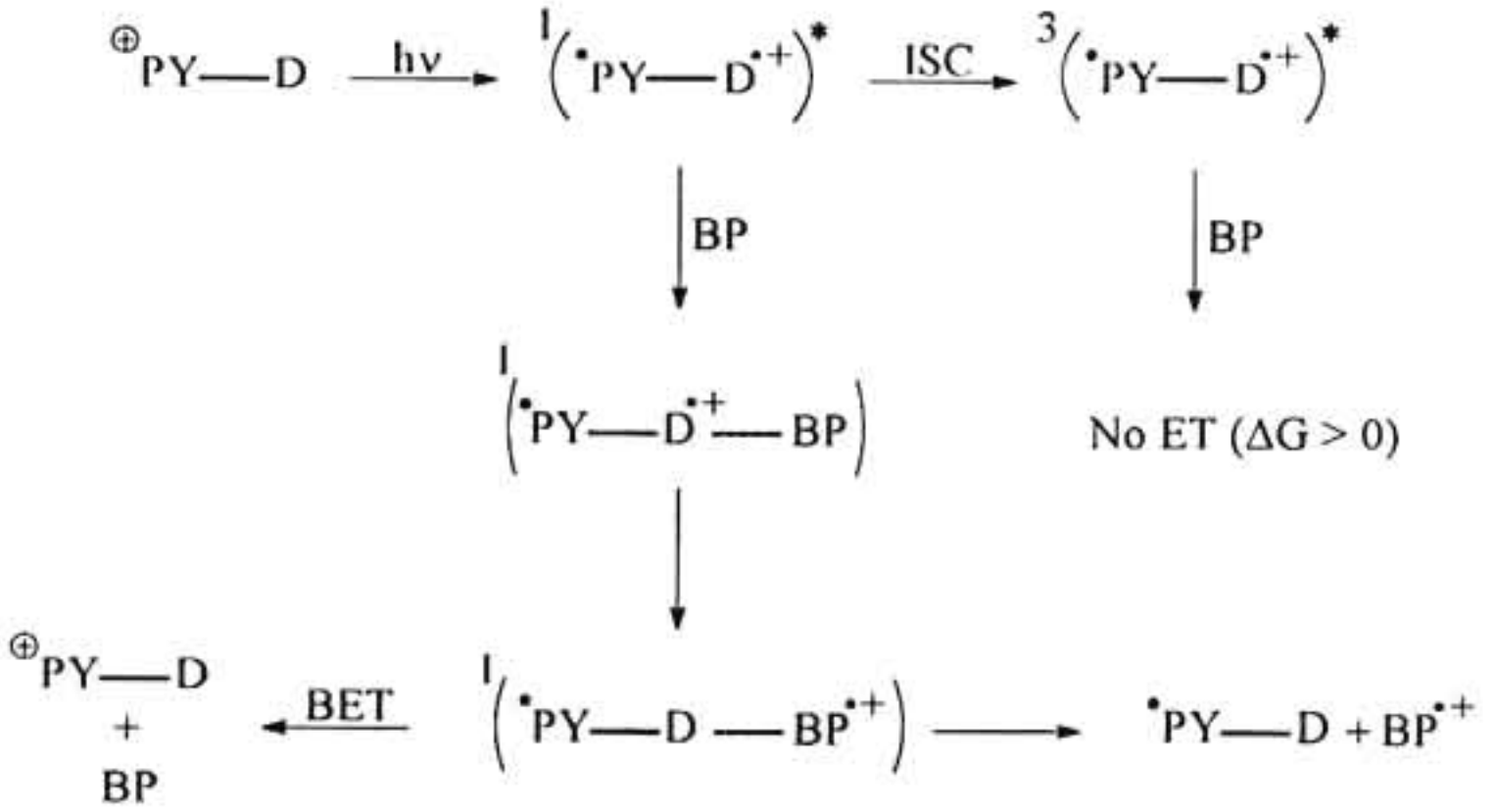

Scheme 3.2

3.3.2. Photophysical and electron transfer studies of 2,6-dimethyl-4-(*p*-acetylphenyl)pyrylium perchlorate (4)

3.3.2.1. Photophysical properties

Absorption maximum of **4** occurred at 336 nm ($\varepsilon = 2.4 \times 10^4$ M^{-1} cm^{-1}) in dichloromethane solution. The fluorescence parameters of this molecule determined in dichloromethane were: $\lambda_{max}(em) = 405$ nm, $\Phi_f = 0.03$, $\tau_f = 2$ ns and

E_S = 77.9 kcal M^{-1}. The very low value of Φ_f is attributed to enhanced intersystem crossing leading to formation of triplet state. **4** exhibited strong phosphorescence emission at 77 K in glycerol galss. Triplet energy (E_T) calculated from the phosphorescence spectrum was 65 kcal M^{-1}. Laser flash photolysis of **4** in degassed dichloromethane gave the transient absorption spectrum shown in Figure 3.14. Oxygen quenching experiments suggested that this transient absorption is due to the triplet of **4**. The extinction coefficient of the T-T absorption (ε = 2.7 x 10^4 M^{-1} cm^{-1}) and the triplet quantum yield (Φ_T = 0.66) were determined in the usual manner. Notice that carbonyl substitution leads to large Φ_T value in this case.

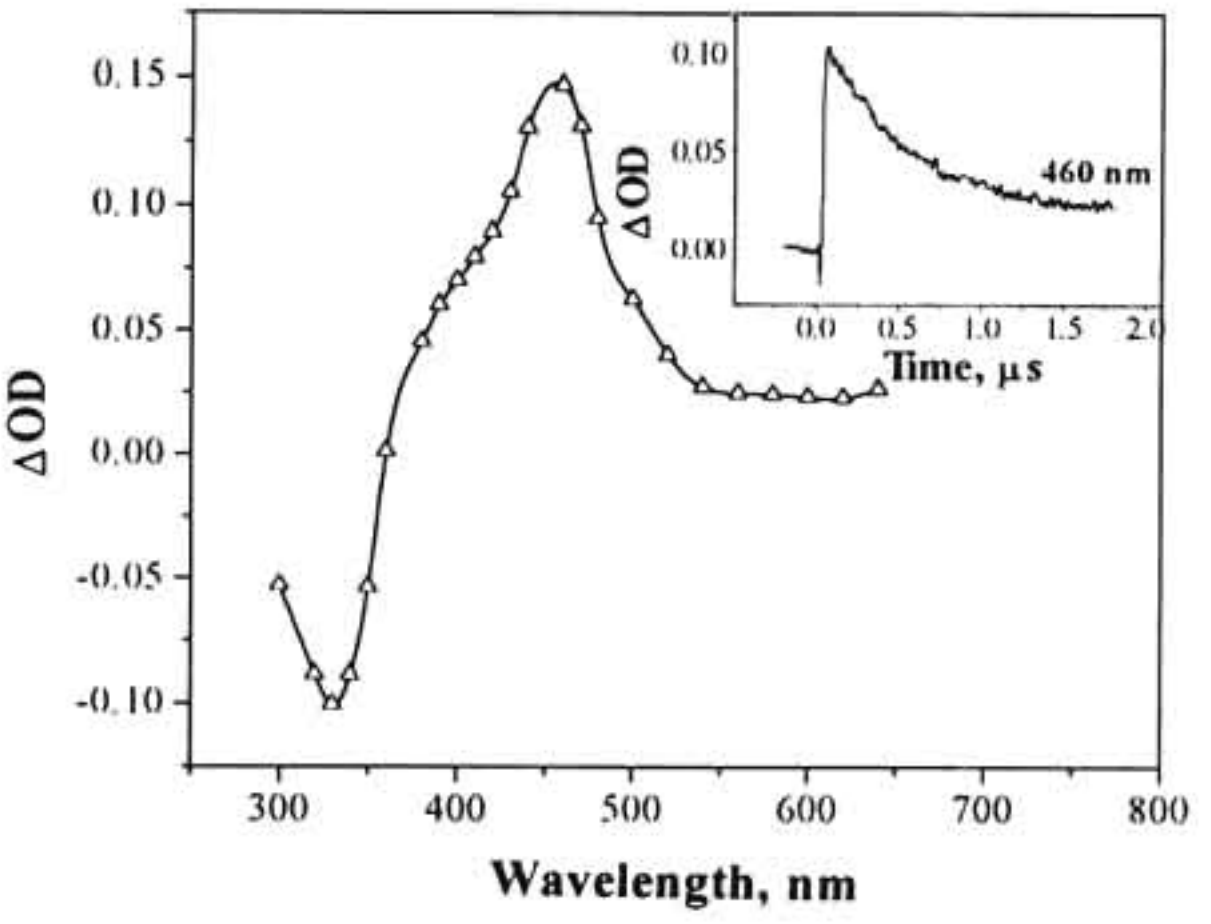

Figure 3.14 Transient absorption spectrum of **4** in dichloromethane recorded at 60 ns after the laser pulse. Inset shows the decay of the triplet at 460 nm.

3.3.2.2. Electron transfer studies

The reduction potential of **4** measuerd in acetonitrile was -0.38 V *vs.* SCE. Using this value, the free energy changes associated with the electron transfer reactions involving singlet (ΔG_{el}^{S} = -23.9 kcal M^{-1}) and triplet (ΔG_{el}^{T} = -10.8 kcal M^{-1}) excited states of **4** and BP were calculated. Large ΔG values suggest diffusion controlled quenching of the excited states. In agreement with this, values of 1.5 x 10^{10} and 9 x 10^{9} M^{-1} s^{-1} were obtained for k_q^{S} (fluorescence quenching) and k_q^{T} (triplet quenching), respectively.

Transient absorption spectrum of **4** in the presence of BP was recorded under triplet quenching conditions. Transient absorption spectra obtained at different time intervals following the laser excitation are shown in Figure 3.15.

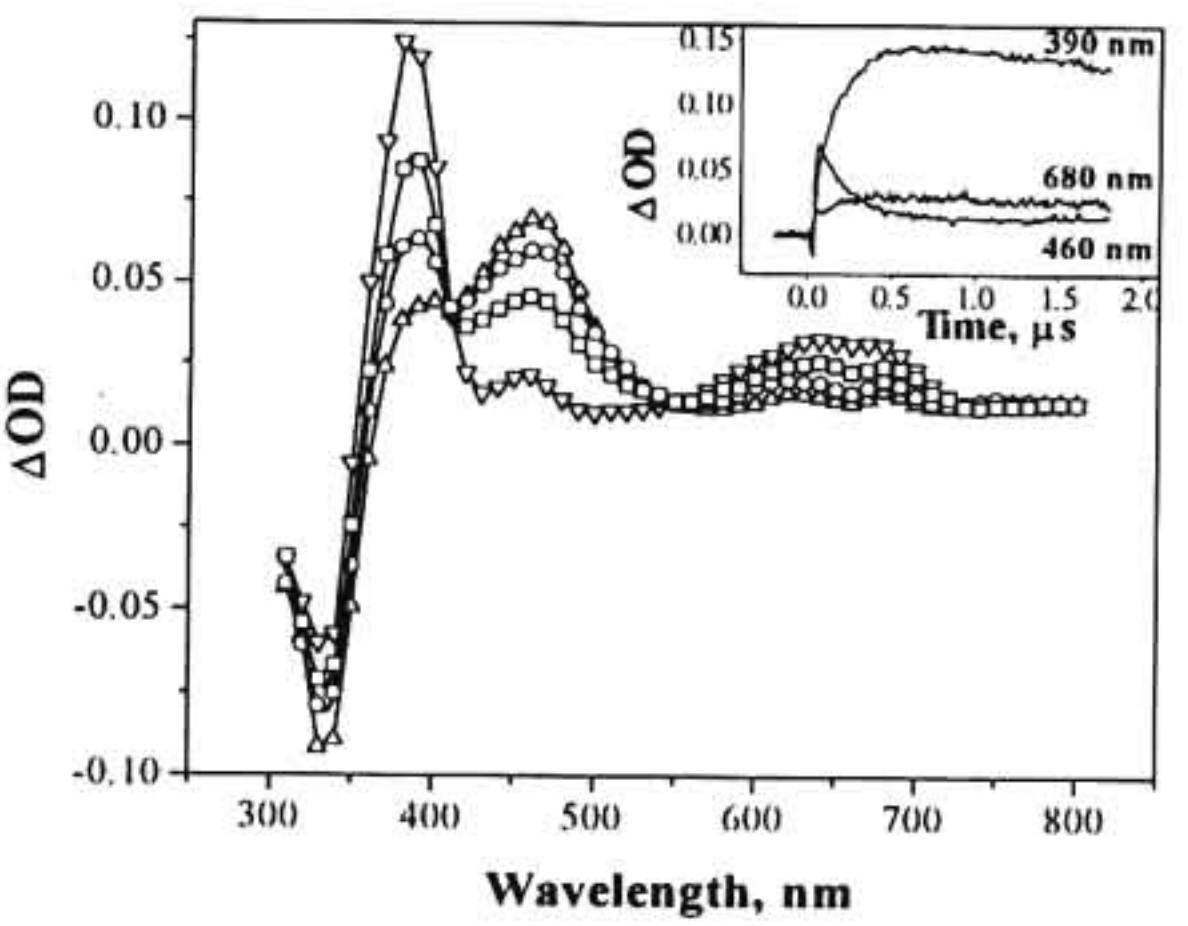

Figure 3.15 Transient absorption spectra at (Δ) 0.1, (O) 0.25, (□) 0.5 and (∇) 1.0 μs following the 355 nm laser pulse excitation of **4** (2 x 10^{-5}M) in the presence of biphenyl (1 x 10^{-4} M) in dichloromethane. Insert shows the growth of the transient at 390 nm , 680 nm and decay at 460.

The transient absorption spectra shows the decay of the triplet at 460 nm and concomitant growths of $BP^{\bullet+}$ at 680 nm and another absorption at 385 nm. This absorption was assigned to the pyranyl radical ($4^{\bullet}$). The decay of the triplet absorption at 460 nm matched very well with the growth of the radical absorption at 385 nm. This suggests that electron transfer from BP to the triplet state of **4** leads directly to the formation of the radical ion pairs.

Transient absorption spectrum was also recorded in the presence of 0.1 M BP. Under these conditions, the singlet excited states are also quenched. Formation of $BP^{\bullet+}$ and $4^{\bullet}$ within the laser pulse was observed in this experiment. Quantum yield of ion formation (Φ_{ion} = 0.71) and rate of back electron transfer (k_{bet} = 1.3 x 10^{11} M^{-1} s^{-1}) were measured for **4**/BP system in the usual manner. The Φ_{ion} value for this compound was the highest observed among pyrylium salts we have studied and is attributed to high triplet quantum yield of **4**. High Φ_{ion} value and low k_{bet} value suggest that this compound is ideally suited for use as a PET sensitizer.

3.3.3. Electron transfer studies of 2,6-di-*tert*-butyl-4-phenylpyrylium perchlorate (5)

In this section, laser flash photolysis studies of **5** in the absence and presence of BP are reported. As mentioned earlier our aim has been to study the effect of steric factor in PET reactions of pyrylium salts. Lin and Schuster have studied the photophysical properties of **5** and its naphthalene sulphonate salt.[34] Hence photophysical properties of **5** are not described here. Laser flash photolysis of **5** in acetonitrile gave the transient absorption spectrum shown in Figure 3.16. The transient was quenched by oxygen and hence the spectrum was assigned to

T-T absorption of **5**. Values of ε_{max}^{T} = 2.8 x 10^4 M^{-1} cm^{-1} and Φ_T = 0.63 were determined for the triplet state of this molecule.

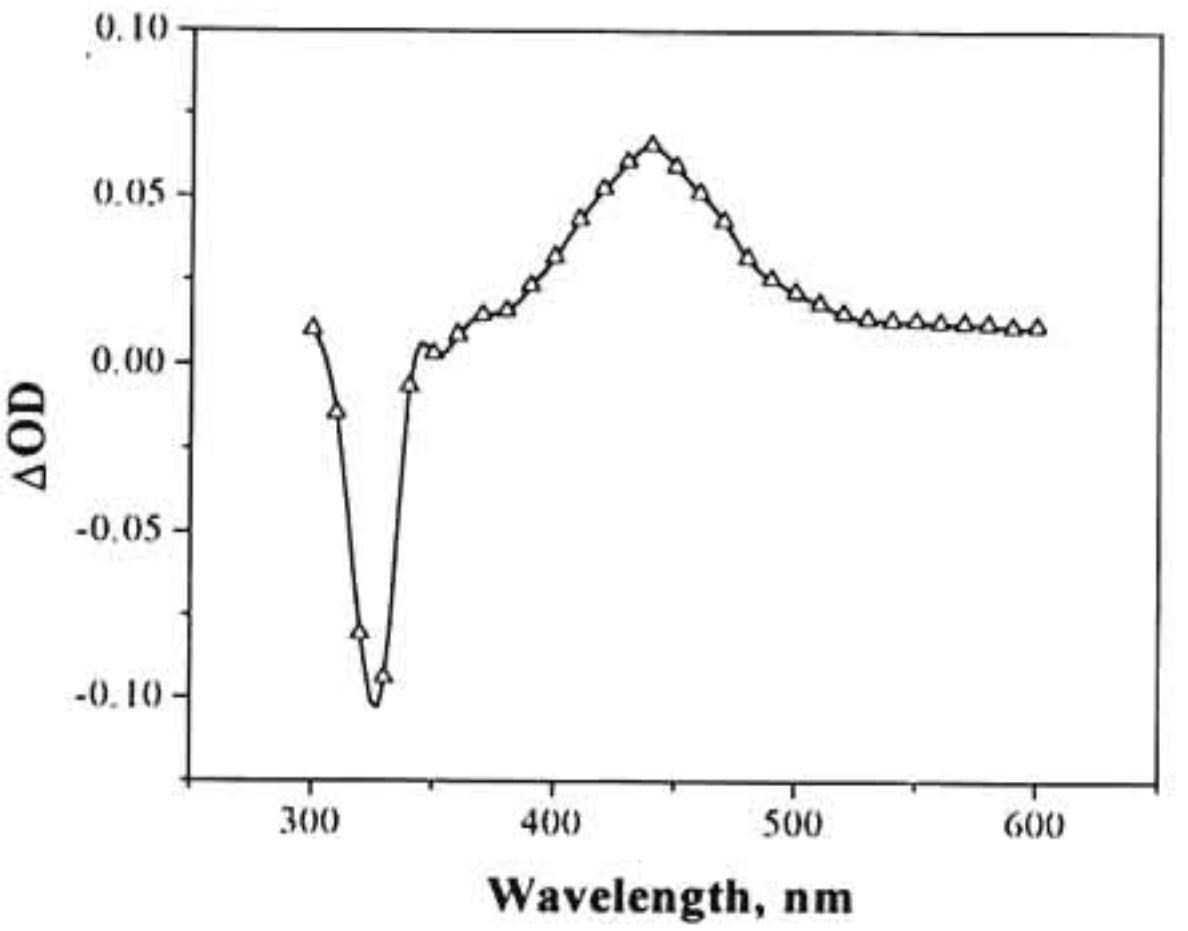

Figure 3.16 Transient absorption spectrum of **5** in acetonitrile recorded at 100 ns after the laser pulse.

Triplets of **5** were quenched by BP with k_q^{T} = 9.8 x 10^9 M^{-1} s^{-1}. The transient absorption spectra recorded under triplet quenching conditions at various time intervals following the laser pulse excitation are shown in Figure 3.17. The spectra showed decay of the triplet at 440 nm and concomitant growths at 680 nm due to $BP^{\bullet-}$ and at 390 nm due to $\mathbf{5}^{\bullet}$. The rate of decay at 440 nm and growth at 390 nm (see insert of figure 3.17) matched very well suggesting that quenching of triplet leads directly to formation of radical ions. Transient absorption spectrum obtained under singlet quenching conditions showed prompt formation of the radical absorptions at 390 and 680 nm.

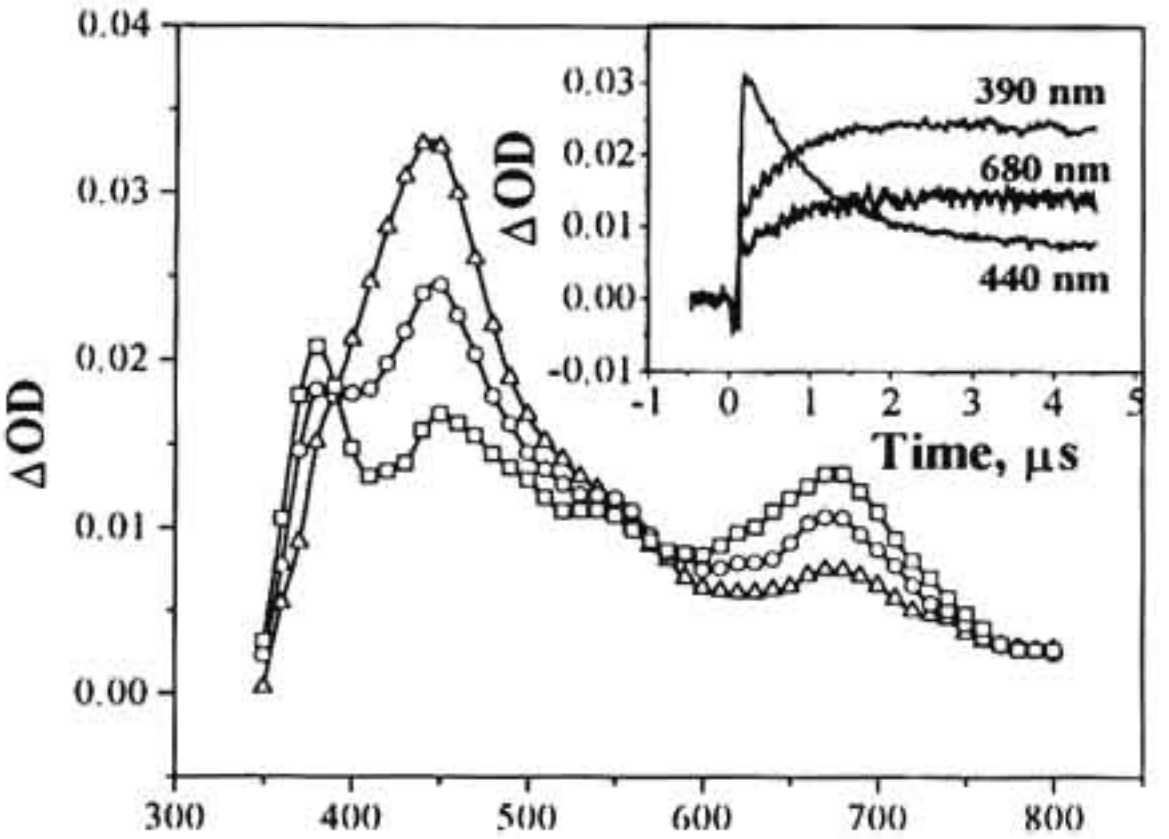

Figure 3.17 Transient absorption spectra at (Δ) 0.1, (O) 0.5 and (□) 1.5 μs following the 355 nm laser pulse excitation of **5** (5×10^{-5}M) in the presence of biphenyl (1×10^{-4} M) in acetonitrile. Insert shows the growth of the transients at 390 nm , 680nm and decay at 440 nm.

In order to evaluate the efficiency of this sensitizer, quantum yields of ion formation and rate of BET were determined. Low k_{bet} (6.7×10^{10} M^{-1} s^{-1}) and relatively high Φ_{ion} (0.46) values were obtained. These results suggest that pyrylium salt **5** can be used as a good sensitizer for PET reactions.

3.3.4. Photophysical and electron transfer studies of dicationic pyrylium salts 6-7

Although several dicationic pyrylium salts are reported in the literature, their photophysical and electron transfer studies have not been reported so far. Because of the presence of two positive charges in the molecule, we expect these salts to be highly oxidizing in nature. They have very broad absorption in the visible region,

which make them suitable for use as PET sensitizers. These aspects have prompted us to undertake a systematic study of a few representative examples.

3.3.4.1. Absorption and emission studies

Dicationic pyrylium salts **6** and **7** are relatively unstable in dichloromethane solution in the presence of light and hence all the studies with these compounds were carried out in acetonitrile solution. Absorption spectra of **6** and **7** in acetonitrile are shown in Figure 3.18. Figure 3.19 shows the fluorescence spectra of these compounds in the same solvent. It can be seen from Figures 3.18 and 3.19 that bromine substitution leads to a red shift in the absorption spectrum and a blue shift in the emission spectrum.

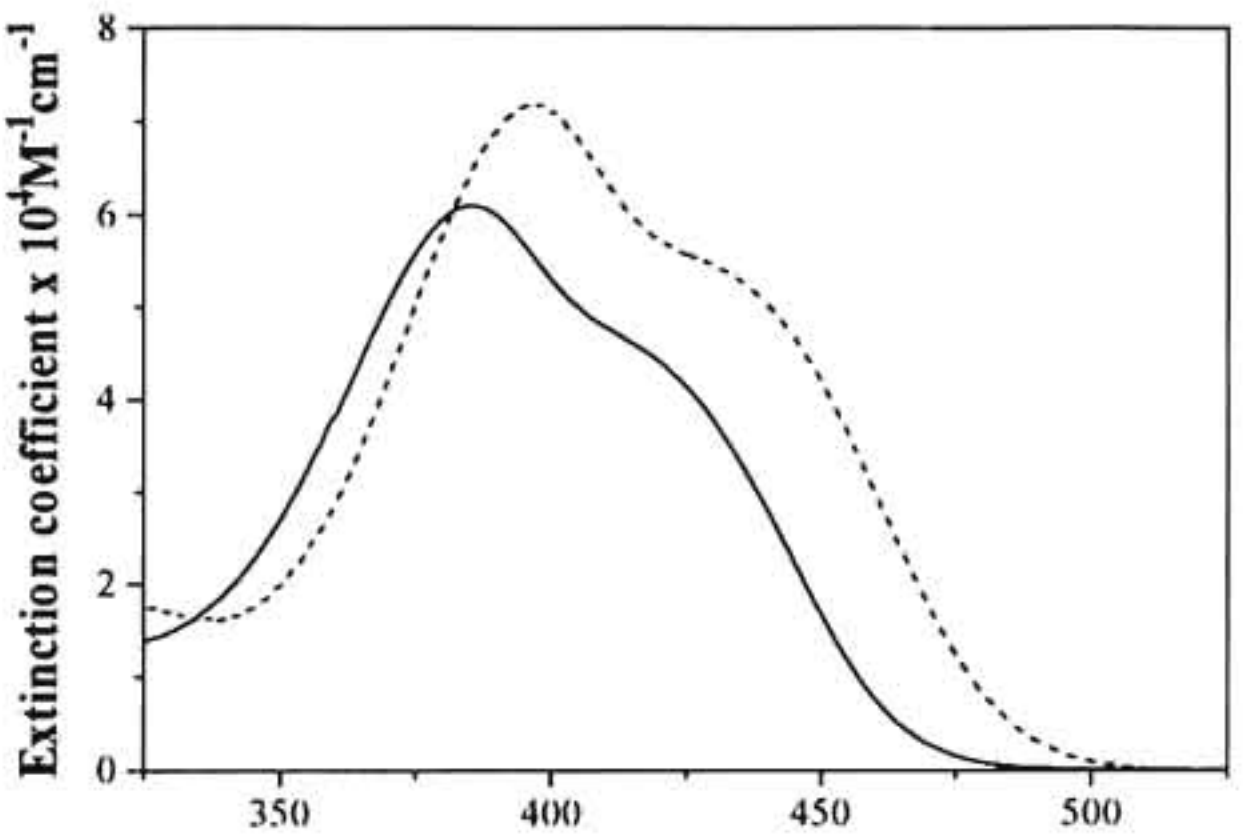

Figure 3.18 Absorption spectra of **6** (—) and **7** (- - - -) in acetonitrile.

Substitution of bromine also leads to a substantial reduction in the fluorescence quantum yield and fluorescence lifetime (Figure 3.20). Decrease in

the Φ_f and τ_f values were attributed to enhanced intersystem crossing induced by the heavy bromine atoms present in **7**. The absorption and emission properties of these pyrylium salts are summarized in Table 3.7.

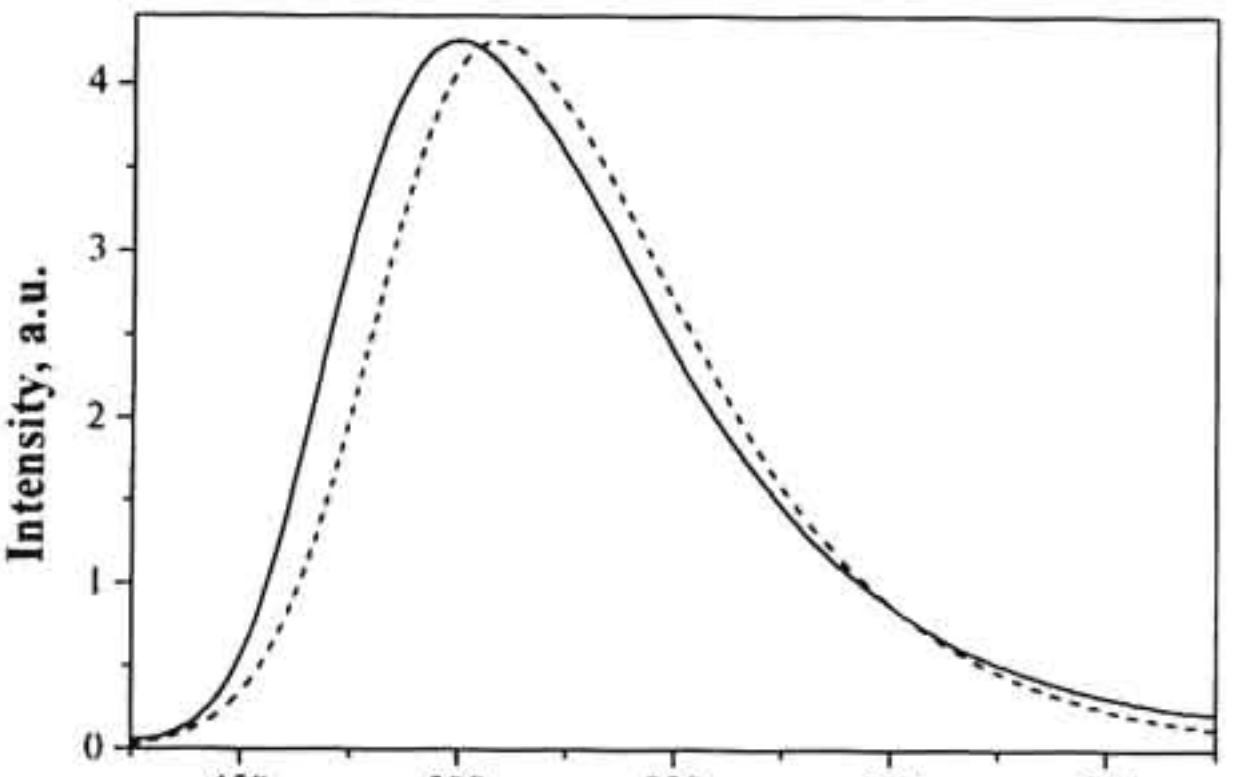

Figure 3.19 Normalized emission spectra of **6** (- - - -) and **7** (—) in acetonitrile.

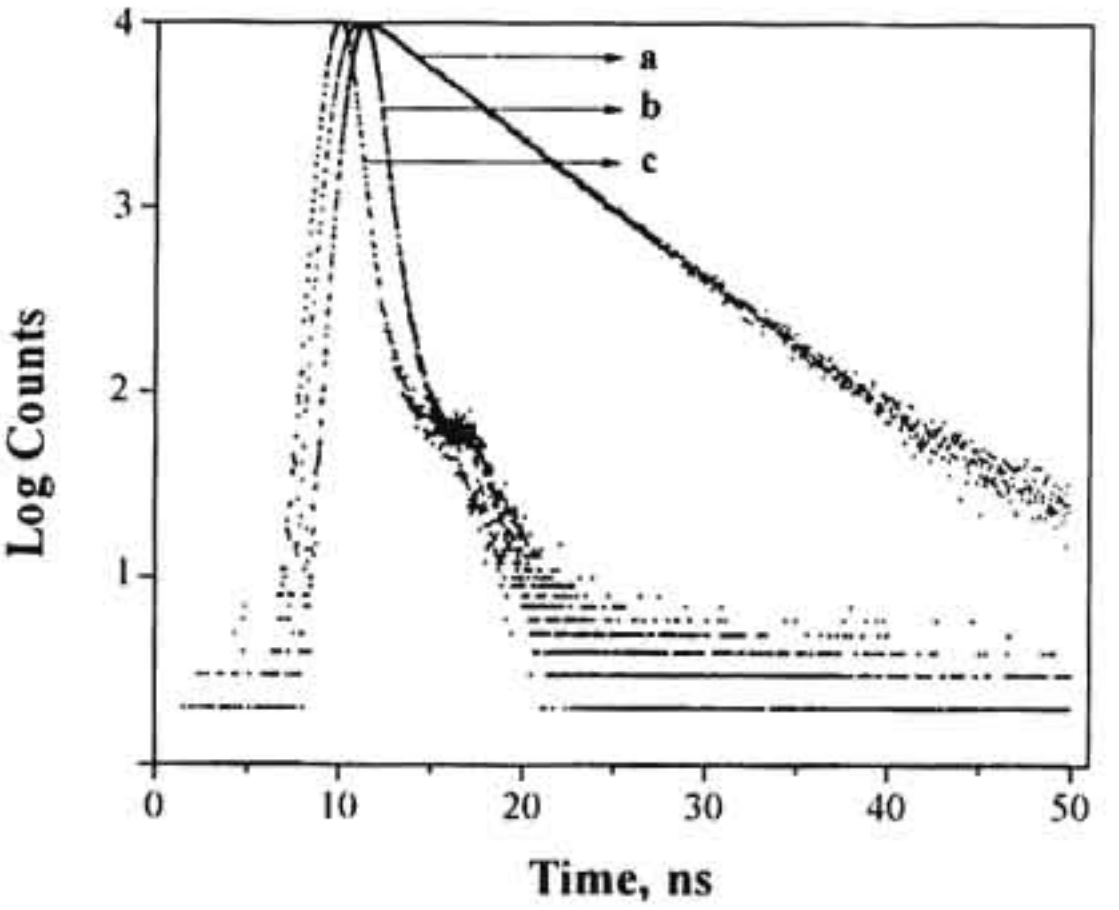

Figure 3.20 Fluorescence decay profiles of **6** (a) and **7** (b) in acetonitrile. (c) is the lamp profile. λ_{ex} = 380 nm, λ_{em} = 500 nm.

Table 3.7 Absorption maxima (λ_{max} (abs)), extinction coefficients (ε_{max}), emission maxima (λ_{max} (em)), fluorescence lifetimes (τ_f), fluorescence quantum yields (Φ_f) and excitation energies ($E_{0,0}$) of pyrylium salts 6 and 7 in acetonitrile.

Compound	λ_{max} (abs) nm	ε_{max} $M^{-1}cm^{-1}$	λ_{max} (em), nm	τ_f, ns	Φ_f	$E_{0,0}$, kcal M^{-1}
6	385	6.1×10^4	508	5.6	0.15	62.0
7	397	7.2×10^4	498	1.2	0.016	59.8

Phosphorescence emission spectrum of **6** was measured in order to determine the triplet energy. Figure 3.21 shows the phosphorescence spectrum of **6** in glycerol glass at 77 K. Since the phosphorescence spectrum did not show any structure, the position of the 0,0 band could not be measured properly. Triplet energy of 58.3 kcal M^{-1} was calculated from the short wavelength end of the phosphorescence spectrum. Note that E_S-E_T = 3.7 kcal M^{-1} for **6**. Assuming the same energy gap, a value of 56.1 kcal M^{-1} was calculated for the triplet energy of **7**.

3.3.4.2. Laser flash photolysis studies

Laser flash photolysis of **6** and **7** in acetonitrile saturated with argon gave transient spectra characterized by absorption maxima at 520 nm and strong bleaching in the region of their ground state absorptions. Transient absorption spectrum of **7** is given in Figure 3.22. Based on oxygen quenching studies, the

transient was characterized as the triplet. The triplet state parameters we have determined are collected in Table 3.8.

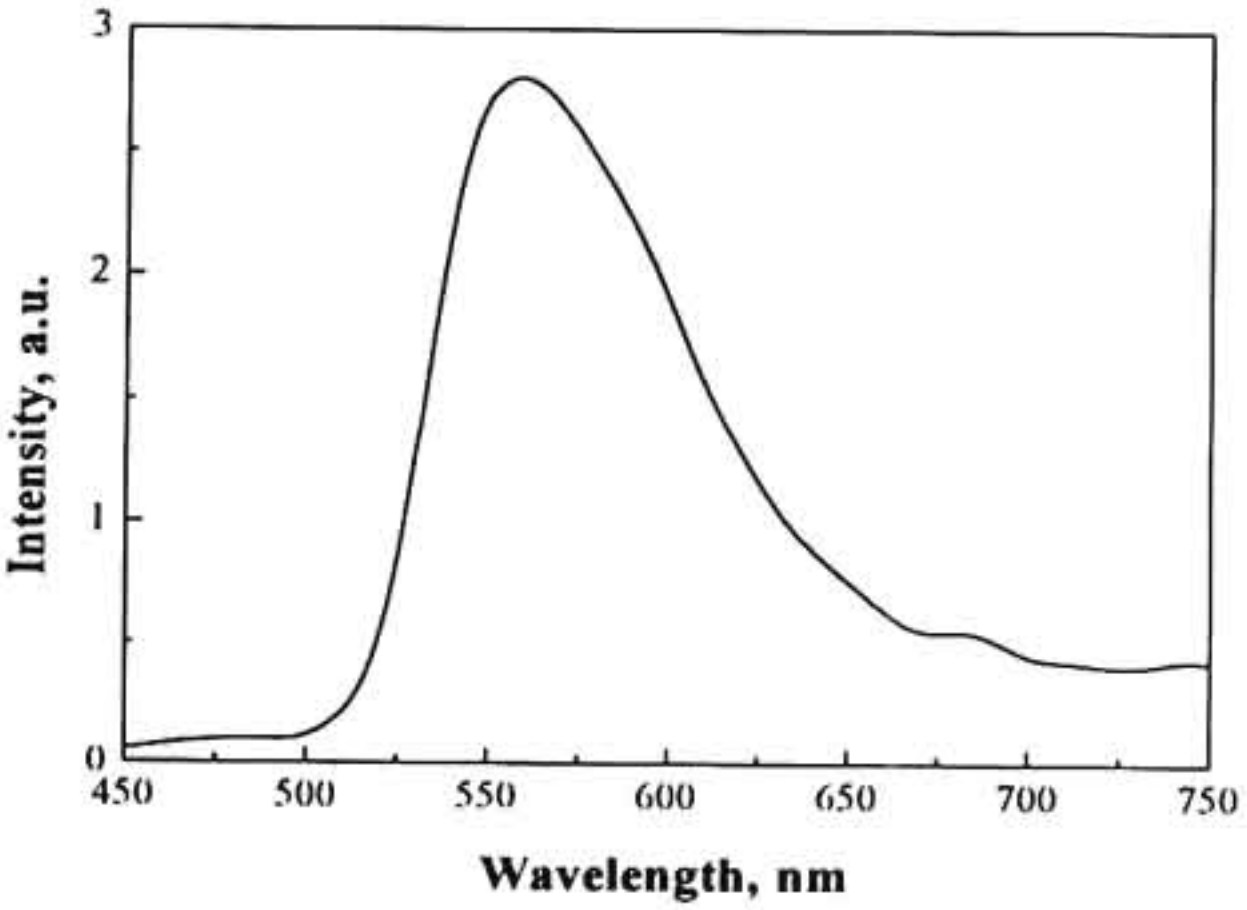

Figure 3.21 Phosphorescence emission spectrum of 6 in glycerol at 77 K.

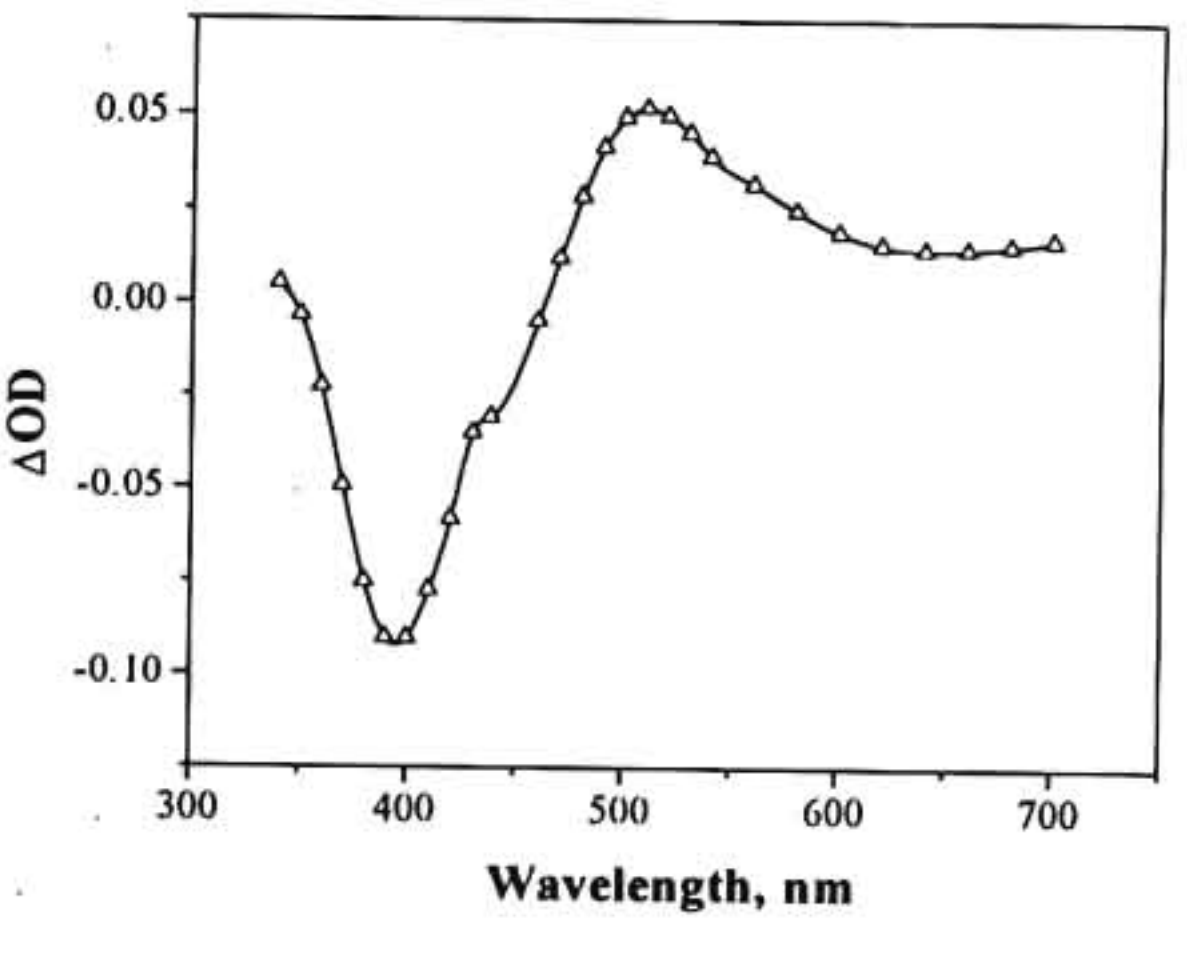

Figure 3.22 Transient absorption spectrum of 7 in acetonitrile recorded at 100 ns after the laser pulse.

Table 3.8 Triplet-triplet absorption maxima (λ^T_{max}), extinction coefficients (ε^T_{max}), triplet quantum yields (Φ_T), triplet lifetimes (τ_T) and oxygen quenching rate constants ($k_q(O_2)$) for pyrylium derivatives 6 and 7.

Compound	λ^T_{max}(Abs), nm	ε^T_{max}(Abs), M^{-1} cm^{-1}	Φ_T	τ_T μs	$k_q(O_2)$ M^{-1} s^{-1}
6	520	3.9×10^4	0.05	4.6	3.9×10^8
7	520	3.3×10^4	0.13	3.8	6.2×10^8

Notice that the decrease in the fluorescence quantum yield of **7** is associated with a corresponding increase in the triplet quantum yield. In both cases, $\Phi_f + \Phi_T << 1$ and suggest the involvement of other nonradiative decay pathways.

3.3.4.3. Electron transfer studies

Cyclic voltammogram of **6** was obtained in acetonitrile solution in the presence of tetra-*n*-butylammonium perchlorate as supporting electrolyte. The first reduction peak appeared at -0.21 V *vs.* SCE. For the dicationic salt **7**, reduction potential could not be measured due to decomposition of the salt at the electrode surface. Hence a value of -0.21 V is assumed for the reduction potential of **7**.

The fluorescence of **6** and **7** were quenched by BP. Plots of the fluorescence intensity *vs.* BP concentration were linear. These plots were analyzed using the Stern-Volmer treatment to obtain the singlet quenching rates (k_q^S). The triplet quenching rate constants were determined by laser flash photolysis

experiments. We have noted that at higher concentrations (> 10^{-3} M), BP forms CT complexes with these salts. Hence, concentrations of BP employed for these studies were kept low (1-5 x 10^{-5} M). In Table 3.9 we have collected the free energies and rate constants of the singlet and triplet mediated electron transfer reactions of **6** and **7** with BP. Note that k_q^S value for **7** is larger than that expected for diffusion controlled quenching. The high value of k_q^S in this case suggested static quenching and is attributed to CT complex formation between BP and **7**.

Transient absorption spectra of **6** and **7** were recorded in the presence of low concentrations of BP. Spectra obtained in both cases were similar. As an example, transient absorption spectrum of **6**/BP system is shown in Figure 3.23.

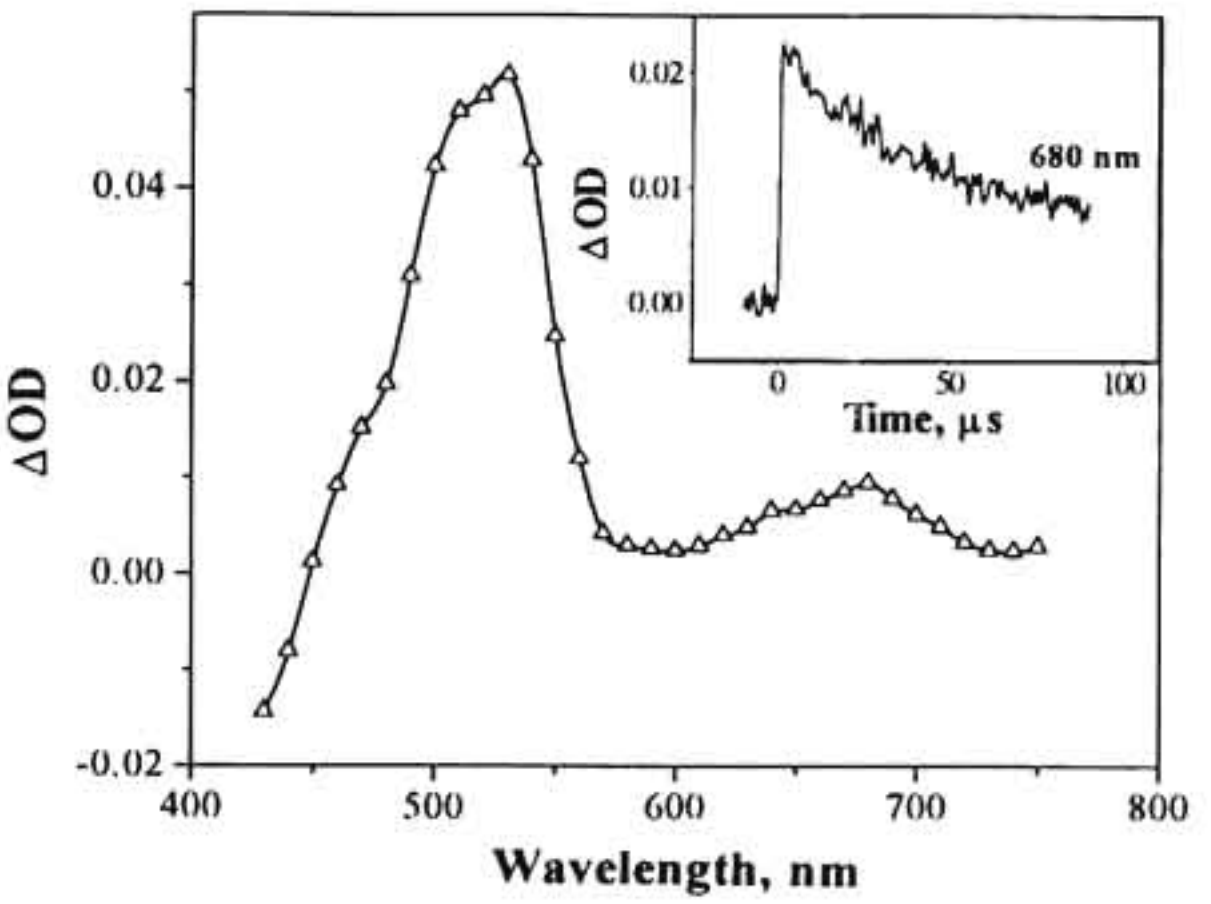

Figure 3.23 Transient absorption spectrum of **6** (2 x 10^{-5} M) in the presence of biphenyl (1 mM) at 1 μs following the laser pulse. Inset shows the transient decay at 680 nm.

In addition to the absorption band due to the triplet at 520 nm (shoulder), the spectrum exhibited bands at 680 nm due to $BP^{\bullet-}$ and at 540 nm due to the pyranyl radical cation ($6^{\bullet+}$). It was observed in these studies that increasing the concentration above 1 x 10^{-3} M leads to a decrease in the yield of the absorptions due to the radical cations. We have attributed this to the formation of a CT complex between BP and dicationic salts **6** and 7. As mentioned previously, CT complex formation leads to facile BET reactions, thereby decreasing the yield of radical ions.

Yields of radical ions and rates of BET reactions were determined at low BP concentrations. These values are also given in Table 3.9. The BET rates obtained in these cases were significantly low compared to the values obtained for other pyrylium salts reported in this thesis. Relatively high Φ_{ion} values were also obtained. We believe that this is a direct consequence of the Coulombic repulsion between the product ion pairs, which result in enhanced yields of radical ions and reduced rates of recombination. Thus dicationic pyrylium salts **6** and 7 can also function as good PET sensitizers if CT complex formation can be avoided.

Table 3.9 Free energies of electron transfer (ΔG_{el}), quenching rate constants (k_q), rates of back electron transfer (k_{bet}) and quantum yields of ion formation (Φ_{ion}) for the PET between BP and pyrylium salts 6 and 7 in acetonitrile solution.

Compound	ΔG_{el}^{S} kcal M^{-1}	k_q^{S}, $M^{-1} s^{-1}$	ΔG_{el}^{T}, kcal M^{-1}	k_q^{T}, $M^{-1}s^{-1}$	k_{bet} $M^{-1}s^{-1}$	Φ_{ion}
6	-11.9	1.9×10^{10}	-8.3	2×10^{10}	2.5×10^{10}	0.21
7	-4.9	7.2×10^{10}	-3.4	2×10^{10}	2.3×10^{10}	0.31

In this Chapter, we have studied the photophysical and electron transfer properties of several pyrylium salts. Several strategies that are in use for the control of BET reactions were tested in the pyrylium class of compounds. Yields of product radicals were higher for pyrylium salts reported in this Chapter (Φ_{ion} = 0.3-0.7) compared to those reported in Chapter 2. Among the several strategies we have employed, design of sensitizers with enhanced triplet quantum yields appears to be the most productive one. For example, pyrylium salts **4** and **5** gave very high yields of ion radicals and shows great potential for use as PET sensitizers. Although pyrylium salts **1**-**3** gave only moderate yields of ion radicals, their absorption at $\lambda > 400$ nm makes them suitable for use in the visible region. Dicationic pyrylium salts also absorb in the visible region, but they tend to form CT complexes with electron rich molecules thereby reducing the yields of radical ions.

3.4. Experimental

Measurements: All melting points are uncorrected and were determined on a Büchi Model 530 melting point apparatus. IR spectra were recorded on a Perkin Elmer Model 882 IR spectrometer. ^{1}H NMR spectra were recorded on a JEOL EX-90 spectrometer. Mass spectra (FAB) were recorded on a JEOL JMS AX503 mass spectrometer. The absorption spectra were recorded on a Shimadzu UV-2100 or a GBC double beam UV-VIS spectrophotometer. Fluorescence spectra were recorded on a SPEX Fluorolog F 112X spectrofluorimeter with a right angled geometry using 1 x 10^{-5} M solutions. Phosphorescence spectra of the compounds in glycerol glass at 77 K were recorded on a SPEX 1934D phosphorimeter. Fluorescence lifetimes were determined using a IBH 5000 U or a Edinburgh

Instruments FL900CD single photon counting system. Electrochemical experiments were performed with a Wenking Model POS 73 potentioscan and pulse generator. Solutions of the pyrylium salts (1 x 10^{-3} M) in acetonitrile, containing 0.1 M tetra-*n*-butylammonium tetrafluoborate as supporting electrolyte were thoroughly degassed before use. A glassy carbon electrode was used as the working electrode and a platinum gauze was used as the counter electrode. Laser flash photolysis experiments were carried out by employing an Applied Photophysics Model LKS-20 Laser Kinetic Spectrometer using GCR-12 Series Quanta Ray Nd:YAG laser. The analyzing and laser beams were fixed at right angles to each other. The laser energy was 60 mJ at 355 nm.

Materials: The pyrylium derivatives **1-4** were synthesized by the general route outlined below.[35]

The appropriate Grignard reagent was prepared through the reaction of corresponding bromo derivative (20 mM) and magnesium (20 mM) in dry THF (20 mL). This reagent was added to a suspension of 2,6-dimethyl-4-pyrone (20 mM) in dry THF (50 mL) at 0°C. The solution was allowed to warm to room temperature and stirred for 30 minutes. Ice cold solution of 10% perchloric acid (100 mL) was added and the precipitated pyrylium salt was collected by filtration. The salt thus obtained was dissolved in dichloromethane and reprecipitated by adding ether. This process was repeated until a constant melting point was obtained. In the case of 4-bromoacetophenone, the carbonyl function was protected by ethyleneglycol before making the Grignard reagent.

2,6-Dimethyl-4-biphenylpyrylium perchlorate (1): Yield 51%; mp 180-181 °C; IR (ν_{max}): 3009, 2963, 2890, 1643, 1092 cm^{-1}; ^1H NMR (90 MHz, $CDCl_3$), δ 3.0

(s, 3 H), 7.3 - 8.3 (m, 11 H); HRMS (FAB) calcd for $C_{19}H_{17}O^+$ (cation) 261.1279, found, 261.1292.

2,6-dimethyl-4-α-naphthylpyrylium perchlorate (2): Yield 28%; mp 159-160 °C; IR (ν_{max}): 3089, 2975, 2918, 1635, 1095 cm^{-1}; ^1H NMR (90 MHz, $CDCl_3$), δ 3.0 (s, 6 H), 7.3 - 8.1 (m, 9 H); HRMS (FAB) calcd for $C_{17}H_{15}O^+$ (cation) 235.1123, found, 235.1129.

2,6-dimethyl-4-β-naphthylpyrylium perchlorate (3): Yield 40%; mp 237 –238 °C; IR (ν_{max}): 3020, 2937, 2869, 1628, 1108 cm^{-1}; ^1H NMR (90 MHz, $CDCl_3$), δ 3.0 (s, 6 H), 8.0 - 9.0 (m, 9 H); HRMS (FAB) calcd for $C_{17}H_{15}O^+$ (cation) 235.1123, found, 235.1142.

2,6-dimethyl-4-(*p*-acetylphenyl)pyrylium perchlorate (4): Yield 20%; mp 134 – 135 °C; IR (ν_{max}): 3087, 2936, 2864, 1636, 1099 cm^{-1}; ^1H NMR (90 MHz, $CDCl_3$), δ 2.6 (s, 3 H) 3.0 (s, 6H), 7.9 – 8.3 (m, 6 H); HRMS (FAB) calcd for $C_{15}H_{15}O_2^+$ (cation) 227.1072, found, 227.1075.

Synthesis of 2,6-di-*t*-butyl-4-phenylpyrylium perchlorate (5)

Synthesis of pyrylium derivative **5** was carried out according to a reported procedure.[34] Phenyl magnesium bromide was prepared through the reaction of bromobenzene (20 mM) and magnesium (20 mM) in dry THF (20 mL). This reagent was added to a suspension of 2,6-di-*t*-butyl-4-pyrone (20 mM) in dry THF (50 mL) at 0°C. The solution was allowed to warm to room temperature and stirred for 30 minutes. Ice cold solution of 10% perchloric acid (100 mL) was added and the precipitated pyrylium salt (**5**) was collected by filtration. The salt thus obtained was dissolved in dichloromethane and reprecipitated by adding

ether. This process was repeated until a constant melting point was obtained. Yield 12%; mp 222 – 223 °C (lit. mp 222 – 223 °C).[34]

Synthesis of dicationic pyrylium salts 6 and 7

Dicationic pyrylium salts **6** and **7** were synthesized according to the general route outlined in Scheme 3.3.[36]

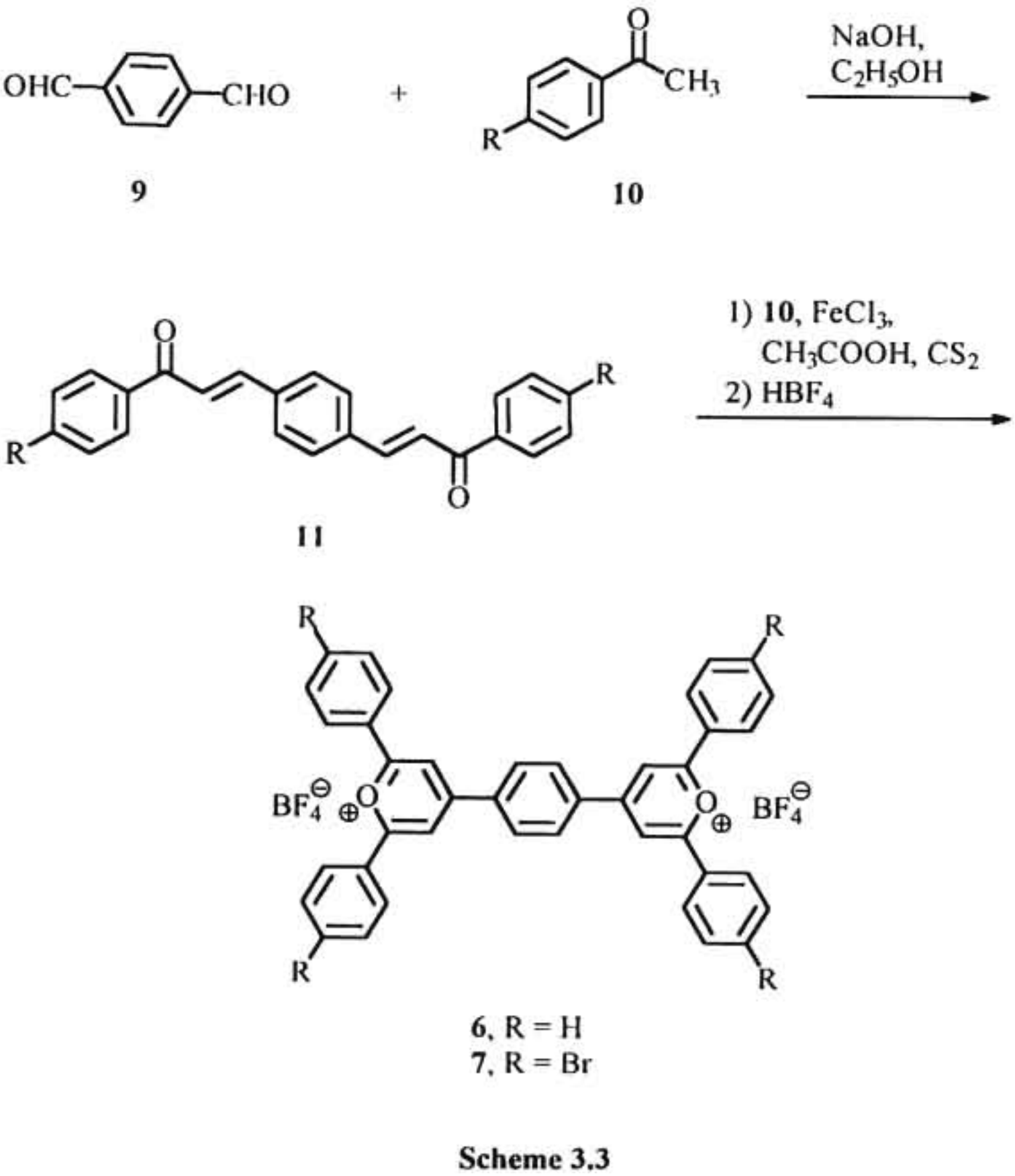

Scheme 3.3

Appropriate bischalcone of terephthalaldehyde was prepared according to the following general procedure. A mixture of Sodium hydroxide (2.05 g, 51 mM), terephthalaldehyde (2.68 g, 20 mM), water (20 mL), ethanol (12 mL) and the appropriate acetophenone derivative (40 mM) was stirred for 10 h and cooled at 0 °C for 12 h. The crystalline product was filtered and recrystallized from a 1:1 mixture of ethanol and chloroform to obtain **11** in about 98% yield. Bischalcone **11** (10 mM) and the appropriate acetophenone derivative (25 mM) were taken in a 1:1 mixture (100 mL) of acetic anhydride and carbon disulphide. The solution was warmed and $FeCl_3$ (0.6 moles) was added slowly with stirring. It was refluxed for 4 h and then cooled in ice for 12 h. The precipitate obtained was washed several times with ether, dissolved in dilute acetic acid and filtered. The filtrate was then treated with 48% tetrafluoroboric acid and the dicationic pyrylium salt obtained was collected by filtration and washed several times with ether.

***p*-Phenylene-[bis-4,4'-(2,6-diphenylpyrylium tetrafluoroborate)] (6)**: Yield 11%; mp >350 °C (lit. mp >350 °C).[36] IR (ν_{max}): 1634, 1089 cm^{-1}; ^1H NMR (90 MHz, $CDCl_3$), δ 7.5 – 8.7 (m, 24 H), 9.2 (4H).

***p*-Phenylene-[bis-4,4'-(2,6-di-*p*-bromophenylpyrylium tetrafluoroborate)] (7)**: Yield 16%; mp 300 - 302 °C; IR (ν_{max}): 1629, 1067 cm^{-1}; ^1H NMR (90 MHz, $CDCl_3$), δ 7.5 – 8.8 (m, 24 H), 9.2 (4H); HRMS (FAB) calcd for $C_{40}H_{24}O_2BBr_4F_4^+$ (cation) 938.8539, found, 938.8538. Anal. Calcd for $C_{40}H_{24}O_2B_2Br_4F_8$: C, 46.79; H, 2.36. Found: C, 45.39; H, 2.54.

Biphenyl used in these studies was a commercial sample and was recrystallized several times before use. Spectroscopic grade solvents were used

throughout and solutions for flash photolysis experiments were deaerated with argon for 15 minutes, prior to the experiments.

3.5. References

1. Mauzerall, D. in *Photoinduced Electron Transfer. Part A*, Fox, M. A.; Channon, M. (Eds.), Elsevier, Amsterdam, **1988**, p. 228.
2. Pragst, F.; Janda, M.; Stibor, I. *Electrochim. Acta* **1980**, *25*, 779.
3. Pragst, F.; Ziebig, R. *Electrochim. Acta* **1978**, *23*, 735.
4. Pragst, F. *Electrochim. Acta* **1976**, *21*, 497.
5. Pragst, F.; Ziebig, R.; Seydewitz, U.; Driesel, D. *Electrochim. Acta* **1980**, *25*, 341.
6. Gird, E.; Balaban, A. T.; *J. Electroanal. Chem.* **1962**, *4*, 48.
7. Degani, I.; Vincenci, C. *Boll. Sci. Fac. Chim. Ind. Bologna* **1967**, *25*, 77.
8. Palchov, V. A.; Zhadanov, Y. A.; Dorofeenko, G. N. *Zh. Org. Khim.* **1965**, *1*, 1171.
9. Polyakova, L. A.; Bilevich, K. A.; Bubnov, N. N.; Dorofeenko, G. N.; Okhlobystin, O. Y. *Dokl. Akad. Nauk.SSSR* **1973**, *212*, 370.
10. Hacquard, C.; Rassat, A. *Molec. Phys.* **1975**, *30*, 1935.
11. Kawata, H.; Niizuma, S. *Bull. Chem. Soc. Jpn.* **1989**, *62*, 2279.
12. Klima, J.; Volke, J.; Urban, J. *Electrochim. Acta* **1991**, *36*, 73.
13. Wintgens, V.; Pouliquen, J.; Kossanyi, J.; Heintz, M. *Nouv. J. Chim.* **1986**, *10*, 345.
14. Wintgens, V.; Pouliquen, J.; Kossanyi, J. *Nouv. J. Chim.* **1985**, *9*, 229.
15. Niizuma, S.; Sato, N.; Kawata, H.; Suzuki, Y.; Toda T.; Kokubun, H. *Bull. Chem. Soc. Jpn.* **1985**, *58*, 2600.
16. Turro, N. J. *Modern Molecular Photochemistry*, Benjamin Cummings Inc. California, **1978**.

17. Rackocsky, S.; Sherr, H. *Biochim. Biophys. Acta* **1982**, *681*, 152.

18. Gould, I. R.; Ege, D.; Moser J. E.; Farid, S. *J. Am. Chem. Soc.* **1990**, *112*, 4290.

19. Berlman, I. B. *Handbook of Fluorescence of Aromatic Molecules*, Academic Press, New York, **1971**.

20. Dewar, M. S. J.; Zoebisch, E. G.; Healy, E. F.; Stewart, J. *J. Am. Chem. Soc.* **1985**, *107*, 3902.

21. PC SPARTAN Graphical Interface Package for Molecular Mechanics and Molecular Orbital Models by Wavefunction Inc. 18401 Von Karman, Suite 370, Irvine, California 92612, USA.

22. Karmazin, V. P.; Kayazhanskii, M. I.; Olenkhnovich, E. P.; Dorofeenko, G. N. *Zh. Prikl. Spektrosk.* **1975**, *22*, 234.

23. Lippert, E. Z. *Naturforsch.* **1955**, *10 A*, 541.

24. Grabowski, Z. R.; Rotkiewicz, K.; Siemiarczuk, A.; Cowley, D. J.; Baumann, W. *Nouv. J. Chim.* **1979**, *3*, 443.

25. Rettig, W. *Angew. Chem. Int. Ed. Engl.* **1986**, *25*, 971.

26. Lutz, H.; Breheret, E.; Lindquist, L. *J. Phys. Chem.* **1973**, *77*, 1758.

27. Carmichael, I.; Hug, G. L. *J. Phys. Chem. Ref. Data* **1986**, *15*, 1.

28. Akaba, R.; Aihara, S.; Sakuragi, H.; Tokumaru, K. *J. Chem. Soc. Perkin Trans.2*. **1991**, 291.

29. Rehm, D.; Weller, A. *Isr. J. Chem.* **1970**, *8*, 259.

30. Kavarnos, G. J. *Fundamentals of Photoinduced Electron Transfer*, VCH, New York, **1993**.

31. Miranda, M. A.; Garcia, H. *Chem. Rev.* **1994**, *94*, 1063.

32. Balzani, V.; Moggi, L.; Scandola, F. in *Supramolecular Photochemistry*, Balzani, V. (Ed.), D. Riedel Publishing Company, Amsterdam, **1987**, p. 1.

33. Guest, D.; Moore, T. A. in *Photoinduced Electron Transfer.Part III*, Mattay, J. (Ed.), Springer Verlag, Heidelberg, **1990**, p. 103.

34. Lin, Z.; Schuster, G. B. *J. Org. Chem.* **1994**, *59*, 1119.

35. Balaban, A. T.; Dinculescu, A.; Dorofeyenko, G. N.; Fischer, G. W.; Koblik, A. V.; Mezheritzkii, V. V.; Schroth, W. *Pyrylium salts: Synthesis, Reactions and Physical Properties*, Katrizky, A. R., (Ed.), *Advances in Heterocyclic Chemistry*, Academic Press: New York, **1982**; Suppliment 2.

36. Dimroth, K.; Reichardt, C. *Liebigs Ann. Chem.* **1969**, *722*, 93.

CHAPTER 4

PHOTOPHYSICAL AND ELECTRON TRANSFER STUDIES OF SELECTED PYRYLIUM DERIVATIVES IN THE PRESENCE OF β-CYCLODEXTRIN

4.1. Abstract

Photophysical properties of pyrylium salts **3-8** were studied in the absence and presence of β-cyclodextrin (β-CD). These studies include absorption spectra, fluorescence spectra, fluorescence quantum yields and fluorescence lifetimes. Our studies have shown that pyrylium salts **3** and **8** did not interact appreciably with β-CD, whereas, **3-7** formed stable inclusion complexes. In the case of **3-7**, the association constants with β-CD were determined using the Benesi-Hildebrand treatment. Electron transfer to the singlet and triplet excited states of the encapsulated pyrylium salts were studied by fluorescence quenching and laser flash photolysis methods. The forward electron transfer rates in the presence of β-CD were slightly lower than those obtained in the absence of β-CD. The back electron transfer rates in the presence of β-CD were approximately 20 times lower. This is attributed to the enhanced binding of the pyranyl radicals to the β-CD cavity.

4.2. Introduction

A major disadvantage that arises in the use of pyrylium salts as PET sensitizers, is the formation of CT complexes between these salts and the donor molecules.[1-3] In CT complexes, photoelectron transfer reaction is generally followed by extremely rapid back electron transfer. Hence formation of the

charge-separated state is suppressed. One way to circumvent this problem is to enforce a separation between the sensitizer and the donor by the use of suitable interfaces. One approach that has been used in the literature with some success, is the use of cyclodextrins (CDs) to selectively encapsulate one of the components. In this Chapter, we have made an attempt to encapsulate selected pyrylium salts in β-CD cavities and study their photophysical and electron transfer properties.

β-CD is a cyclic oligosaccharide made up of seven D-glucopyranose units linked by α-(1,4) bonds (Figure 4.1).[4-6] This molecule resembles a hollow truncated cone (torus) and has approximate C_7 symmetry. The primary hydroxyl groups are located on the narrower side of the torus and the secondary hydroxyl groups are on the broader side. β-CD has an internal diameter of approximately 6.5 Å and a height of 7.9 Å. The most remarkable property of CDs is their ability to form inclusion complexes with a variety of molecules. The inclusion process is analogous to the dynamic solubilization of molecules in micelles. A distinguishing feature of these host systems, however, is the existence of finite size cavities that lead to size and shape selectivity on the molecules they include. Photophysical studies of a large number of molecules have been carried out in the presence of CDs. These studies were generally aimed at probing the inner cavity of the CD and also to understand the inclusion process. Selected examples are listed in the reference section of this Chapter.[7-27]

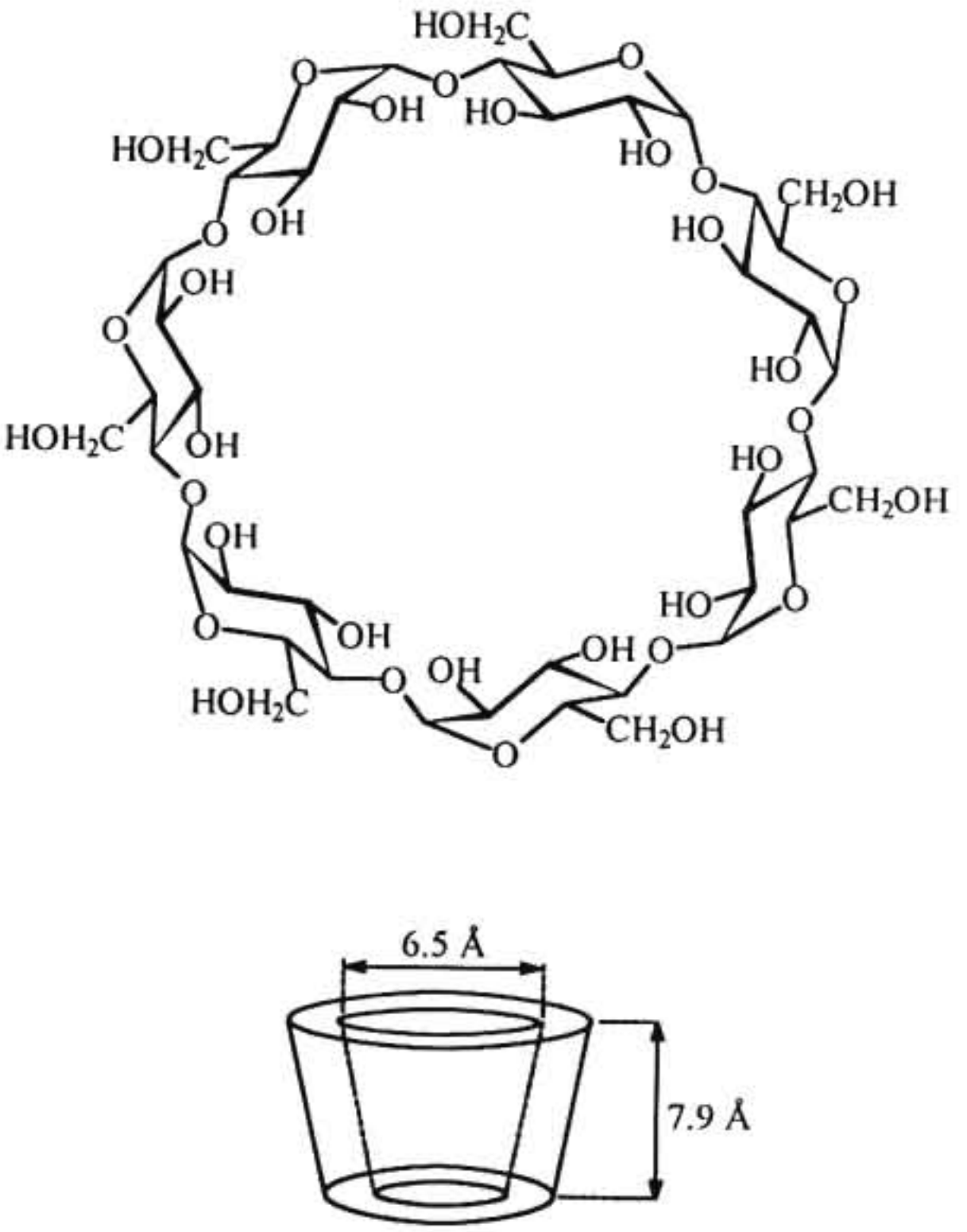

Figure 4.1 Structure and molecular dimensions of β-cyclodextrin.

Few examples of PET reactions of guest molecules incorporated in CD cavities are reported in the literature.[28-46] These studies suggest that CDs can play three different roles in PET reactions. (1) It solubilizes small amounts of organic substrates in water thereby making it possible to study PET of these

molecules in water, (2) it acts as a spacer and prevents CT formation and/or suppresses BET reactions and (3) it acts as a protecting cavity to stabilize the radicals from undergoing BET reactions. In most of the studies dealing with PET reactions of C_{60}-CD complexes in water, the role of CD is to solubilize the C_{60} in water.[28-32] An elegant example of the use of CD as a spacer is provided by the viologen-linked phenothiazine 1(Scheme 4.1).[38,39] Irradiation of 1 did not lead to the formation of cation radicals. This was attributed to the exceedingly short lifetime of the cation radicals due to fast BET. Irradiation in the presence of α- or β-CD gave transient signals corresponding to the radicals of **1**. This is explained on the basis of structure **2** (supported by NMR studies) in which BET is expected to be slow. An example where CD acts as a protecting cavity is provided in the electron transfer quenching of zinc-*meso*-tetra(*N*-propylsulphonato)pyrydiniumporphyrin by anthraquinone-2-sulphonate encapsulated in β-CD.[41] In this case, the photoreduced antharquinone-2-sulphonate remains within the CD cavity and is protected from undergoing fast BET reaction. In general, use of CD as a spacer or a protecting cavity, results in reduced rates for PET reactions compared to that in homogeneous solutions.[46] Compared to the forward reactions, the BET reactions are highly suppressed and this results in the formation of long-lived radical products.[38]

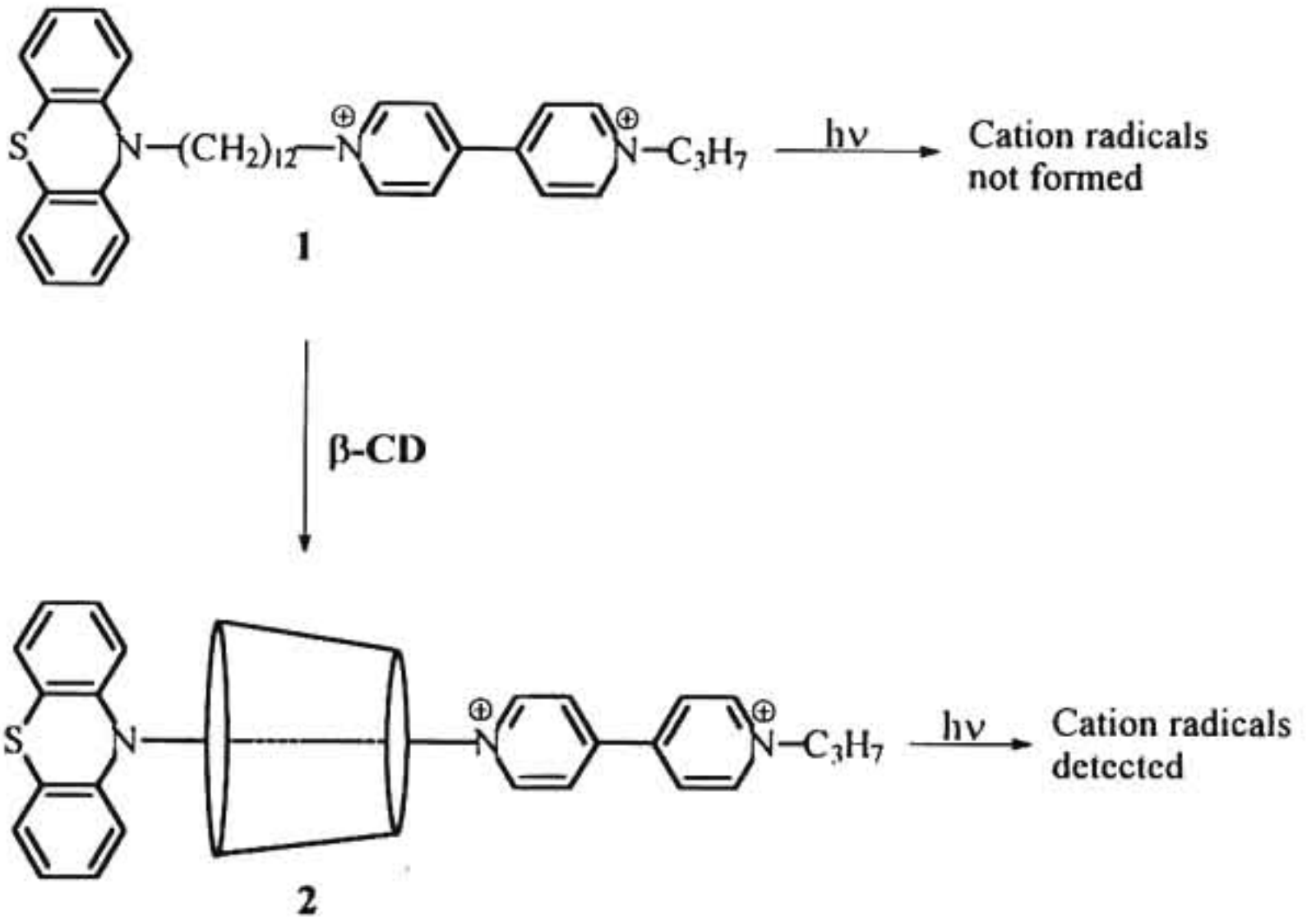

Scheme 4.1

In this Chapter we have attempted to encapsulate a few pyrylium salts in β-CD cavities. The structures of these molecules are given in Chart 4.1. In order to form an inclusion complex, the guest molecule should penetrate the cavity of β-CD, at least partially. In order to see whether the pyrylium salts can penetrate into the cavities, we have calculated the molecular dimensions of our substrates by AM1 methods and the values thus obtained are also indicated along with the structures in Chart 4.1.

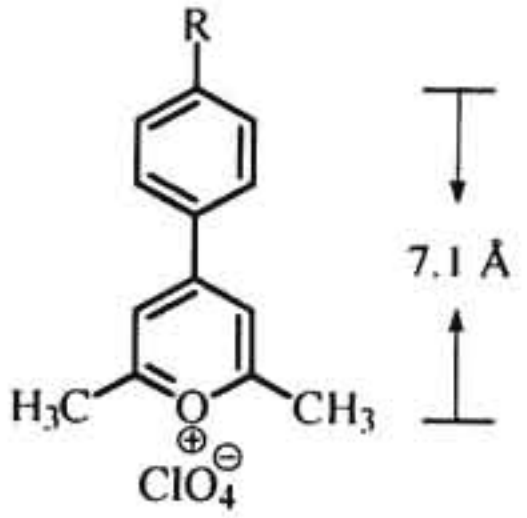

3: R = CH_3
4: R = *n*-C_4H_9
5: R = *n*-C_8H_{17}

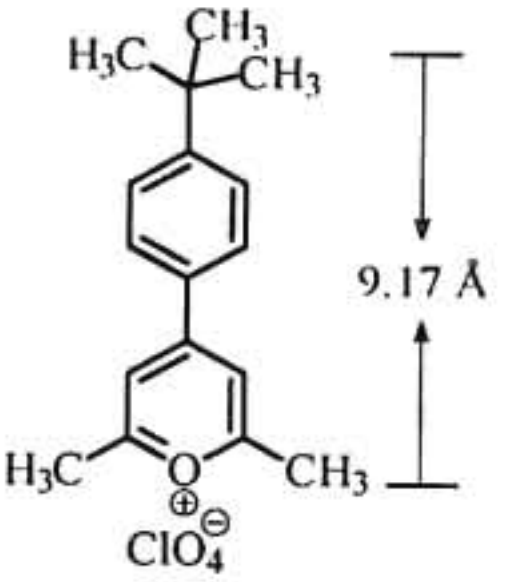

6

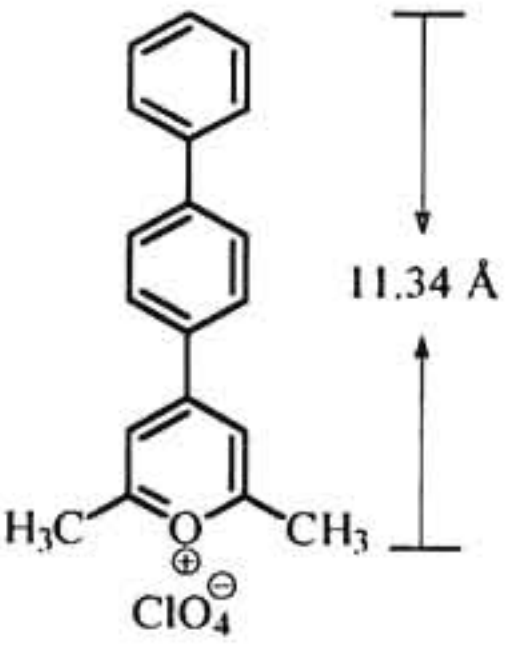

7

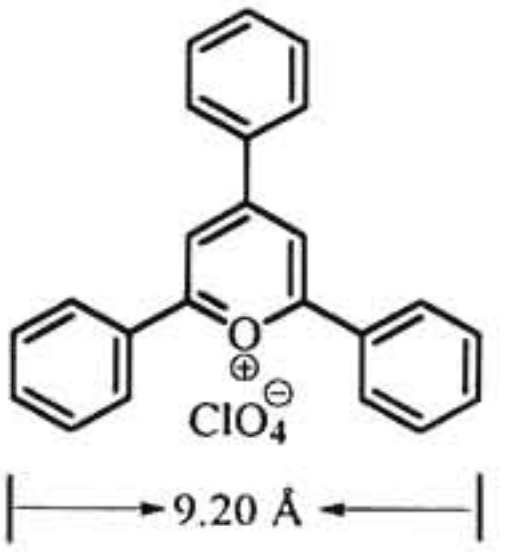

8

Chart 4.1

Photophysical studies of pyrylium salts incorporated in CDs have not been reported in the literature. We have observed that some of the pyrylium salts listed in Chart 4.1 can be incorporated into β-CD cavities. Complexation studies with CDs, however, have to be done in water, where pyrylium salts are reported to be unstable.[47,48] Because of their instability in water, photophysical studies of pyrylium derivatives have rarely been attempted in water. Gird and Balaban observed that pyrylium salts are stable in buffer solutions in the pH range of 0.5-3.5 (citric acid-sodium phosphate or sodium acetate-hydrochloric acid buffers).[49] They have studied the polarographic reduction of several pyrylium salts under these conditions. Cyclodextrins, on the other hand, are not very stable in aqueous acidic solutions.[6] The glycosidic linkages in these molecules tend to hydrolyse at pH < 3.5. Hydrolysis is very slow at room temperature, but occurs at moderate rates above 60 °C. We have observed that both the pyrylium salts and β-CD are stable in a sodium acetate-hydrochloric acid buffer of pH 3.5 at room temperature for several days. Hence all the photophysical studies reported in this chapter were carried out in this buffer solution. Since photophysical studies of pyrylium salts in aqueous buffer solutions have not been reported earlier, these studies are also included in this Chapter.

4.3. Results and Discussion

4.3.1. Absorption spectra

Absorption spectra of **3** and **8** (2×10^{-5} M) in aqueous buffer solutions were unaffected by the addition of millimolar quantities of β-CD, indicating that these substrates have no interaction with β-CD. Absorption spectra of other derivatives, however, were slightly blue shifted in the presence of β-CD. Figure 4.2 shows the

absorption spectra of **4** (2×10^{-5} M) in the absence and presence of β-CD (2.5×10^{-3} M). Although the shift in the absorption maximum is very small, it can be taken as evidence for the association of **4** with β-CD. Similar results were obtained for **5-7**.

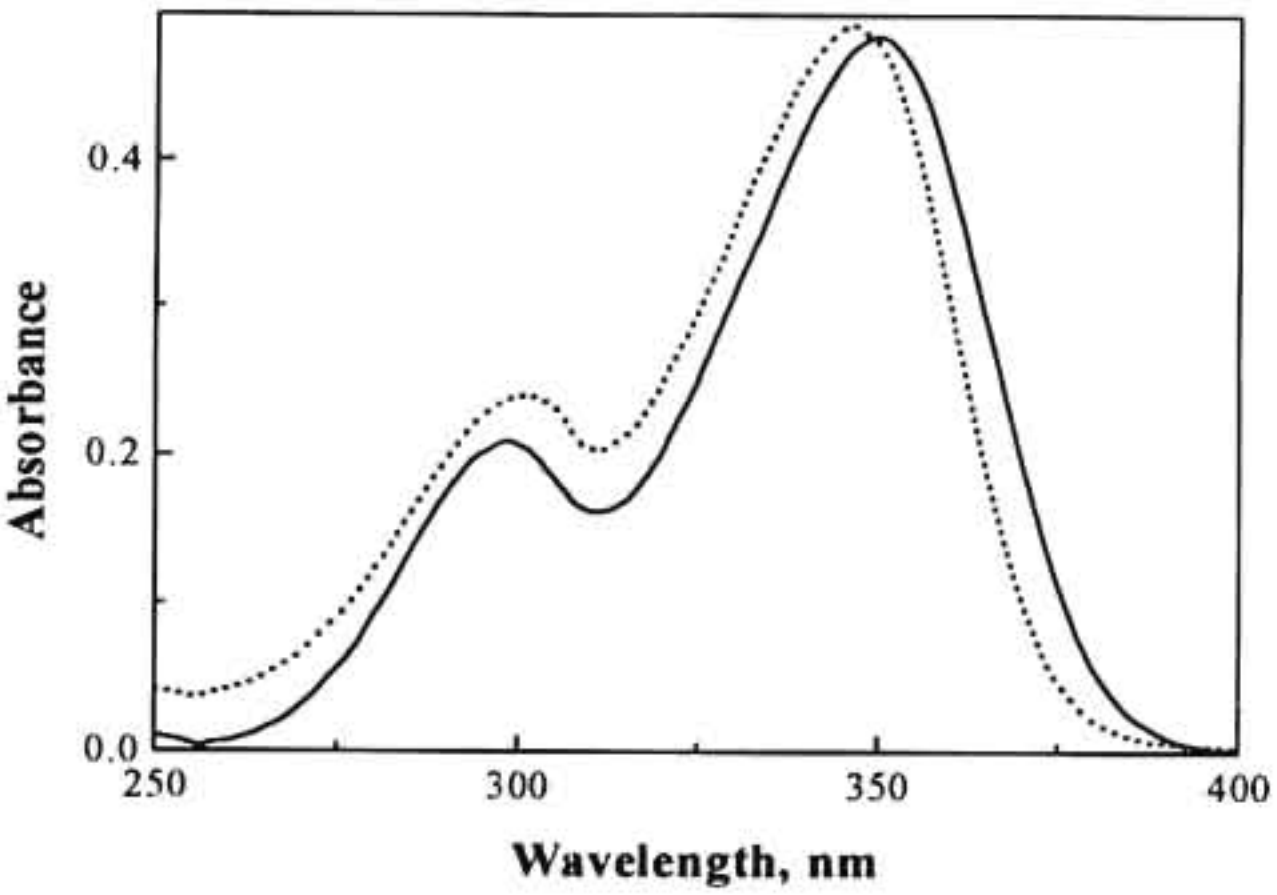

Figure 4.2 Absorption spectra of **5** in the absence (—) and presence (...) of β-CD.

Changes in the absorption spectra can be used to estimate the association constants between the guests and β-CD. However, changes in the absorption spectra of **4-7** in the presence of β-CD were not large enough to allow for accurate analysis of the association processes. Hence no attempt was made to determine the association constants by using the absorption spectral changes.

4.3.2. Fluorescence properties

The fluorescence spectra of **3-8** in the aqueous buffer solutions were similar to those in acetonitrile. The fluorescence quantum yields were, however, lower in

buffer solutions. Addition of small amounts of β-CD did not lead to any change in the fluorescence spectra of **3** and **8**. The fluorescence intensities and lifetimes of these compounds remained unaffected. The fact that the absorption and emission properties of these compounds are unaffected by β-CD, can be taken as conclusive evidence for the absence of inclusion complex formation in these two cases. Since **3** and **8** did not form inclusion complexes, these compounds were not used for other studies described in this Chapter.

Addition of small quantities of β-CD to solutions of **4-7** (4×10^{-6} M), led to changes in their fluorescence properties. In these cases, the fluorescence quantum yields showed a 2-6 fold enhancement in the presence of β-CD. We have used these fluorescence enhancements to analyze the complex formation process and to determine the association constants in these cases.

Formation of complexes between the pyrylium salts **4-7** and β-CD can be analyzed quantitatively by considering the equilibrium given in equation (4.1).

$$PY + \beta\text{-CD} \underset{}{\overset{K}{\rightleftharpoons}} PY{::}\,\beta\text{-CD} \qquad (4.1)$$

In equation (4.1), 'PY' represents the pyrylium salts and 'K' the association constant. Equation (4.1) assumes that a 1:1 complex is formed between β-CD and the pyrylium salts. The association constant is then given by the equation (4.2).

$$K = \frac{[PY{::}\beta\text{-CD}]}{[PY]\,[\beta\text{-CD}]} \qquad (4.2)$$

The solute entry and exit rates into and out of CD cavities are usually of the order of 10^7 M^{-1} s^{-1} and 10^4 M^{-1} s^{-1}, respectively.[19] The rate constants of fluorescence decay for pyrylium salts are usually of the order of 10^9 M^{-1} s^{-1}. Thus, there is very

little chance of any excited pyrylium molecule to enter or exit β-CD cavity during their lifetime. Therefore, we can safely assume that the enhancement of fluorescence intensity is entirely due to the presence of the ground state inclusion complex of pyrylium salt with β-CD. Fluorescence can occur from the associated and unassociated forms of the pyrylium salts. If α is the fraction of pyrylium salts associated, then the observed fluorescence (Φ_{obsd}) is given by equation (4.3).

$$\Phi_{obsd} = \alpha\, \Phi_{[PY::CD]} + (1-\alpha)\, \Phi^0_f \qquad (4.3)$$

where, Φ^0_f is the fluorescence quantum yield in the buffer solution in the absence of β-CD and $\Phi_{[PY::CD]}$ is the fluorescence quantum yield of the inclusion complex. The latter quantity cannot be measured accurately and hence graphical methods are used to determine the association constant. Equation (4.3) can be simplified to equation (4.4).[50,51]

$$\frac{1}{(\Phi^0_f - \Phi_{obsd})} = \frac{1}{(\Phi^0_f - \Phi_{[PY::CD]})} + \frac{1}{K(\Phi^0_f - \Phi_{[PY::CD]})[\beta\text{-CD}]} \qquad (4.4)$$

According to equation (4.4), a plot of $1/(\Phi^0_f - \Phi_{obsd})$ *vs.* 1/[β-CD] should be linear with slope = $1/K(\Phi^0_f - \Phi_{[PY::CD]})$ and intercept = $1/(\Phi^0_f - \Phi_{[PY::CD]})$. The association constant 'K' is then given by,

$$K = \frac{\text{Intercept}}{\text{Slope}} \qquad (4.5)$$

In order to determine K, values of $1/(\Phi^0_f - \Phi_{obsd})$ were plotted against 1/[β-CD] for pyrylium salts **4-7** (Figure 4.3). Straight lines were obtained in all cases, which indicated that the inclusion complexes formed have 1:1 stoichiometry. The K

values determined this way are given in Table 4.1. Note that the association constants obtained for **5** and **6** are very large.

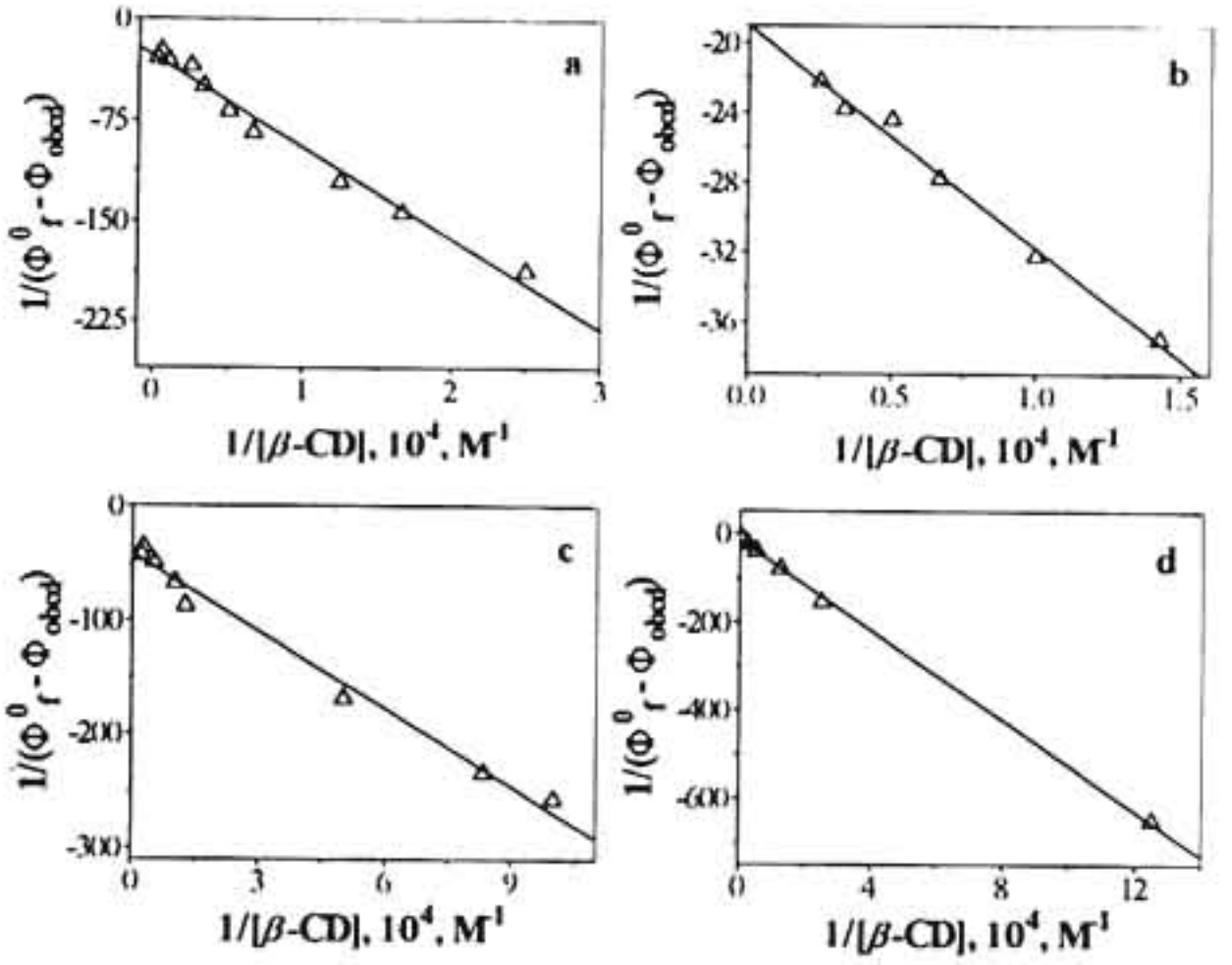

Figure 4.3 Plots of $1/(\Phi^0_f - \Phi_{obsd})$ *vs.* $1/[\beta\text{-CD}]$ for the fluorescence yield enhancement of pyrylium salts (a) **4**, (b) **5**, (c) **6** and (d) **7**.

Eventhough the pyrylium salts **4-7** formed complexes with β-CD, the nature of these complexes was not the same in all cases. This is evident from the fluorescence profiles of these derivatives in the presence of β-CD. Fluorescence profiles of **4** and **6** in the presence of β-CD were similar. The fluorescence enhancement of **6** is shown in Figure 4.4. In this case, the enhancement is associated with the appearance of fine structure, a blue shift of 26 nm for the emission maximum and a narrowing of the spectral bandwidth. The fluorescence spectrum in the presence of β-CD (1×10^{-3} M) is very similar to the spectrum of **6**

in dichloromethane solution. This clearly suggests that **6** is associated within the hydrophobic cavity of β-CD. An important feature in these cases is the presence of an isoemissive point, which suggests that only two forms of the fluorophore are present in the solution.

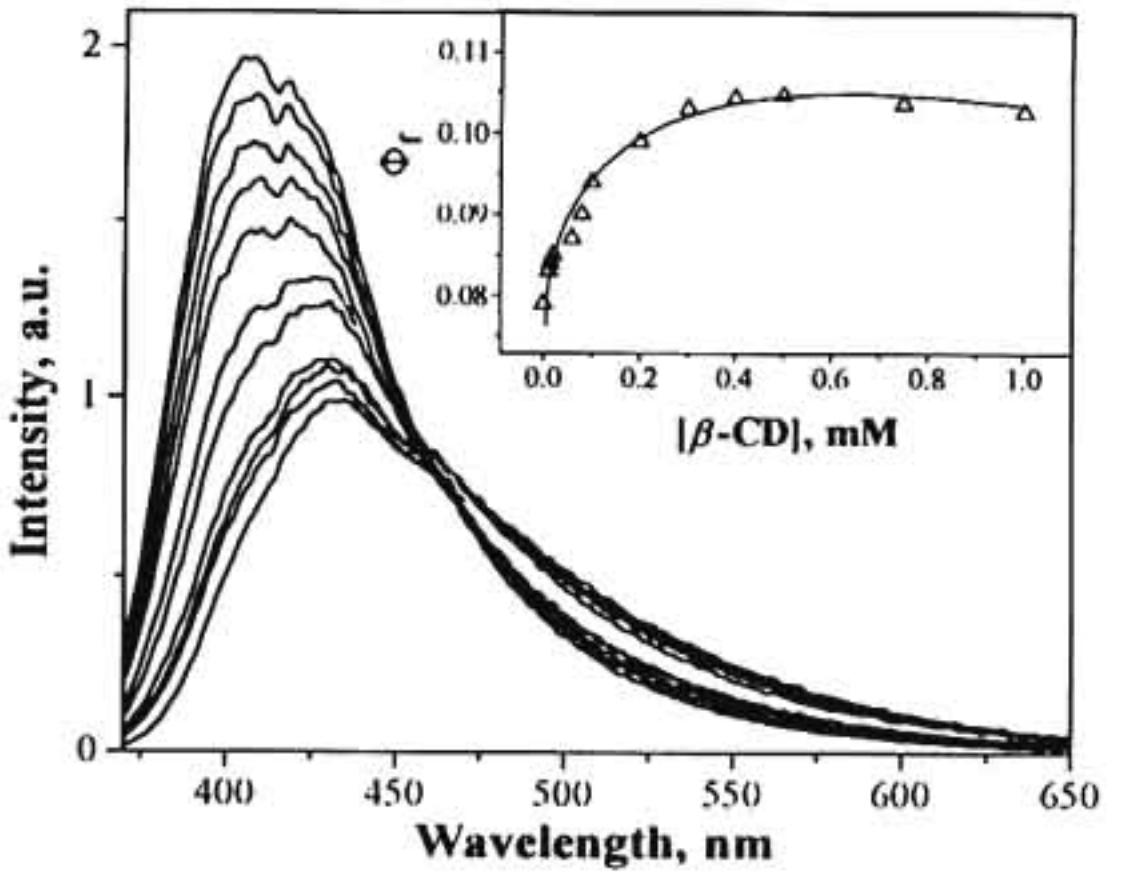

Figure 4.4 Effect of addition of β-CD on the fluorescence spectrum of **6**. Inset shows a plot of fluorescence quantum yield *vs.* [β-CD].

The fluorescence enhancement of **5** in the presence of various concentrations of β-CD is shown in Figure 4.5. Here, even though the intensity showed a two-fold enhancement, the spectral shape was not altered very much. Also, the isoemissive point was not observed. The λ_{max} showed only a moderate blue shift of 15 nm. This indicated that the microenvironment of **5** is not the same as that experienced by **4** and **6**.

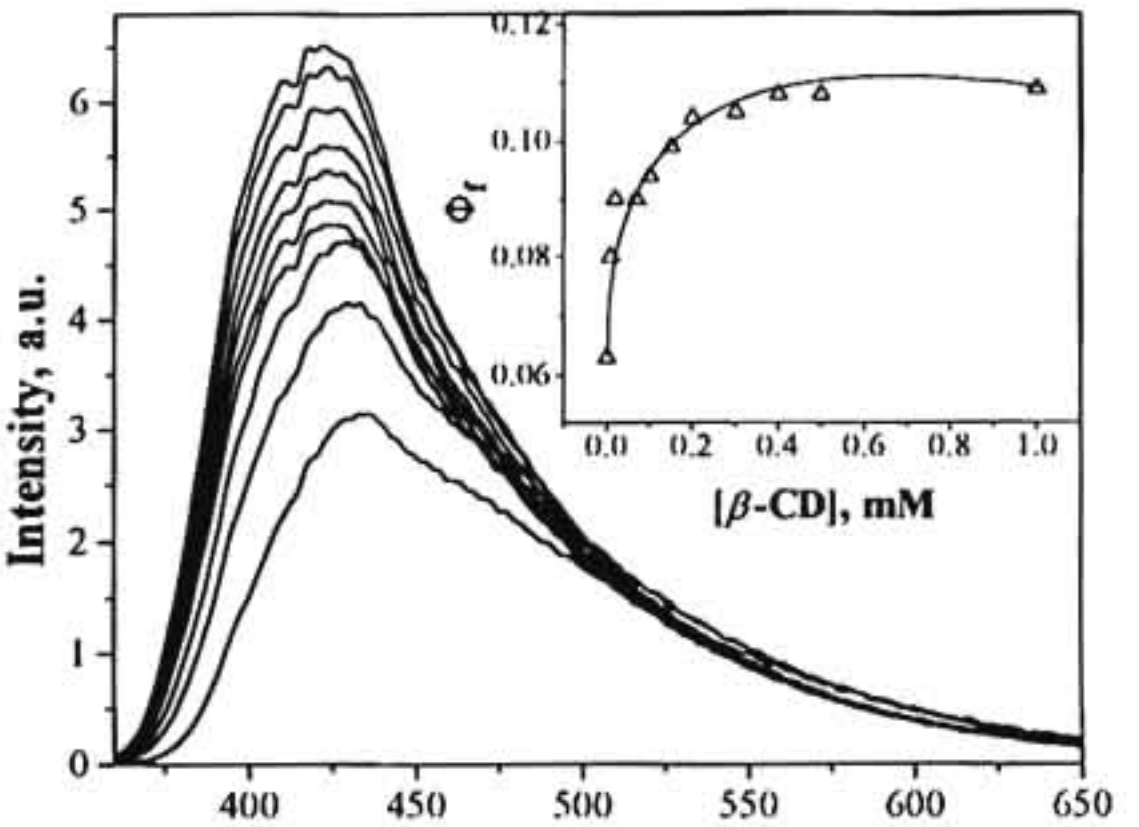

Figure 4.5 Effect of addition of β-CD on the fluorescence spectrum of **5**. Inset shows the plot of fluorescence quantum yield *vs.* [β-CD].

Pyrylium salt **7** exhibited a different type of behaviour in the presence of β-CD. This is shown in Figure 4.6. In this case a 6-fold fluorescence enhancement was observed. Although the emission maximum showed a blue shift of 14 nm, the spectral shape remained unaltered. The insert in Figure 4.6 shows the fluorescence enhancement as a function of β-CD concentration. Note that the saturation behaviour is observed only at relatively large concentrations of β-CD in this case.

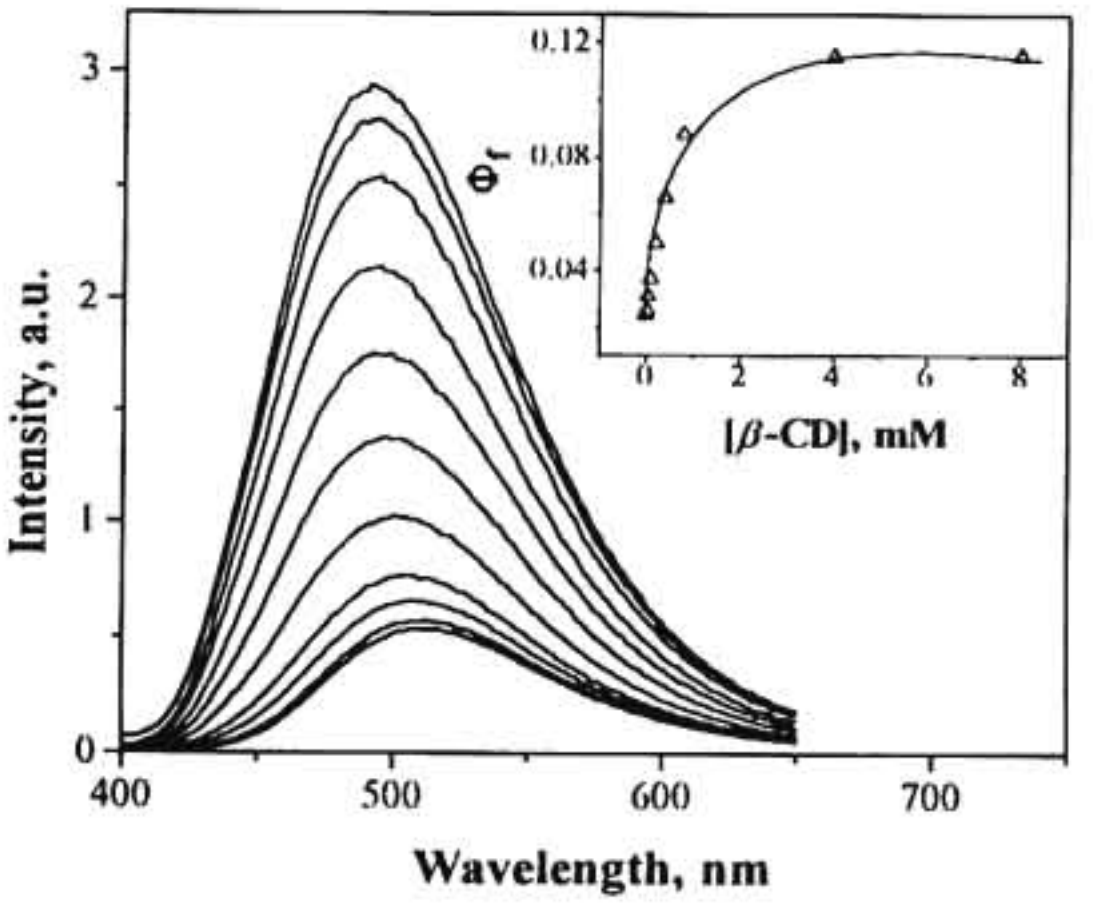

Figure 4.6 Effect of addition of β-CD on the fluorescence spectrum of **7**. Inset shows the plot of fluorescence quantum yield *vs*. [β-CD].

Fluorescence lifetimes (τ_f) of **4-7** were measured in the absence and presence of β-CD. Figure 4.7 shows the fluorescence decay profiles of **5** in the absence and presence of β-CD. In the absence of β-CD, predominantly single exponential decays were obtained. We have fitted the fluorescence decay profiles in the presence of β-CD to single exponential functions. The fits were not very good ($\chi^2 \leq 2$) and the values we have obtained may have some error (vide infra). Nevertheless, we intend to use these values to extract useful information regarding the nature of the complex formed between these pyrylium salts and β-CD.

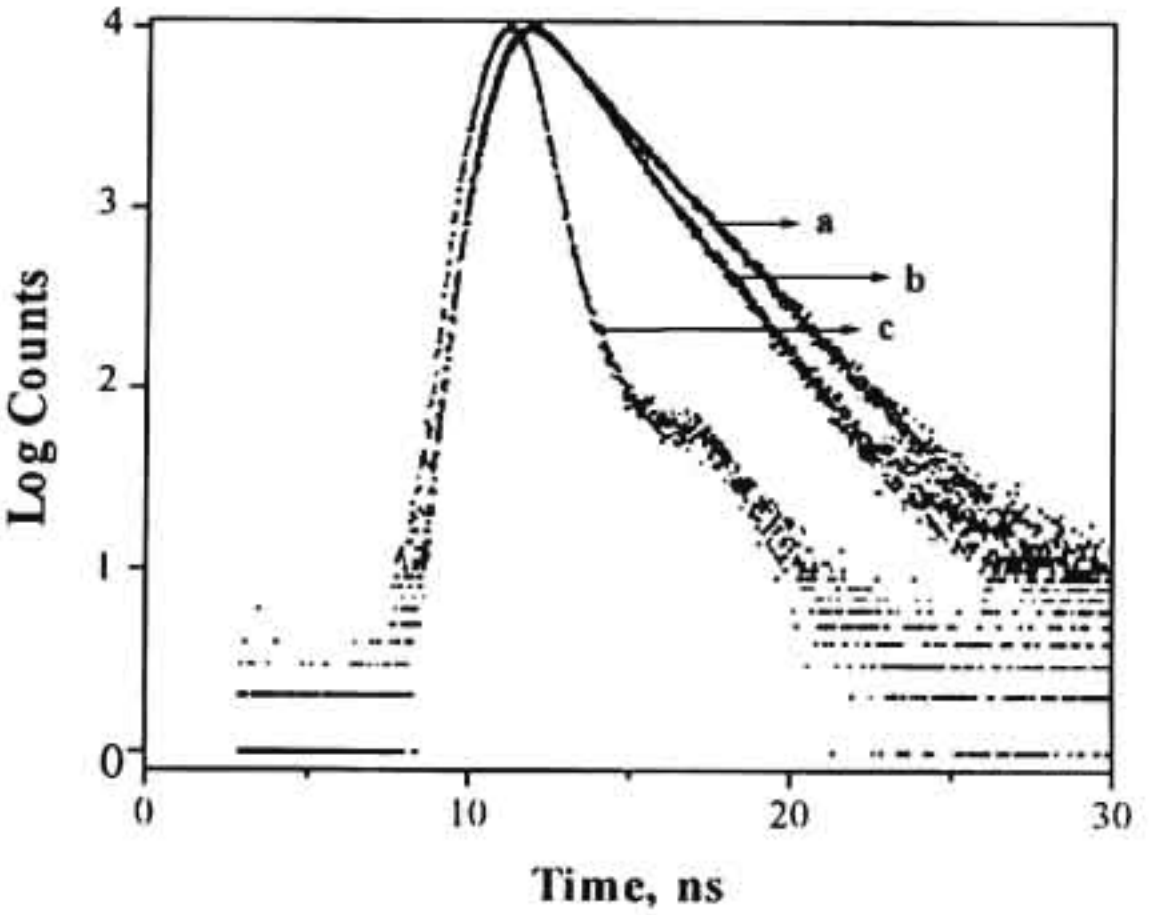

Figure 4.7 Fluorescence decay profile of **5** in the absence (a) and presence (b) of β-CD. The instrument function is shown in (c).

Duveneck et al. observed that the fluorescence decay of *trans*-stilbene in the presence of β-CD is double exponential.[25] The two components of the decay were assigned to loose and tightly bound conformations of *trans*-stilbene within the β-CD cavity. It was shown later that the decay profiles of several anilinonaphthalene sulphonate (ANS) derivatives in the presence of β-CD could not be fitted to single or double exponential functions.[18,27] χ^2 values of 4-40 were reported in these cases.[27] It was suggested that the decay functions could be best fitted by a distribution of fluorescence lifetimes. This suggested the presence of several slightly different conformations of the inclusion complexes in equilibrium, existing in the solution. The fact that we also did not observe good single

exponential decays, supported the presence of slightly different conformations for the pyrylium salt-β-CD complexes. However, the χ^2 values we obtained were much better and hence fitting the decays to a single exponential may be justified.

The fluorescence maxima, quantum yields and lifetimes of pyrylium salts **4-7** in the absence and presence of β-CD are presented in Table 4.1 along with the equilibrium association constants for complex formation.

Table 4.1 Fluorescence maxima (λ_{max}), quantum yields (Φ_f), lifetimes (τ_f) and association constants (K) for pyrylium salts 4-7 in the presence of β-CD. Values given in parenthesis are those in the absence of β-CD.

Compound	λ_{max}(em), nm	Φ_f	τ_f, ns	K, M^{-1}
4	410 (436)	0.072 (0.040)	1.4 (1.5)	4070
5	421 (436)	0.11 (0.063)	1.6 (2.0)	15000
6	410 (436)	0.11 (0.078)	1.8 (2.0)	18400
7	496 (510)	0.11 (0.025)	0.8 (0.2)	2700

An inspection of the table reveals that the association constants vary over a wide range. This clearly suggests that the inclusion complexes do not have the same structure in all cases. In the following section, an attempt is made to draw some conclusions regarding the structure of these inclusion complexes based on the results we obtained.

It is generally accepted that, the binding forces involved in the complex formation are: (1) hydrophobic interactions between the hydrophobic moiety of the guest molecules and the β-CD cavity; (2) release of high-energy water molecules from the cavity in the complex formation process; (3) hydrogen bonding between the functional groups of the guest molecules and hydroxyl groups of β-CD and (4) release of strain energy in the ring frame of cyclodextrin.[6] The latter two aspects are not important in the present case. Regardless of what kind of stabilizing forces are involved, the geometric capability and the polarity of the guest molecules, the medium and the temperature are the most important factors that determine the stability of the inclusion complex. It is suggested that geometric, rather than the chemical, factors are decisive in determining whether the guest molecule can form an inclusion complex with β-CD.[9] If the guest is too small, it will easily pass in and out of the cavity with little or no binding at all. Complex formation with guest molecules significantly larger than the cavity may also be possible, but the complex is formed in such a way that only certain groups or side chains penetrate into the cavity. The stability of the inclusion complexes is generally proportional to the hydrophobic character of the guest molecule. Highly hydrophilic molecules complex very weakly or not at all.

The β-CD cavity has a diameter of 6.0-6.5 Å. An inspection of Chart 4.1 will show that, except for **8**, all other pyrylium salts studied have widths smaller than 6.5 Å. Thus, if molecular size is the only criteria, pyrylium derivatives **3**-**7** should be able to complex with β-CD. Our studies have shown that **3** do not form inclusion complex with β-CD. This indicates that complex formation in these cases is determined by other factors as well. Because of the positive charge present

in the molecule, the pyrylium salts are polar and somewhat hydrophilic in nature. Encapsulation of these salts will be possible only if the pyrylium ring is substituted with hydrophobic moieties. Since **3** does not undergo encapsulation in β-CD, we can safely assume that presence of a phenyl or *p*-toluyl group at the 4-position of the pyrylium ring does not enhance the hydrophobicity of the molecule to the extent required for complex formation. When the 2-, 4- and 6-positions are substituted by phenyl groups as in **8**, the molecule becomes larger than the cavity and inclusion do not take place in this case because of geometric constrains (see Chart 4.1). The fact that **4** -**7** form inclusion complexes with β-CD, suggests that the 4-aryl groups present in these molecules make them sufficiently hydrophobic for inclusion in the cavity. If the association constant can be taken as directly proportional to the hydrophobicity of these groups, the order of hydrophobicity will be *t*-butyl > *n*-octyl > > *n*-butyl > phenyl >> methyl.

The fluorescence profiles of **4**-**7** in the presence of β-CD prompted us to make certain assumptions regarding the structures of the inclusion complexes in these cases. Considering the molecular dimensions, the pyrylium derivatives can enter the cavity only along its long axis, through the wider secondary hydroxyl entrance. In the case of **6**, the very high association constant suggests that the molecule is tightly bound within the cavity and the exit rate is low. Since the length of the molecule is only slightly larger than the height of the cavity, **6** is not exposed very much to the aqueous environment. Observation of an isoemissive point suggests the presence of only one conformation for the inclusion complex. Similarly, the inclusion complex of **4** also has only one conformation. The low association constant in this case is most probably due to a faster exit rate of **4** from

the cavity. In the other two cases, we did not observe isoemissive points. This is most probably due to the presence of slightly different conformations of the inclusion complexes in these cases. In the case of **5**, high value of K suggests tightly bound complex. Since the length of the molecule is much larger than the cavity height, some part of the molecule has to project outside the cavity. Because of the hydrophilicity and positive charge, we expect the pyrylium ring to stick out of the cavity. Thus, we believe that the *n*-octyl group is coiled inside the cavity and the pyrylium chromophore is mostly exposed to the aqueous environment in the most stable conformation of the inclusion complex. This is supported by the fact that the emission maximum is blue shifted by only 15 nm. Presence of different conformations can be attributed to the flexibility of the long alkyl chain. In the case of **7**, one of the aryl rings has to project outside the cavity. Because of this, the hydrophobic stabilization of the complex is low and this results in low association rates. It is difficult to predict the most stable conformation in this case. We believe that the molecule is moving up and down the cavity and the observed fluorescence is the average from several conformational isomers in equilibrium.

The lifetime measurements also suggest that pyrylium salts **4-7** are included within the CD cavity. Compounds **4-6** show a marginal decrease in τ_f and **7** shows an increase in τ_f upon complexation. This is consistent with the results we obtained earlier. Note that, τ_f values for **5** and **6** are larger in polar solvents due to the formation of TICT states (Chapter 2). For these compounds we expect the lifetimes to decrease in less polar media. In the case of **7**, the 4-biphenyl group shortens fluorescence lifetime in polar media due to facile intramolecular electron transfer quenching of the excited state (Chapter 3). Since the CD cavity is less

polar, electron transfer quenching is reduced for molecules encapsulated within the cavity and results in enhanced lifetime. Also, note that the fluorescence enhancement (6-fold) observed in this case is larger. This is also attributed to the reduced rates of intramolecular electron transfer quenching within the CD cavity.

4.3.3. Laser flash photolysis studies

Laser flash photolysis of **4-6** in aqueous buffer solutions led to the formation of transients which exhibit bleaching below 400 nm and absorption above 400 nm. These transients were quenched by oxygen and hence we assign them to the triplets of the substrates. Oxygen quenching rate constants obtained in aqueous media were similar to those reported in other solvents.[52,53] Since the bleaching maxima coincided with the absorption maxima of these compounds, we have estimated the extinction coefficients of the T-T absorptions using the singlet depletion method. The triplet quantum yields (Φ_T) were then determined using relative actinometry (see Chapter 2 for details). Φ_T values thus obtained were very low compared to those in acetonitrile solutions. For all these compounds, the T-T absorption maxima were red shifted by ≈ 20 nm. Triplet lifetimes, however, were larger in the buffer solutions (5-8 μs). The triplets decayed to the ground states and residual absorptions assignable to product formation were not observed in any of these cases. Pyrylium salt **7** did not give good transients under these conditions.

Laser flash photolysis experiments of **4-6** were also carried out in the presence of β-CD. Relatively high concentrations of β-CD were employed in these experiments in order to ensure complete complexation of the pyrylium salts. Laser flash photolysis of β-CD-encapsulated **4-6** also led to the formation of transients, assignable to the triplets of these substrates. A representative example is given in

Figure 4.8. The extinction coefficients and quantum yields of the triplets were determined in the presence of β-CD. Table 4.2 summarizes the absorption maxima, extinction coefficients, quantum yields and oxygen quenching rate constants for **4-6** in the absence and presence of β-CD in aqueous buffer solution.

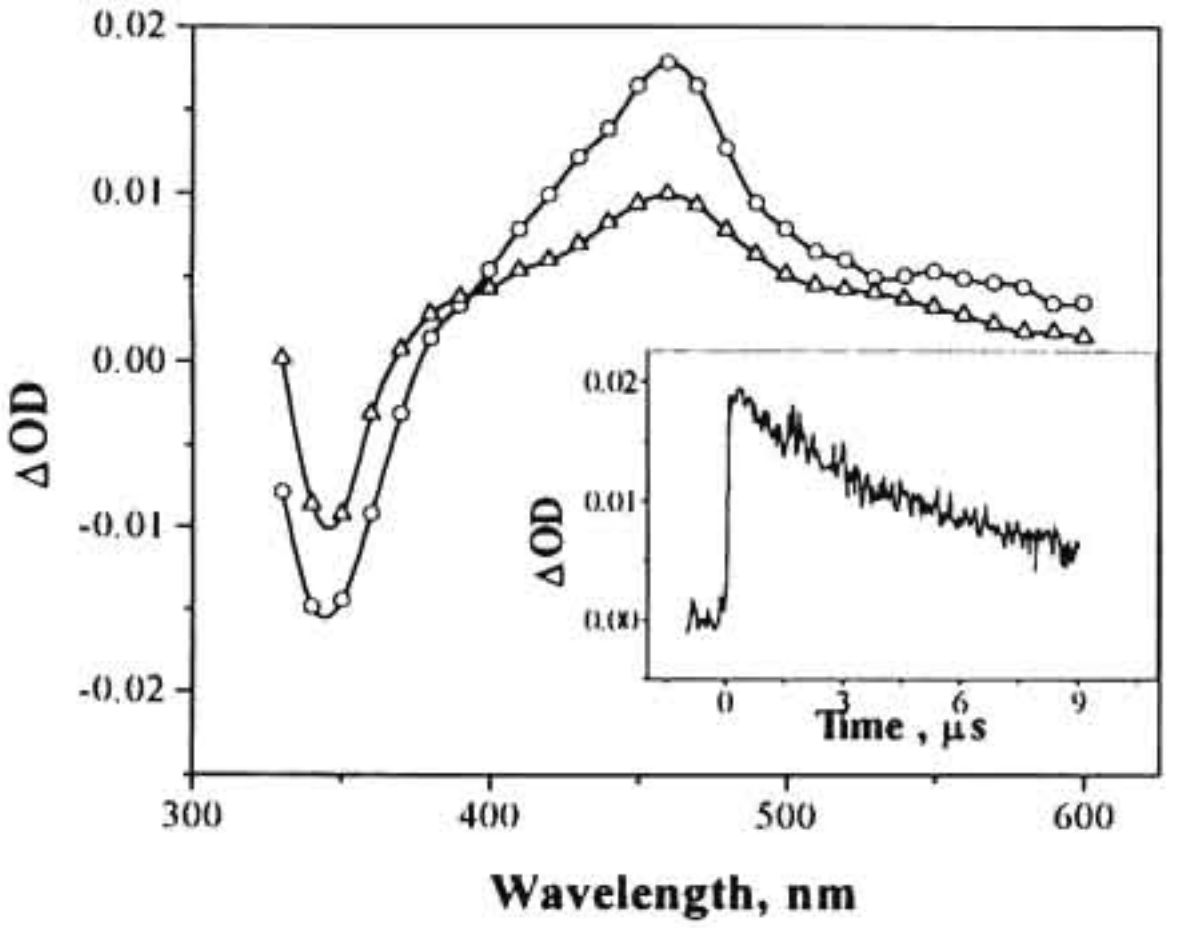

Figure 4.8 Transient absorption spectra of **4** in the absence (O) and presence (Δ) of β-CD. Inset shows the decay profile at 460 nm in the absence of β-CD.

An inspection of Table 4.2 shows that inclusion within β-CD did not have any major effect on the triplet state properties of these molecules. T-T absorption maxima remained unaffected in all cases. Except in the case of **4**, Φ_T and ε_T values also remained unaffected. The triplet lifetimes of all the derivatives, however, were lowered in the presence of β-CD. The lifetimes in the presence of β-CD were similar to those observed in organic solvents. Rates

of quenching of the triplets by oxygen were reduced in the presence of β-CD. This is due to the fact that the pyrylium salts incorporated in the CD cavities are less accessible to quenching by oxygen.

Table 4.2 Absorption maxima, extinction coefficients, quantum yields and oxygen quenching rate constants for 4-6 in the presence of β-CD. The values given in parenthesis are those in the absence of β-CD.

Compound	λ_{max}(T), nm	ε_T, M^{-1} cm^{-1}	Φ_T,	τ_T, μs	$k_q[O_2]$, M^{-1} s^{-1}
4	460 (460)	2.3×10^4 (1.4×10^4)	0.077 (0.12)	1.3 (5.6)	2.7×10^8 (5.0×10^8)
5	460 (460)	3.0×10^4 (2.2×10^4)	0.06 (0.07)	3.8 (8.3)	1.98×10^8 (2.7×10^8)
6	460 (460)	2.8×10^4 (3.5×10^4)	0.067 (0.07)	3.2 (7.6)	2.8×10^8 (4.3×10^8)

4.3.4. Electron transfer studies

In order to study the electron transfer reactions of pyrylium salts in aqueous media in the presence of β-CD, water-soluble quenchers are required. Also the quencher should not displace the pyrylium salts from the cyclodextrin cavities. If this happens, quenching will occur in the aqueous solution and β-CD will have no influence on the quenching process. Lin and Schuster recently observed that sodium-2-naphthalene sulphonate (2-NS) quenched the fluorescence of several 2,6-di-*tert*-butyl-4-arylpyrylium derivatives in organic solvents such as acetonitrile and dimethyl carbonate by electron transfer mechanism.[3] They could not determine the oxidation potential of this molecule

directly. From a plot of the oxidation potentials of substituted naphthalenes against the Hammet σ constants of the substituents, they have estimated E_{ox} = 1.7 V *vs.* SCE for this compound. Using this value for E_{ox}, we have calculated the free energy (ΔG_{el}^{S}) of electron transfer from this molecule to the singlet and triplet excited states of **4-7**. ΔG_{el}^{S} values thus obtained were negative for all compounds, indicating that these reactions are thermodynamically favourable. In order to see whether this quencher molecule has any interaction with *β*-CD, we have carried out absorption and emission measurements of 2-NS in the presence of *β*-CD. The absorption and fluorescence spectra of 2-NS remained unaffected in the presence of *β*-CD, suggesting that this molecule did not undergo inclusion complex formation and prefer to remain in the aqueous phase. Thus we can safely conclude that this molecule will not be able to displace the pyrylium salts from the *β*-CD cavities. Hence, we have used this water-soluble quencher to study the electron transfer reactions of **4-7** in aqueous media in the presence and absence of *β*-CD.

Fluorescence quenching: Fluorescence of **4-7** were quenched by 2-NS in the absence and presence of *β*-CD. The quenching was analyzed by Stern-Volmer kinetics in the usual manner. Stern-Volmer plots obtained for **5-7** in the absence and presence of *β*-CD are shown in Figure 4.9. The quenching rate constants determined from these plots are presented in Table 4.3, along with ΔG values calculated using the Weller equation.

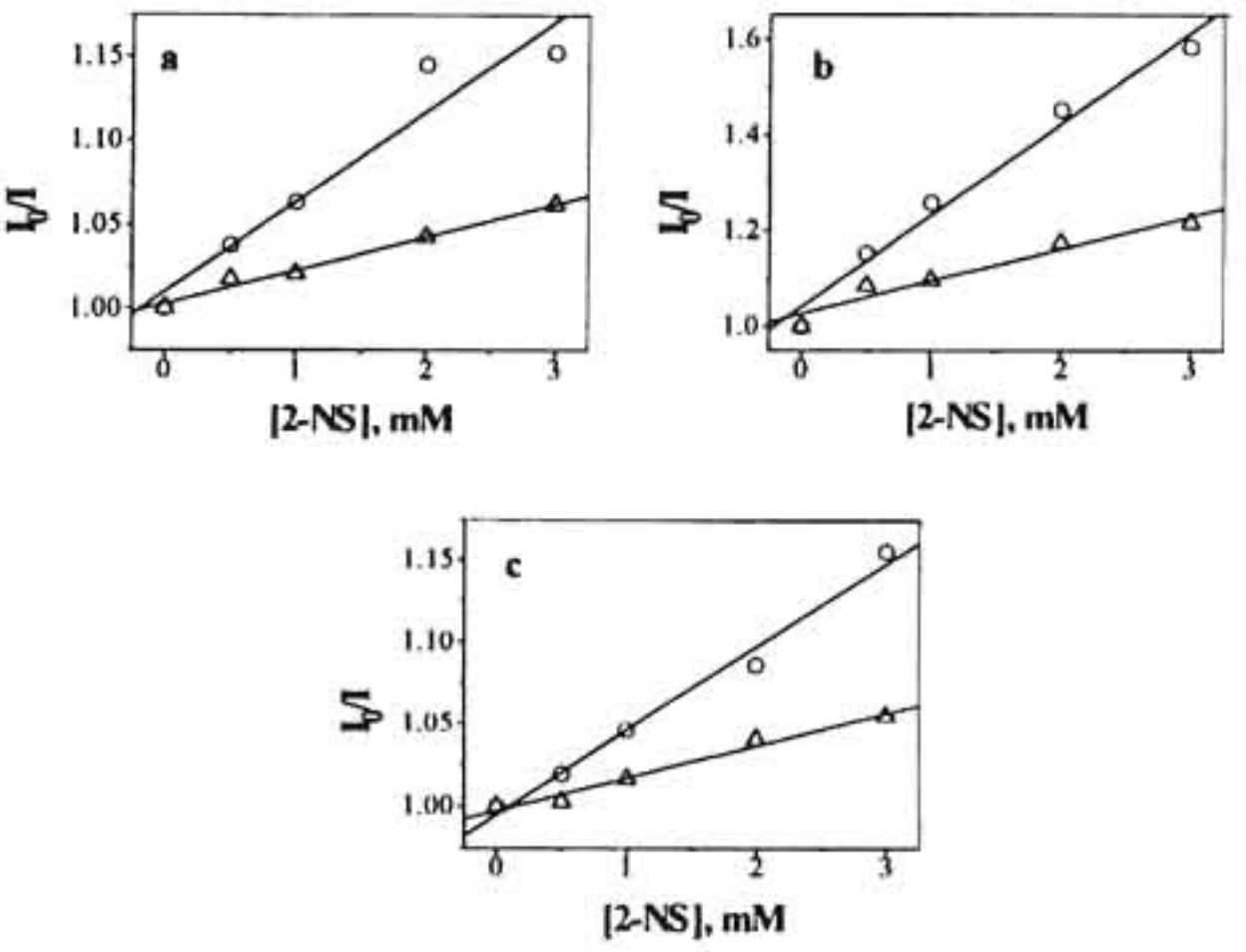

Figure 4.9 Stern-Volmer plots for the fluorescence quenching by 2-NS in the (O) absence and (Δ) presence of β-CD for (**a**) **5**, (**b**) **6**, and (**c**) **7**.

Table 4.3 Quenching rate constants (k_q^S) and ΔG_{el}^S values for the fluorescence quenching of 5-7 in the presence and absence (values in parenthesis) of β-CD.

Compound	k_q^S, $M^{-1}\,s^{-1}$	ΔG_{el}^S, kcal M^{-1}
5	1.36×10^{10} (2.08×10^{10})	-21.2
6	1.11×10^{10} (2.46×10^{10})	-21.2
7	1.93×10^{11} (3.17×10^{11})	-15.0

An examination of the quenching rate constants presented in Table 4.3 reveals that pyrylium salts exhibit different types of quenching behaviour. In the absence of β-CD, quenching rates were in the (2-2.5) x 10^{10} M^{-1} s^{-1} range for **5** and **6**. Lin and Schuster observed k_q^S value of 2.8 x 10^{10} M^{-1} s^{-1} for the quenching of 2,6-di-*tert*-butyl-4-phenylpyrylium perchlorate by naphthalene sulphonate in acetonitrile solution.[3] Although, this value is close to the diffusion limited rate constant, it is higher than that observed (1.4 x 10^{10} M^{-1} s^{-1}) for quenching of the same salt by naphthalene. The higher value obtained in the case of NS was attributed to Coulombic attraction, which will affect the relative motion of the ions when they are close together. In the case of **7**, k_q^S was ten times larger. Large k_q^S values are generally attributed to static quenching.[54] We believe that the positively charged **7** and negatively charged 2-NS associate in the ground state and lead to static quenching of the excited state. For all the substrates, quenching rates were lower in the presence of β-CD. When a fluorophore is residing inside and a quencher is present outside the β-CD cavity, a reduction in the quenching rate is expected. In these cases, the donor and acceptor are separated by a distance equal to the thickness of the wall of β-CD (7 Å). The distance is smaller if the approach of the quencher is through the opening of the cavity. Electron transfer occurs at a distance in these cases. Since the rate of electron transfer depends exponentially on distance, k_q values are reduced. In the case of **7**, although k_q^S is lowered in the presence of β-CD, the observed value is still larger than the diffusion limited value. This suggests that static quenching is observed even in the presence of β-CD indicating that β-CD is not very effective in partitioning the reactants in this case. We attribute this to the low association constant of **7** and β-CD.

Triplet quenching experiments: Attempts were made to quench the triplets of **4-6** by 2-NS in the absence and presence of β-CD. The quencher concentrations employed in these cases were in the range (1-4) x 10^{-4} M. Less than 10% of the singlets of **4-7** were quenched under these conditions. The quenching rate constants were determined by plotting the observed pseudo-first-order rate constants against the quencher concentration as described in Chapter 2. The quenching rate constants obtained in the absence of β-CD were in the range (3.5-5) x 10^9 M^{-1} s^{-1} (Table 4.4). Slightly lower values were obtained in the presence of β-CD and, as in the case of singlet quenching, this is attributed to the spatial separation of the donor and acceptor.

Table 4.4 Quenching rate constants (k_q^T) and free energy change (ΔG_{et}^T) for electron transfer from the triplet excited states of compounds 4-6 in the presence and absence (values in parenthesis) of β-CD.

Compound	k_q^T, M^{-1} s^{-1}	ΔG_{et}^T, kcal M^{-1}
4	2.2 x 10^9 (3.6 x 10^9)	-7.4
5	1.0 x 10^9 (3.8 x 10^9)	-7.4
6	1.7 x 10^9 (4.9 x 10^9)	-7.4

Transient absorption spectra: Lin and Schuster studied the quenching of several pyrylium salts by 2-NS.[3] Laser flash photolysis in these cases led to the formation of transients which were assigned to pyranyl radicals (λ_{max} = 430-480 nm) and 2-

NS radical cation (λ_{max} = 600-700 nm). Based on these results they have suggested that quenching in these cases occurred by electron transfer from 2-NS to the pyrylium salts. In order to see whether electron transfer occurred in our systems, we have recorded the transient absorption spectra of **4-7** in presence of 2-NS. A representative example is given in Figure 4.10.

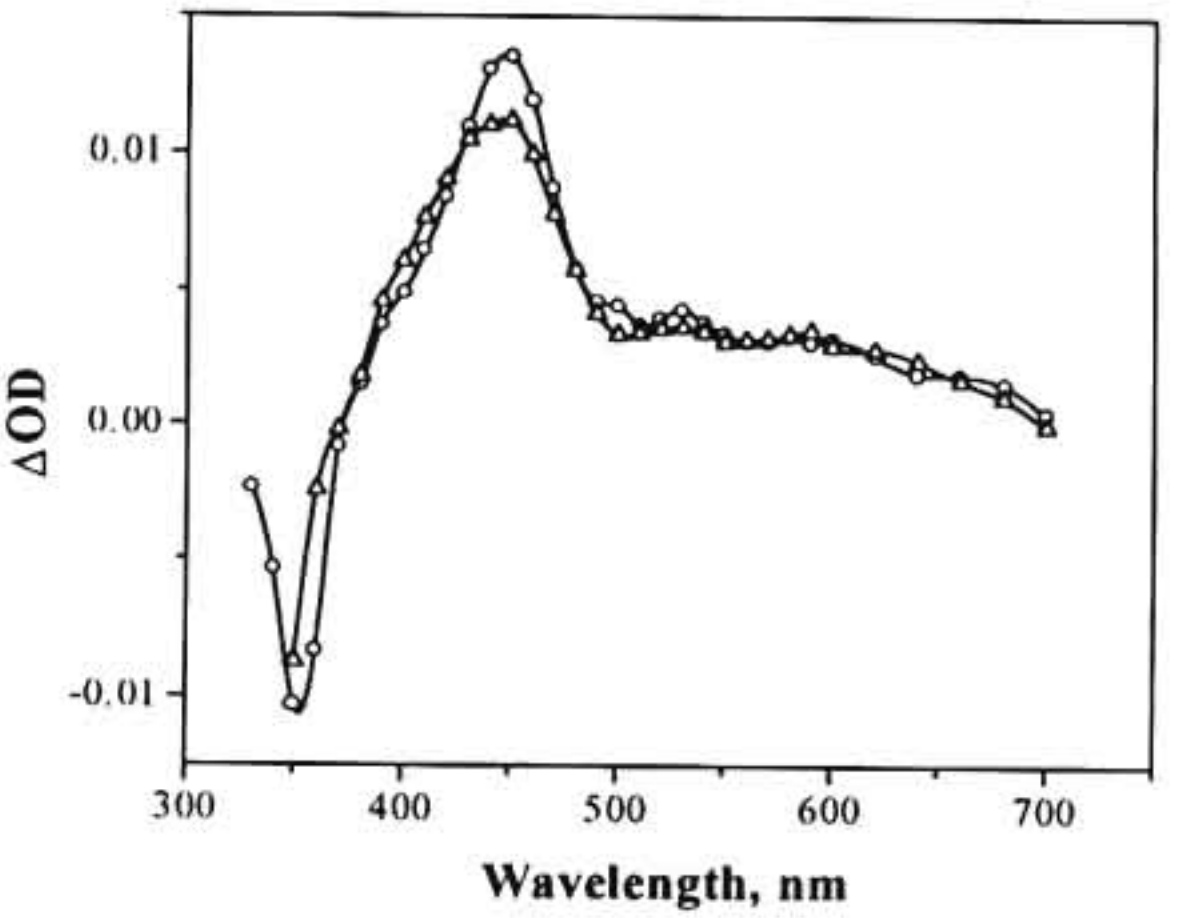

Figure 4.10 Transient absorption spectra of **6** the presence of 0.01 M 2-NS. (O) β-CD = 0 mM and (Δ) β-CD = 2.5 mM.

The transient absorption spectrum showed a maximum at 420-440 nm and small absorptions in the 600-700 nm region. The 440 nm absorption was assigned to the pyranyl radical based on literature reports and our own earlier results, and the long wavelength absorption was assigned to 2-NS radical cation. Thus it is clear that quenching of the singlets and triplets of **4-7** by 2-NS occurs by an electron transfer mechanism. Transient absorption spectra of the above systems in the presence of

β-CD were also similar (Figure 4.10). This confirmed that electron transfer occurs even when the pyrylium salt is encapsulated within β-CD and quencher is present in the aqueous phase.

The most important results of these studies is the substantial reduction of the BET rates in the presence of β-CD. We have observed that the lifetimes of the radicals were enhanced approximately 20 times in the presence of β-CD. This is shown in the kinetic traces in Figure 4.11, which shows the decay of the 440 nm species in the absence and presence of β-CD.

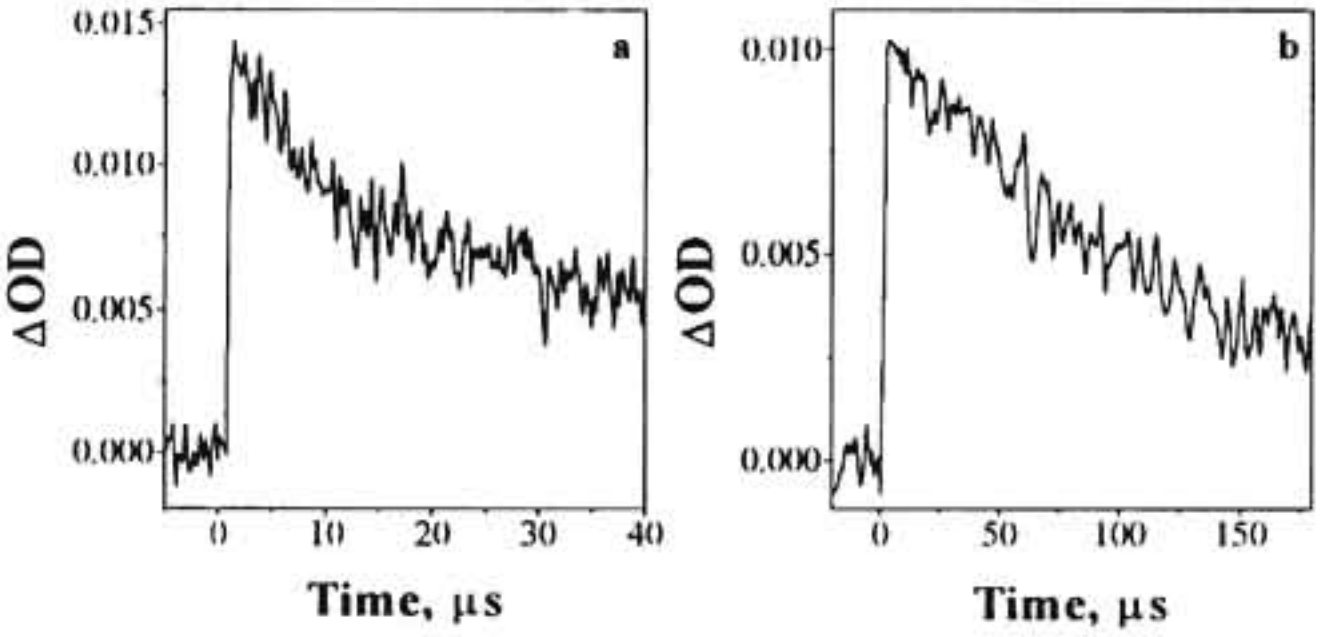

Figure 4.11 Kinetic traces in the (**a**) absence and (**b**) presence of β-CD for **6** / **2-NS** system.

In the absence of β-CD, the transients decayed in about 20 μs time. The small residual absorption in this case is attributed to product formation. In the presence of β-CD, decay of the radical species is not complete even at 150 μs. Residual absorptions attributable to product formation is absent in this case. This clearly indicated that the radicals are protected within the β-CD cavity for relatively long

periods. Reduced rates of BET in these cases can be attributed to two factors: (1) the spatial separation of the donor and acceptor achieved by encapsulation and (2) increased hydrophobicity of the radicals compared to the cationic pyrylium salts.

In a recent report, Mirzoian and Kaifer studied the binding abilities of viologen derivatives and their one and two electron reduction products with β-CD using cyclic voltammetry.[55] They have observed that the dicationic viologens have no affinity towards cyclodextrins. The two electron reduction products (neutral form) formed extremely stable inclusion complexes with association constants in the range 10^3-10^4 M^{-1}. The radical cations (single electron reduction products) exhibited intermediate binding affinities ($K \approx 10^2$ M^{-1}). Enhanced binding of the radical cations and neutral forms is due to their hydrophobicity. This study clearly established that the radicals are more hydrophobic compared to the cations. Pyrylium salts also present a similar case. Based on the study of Mirzoian and Kaifer, we propose that the neutral pyranyl radicals will be more hydrophobic compared to the cationic pyrylium salts[55]. Thus, compared to the pyrylium salts, the binding constants of the radicals with β-CD will be higher.

Based on our fluorescence studies we have suggested that in the pyrylium salt-β-CD inclusion complex, the pyrylium ring is partly exposed to the aqueous environment. Upon electron transfer from 2-NS, the charge on the pyrylium ring is neutralized. The radical formed is more hydrophobic and will have better binding affinity with β-CD. Thus, the pyranyl radical formed may move towards the interior of the cavity and the 2-NS radical cation formed may move away from the β-CD. This would lead to an effective separation of the products of PET reactions

and can account for the approximately 20 times enhancement of the radical lifetime in the presence of β-CD.

In this Chapter, we have described the photophysical and electron transfer properties of selected pyrylium derivatives in aqueous solutions in the absence and presence of β-CD. Our studies showed that pyrylium salts with proper size and hydrophobic groups can be encapsulated into the β-CD cavities. For those pyrylium salts, which form inclusion complexes, the fluorescence enhancements were measured and used in the calculation of the binding constants. We have shown that encapsulated pyrylium salts can undergo electron transfer reactions. The radicals obtained in these cases were long-lived compared to those in the absence of β-CD. Our results suggest that β-CD can be employed in suitable cases to control BET reactions to some extent.

4.4. Experimental

Measurements: All melting points are uncorrected and were determined on a Büchi Model 530 melting point apparatus. IR spectra were recorded on a Perkin Elmer Model 882 IR spectrometer. ^{1}H NMR spectra were recorded on a JEOL EX-90 spectrometer. The absorption spectra were recorded on a Shimadzu UV-2100 or a GBC double beam UV-VIS spectrophotometer. Fluorescence spectra were recorded on a SPEX Fluorolog F 112X spectrofluorimeter with a right-angle geometry using 4 x 10^{-6} M solutions. Fluorescence lifetimes were determined using Edinburgh Instruments FL900CD single photon counting system. Laser flash photolysis experiments were carried out by employing an Applied Photophysics Model LKS-20 Laser Kinetic Spectrometer using GCR-12 Series

Quanta Ray Nd:YAG laser. The analyzing and laser beams were fixed at right angles to each other. The laser energy was 60 mJ at 355 nm.

Materials: Synthesis of **4** is described below. Compound **8** was prepared according to a reported procedure.[56] Syntheses of other pyrylium derivatives are described in earlier chapters of this thesis. β-CD purchased from Aldrich was used as received. 2-NS was prepared according to a reported procedure[57] and was recrystallized before use.

Synthesis of 2,6-dimethyl-4-(*p*-*n*-butylphenyl)pyrylium perchlorate (4)

4-(*n*-Butylphenyl)magnesium bromide was prepared through the reaction of 1-(4-bromophenyl)butane (20 mM) and magnesium (20 mM) in dry THF (20 mL). This reagent was added to a suspension of 2,6-dimethyl-4-pyrone (20 mM) in dry THF (50 mL) at 0 °C. The solution was allowed to warm up to room temperature and stirred for 30 minutes. Ice cold solution of 10% perchloric acid (100 mL) was added and the precipitated pyrylium salt (**4**) was collected by filtration. The salt thus obtained was dissolved in dichloromethane and reprecipitated by adding ether. This process was repeated several times to give 2.1 g (31 %) of a pure product, mp 120-121 °C; IR (ν_{max}): 3094, 2935, 2861, 1647, 1095 cm^{-1}; ^1H NMR (90 MHz, $CDCl_3$), δ 0.9 - 1.6 (m, 9 H), 2.9 (s, 6 H), 7.3 - 8.2 (m, 6 H); Anal. Calcd for $C_{17}H_{21}O_5Cl$: C, 59.98; H, 6.22. Found: C, 59.71; H 6.35.

All experiments were carried out in aqueous buffer solutions of pH 3.5. Double distilled water was used for preparing solutions. Solutions for flash photolysis experiments were deaerated with argon for 15 minutes, prior to the experiments.

4.5. References

1. Wintgens, V.; Pouliquen, J.; Kossanyi, J. *Nouv. J. Chim.* **1985**, *9*, 229.
2. Wintgens, V.; Pouliquen, J.; Simalty, M.; Kossanyi, J.; Justesen, F. K.; Eriksen, J. *J. Photochem.* **1984**, *26*, 131.
3. Lin, Z.; Schuster, G. B. *J. Org. Chem.* **1994**, *59*, 1119.
4. Atwood, J. L.; Davis, J. E. D.; Mac Nicol, D. D. (Eds.), *Inclusion Compounds*, Academic Press, London, **1984**, Vol. 2 and 3.
5. Saenger, W. *Angew. Chem. Int. Ed. Engl.* **1980**, *19*, 344.
6. Li, S.; Purdy, W. C. *Chem. Rev.* **1992**, *92*, 1457.
7. Ueno, A.; Osa, T. in *Photochemistry in Organized and Constrained Media*, Ramamurthy, V. (Ed.), VCH Publishers, New York, **1991**.
8. Ramamurthy, V.; Eaton, D. F. *Acc. Chem. Res.* **1988**, *21*, 300.
9. Kalyanasundaram, K. *Photochemistry in Microheterogeneous Systems*, Academic Press, New York, **1987**.
10. Bortolus, P.; Monti, S. *Adv. Photochem.* **1996**, *21*, 1.
11. Cramer, F.; Saenger, W.; Spatz, H. C. *J. Am. Chem. Soc.* **1967**, *89*, 14.
12. Kinoshita, T.; Linuma, F.; Tsuji, A. *Biochem. Biophys. Res. Commun.* **1976**, *51*, 666.
13. Hoshino, M.; Imamura, M.; Ikehara, K. *J. Phys.Chem.* **1981**, *85*, 1820.
14. Yorozu, T.; Hoshino, M.; Imamura, M.; Shizuka, H. *J. Phys. Chem.* **1982**, *86*, 4422.
15. Turro, N. J.; Okubo, T.; Weed, G. *Photochem. Photobiol.* **1982**, *35*, 325.
16. Turro, N. J.; Okubo, T.; Chung, C. –J. *J. Am. Chem. Soc.* **1982**, *104*, 3954.
17. Turro, N. J.; Cox, G. S.; Ki, X. *Photochem. Photobiol.* **1983**, *36*, 149.

18. Bright, F. V.; Catena, G. C.; Huang, J. *J. Am. Chem. Soc.* **1990**, *112*, 1343.

19. Park, J. W.; Song, H. J. *J. Phys. Chem.* **1989**, *93*, 6454.

20. Hashimoto, S.; Thomas, J. K. *J. Am. Chem. Soc.* **1985**, *107*, 4655.

21. Nelson, G.; Warner, I. M. *J. Phys. Chem.* **1990**, *94*, 576.

22. Das, S.; Thomas, K. G.; George, M. V.; Kamat, P. V. *J. Chem. Soc. Faraday Trans.* **1992**, *88*, 3419.

23. Sanramé, C. N.; de Rossi, R. H.; Argüello, G. A. *J. Phys. Chem.* **1996**, *100*, 8151.

24. Wagner, B. D.; MacDonald, P. J. *J. Photochem. Photobiol. A: Chem.* **1998**, *114*, 151.

25. Duveneck, G. L.; Sitzmann, E. V.; Eisenthal, K. B.; Turro, N. J. *J. Phys. Chem.* **1989**, *93*, 7166.

26. Tran, C. D.; Fendler, J. H. *J. Phys. Chem.* **1984**, *88*, 2167.

27. Huang, J.; Bright, F. V. *J. Phys. Chem.* **1990**, *94*, 8457.

28. Dimitrijevic, N. M.; Kamat, P. V. *J. Phys. Chem.* **1993**, *97*, 7623.

29. Guldi, D. M.; Hungerbuehler, H.; Janata, E.; Asmus, K. D. *J. Phys. Chem.* **1993**, *97*, 11258.

30. Guldi, D. M.; Huie, R. E.; Neta, P.; Hungerbuehler, H.; Asmus, K. D. *Chem. Phys. Lett.* **1994**, *223*, 511.

31. Guldi, D. M. *Res. Chem. Intermed.* **1997**, *23*, 653.

32. Priyadarshini, K. I.; Mohan, H.; Mittal, J. P. *Proc. Electrochem. Soc.* **1994**, *94*, 921.

33. Willner, I.; Eichen, Y.; Willner, B. *Res. Chem. Intermed.* **1994**, *20*, 681.

34. Lee, D. K.; Kang, Y. S.; Kevan, L. *J. Phys. Chem.* **1997**, *101*, 519.

35. Kim, Y. H.; Cho, D. W.; Song, N. W.; Kim, D.; Yoon, M. *J. Photochem. Photobiol. A: Chem.* **1997**, *106*, 161.

36. Yonemura, H.; Nakamura, H.; Matsuo, T. *Chem. Phys.* **1992**, *162*, 69.

37. Fujiwara, Y.; Aoki, T.; Yoda, K.; Cao, H.; Mukai, M.; Haino, T.; Fukazawa, Y.; Tanimoto,Y.; Yonemura, H. *Chem. Phys. Lett.* **1996**, *259*, 361.

38. Yonemura, H.; Nakamura, H.; Matsuo, T. *Chem. Phys. Lett.* **1989**, *155*, 157.

39. Yonemura, H.; Saito, H.; Matsushima, S.; Nakamura, H.; Matsuo, T. *Tetrahedron Lett.* **1989**, *30*, 3143.

40. Yonemoto, E. H.; Saupe, G. B.; Schmehl, R. H.; Hubig, S. M.; Riley, R. L.; Iverson, B. L.; Mallouk, T. E. *J. Am. Chem. Soc.* **1994**, *116*, 4786.

41. Adar, E.; Degani, Y.; Goren, Z.; Willner, I. *J. Am. Chem. Soc.* **1986**, *108*, 4696.

42. Wilmer, I.; Adar, E.; Goren, Z.; Steinberger, B. *New. J. Chem.* **1987**, *11*, 769.

43. Kano, K.; Takenoshita, I.; Ogawa, T. *J. Phys. Chem.* **1982**, *86*, 1833.

44. Kano, K.; Takenoshita, I.; Ogawa, T. *Chem. Lett.* **1980**, 1035.

45. Kobashi, H.; Takahashi, M.; Muramatsu, Y.; Morita, T. *Bull. Chem. Soc. Jpn.* **1981**, *54*, 2815.

46. Hamai, S. *Bull. Chem. Soc. Jpn.* **1982**, *55*, 2721.

47. Awartani, R.; Sakizadeh, K.; Gabrielsen, B. *J. Chem. Educ.* **1986**, *63*, 172.

48. Sivakumar, A.; Parimala, S.; Ramamurthy, P. *J. Photochem. Photobiol. A: Chem.* **1996**, *94*, 129.

49. Gird, E.; Balaban, A. T. *J. Electroanal. Chem.* **1962**, *4*, 48.

50. Gopidas, K. R.; Bohorquez, M.; Kamat, P. V. *J. Phys. Chem.* **1990**, *94*, 6435.

51. Kamat, P. V.; Chauvet, J. –P.; Fessenden, R. W. *J. Phys. Chem.* **1986**, *90*, 1389.

52. Akaba, R.; Sakuragi, H.; Tokumaru, K. *J. Chem. Soc. Perkin Trans. 2* **1991**, 291.

53. Akaba, R.; Aihara, S.; Sakuragi, H.; Tokumaru, K. *J. Chem. Soc. Chem. Commun.* **1987**, 1262.

54. Lakowicz, J. R. *Principles of Fluorescence Spectroscopy*, Plenum Press, New York, **1983**.

55. Mirzoian, A.; Kaifer, A. E. *Chem. Eur. J.* **1997**, *3*, 1052.

56. Baldovi, M. V.; Garcia, H.; Miranda, M. A.; Primo, J. *Monatsch. Chem.* **1990**, *121*, 371.

57. Furniss, B. S.; Hannaford, A. J.; Rogers, V.; Smith, P. W. G.; Tatchell, A. R. (Eds.), *Vogel's Textbook of Practical Organic Chemistry*, Longman, England, **1984**, p. 643.